THE UNIVERSITY *of* EDINBURGH

A study of dissolved organic matter in peatlands: molecular characterisation of a dynamic carbon reservoir

Luke McDonald Ridley

A thesis submitted for the degree of Doctor of Philosophy, 2012
University of Edinburgh

Declaration

Ruth Flerus carried out the ESI-FT-ICR-MS analysis and data acquisition (discussed in Chapter 6). CuO oxidation GC-MS analysis and quantification of phenolic compounds in the solid phase was carried out Jason Dallas-Ross and Dafydd Elias, who also assisted in the field in June 2010. All subsequent data analysis and interpretation was carried out by the candidate. All other sample analysis and data collection was carried out by the candidate.

The candidate declares that:

(a) that the thesis has been composed by the candidate, and
(b) either that the work is the candidate's own, or, if the candidate has been a member of a research group, that the candidate has made a substantial contribution to the work, such contribution being clearly indicated, and
(c) that the work has not been submitted for any other degree or professional qualification except as specified.

Signed:

Abstract

Northern peatlands represent a significant carbon reservoir, containing approximately a third of the terrestrial carbon pool. The stability of these carbon stores is poorly understood, and processes of accumulation and degradation appear to be finely balanced. Over the last decade, it has become increasingly clear that losses of dissolved organic carbon (DOC) from peatlands can be of considerable size and this flux appears to have increased substantially over the last 20 years. Despite its significance, the chemical composition of peatland-derived DOC remains poorly understood. This study aimed to characterise dissolved organic matter (DOM) at the molecular level using a novel combination of techniques. The study site (Cors Fochno, Wales, UK) is an ombrotrophic bog on which a number of studies into carbon cycling and hydrology have been carried out, providing a useful context for this project.

The size and compositions of the DOC pool was monitored over 18 months, from three banks of piezometers, sampling from depths of 15 cm to 6 m. DOM which is representative of bog runoff was also monitored. DOC concentrations varied considerably between locations, spanning an order of magnitude (11.4 to 114 mgC l^{-1}). Several relationships between DOC concentration and environmental and physical factors were established: DOC levels near the surface of the peatland varied with temperature, those in the runoff were most affected by recent rainfall events and the apparent DOC concentration at depth was related to the hydraulic conductivity of peat at that depth. The annual flux of DOC from the site was estimated at 113 tonnes, or 17.4 gC m^{-2}.

Only a small portion of the DOC pool could be characterised by analysis of dissolved combined amino acids (DCAA) and dissolved carbohydrates (as neutral sugars). Non-protein amino acids were most abundant in runoff samples, suggesting microbial reworking of DOM on entering drainage systems. DCAA yields decreased with depth, and the DCAA pool in deeper peat layers was characterised by more hydrophobic compounds. Interpretation of semi-quantitative

results from TMAH thermochemolysis GC-MS analysis suggested oxidative degradation of organic matter near the surface of the peatland and photochemical degradation where DOM entered drainage networks, and this was supported by novel interpretation of results from ultrahigh resolution mass spectrometry analysis. The deepest porewaters were dominated by *n*-alkanes, with notable contributions from fatty acids, suggesting a plant wax source for this DOM.

The highest DOC concentrations were found at intermediate depth from a site midway between the centre of the bog and the southern boundary where hydraulic conductivities were low, and DOM from these piezometers were characterised by high contributions from a suite of phenolic compounds (with mainly *para*-hydroxyphenyl structures). These compounds have been linked to *Sphagnum* species, and are known to be functionally important to the development and maintenance of the unusual chemical environment in peatlands which slows decay rates, reduces microbial activity, and allows the sequestration of the large carbon reservoir.
The findings of this study highlight the dynamic nature of peatland derived DOM, both in the size of the carbon pool and its composition which change dramatically with both season and depth.

This thesis is dedicated to my dad who was dauntlessly fighting his own battles throughout this project, and whose victory gives our family much to smile about every day.

"Si ce n'est pas toi, petit,
qui commence a changer le monde,
qui le fera?"

Unknown author

Given to me on a postcard by my mum
before I left home for university.

Acknowledgements

Thank you to NERC for funding this project, and to DAAD and the British Council for giving me the opportunity to collaborate with European colleagues, resulting in the ESI-FT-ICR-MS work presented in Chapter 6 of this thesis.

In addition to acknowledging the support and advice of all my supervisory team, Greg Cowie, Geoff Abbott, Andy Baird and Maurizio Mencucinni, I would like to say a special thank you to Andy, whose help in the field and during the writing process has been invaluable. Mike Bailey at CCW was also a huge help, and great champion of scientific studies at Cors Fochno.

A special thanks must also be given to Steve Mowbray, who introduced me to the wonders of working in an organic geochemistry lab, and whose expert knowledge I called upon countless times. Thanks also to Paul Donohoe at Newcastle University for his help with the acquisition of TMAH thermochemolysis data, and to Alan Pike and Jim Sm
ith for their help with the manufacture of field equipment (with some entertainment along the way). Thanks also to Ruth Flerus, Philippe Schmitt-Kopplin and Boris Koch for their generosity, inspiration and help while I was getting to grips with ESI-FT-ICR-MS.

For their huge efforts in the field, both manual and morale boosting, I'd like to thank Alice Milner, Alun Evans, Daf Elias, Jason Dallas-Ross and Terry Alexander. A special mention goes to Alun, who has helped immeasurably over the past three and a half years. Thanks also to Imalda Stamp for her support on and off the bog, to Rhona and Phil at Borth House B&B, and to Walter Geibert who was always willing to offer advice and support over coffee. And thanks to my informal peat network (AKA Kathleen Allan and Antony Phin) for all the peatmeets, and for proof reading chapters. On that front, thanks also to Drs Antony Bloom, Bronwen Whitney, Tom Russon and Gillian McCay for their very helpful comments and advice.

Finally, a huge thanks to my friends, housemates and office buddies, without whom this would not have been four of the most enjoyable and rewarding years of my life. I can't mention everyone, but Matthew Unterman, Amber Annett, Tom, Gillian, Sian Henley, Rachel Kilgallon, Johanass Miocic, Robyn Tuerena, Lizzie Entwhistle, Maddy Berg, Nancy Burns, Rhian Meara, Luke Smallman, Catherine Harper, Andrew Schurer and Dan Hobley all deserve special mentions.

Contents

List of figures

List of Tables

Chapter 1: Introduction and project rationale

1.1 Northern peatlands as carbon reservoirs:

Peatlands are a major carbon reservoir, accounting for approximately half (~5 Pg) of the total soil carbon stock for the UK (Dawson & Smith, 2007). They also cover a significant proportion of the country's land mass, some 14%, and this number increases to 31% when considering just Scotland. (Billett et al., 2006). Although peat stocks in the UK have traditionally been exploited for use as a fuel and more recently as a growing medium, these practices have become much less common and there is now an emphasis being placed on conservation of peatlands as a habitat. This study will focus on Cors Fochno, an estuarine raised bog in mid-Wales. However, the vast majority of peatland research (especially in the UK) is conducted on other types of peatland (e.g. blanket bogs in the UK, boreal bogs in the rest of Northern Europe) and so the following introduction will draw on some references from these other types of northern peatland.

Northern peatlands play a significant role in the global carbon cycle and contain between 250 and 450 Pg of C, approximately a third of the global terrestrial organic carbon pool (Gorham, 1991). Peatlands are predominantly located in mid to high latitudes (Figure 1.1) where temperatures are relatively low and the peat layer can remain saturated for much of the year. In this environment, carbon is effectively stored through the build up of acidic and anoxic conditions which inhibit many enzymatic degradation reactions. *Sphagnum* mosses are particularly important for the onset of a chemical environment which suppresses decomposition of organic matter. More than half the world's peat originates from *Sphagnum*, representing 10-15% of the terrestrial carbon stock (Fenner et al., 2004). The unusual physiology and biochemistry of *Sphagnum*, including its water holding capacity (Rydin et al., 2006), cation exchange capacity (Painter, 1991) and the presence of unusual polyphenolics (Verhoeven & Liefveld, 1997) and oxopolysaccharides (Hàjek et al., 2011) lead to some of the defining characteristics of northern peatlands. This will be discussed further in the

introduction to Chapter 4. Low degradation rates, due to both the quality of organic matter and the chemical environment, then lead to the formation of thick layers of poorly decomposed and recalcitrant organic deposits.

The thickness of these organic layers, and therefore the total carbon reservoir size, is dependent on the balance between net biomass accumulation rate in the acrotelm (the upper portion of peat which is bordered by the land surface and lowest annual-average water table position; this area is intermittently aerobic) and the integrated biomass decay rate in the catotelm (that portion of the peat which is always below the water table and anaerobic, and in which long term storage of carbon occurs). The accumulation of metres of organic material is possible because degradation rates in the catotelm are very slow, as much as three orders of magnitude slower than rates near the water table, where the majority of decomposition occurs (Beer and Blodau, 2007). Understanding the relationship between these two processes and the controls upon them is essential if we hope to be able to predict how peatlands will react to future environmental forcing, both natural and anthropogenic.

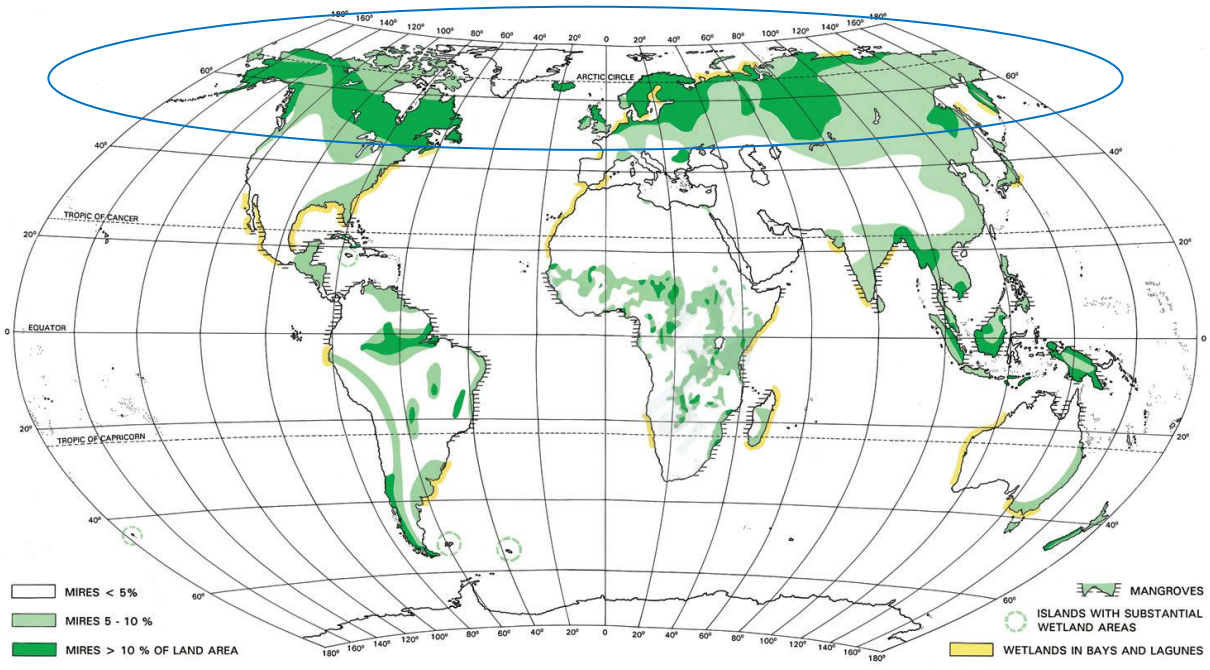

Figure 1.1.Global distribution of wetlands. Source: International Peat Society (2007). The region circled in blue is dominated by the northern peatlands of Northern Europe, North America, and Russia.

The majority of the carbon stored within peat bogs is poorly decomposed or recalcitrant solid-phase organic matter; however, there is also a substantial amount of C present in the form of dissolved organic carbon (DOC), defined as the portion of porewater carbon not extracted by filtering at 0.45 μm. For the purposes of this work, the term porewater is used to describe water samples obtained by extraction of water from piezometers. Dissolved organic carbon is found in concentrations from 3-400 mg l^{-1} in natural peatlands, with average concentrations of approximately 30 mg l^{-1} reported (Thurman, 1985). Estimates of the flux of DOC from northern peatland systems range from 5-40 g $m^{-2}yr^{-1}$ (Moore et al., 1997; Scott et al., 2001; Thurman, 1985) although there is still debate as to the extent of loss of organic carbon within the stream continuum and the best methods for measuring and reporting this flux; therefore, these numbers may underestimate the actual loss from the peatland (Billett et al., 2004; Worrall et al., 2006a; Dawson et al., 2004; Eimers et al., 2008). Estimates of DOC fluxes from raised bogs range from 16.2 gC m^{-2} yr^{-1} (Blodau et al. 2007) to 30.4 gC m^{-2} yr^{-1} total OC (Billett et al. 2004). These estimates are similar to estimates of accumulation rates for northern peatlands (~20-25 gCm^{-2} yr^{-1} Moore et al., 1998; Turunen et al., 2002). Limpens et al. (2008) collated data from a number of studies, and reported that DOC or dissolved carbon fluxes were approximately a third to a quarter of the magnitude of net ecosystem exchange, or around half of carbon accumulation (the remainder being the methane loss to the atmosphere).

The majority of previous studies into carbon storage in northern peatland systems have focussed on fluxes between the atmosphere and land surface: the uptake of CO_2 during photosynthesis and the release of CO_2 and CH_4 during respiration (Billett et al., 2004 and references therein). See Figure 1.2 for a schematic of the major components of the carbon cycle in northern peatlands, adapted from Moore et al. (1998). Studies by Billett et al. (2004) and Dawson et al. (2004) highlight the need for the inclusion of groundwater and runoff fluxes in carbon budget studies and also the loss of carbon from surface waters through CO_2 evasion. These studies come amid an increasing level of awareness of the important role dissolved organic carbon (DOC) plays in maintaining peat carbon reservoirs.

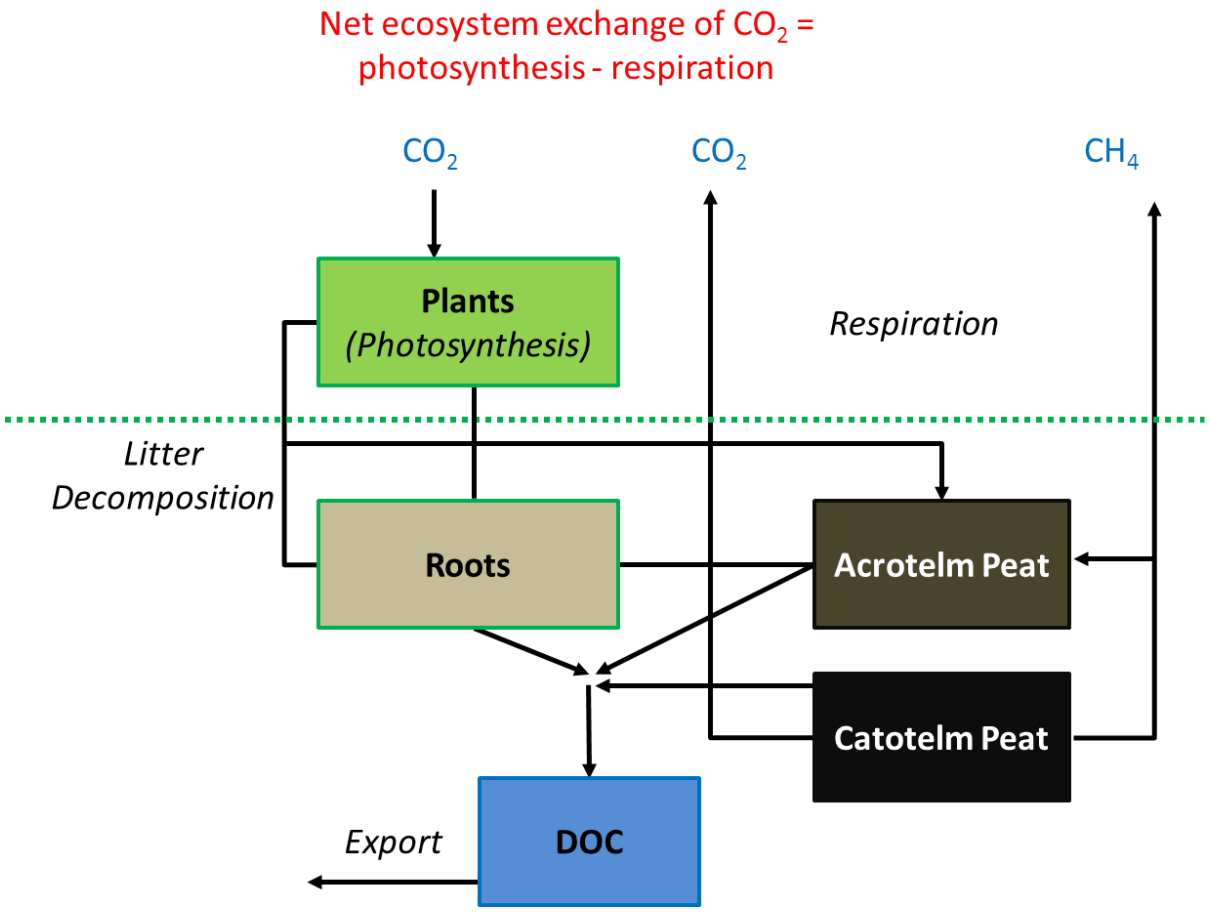

Figure 1.2: Schematic of the major components of the carbon cycle in northern peatlands, adapted from Moore et al. (1998).

The next sections of this chapter will focus on the stability or vulnerability of northern peatlands as carbon reservoirs, firstly with respect to changing climate and then to other anthropogenic influences.

1.2 Peatlands dynamics: the possible impact of future climate change

Peatlands have been accumulating carbon since the end of the last ice age with large increases in carbon storage between 5,000 and 8,000 years BP (Billett et al., 2007). Rates of accumulation over the last few centuries are estimated at ~230 kg C ha^{-1} yr^{-1} although a high degree of uncertainty remains over these estimates (Moore et al., 1998). Although there is a large quantity of carbon currently stored in northern peatlands, it is unclear how stable these

carbon reservoirs are: it has been demonstrated that some peatlands display seasonal changes in their carbon balance, storing carbon during the summer then becoming net carbon sources during the winter (Billett et al., 2004). Using climate-change models, it has been predicted that northern peatlands will become net carbon sources within this century (e.g. Wieder, 2001). As temperatures rise, microbial activity is predicted to increase and degradation of previously stable recalcitrant carbon stores could release large amounts of carbon into the atmosphere and marine system (Davidson & Janssens, 2006). Alongside temperature increases, it is thought that there will be associated changes to rainfall patterns with more frequent storm events and periods of drought (IPCC 4th Assessment Report, 2007). It is therefore generally recognised that although increasing temperatures are likely to have an effect on the carbon balance within peat systems, the major impact of climate change is likely to be indirect, caused by changing hydrological and seasonal conditions (Gorham, 1991).

Any changes in climate as a result of global warming may well have a profound effect on DOC dynamics in the peat system: DOC production is mediated by a number of factors including temperature and moisture, and its export is controlled by hydrological conditions; indeed, there is a growing body of evidence that DOC fluxes from peatlands are already responding to changing environmental conditions.

1.2.1 Increased DOC fluxes - possible climatic controls:

In 2001, Freeman et al. conducted a study of the UK acid water monitoring network and found that, over the previous 12 years, concentrations of DOC had increased by up to 65% and that in 20 of the 22 sites covered the increases were "significant". This increase in DOC concentrations in surface waters has been observed in numerous subsequent studies in the UK, Scandinavia and North America: Worrall et al. (2004) found that DOC concentrations increased significantly in 77% of the 198 UK catchments they studied on timescales of between 9 and 42 years; Erlandsson et al. (2008) report an average increase in absorbance at

420nm wavelength[1] of 1.47% per annum for 28 large Swedish rivers over 35 years; and Stoddard et al. (2003) found that in a study of 292 sites across northern and eastern U.S., all regions exhibited increased DOC concentrations between 1990 and 2000 with a median increase of 0.05 mg $l^{-1}yr^{-1}$, corresponding to a region-wide 10% increase.

A number of mechanisms have been proposed as driving increasing DOC concentrations within surface waters. Initially, increased atmospheric temperature was invoked as the driving force because increasing temperature increases biological activity and hence bacterial production of DOC (Freeman et al., 2001). Further studies have found correlations between increasing seasonal temperatures and DOC export (Worrall et al., 2003) although temperature changes cannot account for all the increases in the flux term (Evans et al., 2007; Worrall et al., 2004). If temperatures increase there may be a subsequent lowering of the water table, particularly during the summer months, through increased evapotranspiration. This would increase the depth of the oxidised zone and thereby enhance biological degradation of organic matter (Gorham, 1991), but there is little evidence that long-term trends in water-table level are responsible for observed increases in riverine DOC levels or that the effects of droughts continue over timescales of several years (Worrall et al., 2004; Worrall & Burt, 2007a; Worrall & Burt, 2007b). Conversely, Strack et al. (2008) carried out water-table drawdown experiments over an eleven year period; the results suggested that there was a significant impact on DOC production over the full period of the experiment, but that the increased DOC fluxes were not indicative of destabilisation of the carbon reservoir but of increased biomass production and a shift in vegetation patterns.

Increasing temperature may also increase the frequency of severe droughts, and these have been suggested as a mechanism for increasing surface-water DOC concentrations. Freeman et al. (2001) suggested that hydrolase enzymes are inhibited by the presence of phenolic compounds; these can build up in peat bogs due to the high oxygen demand of phenol oxidase. If water tables are lowered, the transport of oxygen to areas that were previously

[1] Absorbance at 420nm wavelength is frequently used as a proxy for the DOM concentration of natural freshwaters in water quality monitoring programs.

anaerobic can increase phenol oxidase activity which in turn allows for higher hydrolase activity and breakdown of organic matter generally. This effect is not limited temporally to the time of the drought: once the water table returns to its normal height, hydrolase activity can continue until the phenolic compounds once again build up to a level where activity is inhibited. This "enzyme latch" mechanism has been supported by subsequent studies (Worrall et al., 2004) but there is still little microbiological evidence for its occurrence (Evans et al., 2006; Worrall et al., 2006).

1.2.2 Increased DOC fluxes - possible non-climatic controls:

Although in the current political climate it is tempting to attribute observed changes in the environment to human-induced climate change, there are a number of other drivers which could be contributing to increased DOC fluxes. There have been several significant changes in deposition patterns in the UK over timescales similar to those of the observed DOC increases, and a number of studies have investigated whether these could be causing the trends seen in UK surface waters. Evans et al. (2006) were the first to cite changes in deposition patterns as a driver for DOC concentration increases, arguing that climatic effects could not produce the large increases in DOC concentrations found; instead, this study invokes decreasing sulphate concentrations in rain-water as the cause, and found a significant inverse relationship between DOC and SO_4^{2-} concentration in soil solution. Decreasing sulphate deposition has been cited as a major influence on DOC increases in Scandinavia (Erlandsson et al., 2008) and in North America (Stoddard et al., 2003) and evidence from ^{14}C studies in the UK have suggested recovery from acidification is the main driver in increasing DOC fluxes (Evans et al., 2007).

Draw-down of the water-table has historically occurred over large areas of the UK's peatlands as a result of efforts to improve the agricultural worth of these areas, but due to the low level of improved productivity and associated negative environmental impacts (e.g. reduced water quality in peat-draining catchments) there have recently been notable efforts to re-wet peatlands, and wetlands more generally, and restore them to self sustaining

ecosystems. Wallage et al. (2006) investigated the impact of drain-blocking within a peatland on DOC dynamics and have shown that peats with substantial cuttings and no drain-blocking export significantly more DOC, and it is therefore possible that changes in land management are in places masking the trend in increasing DOC export.

Although many questions remain unanswered as to why DOC concentrations are increasing in UK surface waters, there seems to be a consensus that the mechanisms described above are not mutually exclusive: it is likely that a number of them could together be causing the underlying trends observed, and that although temperature changes alone cannot account for the increases seen, temperature rises and other secondary changes in the soil environment resulting from climate change, acid deposition and land management could result in increased DOC losses from peatlands. It is not known whether increased DOC fluxes from peatlands indicate destabilisation of a large carbon reservoir, whether increased DOC flux is matched by increased biomass growth, or whether the increased DOC flux from peatlands merely represents a recovery from acidification and a return to more natural conditions.

1.3 Mechanisms for the production and export of DOC in peatlands

Peatland DOC is composed of a mixture of high molecular weight compounds (including phenolics and humic and fulvic acids) and low molecular weight compounds, which include carbohydrates, amino acids, fatty acids and hydrocarbons (Fenner et al., 2004; Thurman, 1985). The majority of the DOC pool is composed of more recalcitrant organic matter (OM), with humic substances accounting for 70-90% of the DOC pool (Thurman, 1985). DOC is produced via the decomposition of recalcitrant high molecular weight organic substances (mainly partially degraded primary plant material, Fenner et al., 2004), where the breaking of long carbon chains creates a heterogeneous mixture of organic compounds with different degrees of hydrophilicity. Other important sources include secretions from both photosynthetic and heterotrophic organisms, bacteria and viral particles (Fenner et al., 2004

and references therein). DOC concentrations increase with increased primary productivity (Freeman et al., 2004) and can therefore change with season and environmental conditions.

Dissolved organic matter (DOM) resulting from fresh plant material will either be remineralised and recycled within the acrotelm, or undergo molecular transformations such as polycondensation (Strack et al., 2011) and Maillard reactions (Kabitz& Geyer, 2002) which increase the recalcitrance of the DOM pool and removes compounds from the labile, fast-turnover OM pool (Blodau et al., 2007). Degradation of natural biopolymers occurs in a stepwise manner (Strack et al., 2011), including extracellular hydrolysis of polymers, fermentation of the resulting monomers and fatty acids and finally utilisation of acetate by microbial communities (Beer and Blodau, 2007).

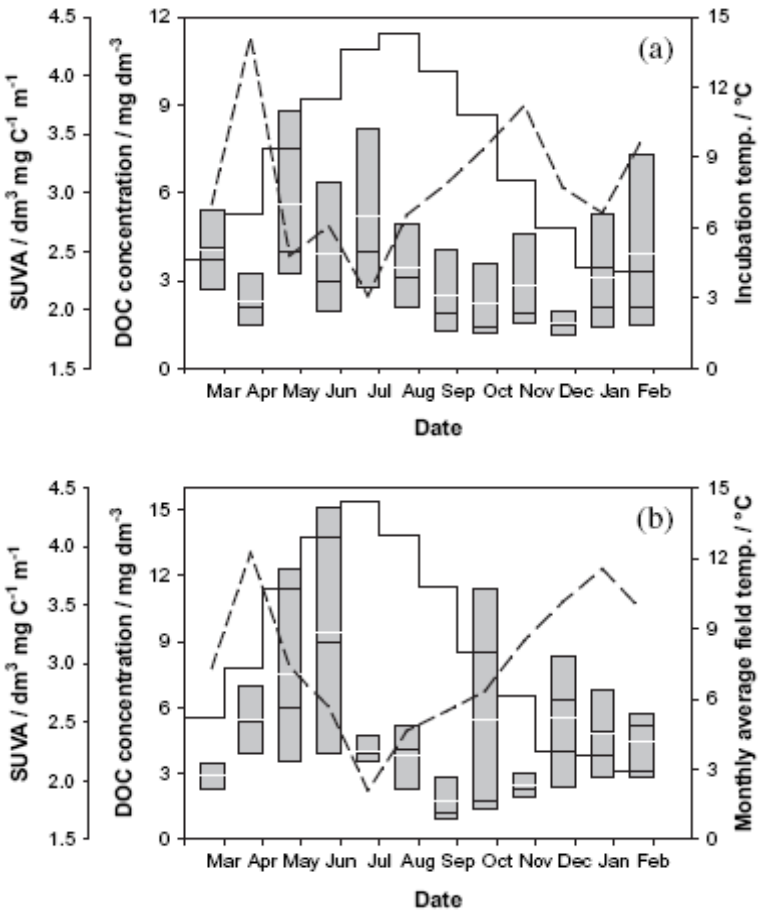

Figure 1.3: Monthly variation in DOC concentration and SUVA [carbon normalised (specific) UV absorbance] of core leachates with temperature (a) for laboratory-incubated cores and (b) monthly field-collected cores collected from March 2003 to February 2004 from a moorland hillslope site at Glensaugh, NE Scotland. Box plotsshow 25 to 75 percentile range for DOC concentrations: median and mean concentrations are represented by black and white lines respectively. The dashed line shows the SUVA and the stepped solid line the temperature. From Stutteret al. (2007).

Research on DOC production and mobilisation within peatlands is sparse, when compared to forested ecosystems for example (Stutter et al., 2007 and references therein). In forest soils there is a seasonal pattern in release of labile hydrophilic DOC which results from plant litter decomposition. This seasonal pulse in highly bioavailable DOC which occurs in the spring then primes the decomposition of more recalcitrant, hydrophobic organic matter resulting in DOC with an older native C source being produced later in the summer (Hagedorn et al., 2004). Stutter et al. (2007) have shown that this mechanism may also be creating seasonal pulses in peatland soils. Their study of both field and laboratory-incubated soil cores showed that DOC concentrations in spring and early summer were high and that there seemed to be a high proportion of labile carbon within this pool (Figure1.3). This pattern is thought to be caused by increasing temperatures which in turn increase microbial activity, releasing DOM during the incomplete decomposition of humic organic matter. As microbial activity continues throughout the summer, the labile, lower molecular weight fraction of DOM is respired and the DOC pool becomes increasingly aromatic and recalcitrant in nature, and this is accompanied by a decrease in concentrations of DOC found within the cores.

The mechanism proposed by Stutter et al. (2007) is in agreement with previous work: Scott et al. (2001) have shown that after summer droughts, the humic substances they isolated from peat pond-waters gradually became more aromatic with less carboxylic acid content through the autumn and into winter; Dawson et al. (2008) have demonstrated that soil organic matter is more hydrophilic during the summer, due possibly to increased cleaving activity during this period, with less soluble DOM being produced during the winter months. This study also suggests that controls on DOM concentrations and fluxes depend on the rainfall regimens of the catchment being considered – in wetter areas, DOM concentrations appeared to be controlled by the rates of production whereas DOM concentrations in dryer catchments were found to be export limited (Dawson et al., 2008).

1.4 Research questions and aims of the project

Understanding how both the quality and quantity of DOM in the peatland system vary over both spatial and temporal scales is necessary in order to adequately predict how peatlands are reacting, and will react in the future, to changing climate. As discussed above, DOC concentrations are thought to have responded to recent changes in the environment, but elucidating what the drivers are for observed changes has proved challenging for the scientific community. No attempts to monitor or investigate DOC loss from Cors Fochno have previously been made, so a network of piezometers has been installed across the bog for this project. Monitoring of DOC concentrations in porewater obtained from these banks of piezometers has been carried out over 18 months, giving an insight into the carbon dynamics of this site. From this DOC monitoring effort, along with environmental measurements collected over the 18 months, an estimate of DOC loss from the site can be made. This new data-set will be used to assess the heterogeneity of organic carbon concentrations at different depths, location and how these concentrations change over a full seasonal cycle.

Organic matter found in natural waters is composed of a complex mix of compounds (see Section 1.3 above), some of which can be traced to the source of the organic matter, and some of which may be indicative of degradation pathways or mechanisms (e.g. release of a pulse of labile DOM in the spring which then primes degradation of older recalcitrant OM). Current knowledge on the molecular makeup of peatland DOM is sparse, and so an important aim of this work is characterisation of the DOM pool, assigning portions of the organic carbon pool to classes or groups of compounds (e.g. the percentage of DOC present as hydrolysable amino acids). Molecular characterisation of the individual components of these pools generates further information on DOM sources and transformations, and may also indicate the recalcitrance (therefore longevity) of this carbon reservoir. With this in mind, an in-depth molecular characterisation of DOM from across different locations, depths and over more than a full seasonal cycle has been undertaken using a novel combination of techniques.

Dissolved combined amino acid (DCAA) analysis provides information on the sources of DOM and on carbon cycling within the peatland ecosystem. In addition to quantifying the yield of DCAA by a vapour phase hydrolysis and high-performance liquid chromatography (HPLC), 18 individual amino acids have been quantified. Analysis of the dissolved carbohydrate pool can also indicate plant or microbial organic matter sources. To the author's knowledge, no molecular characterisation of dissolved neutral sugars has been published from waters derived from peatlands. A strong/weak hydrolysis of water samples from Cors Fochno, followed by gas chromatography (quantifying 9 individual neutral sugars), provides novel information on the magnitude and molecular composition of this DOM component. Finally, the application of a thermochemolysis gas chromatography mass spectrometry technique in the presence of tetramethyl ammonium hydroxide (TMAH) provides a semi-quantitative assessment of lipids (*n*-alkanes and fatty acids) and functionally important aromatic compounds, including hydrolysable tannins, lignin and polymeric phenolic compounds.

Another significant question for this study is that of how, and from what pools of organic matter, DOM is produced. The relationships between solid phase- and dissolved- organic matter will be explored, using techniques which not only indicate the quantity of organic matter present, but also indicate its origin and quality. The site also acts as an important source of energy and organic carbon to surrounding water-bodies and the nearby Dyfi estuary. The quality and stability of this DOM pool will have a profound impact on the fate of these compounds, and so water which is characteristic of peatland-runoff has also been molecularly characterised, and an estimate of this flux term made. Principal component analysis (PCA) using variables from multiple analysis techniques provides further information on the transformations which DOM undergoes as it moves through the peatland environment.

Finally, an ultrahigh resolution mass spectrometry technique (electrospray ionisation Fourier transform ion cyclotron resonance mass spectrometry, ESI-FT-ICR-MS) will be utilised to analyse four samples from across the peatland, representing four of the key

chemical environments found at the site. This powerful method can provide a vast amount of information on the molecular makeup of the DOM pool, and is the only technique capable of molecularly characterising the complex mixture of humic and non-humic substances present in natural organic matter (NOM). Novel visualisation tools have been created for the interpretation of these data, which will be used to further explore the relationships between molecules in DOM from Cors Fochno.

In summary, this study had the following aims and objectives:

- To quantify DOC concentrations across different locations and depths over more than a full annual cycle in order to ascertain how DOC concentrations change over both time and space, the heterogeneity of DOC concentrations with depth and location, and to gain an insight into controls upon the magnitude of this important carbon pool,
- To quantify both the total yield and relative contribution of individual components of the DCAA and dissolved neutral sugar pools, using a sub-set of samples from different depths, seasons and locations,
- To use TMAH thermochemolysis to provide a semi-quantitative assessment of lipids (*n*-alkanes and fatty acids) and functionally important aromatic compounds, again from a sub-set of samples as above,
- To compare the DOM pool against solid phase peat cores using complimentary techniques,
- To use a ultrahigh resolution mass spectrometry technique to investigate humic substances within peatland porewater,
- Using the information gained from the above molecular characterisation, to assess the sources of peatland DOM and the molecular transformations or alterations this OM undergoes in different environments in the peatland.

In addition to the above, although it was not originally planned (and the sampling setup and availability ofsupplementaryinformation are therefore not optimum), an attempt will be made in Chapter 3 to estimate the flux of DOC from Cors Fochno.

Chapter 2: Methods and site description:

2.1 Site description

Cors Fochno (Borth Bog) is an estuarine raised bog which covers ~650 ha and is located 8 km north of Aberystwyth (UK) at 52°30'N, 04°01'W. The site, which was chosen because of its representativeness of a wide class of northern peatland, has been host to a number of research projects in the recent past, providing a large amount of contextual data from which this study can draw. The peat layer extends to a depth of >6.5 m at the centre of the main dome, which is 2-3 m higher than the margins of the site and approximately 5.5 m above sea level. The site receives on average 122.2 cm rain per year (Figure 2.1).

The main dome of the bog is ombrotrophic (rain-fed) and patterned with low-amplitude hummocks, lawns and hollows which are dominated by the species detailed in Table 2.1. Towards the edges of the site, the patterning becomes less well defined, and much of this area has been previously utilised as a source of fuel, with shallow (~30 cm) hand cuttings approximately 5 m wide running perpendicular to the site boundary (see Figure 2.2). Countryside Council for Wales (CCW) who run the site have been making efforts to raise the water table following previous drainage and cutting, and their efforts have met with considerable success, creating particularly wet conditions around the boundary between the pristine and previously cut sections of the bog. The northern half of the bog has been affected by a number of draining schemes from 1820 to the 1940's, but the focus of this study is on the central area containing the main dome and area to the south-southeast of this.

Micro-habitat	Vegetation type	Examples of dominant species
Low ridge/ hummock	vascular plants	*Calluna vulgaris* (L.) Hull.
	small-leaved Sphagna	*Sphagnum capillifolium* (Ehrh.) Hedw. *Sphagnum fuscum* (Schimp.) Klinggr.
Hollows/ shallow pools	Sphagna	*Sphagnum pulchrum* (Lindb. ex Braithw.) Warnst.
	vascular plants	*Rhynchospora alba* (L.) Vahl. *Menyanthestrifoliata* L.
Intermediate areas	large-leaved Sphagna	*Sphagnum magellanicum* Brid.
	sedges	*Eriophorum angustifolium* Honck.
Dome margins	vascular plants	*Calluna vulgaris* (L.) Hull. *Eriophorum vaginatum* L. *Myrica gale* L.

Table 2.1: Dominant vegetation types and species found at the investigation site (Cors Fochno) on 4 micro-habitats. Data from Baird et al. (2008).

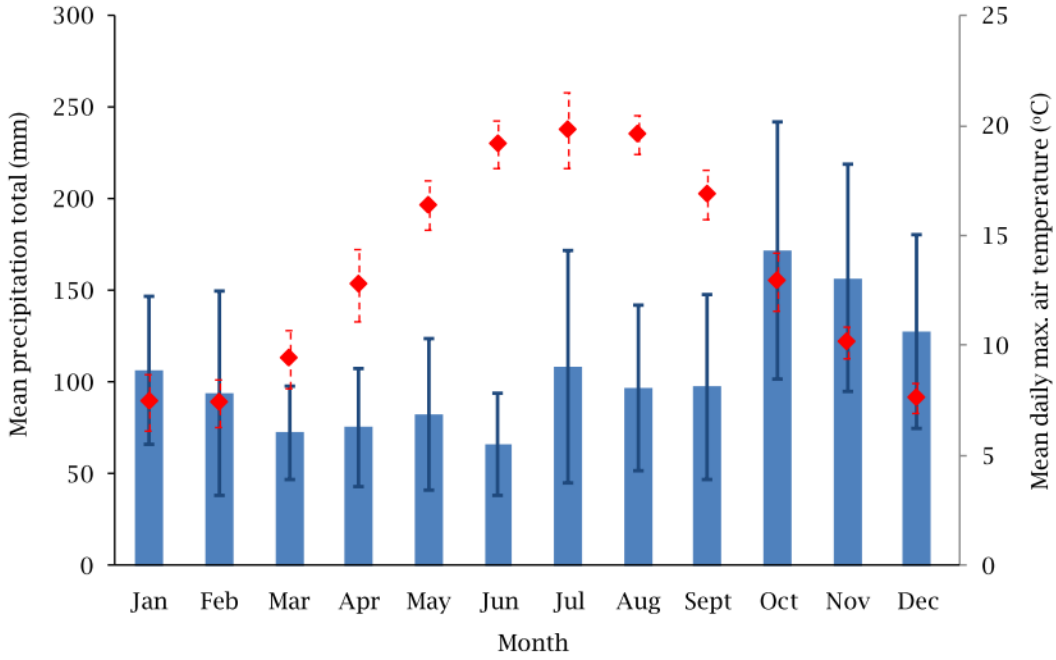

Figure 2.1: monthly mean precipitation (blue bars) and daily maximum air temperatures (red diamonds) for Cors Fochno (Fron-dirion Met. Station (elevation 65 m, 1.4 km from Cors Fochno), Tal-y-bont, 2000 – 2009). T-bars represent standard deviation of data over 10 year period. Figure from Stamp (2011).

The bog forms part of a designated UNESCO biosphere reserve and is a Special Area of Conservation (SAC). The main dome of the bog is recognised by the Joint Nature Conservation Committee (JNCC) as the largest area of primary near-natural raised bog in an estuarine position within the UK. In order to minimise damage to this sensitive site, the majority of work was carried out on sites easily accessible from either the borders of the site or via a boardwalk which has been placed on the bog in order to provide access to the main dome while minimising the risk of damage to sphagna by trampling.

The site is bounded to the south and west by a perimeter drain (Pwll Ddu ditch) which runs into the River Leri just to the west of the site. The Leri then runs into the Dovey (Dyfi) estuary approximately 1½ km north of the site. Figure 2.2 shows an aerial photo of the site overlain with the positions of major boundaries, runoff channels and sampling sites. The main access to the site is from the north, but smaller access routes are available from the south east and south west.

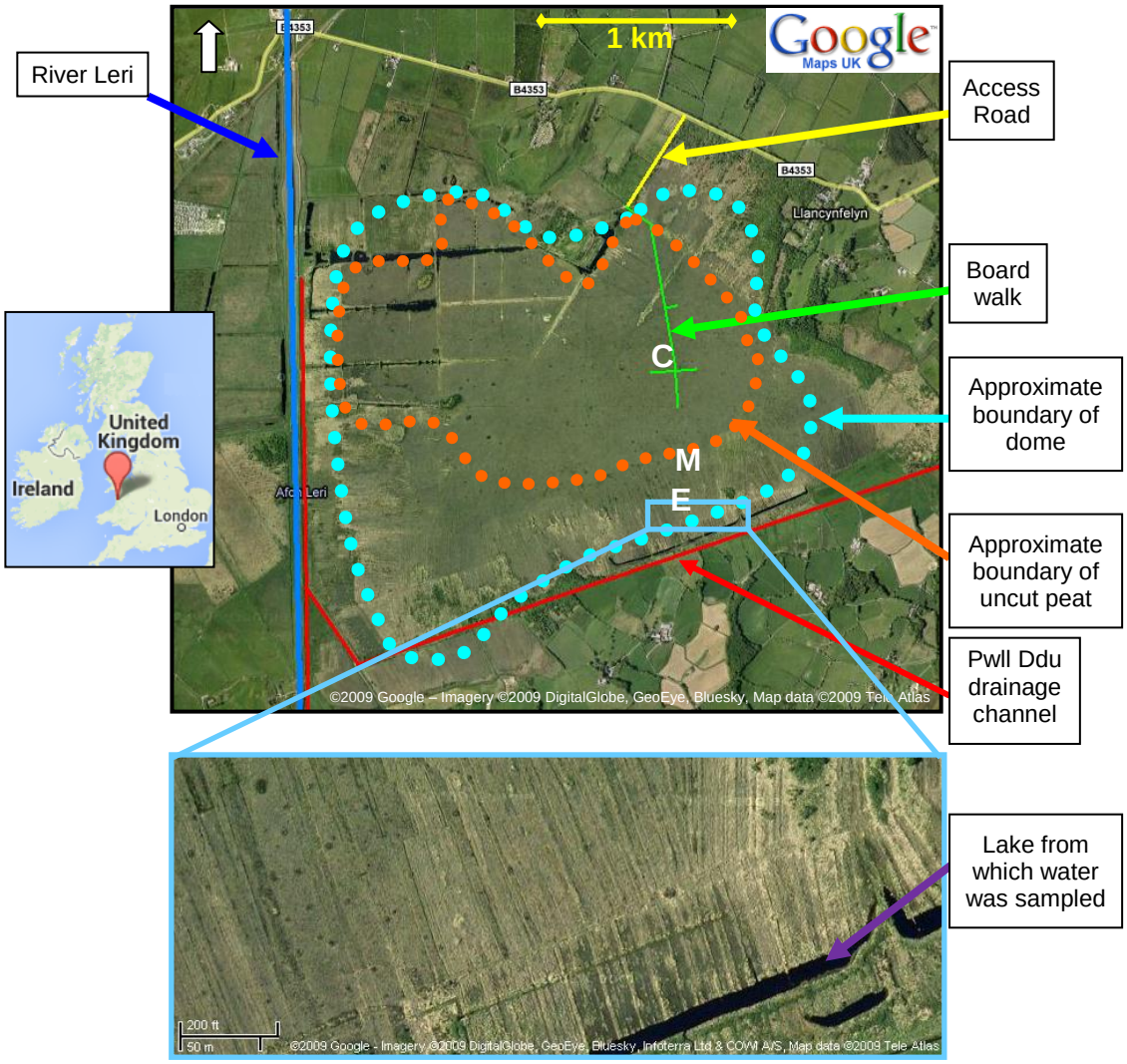

Figure 2.2: aerial photo overlain with details of the main features of the site (white arrow indicates north). Top image shows path of the main drainage channel (Pwll Ddu) and the River Leri, as well as boundaries of the site and access points. The bottom image shows greater detail of cuttings in the south of the site as well as one of the small lakes which was dug as part of restoration efforts by CCW. Small map on left indicates position of the site in the UK. The letters in white (C, M and E) represent the sampling locations where banks of piezometers have been installed (referred to as Centre, Mid and Edge respectively). See Sections 2.2 and 2.3 for further details.

2.2 Sampling design and rationale

As stated in Chapter 1 Section 1.4, this study aimed to quantify and characterise both the bulk DOM pool (through measurements of DOC) and individual components of it (e.g. dissolved neutral sugars) over a range of locations, depths and spanning more than a full seasonal cycle. In order to capture more than a full seasonal cycle, water

samples were collected over 18 months at approximately three monthly intervals. In order to sample at different depths and locations, sites were identified where arrays or banks of piezometers could be installed from which water samples could be taken.

It was decided that the first location should be at the centre of the bog where the peat is at its deepest and where the peatland is in almost pristine condition. Due to the fragile nature of the peatland surface (which is susceptible to trampling) the Central piezometer bank was installed close enough to the boardwalk (indicated on Figure 2.2) that sampling could be carried out from this structure. Several short sections of boardwalk run perpendicular to the main path, and choosing an area of peat adjacent to one of these short sections minimised the risk of being disturbed during sampling. The location also benefitted from being far enough from other scientific work being carried out on the site (investigating methane emission rates and ebullition events at the site, Stamp, 2011) that neither study would be disturbed or influenced by the other. The peat at the Central location on the bog is >6.5 m deep and in order to sample to this depth a piezometer sampling at 6 m was installed. Further piezometers were installed at shallower depths, with higher resolution sampling around approximately the depth of the acrotelm/catotelm interchange and in less frequent sampling at >2 m depth below the peat surface (see Section 2.3 below for piezometer design and list of depths).

Modelling work carried out by Baird et al. (2006) has suggested that, from the Central site, the direction of subsurface lateral water movement is southwards, towards several long stretches of open water (lakes) running along the southern border of the site. Two further banks or arrays of piezometers were installed along a transect from the Central site to the lakes. The exact placement of these banks was influenced by access: the Mid-bog site (midway between the centre and edge) was again situated adjacent to a section of abandoned boardwalk, and the Edge bank was installed where a safe path could be found across the bog. The peat was shallower in both these locations, and so a 6 m piezometer could not be installed. Other than this, piezometers were installed at the same depths as the Central site (as detailed in

Section 2.3 below). Finally, samples were taken from the Lake near the Edge site. The main direction of water flow runs perpendicular to these long sections of open water, and so it was hoped that water samples from the Lake represent (to an extent) the water which is exported from the site. This will be discussed further in Chapter 3, Section 3.2.2.

2.3Sampling methods

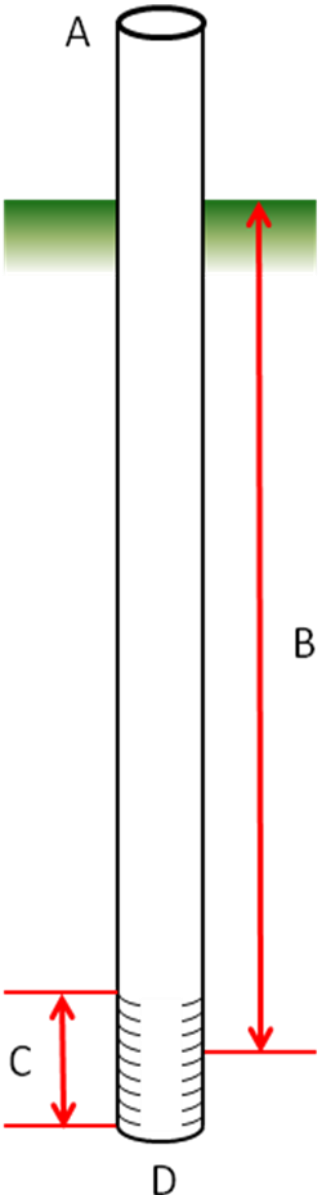

Samples were collected from three series of piezometers (nine at the central position, eight in the mid, and ten at the edge) which were installed as part of this study in the spring and summer of 2009.

Piezometers were made from high density polyethylene tubing with an internal diameter of 25 mm (van Walt UK Ltd.). The majority of the piezometer was enclosed, with a small section of the tubing near the base of the piezometer acting as the water inlet. The water inlet section of the tubing was 20 cm long in the majority of wells (30 cm for the deepest well) and consisted of two series of 30 mm horizontal slots, each slot being 0.3 mm wide, placed every 5 mm down the inlet tubing (van Walt UK Ltd.). Piezometers were capped between sampling visits and sealed at their base (see Figure 2.3).

Figure 2.3: Piezometer design for depths >50 cm; A) piezometers capped to minimise input of rainwater and particulate organic matter; B) depth given for piezometer sampling depth is the distance between the middle of the inlet section and the peat surface; C) water inlet section of 20 cm (30 cm in deepest (6 m) piezometer; D) piezometer closed at base.

Piezometers sampling depths of less than 50 cm were somewhat simpler in design, consisting only of high density polyethylene tubing with a gauze filter on the base to allow inflow of water. Before installation of piezometers, holes were created (using an extendable auger) in order to minimise compaction and entrainment of overlying peat material as piezometers were inserted into place. Piezometers were installed with a long plug inserted into them (consisting of a sealed length of tubing attached to string for ease of removal) in order that the force of pushing them into place did not break the seal at the base of the piezometer, and that they did not fill up with small particulate matter during installation. In order to sample from a range of depths, banks of piezometers were installed. Depths were chosen to sample around the acrotelm/catotelm boundary at higher resolution than at depth, with four piezometers sampling from the top 1 m of peat.

The central bank (Central site) of piezometers (Figure 2.4) was installed at the centre of the main dome, where the bog is in near-pristine condition. This bank of piezometers samples from depths of 6 m, 3 m, 2 m, 1.5 m, 1 m, 50 cm, 30 cm and 15 cm, and the piezometers are situated in a lawn-like area (the lower-lying topographical feature in the central part of the bog are mainly sphagnum-dominated lawns). All piezometers were placed 50 cm apart to minimise any groundwater interaction. The Mid site bank of piezometers was installed to the south of the Central site, in an area which has been impacted by water table management. These piezometers sample from depths of 3 m, 2 m, 1.5 m, 1 m, 50 cm, 30 cm and 15 cm. Drain blocking has raised the water table in this area, and subsequently the middle bank of piezometers sample from a more hollow-like feature. The final bank of piezometers was installed on the southern edge of the site, in an area which has been previously cut. These piezometers sample from depths of 3 m, 2 m, 1.5 m, 1 m, 50 cm, 30 cm and 15 cm, with depths from 50 cm to 15 cm duplicated to sample from two contrasting topographies which are typical of this area: a baulk, created by previous draining (resembling a natural hummock) and an area of old cutting (resembling a lawn). All piezometers were in place for over 3 months prior to sampling, in order to minimise any artefacts arising from the entrainment of oxygen with depth and any

resulting changes in redox conditions in the peat immediately surrounding the wells. An additional four pairs of shallow piezometers (15 and 30 cm) were installed within 10 m of the main Central piezometer array in order to obtain large sample sizes when required (e.g. for methods testing and FT-ICR-MS as detailed in Section 2.4.7).

Figure 2.4: Schematic of piezometers in central bank and photograph of central site taken during installation of sample wells (six deepest piezometers shown installed).

The three banks of piezometers lie roughly along a transect from the main dome to the edge of the bog. This transect coincides with a region of the bog on which hydrological modelling work has been carried out, as part of a previous project (Baird et al., 2006). Several series of auto-logging pressure transducers have been installed on this segment of the site over a number of years, and the data from these have been used to construct a hydrological model for the site (DigiBog).

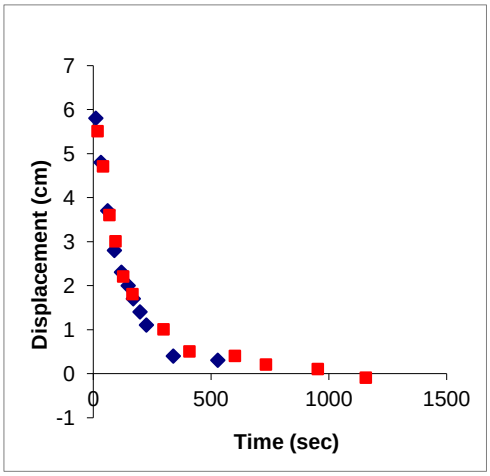

Figure 2.5: duplicate slug removal test results from central 2 m well.

The hydraulic conductivity of all sample wells ≥ 50 cm in depth was carried out using a slug-withdrawal test, following the procedure described by Baird et al. (2008). Slugs consisted of 15 cm lengths of sealed PVC tubing which had been filled with a ballast of sand. Water tables were measured prior to slug insertion, and allowed to return to this original level (± 5%) before the slugs were removed. On removal, the water level was measured as frequently as possible (~ 3 times per minute) during the initial rapid

recovery of the water table, and with lower frequency as the water level approached its initial height.

Water levels were measured manually by blowing through a piece of tubing inserted into the well; by listening for bubbling, it was possible to assess when the tip of the tubing was at the water surface, and by measuring the length of bubble tubing inserted into the well and the height of the piezometer tubing above the peat surface, a water level could be obtained.

Measurements were taken until the water table had recovered to at least 90% of the original displacement, or for 3 hours where recovery was very slow. Duplicate measurements (Figure 2.5) indicated reasonable reproducibility. Data obtained using the slug-withdrawal test was used to estimate K values for all wells using Hvorslev's (1951) equation:

$$K = -\frac{A}{Ft}\ln\left(\frac{h}{h_0}\right) \quad (2.1)$$

Where A is the inner cross-sectional area of the piezometer tubing, t is time at which head difference h is measured, and h_0 is the initial head difference and F is the shape factor for the piezometer intake. For the piezometer design used in this study, an F value of 55.59 cm was used. Baird et al. (2008) recommend that equation 2.1 be used when the water table is close to full recovery, i.e. where $h/h_0 < 0.05$. Timing constraints in the field and very slow recovery rates[a] in some wells meant that this was not always the case, and therefore the absolute values of the lowest K estimates must be regarded with caution.

[a] The slowest recovery (Edge site, 1 m depth) only reached 30% after 223 minutes.

2.3.1 Porewater sampling and preservation

On the day prior to water-sample collection, all piezometers were drained[b] so that sampling would be of freshly re-charged peat porewater. Water was pulled from piezometers via a syringe(with 7 m of Tygon PVC-based lab tubing attached), and immediately vacuum filtered through 0.7μm GFF filters (as a pre-filtration step) followed by filtration though a Whatman GMF 22 mm GD/X 0.45 μm syringe filter unit. These units are chemically inert, provide the standard pore size for DOC filtration, and allow easy filtration in the field. Water samples were then stored in pre acid-washed and fired 24 ml Wheaton glass sample vials (leaving no air in the vial) and sealed with a PTFE cap before being stored in an ice box for transport and subsequently at 4 °C in the dark.These sample containers were chosen as they were known to not introduce organic contaminants to samples and our lab has found no loss of DOC via adsorbtion onto the fired glass. Water samples were also taken from one of the small lakes on the southern edge of the site (figure 2.2) using the same protocol.

Acidification or freezing have been used in the past to preserve samples of DOM, but Spencer et al. (2007) found that both these preservation techniques had significant and variable effects on both the UV-visible and fluorescence excitation-emission matrix spectrophotometric properties of upland-derived DOM. Furthermore, when acidification of our samples was tested (using 200 μl 6N HCl per 24 ml vial of sample), there was easily visible precipitation/coagulation of organic matter within sample vials. In light of these facts, filtration and refrigeration in the dark were the only preservation techniques used in this study. Repeat DOC concentration measurements showed only a 3-4% variation over 6 months of storage (see Appendix A), which is within the error range of the analysis.

[b] The deepest Central piezometer, (6 m) had a higher hydraulic conductivity than all other piezometers, and subsequently could not be fully drained. In this case, in excess of two full well-volumes of water were removed prior to sampling.

2.3.2 Solid peat sampling, preparation and preservation

Peat cores were sampled in June 2010. Custom-built corers made from ~ 60 cm of plastic tubing (15 cm internal diameter) were used to extract cores of between 35 and 55 cm length of solid peat. In order to minimise compaction and water movement during coring, a cut a few centimetres deep was made into the peat surface (using a serrated knife and robust scissors) using the corer as a guide. The plastic corer was then pushed gently into the peat, and the solid material surrounding the corer was carefully dug out, creating a gap of a few inches around the core. This process was repeated, essentially digging the corer gently into the peat, until the corer was as deep as possible while still being extractable by hand (i.e. a full arm length deep). Excess peat from below the base of the corer was then used as a temporary plug while the core was quickly removed, then placed in strong plastic sacks, wrapped very tightly (removing all air) and securely fastened with strong tape. Tape wrapped around the entire base of the plastic sacking prevented drainage of water from the core. Cores were transported upright in a rack and stored where possible at 4°C until sectioning of the core material could be undertaken in Edinburgh.

Preparation of individual solid peat samples was carried out by first extruding the core from the coring tube using a custom built disc which was pushed through the tubing from below. As the core was extracted, it was sliced into 2 cm thick discs. A subsample from each disc of approximately 20 g was weighed out (avoiding the outer portions of the slice which had been in contact with plastics and may have contained peat material from shallower depthsentrained during coring), frozen, freeze dried and then weighed again in order to calculate the moisture content of each peat slice. Freeze dried samples were then ground to a fine homogenous powder using a centrifugal mill and stored frozen until analysis.

2.4 Chemical analysis of samples – overview and rationale

All water samples collected were analysed for DOC and TDN initially in order to quantify DOC concentrations across different locations and depths over more than a full annual cycle (the initial aim of this study, see Chapter 1, section 1.4). The next series of objectives focussed on obtaining quantitative and semi-quantitative molecular information to characterise the DOM pool using a sub-set of samples from different depths, seasons and locations.

Quantification of individual components which make up the amino acid, carbohydrate and phenolic compound pools requires complex, multi-step hydrolysis procedures and long detection development times, but the Organic Geochemistry group at University of Edinburgh have expertise at using these techniques on marine and solid peat samples. In addition, Geoff Abbott's group at Newcastle University has optimised a thermochemolysis gas chromatography mass spectrometry technique in the presence of tetramethyl ammonium hydroxide (TMAH) for the analysis of lipids and phenolic compounds in solid peat and organic rich soils. Finally, an opportunity was found (via a joint DAAD and British Council exchange) to analyse a small number of samples using a cutting edge ultrahigh resolution mass spectrometry technique, working with colleagues in the Alfred Wegener Institute for Polar and Marine Research (Bremerhaven, Germany) and Helmholtz Zentrum München (Neuherburg, Germany). See Table 2.2 for an overview of these samples.

This study aimed to combine these techniques and use them to investigate the OM found in the dissolved phase (see Chapter 1, Section 1.4 for study objectives). Not all samples could be analysed using all the techniques, for reasons of both cost and time; therefore, a subset of samples was selected to cover a range of seasons, depths and locations. The shallower samples from the Central piezometers bank samples taken from the Lake were prioritised from all seasons, as shallower regions of the peat may be affected more by seasonal changes in variables such as temperature and water table (with related changes in microbial and plant activity). The Central and Lake

locations were chosen for this seasonal focus as they best represent near-natural raised bog conditions and water exported from the peatland respectively.

Analysis	Sample required	Number of samples analysed	Comments
DOC/TDN	2 ml	154	All water samples analysed to dissolved organic carbon and total dissolved nitrogen
CN (elemental)	4 g	44	All solid samples analysed for carbon and nitrogen content
Dissolved combined amino acids	2 ml	84	18 individual amino acids quantified by hydrolysis – information on DOM source, microbial activity and carbon cycling
Solid amino acids	15 mg	22	18 individual amino acids quantified for comparison with dissolved phase
Carbohydrates (dissolved)	9 ml	43	8 neutral sugars quantified, poor recovery and many samples lost during analysis but entirely novel data set produced
Carbohydrates (solid)	25 mg	22	9 neutral sugars quantified for comparison with the dissolved phase
Phenolic compounds	250 mg	12	11 lignin proxies quantified for comparison with the dissolved phase
TMAH thermochemolysis	18 ml	53	Semi quantitative, novel approaches required to compensate for non-optimised instrumental set up, large suite of products indicative of lipids, phenolics and other sources
ESI-FT-ICR-MS	~250 ml	4	Cutting edge ultrahigh resolution mass spectrometry technique, generates thousands of molecular formulae from humic substances although no structural information. Novel visualisation techniques and analytical approaches used in this study

Table 2.2: Overview of analysis techniques, with sample volume or mass requirements, number of samples from which data was obtained and comments on the strengths and information gained. Rows in blue denote dissolves phase analyses, orange denote solid phase.

Depth profiles from all locations (Central, Mid-bog and Edge) were characterised from samples taken December 2009. See Figure 2.6 for a schematic of sampling locations, depths and seasons with details of analyses for each water sample.

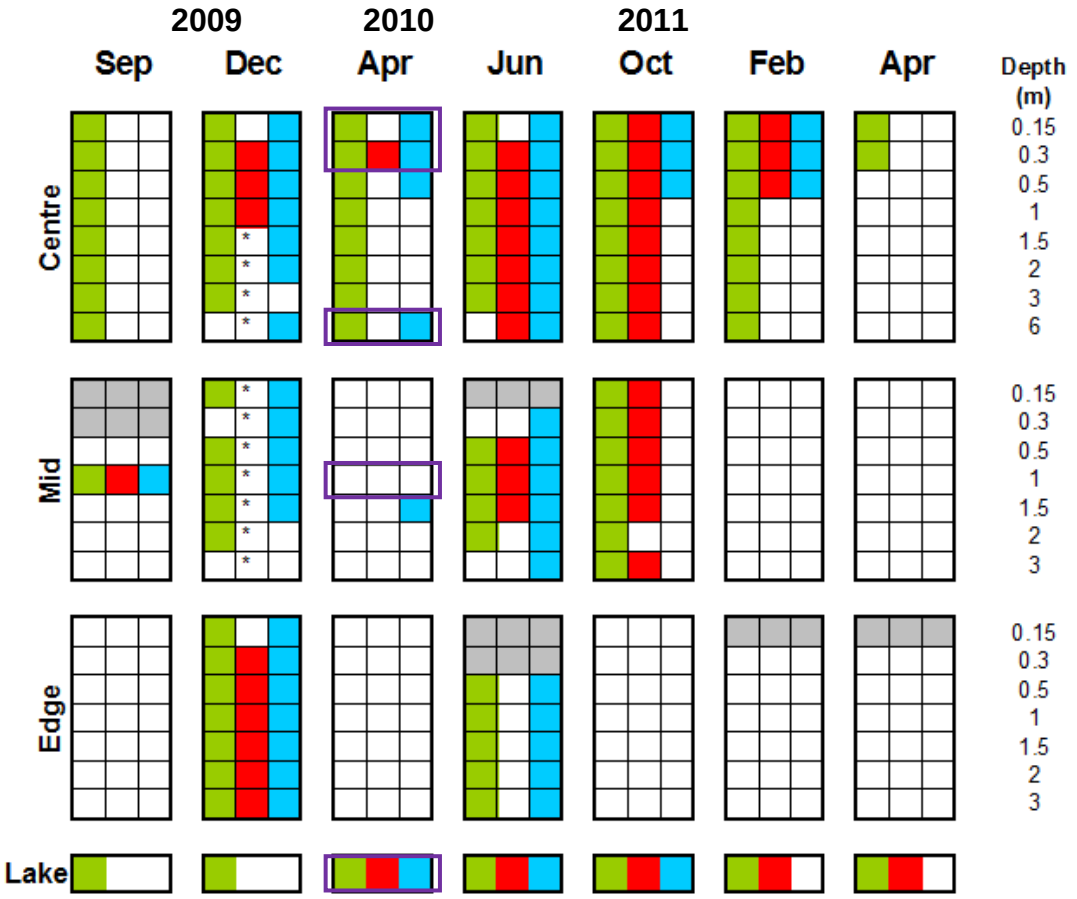

Figure 2.6: Schematic of all sampling depths (on right hand side) and occasions with which individual sample was used for each analysis. **Green** indicates DCAA, **Red** dissolved carbohydrates, **Light Blue** TMAH thermochemolysis. Grey boxes indicate no sample collected from this well on this occasion. **Purple boxes** indicate samples used for ESI-FT-ICR-MS analysis. * indicates those samples partly used during testing of an ultrafiltration technique which was subsequently found to introduce high blanks. As such, the remaining sample size was too small to obtain adequate recovery of dissolved carbohydrates.

Further depths samples were characterised from June 2011 and October 2011, although the full suite of data wasn't obtained for any one depth profile due to a combination of instrumental difficulties and poor recoveries (e.g. numerous samples were lost during TMAH analysis due to an instrumental error where injection onto the gas chromatography column failed, and one run of 24 samples analysed for dissolved carbohydrates resulted in very poor recoveries where only 11 samples were quantifiable). Due to sample size requirements, it was not possible to repeat TMAH thermochemolysis or dissolved carbohydrate analysis where samples were lost.

Although significant instrumental and analyticalproblems were encountered, Figure 2.6 shows that several profiles of depth, in different seasons and locations, were successfully analysed, if not for the full combination of techniques. Using the data set available, this combination of techniques it was possible compare the DOM pool against solid phase peat cores and use the information gained to assess the sources of peatland DOM and the molecular transformations or alterations this OM undergoes in different environments in the peatland.

2.4.1 CN analysis

Freeze dried solid peat samples (3-4 mg) were weighed into silver capsules. Samples were then treated with small aliquots of 6 N double distilled HCl until no bubbling was observed and left on a heating block at 150°C for 24 hours in order to remove any inorganic carbon prior to analysis (in practice a large excess of acid was likely to have been used as the inorganic content of core material was very low). Carbon and nitrogen elemental analysis was then carried out using a CE Instruments NA2500 Elemental Analyser.

2.4.2 Dissolved organic carbon (DOC) and total dissolved nitrogen (TDN)

DOC analysis of water samples was carried out within a week of sampling by high-temperature catalytic oxidation using a Shimadzu TOC-V instrument fitted with a non-dispersive infrared detector and TDN was analysed from the sample via an online total nitrogen module fitted with a chemiluminescence detector. Samples were diluted by a factor of 10 prior to analysis with milliQ grade ultrapure water (18.2 MΩ cm^{-1}) which had been passed through an online UV oxidation compartment (hereafter referred to as ultrapure water). Precision of the analysis was found to be very high (< 3% relative standard deviation, n=8) and therefore error bars are not routinely shown on DOC and TDN concentration results.

2.4.3 Carbohydrate analysis by strong acid/weak acid hydrolysis

Analysis was adapted from the methods of Cowie and Hedges (1984). For analysis of solid phase peat, approximately 25 mg of homogenised freeze-dried peat was weighed into 10 ml Pyrex tubes and wetted with 0.5 ml 12 M H_2SO_4. For analysis of porewater samples, 9 ml of sample was freeze-dried in Pyrex tubes to which 0.5 ml 12 M H_2SO_4 was then added.

The hydrolysis mixtures were then sealed with a Teflon lined cap and stirred with a magnetic stirrer for 1 hour (the strong acid hydrolysis stage). The mixture was then diluted to 1.2 M with ultrapure water and the mixture placed in a heating block at 120°C and stirred for a further hour before being transferred to an ice bath to halt the hydrolysis (weak acid hydrolysis stage).

100 µl adonitol was added as an internal standard with 100 µl glycerol solution (100 mg glycerol to 1 ml pyridine) and mixed thoroughly before being transferred to Teflon centrifuge tubes containing ~2 g strontium carbonate to neutralise the hydrolysate. The liquid phase was then separated via centrifuge (8000 rpm for 5 minutes) and passed sequentially through cation then anion exchange columns. These were then rinsed with 6 ml ultrapure water to ensure maximum recovery of samples. Analysis of blanks passed through columns after this rinse showed negligible concentrations of carbohydrates. The resulting solution was then dried in a vacuum centrifuge for 9 hours before being re-dissolved in a solution of 0.2% lithium perchlorate in pyridine (150 µl for dissolved phase samples, 300 µl for solid phase samples). The resulting solution was then heated to 60°C for 48 hours on an aluminium hotplate in order that the sugar isomers could reach equilibrium in the presence of the $LiClO_4$ catalyst. The trimethylsilyl derivatives of each sugar were formed by addition of bis(trimethylsily)trifluoroacetamide (BSTFA) and were analysed using an HP 5890 Series II single column gas chromatograph fitted with a 0.25mm fused silica capillary column using a split injection and a flame ionisation detector.

Individual sugars were quantified by comparing peak intensity relative to the response of the internal standard. Response factors and retention times were calculated from the analysis of mixed standards (placed in the sample run between every five samples). For those compounds which gave multiple peaks within a spectra, the quantified peaks (taken from Cowie and Hedges, 1984) were the 2nd arabinose peak, the 3rd xylose peak, the 2ndgalactose peak and the 2nd glucose peak (all other sugars only show one major peak in chromatograms).

Repeat analysis of samples showed that the reproducibility of the method was good during solid phase analysis (≤ 10% relative standard deviation for each individual peak, n=4) and the relative standard deviation of the total yield was < 5%. The precision decreased where yields were low (as was the case for the dissolved phase analysis), with substantially higher standard deviations for individual peaks (see Table 2.3). Ribose peaks were poorly resolved when yields were low, therefore ribose has not been considered when discussing the molar percentages of individual sugars in the dissolved phase.

	Standard deviation of repeat analysis of individual sugars and total yield (n=4)								
	Ara	Rha	Rib	Xyl	Fuc	Man	Gal	Glu	TCHO
Solid analysis	9.4%	9.5%	10.0%	4.1%	6.8%	8.8%	7.1%	4.1%	4.6%
Dissolved analysis	23.1%	8.5%	-	22.5%	6.1%	13.9%	14.6%	45.3%	15.0%

Table 2.3: The precision of the analysis for individual neutral sugars and total yield (TCHO) in both the solid and dissolved phases. Individual sugars: arabinose (Ara), rhamnose (Rha), ribose (Rib), xylose (Xyl), fucose (Fuc), mannose (Man), galactose (Gal) and glucose (Glu). The ribose peak was small and poorly resolved in the dissolved phase and will not be included in discussion of results.

It was hoped that, to compliment the above method, total dissolved mono- and polysaccharides could be ascertained by modifying the methods of Myklestad et al. (1997) who used a spectrophotometric method utilising the reagent 2,4,6-tripyridyl-*s*-triazine (TPTZ) to analyse seawater samples. However, after testing it was found that the relatively high reduced iron concentrations in our samples (compared to

seawater and drinking-water samples which have previously been analysed using the technique) introduced too high a matrix blank value for the method to give meaningful results.

2.4.4 Amino acid analysis

Analysis of solid peat material was carried out using an acid hydrolysis method adapted from Cowie and Hedges (1992). Analysis of dissolved combined amino acids was carried out using a vapour-phase hydrolysis method adapted from Tsugita et al. (1987).

2.4.4.1 Amino acid hydrolysis of solid peat

Approximately 15 mg of homogenised freeze-dried sample was weighed into pre-fired flame-sealable ampoules with 1 ml double distilled 6 N HCl that had been degassed with nitrogen. The ampoules were then flushed with argon, flame-sealed and placed in a heating block at 155 °C for 70 mins. The post-hydrolysis treatment and method was identical to that of the dissolved combined amino acids, which follows below.

2.4.4.2 Amino acid hydrolysis of DOM from water samples

2 ml of water sample was freeze dried within a small (3.5 ml) pre-fired glass sample tube. 3 ml of sample was used where DOC concentrations were found to be particularly low. This tube was then placed inside a larger Pyrex tube and kept from touching the walls of the larger tube by use of a Teflon ring. A 7.7 N acid mixture was made up by dissolving 10 mg phenol and 20 mg ascorbic acid into 1 ml trifluoroacetic acid (TFA), 6.5 ml 12 N HCl and 2.5 ml ultrapure water and then degassed with nitrogen. 200 µl of this acid mixture was carefully transferred to the

outer tube which was then flushed with argon and sealed with a Teflon-lined cap before being placed in a heating block at 165 °C for 60 minutes.

2.4.4.3 Amino acid hydrolysis analysis – quantification by high-performance liquid chromatography (HPLC)

For both the above amino acid analysismethods, after hydrolysis, three charge matched recovery standards (α-aminobutyric acid, hydroxylysine and fluorophenylalanine)were added in equal parts to the hydrolysed sample, and this mixture was then dried and stored frozen until analysis. For this, samples were taken back up into aqueous solution with ultrapure water using a sonic bath and vortex stirrer to maximise sample recovery. The pH was then adjusted to between 9 and 10.5 using ultrapure KOH and double distilled 6N HCl and filtered through 0.45 μm Whatman GMF filter units using fired glass syringes. The sample was then split where possible (with a reference sample being stored frozen) and analysed for individual amino acids using an HP 1100 series HPLC fitted with a C_{18} column, a chilled autosampler and programmable fluorescence detector (with an excitation wavelength of 330 nm and monitoring emissions at > 450 nm). Primary amines were derivatised online with an orthophthalaldehyde (OPA) solution (15 mg OPA, 2 drops of Brij 35 solution, 2 drops of mercaptoethanol and 500 μl methanol made up in 0.8 M boric acid pH adjusted to 10.5 with ultrapure KOH). A binary gradient between solvent A (a 35mmol sodium acetate solution with 5% tetrahydrofuran adjusted to pH 5.6) and solvent B (HPLC-grade methanol) was used, ramping from 10% B to 70% B over 30 minutes.

Individual amino acids were quantified relative to the charge matched recovery standards. The reproducibility of amino acid analysis was found to be good, where replicate analysis (n=4) showed a relative standard deviation of the total yield being 1.5% in the solid phase and 6.2% in the dissolved phase where signal strength was lower. On repeat analysis of the solid phase, the majority of individual sugars had

relative standard deviations less than 3%, and only threonine, γ-aminobutyric acid, methionine and ornithine hadhigher relative standard deviations (14.6%, 20.4%, 5.4% and 13.6% respectively) due in part to the low yields of these compounds.

Analysis of the dissolved phase required the use of much smaller sample sizes (~0.05 mgOC compared to ~7.5 mgOC in the solid phase) and thus the reproducibility understandably decreased; the relative standard deviations of individual amino acids rose to ~10% for the majority of amino acids, and was significantly higher for histidine, threonine, tyrosine, β-alanine, γ-aminobutyric acid and methionine (26.2%, 32.6%, 25.3%, 16.0%, 21.5% and 56.3% respectively). Where discussions do focus on these lower-yield amino acids, the uncertainties will be clearly outlined and averages of a number of samples used for the identification of trends.

2.4.5 Phenol analysis by CuO oxidation of solid peat

The CuO oxidation method was taken from Hedges & Ertel (1982) with modifications from Goni & Hedges (1992) and Opsahl & Benner (1995, 1997).In an oxygen free environment (flushed glove bag with flowing nitrogen atmosphere) 250 mg of homogeneous freeze dried peat sample was placed in a steel bomb with 100 mg $Fe(NH_4)_2(SO_4)_2.6H_2O$ and 1 g CuO. 8ml of 2 M NaOH was added and the bombs tightly sealed, then placed in a rotary oven at 155°C for 3 hours. Once cool, internal standards (cinnamic acid and ethylvanillin) were added, thoroughly mixed, and the reaction solution centrifuged at 8000 rpm for 5 minutes.

The supernatant was then decanted into Teflon centrifuge tubes, and a further two extractions with 8 ml 1 M NaOH were carried out on the remaining solid material in order to maximise sample recovery. The extract solution was then acidified to pH 1-2 with 6 N double distilled HCl and triple extracted with small aliquots of freshly distilled ethyl acetate. The centrifuge tubes were centrifuged at 7000 rpm for 3 minutes before carefully transferring the organicsolvent layer to pre-fired round

bottom flasks. Anhydrous sodium sulphate was added to samples as a drying agent, and solutions were passed through anhydrous sodium sulphate columns and collected in glass vials under a stream of argon. Dried samples were stored in pyridine and frozen until ready for analysis then re-dissolved in pyridine and derivatised with BSTFA prior to analysis using an HP 5890 series II dual column gas chromatograph.

No repeat-analysis data is available from the measurement of phenols in solid cores due to the time constraints of the undergraduate projects during which samples were analysed, and no tests of the method's precision have been carried out using the same instrumentation using similar samples. Opsahl & Benner (1995) found analytical precision to be between 5-15% using the same method and detection set up, with values towards the lower end of this range where abundances were high.

2.4.6 TMAH thermochemolysis and GC-MS of DOM

On-line thermally assisted hydrolysis and methylation (THM) in the presence of tetramethylammonium hydroxide (TMAH) and gas chromatography mass spectrometry (GC-MS) was carried out using the methods of Mason et al. (2009).

2.4.6.1 TMAH thermochemolysis sample preparation and GC-MS instrumental setup

18 ml of water sample was freeze-dried in acid washed, pre-fired and weighed 20 ml scintillation vials. This resulted in ~2 mg solid material which was calculated (from DOC concentrations of the original sample) to be ~30% organic carbon. ~1.5 mg of freeze dried material was weighed into quartz pyrolysis tubes plugged with pre-extracted silica wool. An internal standard, 5α-androstane, was added with 5 μl of aqueous TMAH solution (25%; w/w) immediately prior to analysis.

Analysis was performed on a Chemical Data Systems (CDS) 1000 pyroprobe unit fitted with a platinum coil and a CDS 1500 valved interface (320°C) with a Hewlett-Packard 6890GC split injector (320°C) linked to a Hewlett-Packard 5973MSD (electron voltage 70 eV, emission current 35 uA, source temperature 230°C, quadrupole temperature 150°C, multiplier voltage 2200V, interface temperature 320°C). The sample was placed in the platinum coil and sealed into the valved interface. The methylation/hydrolysis was carried out at 610°C for 10 seconds with the GC split open. Separation was performed on a fused silica capillary column (60 m,0.25 mm internal diameter). The GC was held at 50°C for 5 minutes and then the temperature programmed from 50°C to 320°C at 4°C min^{-1} and held atthe final temperature for 15 minutes, (total run time 95 minutes). Helium was used as the carrier gas (constant flow 1mlmin^{-1}, initial pressure of 110 kPa, split at 30 ml min^{-1}).Data acquisition was controlled by a HP kayakXA chemstation computer, in full scan mode (50-700 amu).

2.4.6.2 Quantification and co-eluting peaks from TMAH thermochemolysis

The instrumental set-up described above was developed for analysis of solid peat material and organic rich soil samples. The set-up was not optimised for analysis of freeze-dried DOM (which had not been previously attempted) and this caused challenges when attempting to quantify peaks from the resulting spectra. Therefore, two novel techniques were developed to estimate the contribution of co-eluting peaks and to provide a semi-quantitative comparison of peak areas between samples as described below.

Peaks were identified from the full scan mass spectrum (50-700 amu) of each peak, using ion fragmentation patterns and subsequent comparison to the NIST98 mass spectrum library, and to the relative retention times reported by other studies (i.e.

Frazier et al., 2003; Frazier et al., 2005; Templier et al., 2005). Where a peak could not be confidently identified, it has been left unlabelled.

In order to explore changes in composition between samples, a list of the dominantthermochemolysis productswas compiled (see Table 2.4). These cover the major products of the TMAH thermochemolysis, including 18 methoxy-benzenes, 8 alkylbenzenes, 8 phenols, 14 fatty acid methyl esters (FAMEs), 9 *n*-alkanes, 4 carbohydrate-related compounds, and 8 naphthalenes. Other minor thermochemolysis products which have been investigated in previous studies of NOM using TMAH thermochemolysis were also included on the list, where present in our samples. The list of key species was amended slightly for the interpretation of the mid-depth samples, as they contained a more varied array of compounds. The integrated area under each peak of interest was calculated, and these numbers used to quantify differences in the molecular composition of samples.

Quantified compounds		Continued…	
1,1'Biphenyl	2-methoxy-	Benzoic acid	3-methoxy-4-methyl-
Benzene	methoxy-	Acetophenone	4'-methoxy-
Benzene	1-methoxy-4-methyl-	Benzene	1,2,4-trimethoxy-
Benzoic acid ME		Benzoic acid ME	4-methoxy-
Benzene	1-ethyl-4-methoxy-	Benzene	1,3,5-trimethoxy-
Benzene	1,2-dimethoxy-	Ethanone	1-(3,4-dimethoxyphenyl)-
Benzene	1-ethenyl-4-methoxy-	Benzoic acid ME	3,4-dimethoxy-
Benzene	1,4-dimethoxy-	Ethanone	1-(3,4,5-trimethoxyphenyl)-
Benzene	1-ethenyl-4-methoxy-	2-Propenoic acid ME	3-(4-methoxyphenyl)-
Benzeneacetic acid ME	4-methoxy-	Benzoic acid ME	3,4,5-trimethoxy-
Benzoic acid ME	3,5-dimethoxy-	2-Propenoic acid ME	3-(3,4-dimethoxyphenyl)-
Styrene		Benzene	1,1'-(1-methylethylidene)bis[4-methoxy-
Benzene	ethyl-	Benzene	1,3,5-trimethyl-
Xylene		Benzene	1,2,3-trimethyl-
Benzene	1-ethyl-3-methyl-	Benzene	1-ethyl-2-methyl-
Phenol		Benzene	1-propynyl-
Phenol	2-methyl-	Phenol	4-ethyl-
Phenol	4-methyl-	Phenol	2,4,6-trimethyl-
Phenol	2,5-dimethyl-	Phenol	2,3,5-trimethyl-
Phenol	2,4-dimethyl-	2-cyclopenten-1-one	2,3-dimethyl-
2-cyclopenten-1-one	2-methyl-	2-Cyclopenten-1-one	2,3,4-trimethyl-
2-cyclopenten-1-one	3-methyl-	Nonanedioic acid di-ME	
Hexanoic acid ME		9-Hexadecanoic acid ME	
Butanedioic acid di-ME		Hexadecanoic acid ME	
Octanoic acid ME		9-Octadecenoic acid ME	
Nonanoic acid ME		8-Octadecenoic acid ME	
Decanoic acid ME		Octadecanoic acid ME	
Octanedioic acid di-ME		Tetracosanoic acid ME	
Dodecanoic acid ME		Hexacosanoic acid ME	
2-Octenoic acid ME		Octacosanoic acid ME	
Furancarboxylic acid ME		Tetradecanoate	methyl-
Ethanone	1-(2-furanyl)-	2-Decenoic acid ME	
2-Furancarboxaldehyde	5-methyl-	Furan	2,3,5-trimethyl-
1-Dodecene		Furfural	
Dodecane		Benzofuran	
2-Dodecene (Z)		Benzene	methylthio-
4-Dodecene (Z)		Benzofuran	2-methyl-
Eicosane		Cyclododecane	
Heneicosane		Naphthalene	
Docosane		Naphthalene	1-methyl-
Tricosane		Naphthalene	2-methyl-
Tetracosane		Naphthalene	2,7-dimethyl-
Pentacosane		Naphthalene	2,3-dimethyl-
Hexacosane		Naphthalene	1,8-dimethyl-
Heptacosane		Naphthalene	1,4,6-trimethyl-
Octacosane		Naphthalene	1,4,6-trimethyl-
1H-Isoindole-1,3(2H)-dione	2-methyl-	Prop-2-ene	2-(4-methoxyphenyl)-
Cyclooctane	1,2-dimethyl-	But-2-enoic acid ME	3-(4-methoxyphenyl)-
Sulphide	diphenyl-	But-3-enoic acid ME	3-(4-methoxyphenyl)-

Table 2.4: Peaks for which the integrated peak area from TMAH thermochemolysis total ion counts (TICs) was quantified.

Where compounds co-eluted but could still be confidently identified, a novel method for estimating the relative contribution of each compound to the TIC was developed.The integrated area of each of the co-eluting peaks in single ion mode was recorded (using the base ion for the compound in question). Because the integrated area of some compounds' peaks are dominated by thebase ion, whereas some will have a larger number of major ions contributing to the total ion count (TIC), a correction factor is needed in order to scale the base ion according to its contribution to the TIC. To achieve this, a mass spectrum for the compound in question was obtained from a sample in which it did not co-elute, and the relative contribution of the base ion to the TIC determined.

Subsequently, to assign anarea to each of the co-eluting peaks, the ratio of the corrected single ion peak areas was applied to the TIC integrated area; that is:

$$\text{Adjusted area A} = \text{Combined TIC area} \times [(SIC_A / CF_A) / ((SIC_A / CF_A) + (SIC_B / CF_B))] \quad (2.2)$$

Where compound A and B co-elute, SIA_A refers to the area under the corresponding peak in single ion mode where the m/z selected is that of the base ion for compound A, and $CF_A$is a correction factor which is the contribution of the base ion to the TIC of compound A.

An example calculation:

Figure 2.7 shows a portion of the TIC (black) and single ion counts (red for m/z 108, blue for m/z 74) to show a coeluting peak at 16.59 min from the analysis of a June 2010 sample from 150cm at the centre of the bog. The peak at m/z 74 is due to the presence of hexanioc acid ME, and the peak at m/z 108 results from methoxybenzene. The integrated peak area from the TIC is 3,732,457, at m/z=74 it is 407,168 and at m/z=108 it is 571,869.

The correction factor is calculated using a non-co-eluting peak from another sample. Figure 2.7shows the mass spectra for a hexanoic acid ME peak (from Oct 2010 Central site, 30cm) and methoxybenzene peak (from Jun 2010, Mid-bog site, 1.5m). The base peak'sintegrated areain single ion (74 amu) mode is 14,947 out of a total count of 44,791, therefore the m/z 74 ion accounts for 33.4% of the TIC. The same calculation for methoxybenzene gives a contribution to the TIC from the base peak (m/z 108) of 31.6%.

The assigned integrated area for hexanoic acid ME is calculated as follows:

3,732,457 x [(407,168 / 0.334) / ((571,869 / 0.316) + (407,168 / 0.334))] = 1,502,293

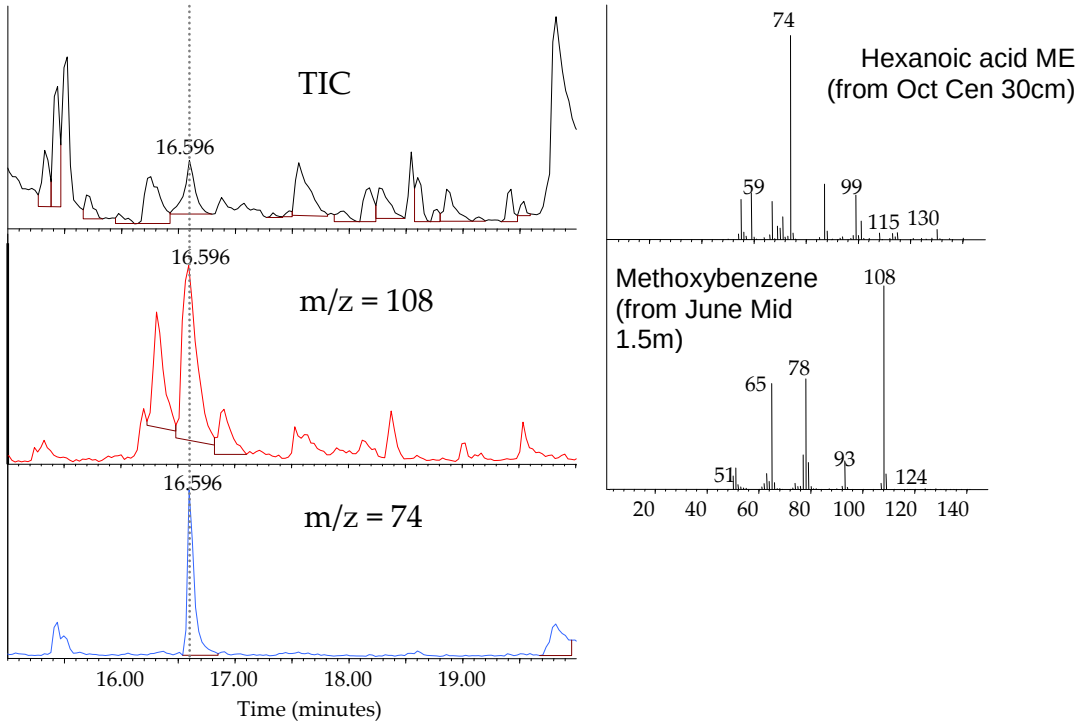

Figure 2.7. Total ion count (upper left) and single ion count at m/z 108 (red, middle left) and m/z 74 (blue, lower left) showing the peak at 16.59 min from Jun '10, Centre 150 cm sample to be a coelution of hexanoic acid ME and methoxybenzene, the mass spectra for which are shown on the right with sample label.

It was found that the fatty acid methyl esters (FAMEs) co-eluted in a large number of samples, but they can be easily identified in single ion mode (m/z 74). For this reason, in addition to being quantified using the method above, all saturated alkyl-

chain FAMES which were commonly found in samples (hexanoic-, octanoic-, nonanoic-, decanoic-, dodecanoic-, hexadecanoic-, octadecanoic and tetracosanoic acid methyl esters) were quantified in single ion mode. These data cannot be directly compared to the main data-set, but do provide a better comparison of how the composition (e.g. chain length) of FAMEs changes between samples.

A direct comparison of peak areas between samples may not represent differences between chemical compositions as the response of the analysis technique will be variable. Fully quantitative studies of natural organic matter (NOM) using TMAH thermochemolysis are difficult due to lack of standards (leading to uncertain response factors for some compounds) and differences in the chemical mechanisms involved in the hydrolysis and methylation, depending on the ratio of TMAH to certain functional groups within samples (Templier et al., 2005). Because of this, numerous studies only use a qualitative or semi-quantitative approach (e.g. Deport et al., 2006; Estournel-Pelardy et al., 2011; Fabbri & Helleur, 1999; Gallois et al., 2007; Guignard et al., 2005; Lehtonen et al., 2009; Mason et al., 2012; Peuravuori & Pihlaja, 2007; Swain et al., 2010; Templier et al., 2005). Our initial analytical approach involved the addition of an internal standard to samplesprior to analysis. Assuming a relative response factor of 1 for all peaks, this would allow quantification of peaks. The 5α-androstane standard should simply be volatised during the thermochemolysis run, and has been used successfully in previous studies (e.g. Abbott et al., 2013; Swain et al., 2010). Upon analysis of sample data however,it was found that, due to the non-optimal instrument set-up,the response of the 5α-androstane standard variedsignificantly and non-systematically between samples[c], and the signal in some samples was small enough that the internal standard peak could not be accurately quantified.

[c]relative standard deviation of peak area = 122%, the 5th highest relative standard deviation observed in peak areas of all quantified peaks.

In order to address this problem and make representative comparisons between chromatograms, a number of semi-quantitative approaches could be taken. Firstly, peak areas could be compared as percentages of the TIC for the entire chromatogram or all quantified peaks. Another approach would be to consider all peaks relative to the largest peak in the chromatogram. However, both these approaches have drawbacks, especially if samples vary considerably with regards dominant species present; changes in one major peak or compound class will affect the relative peak area of all samples.

When considering changes in peak areas *between samples*, all peaks can be compared to a referencing peak (e.g. the largest peak within a certain time-window, or a peak which has a stable response in all spectra), around which the variations in other peak areas can be anchored[d]. This peak must be one which a) shows little variation in signal between samples, b) does not co-elute with other peaks and c) has a high response in all samples. The average and standard deviation of the area of all quantified sample peaks was tabulated in order to find the best candidate to be used as this referencing peak. A xylene (1,4-dimethylbenzene) peak at 14.477 min was identified as both the peak with highest response across all samples and with the lowest variability between samples (relative standard deviation of 40%). Where relative peak areas are given in subsequent chapters, they will be as values relative to a peak height of 100 for this xylene referencing peak.

2.4.7 Electrospray ionisation Fourier transform ion cyclotron resonance mass spectrometry (ESI FT-ICR-MS) of DOM

Filtered water samples were acidified and extracted using PPL solid phase extraction (SPE) cartridges (1 g, Varian Mega Bond Elut) as follows. 0.1 ml ultrapure conc. HCl was added for each 100 ml of sample in fired and acid washed Pyrex sample bottles

[d] This approach is commonly used in the interpretation of FT-ICR-MS spectra, as in Chapter 6.

(~500 ml total was collected) in the field and then transported back to the laboratory in cool boxes with ice-packs in the dark (sample bottles wrapped in aluminium foil). SPE cartridges were rinsed with a cartridge volume of Hipersolv HPLC grade methanol then activated with two cartridge volumes of dilute HCl (pH 2 made up with 60 μl double distilled 6 N HCl in 75 ml ultrapure water) and mounted onto a stand. The acidified sample was agitated to ensure it was well mixed, then passed through a cartridge in small aliquots.

Once 100 ml of sample had been passed through it, the cartridge was washed with 2 volumes of the dilute HCl and then dried completely by gently passing nitrogen though it.The DOM sample was then eluted off the SPE material using 2 ml of Hipersolv HPLC grade methanol and collected in three 2 ml chromacolautosampler vials, the headspace of which was filled with nitrogen gas. These were then sealed with a PTFE backed silicon rubber cap and shipped to Helmholtz Zentrum München (Germany) for analysis.

Samples were analysed in 50:50 methanol/water with electrospray ionisation (ESI, Apollo II electrospray source) in negative mode (capillary voltage of 4 kV) at an infusion flow rate of 2 μl min^{-1} on an Apex Qe mass spectrometer (Bruker Daltronics Inc., Billerica USA) equipped with a 9.4 T superconducting magnet (Bruker Biospin, Wissembourg, France). Methanol blanks were run prior to analysis, and any large peaks from these blanks discounted from further analysis. Spectra were calibrated internally with mass peaks 339.10854, 369.11911, 411.12967 and 469.13515 which have been repeatedly found in NOM samples (e.g. Schmidt et al., 2009; Flerus et al., 2011; and Flerus et al., 2012). 512 scans were added to acquire one spectrum. The mass accuracy for internal calibration peaks was found to be below ± 0.05 ppm.

Peaks within mass spectra were assigned molecular formula for the m/z range 200 – 650. For each identified peak (signal to noise ratio, S/N, ≥ 5 as calculated using Data analysis 3.4, BrukerDaltronics) elemental formulae were calculated with a mass accuracy range of ± 0.5 ppm. The elemental composition of molecules was allowed to

range between the following $0 < C \leq 67$, $0 < H \leq 150$, $0 \leq O \leq 50$, $0 \leq N \leq 4$, $0 \leq S \leq 2$. The "nitrogen rule" was followed and O/C was limited to ≤ 1.2 (as Flerus et al., 2012).

Chapter 3: Dissolved organic carbon (DOC) dynamics with season and location, and an estimate of DOC loss from Cors Fochno

This chapter will focus on what can be ascertained about the peatland system from understanding how DOC concentrations vary, both temporally and spatially. The concentration of DOC and TDN were measured in all water samples taken. This information on the OC and N content of pore-waters, while simple, gives an insight into carbon cycling and dynamics in the peatland, and allows for further in-depth analysis to be targeted on key samples. Variations in DOC concentrations between different locations across the bog, and with depth in the peat profiles, may indicate accumulation or loss processes. Finally, understanding how DOC concentrations change seasonally, when incorporated with environmental data such as rainfall, allows for an estimate of the DOC loss from the entire peatland system.

3.1 Objectives and approaches taken

This chapter aims specifically to address the first objective given at the end of Chapter 1, Section 1.4:

- To quantify DOC concentrations across different locations and depths over more than a full annual cycle in order to ascertain how DOC concentrations change over both time and space, the heterogeneity of DOC concentrations with depth and location, and to gain an insight into controls upon the magnitude of this important carbon pool

In addition, a flux estimate for DOC export from Cors Fochno will be made.

In order to achieve this, data will be presented as depth profiles with season and location for visual comparison. Relationships between variables (e.g. groundwater temperature and DOC concentration) will be explored using regression analysis, (with R^2 and P values calculated from Excel data analysis add-on Analysis Toolpak).

The affect of water table fluctuations on DOC concentrations with several different memory effects will also be investigated by use of regression analysisin Section 3.3. These memory effects will be generated by combining different lag times (on the scale of weeks) with either net changes in water table height, or gross increases or decreases in water table height.

Finally, DOC concentrations in runoff waters throughout the year will be modelled using the relationships found, and this modelled DOC concentration, combined with an estimate for the water loss from the site (as belowground runoff), will be used to estimate the annual export of DOC from Cors Fochno. This modelling will be described fully in Section 3.4.

3.2DOC concentrations – variations with depth, location and season

DOC concentrations found in pore waters vary by exactly a factor of ten across all seasons and sites, the lowest concentration (11.4 mgC l^{-1}) being found at 6 m below the central site in April 2011, and the highest (114 mgC l^{-1}) at 1 m depth at the Mid-bog site, sampled in December 2009. The average concentration is 41.5 mgC l^{-1} and the median value is 39.9 mgC l^{-1}. The standard deviation of all values is 18.4 mgC l^{-1} (relative value of 44%).

Average concentrations of DOC in both the Mid and Edge sites are significantly higher (51 and 49 mgC l^{-1} respectively) compared to the average concentration at the Central site (26 mgCl^{-1}). The lower organic carbon content of the central waters is possibly due to the hydrology of the peatland and the proximity of the Central site to the main dome. Porewaters from the centre of the bog will be derived solely from precipitation (with little if any lateral movement through the peatland before reaching the sampling locations), whereas further towards the edges of the bog, water sampled will be a mixture of recent precipitation and porewater that has been flowing towards the bog-margin, accumulating carbon as it progresses. However, a simple accumulation process does not explain the overall trend in DOC

concentrations with location, as porewaters from the bog margin do not have the highest average DOC content[1].

When depth profiles are considered, it becomes clear that the high average DOC concentrations observed at the Mid-bog site are in part due to very high concentrations of OC at intermediate depth at this site. If only samples from the upper layers of the peat profile (approximately the acrotelm according to the diplotelmic model) are considered (≤50 cm), an accumulation mechanism for controls on DOC becomes more plausible, with average concentrations rising from 31 mgC l^{-1} at the Centre site, 35 mgC l^{-1} at the Mid-bog site, and 48 mgC l^{-1} at the Edge of the bog.

In September 2009 (the first month of sampling), a peak in the DOC content of porewaters sampled from the Mid-bog site is present at 1 m below the peat surface (97.7 mgC l^{-1} compared with a range from 30.3 to 74.8 mgC l^{-1} for the remaining samples), which was initially thought to be an outlier (Figure 3.1). In December 2009, this peak in DOC content becomes more pronounced (maximum concentration 114.0 mgC l^{-1}), and a similar phenomenon appears across the site, occurring at 1.5 m below the peat surface at the Centre of the bog, 1 m below at the Mid-bog site, and appearing at 50 cm at the Edge of the bog. In all subsequent months, there is a broad peak in DOC concentrations at intermediate-depth in the Mid-bog site, but this feature is absent from both Centre and Edge samples.

[1] This is somewhat complicated by possible changes in the residence time of water in the peat as it approaches the bog margin, where lateral flow rates are faster (e.g. Baird et al., 2008); as flow rates increase, water will spend less time per metre of peat along its flowpath, decreasing the amount of carbon that can be accumulated in the latter stages of the water's journey.

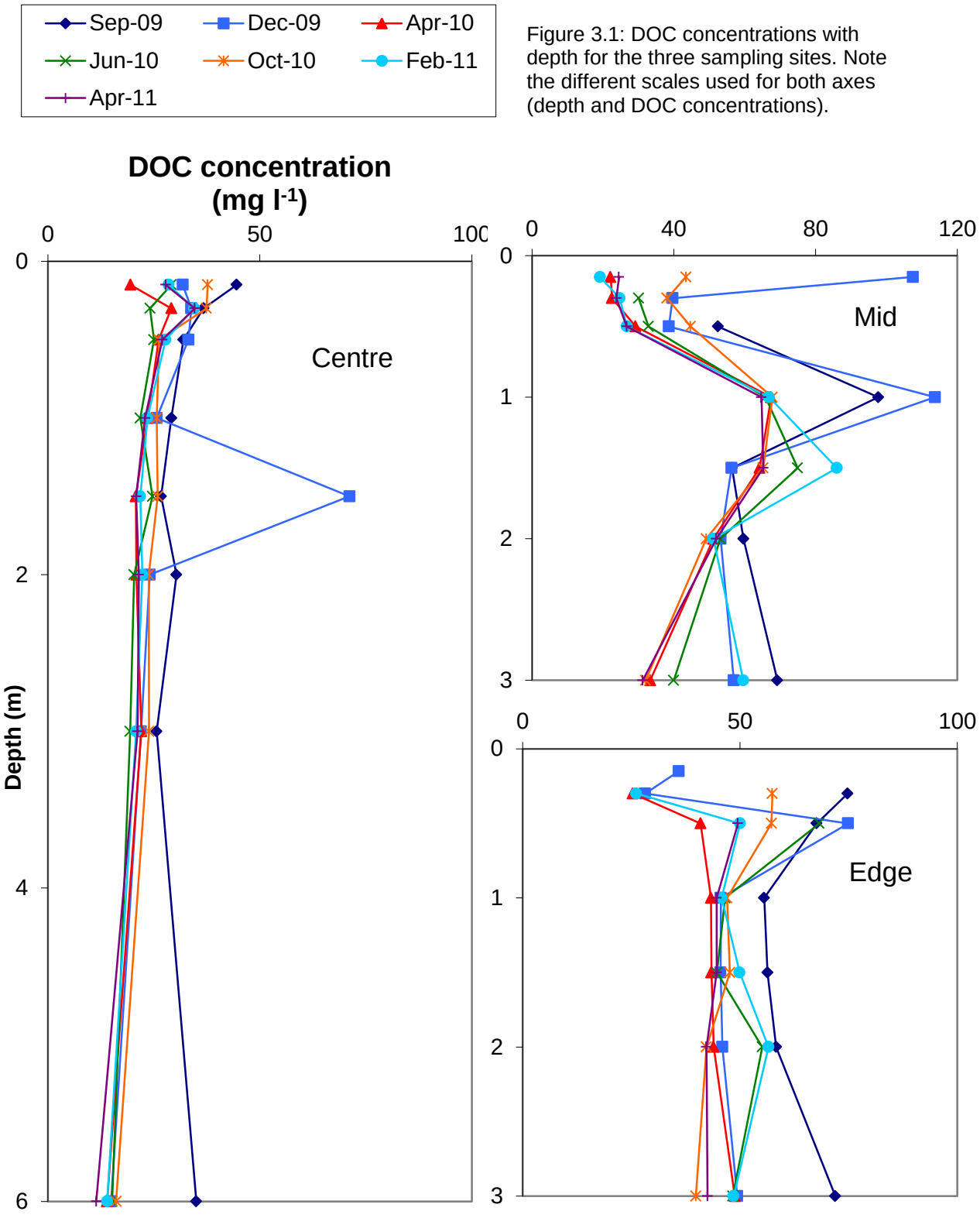

Figure 3.1: DOC concentrations with depth for the three sampling sites. Note the different scales used for both axes (depth and DOC concentrations).

The shape and size of this Mid-bog DOC peak changes seasonally, but maximum concentrations are always found at either 1 m or 1.5 m depth, and the peak is always

contained within a depth of 1-2 m, that is, depths of 50 cm and 3 m appear to be unaffected by this feature.

3.2.1 Other locations - Investigating those samples with high DOC concentrations

Concentrations of DOC were occasionally very high in water samples from intermediate-depth wells and, anecdotally, it was noted that these wells often recovered very slowly from piezometer drainage (carried out on the day before sampling as described in Chapter 2). In order to investigate whether there was a relationship between the hydraulic conductivity of wells and the average DOC content of their samples, slug-withdrawal tests were conducted on all wells of depth ≥ 50 cm and K values estimated. K values varied widely across sites and depths, spanning more than three orders of magnitude (Figure 3.2A). The highest hydraulic conductivity was found, somewhat surprisingly, from the deepest well, the 6 m piezometer from the Central site. After only 43 seconds, the well recorded 98% recovery, which resulted in an estimated K value of 0.00668 cm sec^{-1}. As noted in Chapter 2, it was not possible to test the most slowly-recovering wells to near full recovery, and therefore the absolute values of K estimates must be regarded with caution. For this reason, although repeat tests were carried out, no error bars are shown on Figure 3.2 so as not to mislead the reader.

Figure 3.2A shows the DOC concentrations of water samples taken from piezometers on the same sampling occasion as the slug tests were carried out (April 2011). The estimated K values for piezometers appeared to mirror the pattern presented in DOC concentrations with depth, with high DOC being (repeatedly) obtained from piezometers with low hydraulic conductivities.

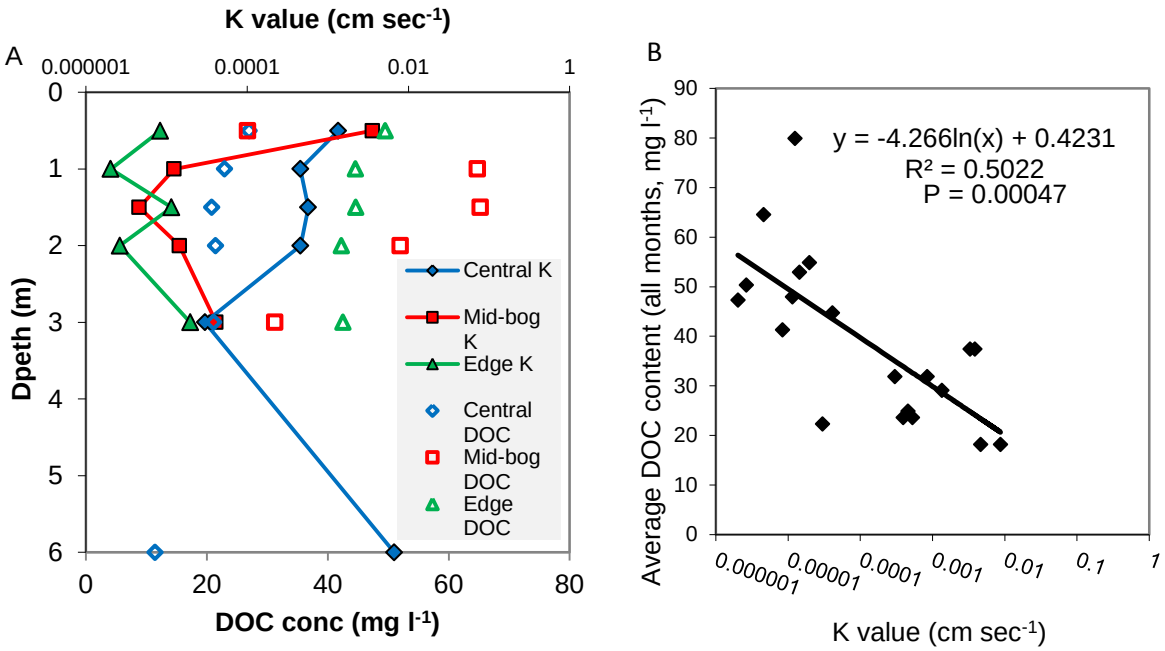

Figures 3.2A: (Left), estimated K values (mean values where multiple tests were performed on one piezometer) from slug-withdrawal tests for all three sites with depth (site by colour) and DOC concentrations from the same sampling period (April 2011) for reference; Figure 3.2B: (Right), average DOC concentrations (from all sampling seasons) plotted against estimated K values.

To explore this relationship, Figure 3.2B shows K value estimates plotted against the averaged DOC concentration from all sample wells (depth ≥ 50 cm), averaged over all 7 sampling periods. There is a statistically significant negative relationship between these two variables, with higher average DOC concentrations in those wells which have the lowest estimated hydraulic conductivity. It is possible that this relationship is due to differences in the origin of the sampled water (after draining piezometers the previous day) as follows:

- When water is drawn from a piezometer which is situated in peat of relatively high hydraulic conductivity, water is replaced quickly as water can move easily from the surrounding peat;
- When water is drawn from a piezometer which is situated in peat of relatively low hydraulic conductivity, water is only replaced very slowly, creating a pressure differential in the surrounding peat; this could then lead to water being extracted from small pore-spaces which may be essentially hydraulically isolated from the surrounding pore-waters under normal conditions. The water held in these small pores may have very long residence times, leading to unusual DOC dynamics. While others have noticed similar

effects (pers. Comm. A. Armstrong), to the author's knowledge, no published work has addressed or tested this theory.

3.2.2 Other locations: DOC concentrations at the Lake site

Water samples were also obtained from one of the lakes (Lake site) on the southern edge of the bog. These lakes provide an excellent opportunity to study the water which leaves the bog via both above-ground and below-ground runoff. The lakes extend in a line perpendicular to the flow of water (from the central dome to the surrounding drainage channels), and will thus intercept a mixture of all flows from this section of the bog, including any overland, sub-surface or deep run-off. Concentrations of DOC from the lake range from 14.0 to 34.4 mgC l^{-1} over the 7 sampling seasons with the highest values found in September 2009 and the lowest in December of the same year. In order to establish what mechanism might control the large scale DOC dynamics across the bog, comparisons of concentration data to water table and temperature were made.

3.3 DOC concentrations: comparison to water table and temperature

Logging pressure transducers (Schlumberger Mini Divers) have been deployed in dip-wells situated across the site for more than three years, and good coverage is available for the entirety of the sampling period of this study, although data from any one individual dip-well may not be continuous. The data from dip-wells were collated and adjusted for atmospheric pressure by R. Low (Rigare consultancy) who has been contracted by CCW who own the majority of the instruments. The loggers are stationed in over 10 locations over the bog, but as all logging stations on the site show similar trends in relative water table height, data from a single dip well will be considered. Logging station 3, situated close to the Mid bank of piezometers, was chosen for comparison with our data; data-coverage from this site was almost continuous for the duration of sampling, and the dip-well is in close proximity to the sites used in this study (see figure 3.3).

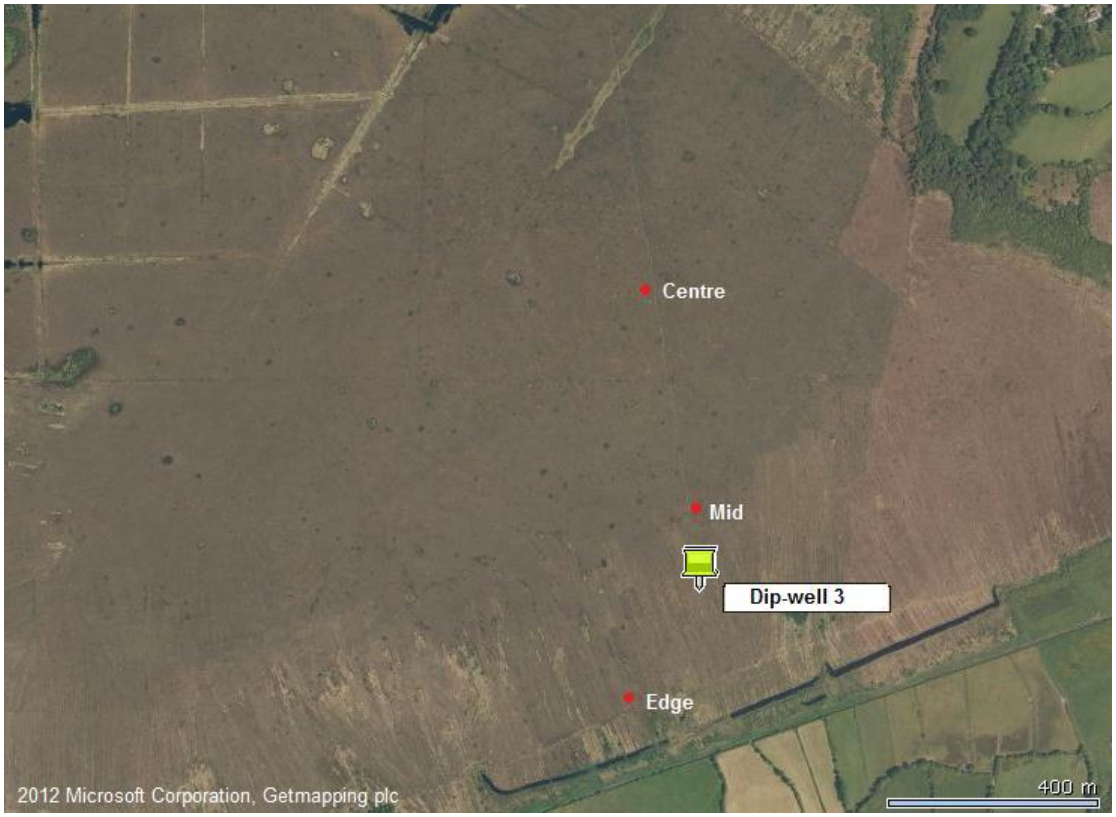

Figure 3.3: Location of dip-well three in relation to sample sites used in this study.

Figure 3.4 shows water table changes over a period of three years from March 2009 to March 2012. The dates on which the samples were obtained for this study are represented by vertical red lines and, for reference, the range of DOC concentrations found in near surface samples (15 cm and 30 cm) across the site are shown on these vertical lines – the yellow circle is the mean value for all shallow sites, with the red bars showing the range of values found. It should be noted that although only a small range of values were found in June 2010, this is because the majority of shallow piezometers were above the water table during this season, and this range is only from three samples. Figure 3.5 shows a similar plot, but with Lake concentrations indicated (green diamonds). The green lines are the results of a simple model which is discussed in Section 3.4.

The logging pressure transducer at dip-well 3 also logged water temperature in the dip-well continuously, and this provided the best available record of subsurface temperature. Comparison of average DOC concentration at the central site (15 cm

and 30 cm combined) against subsurface temperature at time of sampling shows a strong and statistically significant correlation ($R^2 = 0.7339$, $p < 0.02$, Figure 3.6). Comparison of the Lake concentrations with temperature shows only a weak correlation which is not statistically significant.

On initial inspection there appears to be little relationship between DOC concentration at central piezometers and water table height *at the time of sampling*. However, in order to adequately explore whether there is a relationship between water table measurements (two-hourly) and DOC concentrations (sporadic: ~three-monthly) some term to describe the recent history of water table changes is required. Three different terms have been considered: a) net change in water table height, b) summed water table increases, and c) summed water table decreases. Each of these terms was considered over 5 timescales, that is, the relationship between DOC concentrations and water table changes was explored with 5 different memory periods, namely 1, 2, 4, 6 and 8 weeks. This memory effect is utilised for water table height, which changes quickly, and so important recent changes could easily be missed on the day of sampling. The same was not considered necessary for temperature, as sub-surface temperatures change slowly, recording a seasonal signal rather than a daily or hourly one.

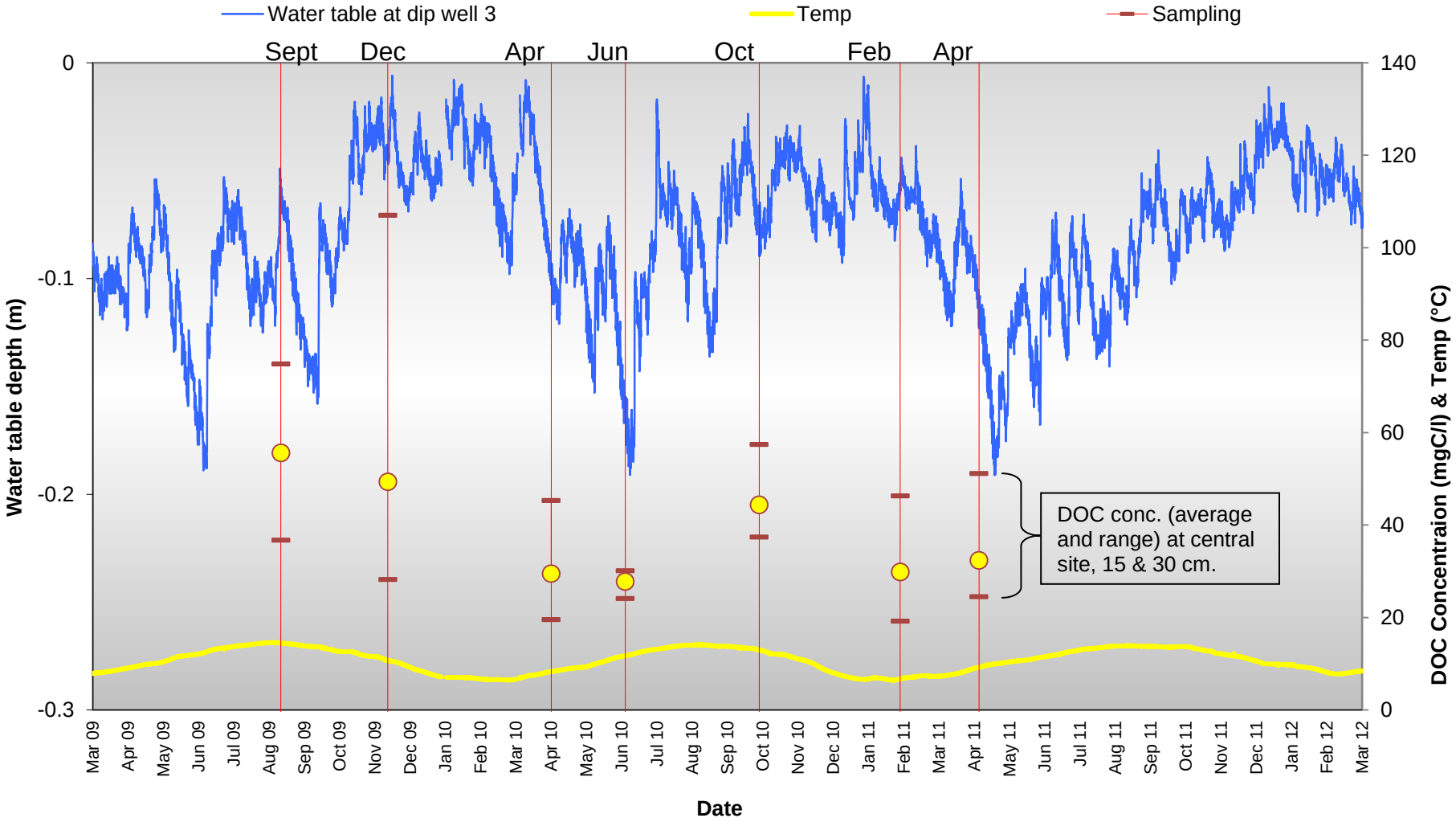

Figure 3.4: Water table depth over a three year period (blue) and water temperature (yellow) measured every two hours by logging pressure transducer at dip-well 3. Dates of water sampling denoted by vertical red lines. Yellow circles and dark red dashes on these lines represent the mean and range of values respectively of DOC concentrations from all shallow (15 & 30 cm) piezometers on that sampling date. See Chapter 4, Figure 4.7 for the same temperature measurements on a larger scale.

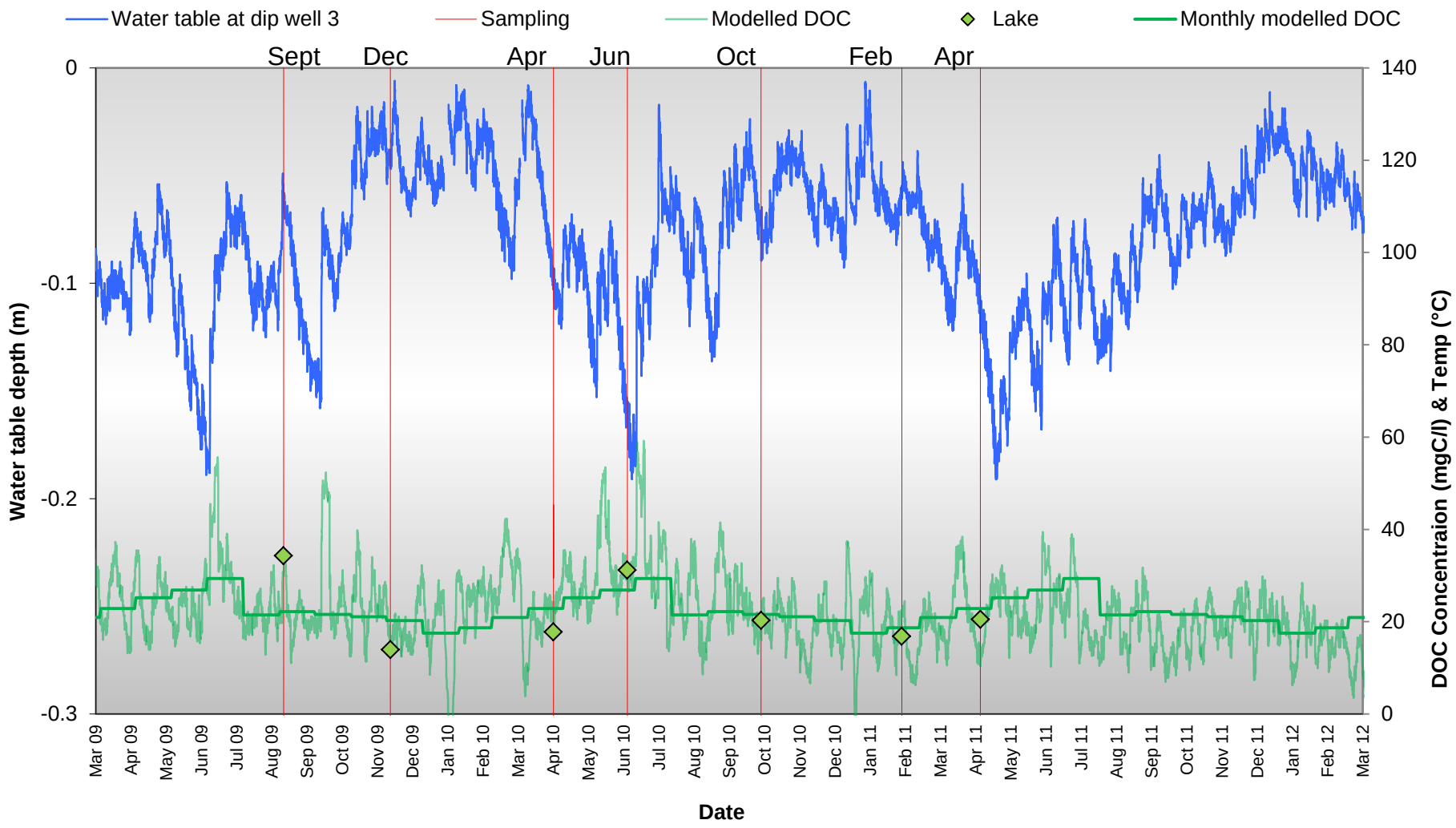

Figure 3.5: Water table depth over a three year period (blue) with sampling dates denoted by vertical red lines. Green diamonds represent Lake DOC concentrations. Light green line is modelled Lake DOC concentrations and solid green line is monthly averaged modelled Lake DOC concentrations used for flux estimate.

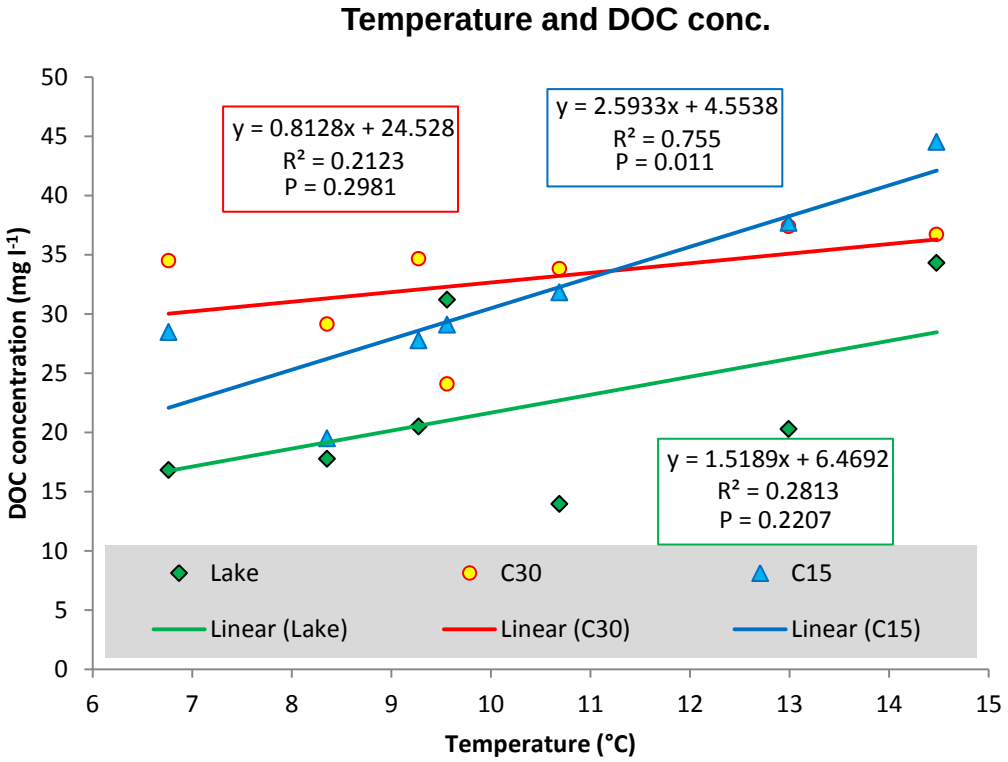

Figure 3.6: DOC concentration of Lake (green diamonds), Central 15 cm (C15 in blue) and 30 cm central piezometers (red with yellow fill), plotted against sub-surface temperature at time of sampling.

Running sums of net water table change were calculated for the 5 time periods (1, 2, 4, 6 and 8 weeks) and a value found for each of the 7 sampling dates. Running sums of water table increases and decreases were also calculated. In order to test whether there was some relationship between these terms and DOC concentrations, simple regression analysis was carried out, firstly against the concentration of DOC in the lake (which is semi-representative of runoff), and then in the 15 cm sample from the centre of the bog. Three examples of plots of these relationships are shown in Figure 3.7, and where significant relationships were found ($P < 0.05$) the equations, R^2 values and P values are presented in Table 3.1.

Plots of Lake DOC concentration versus water table fluctuations over time:

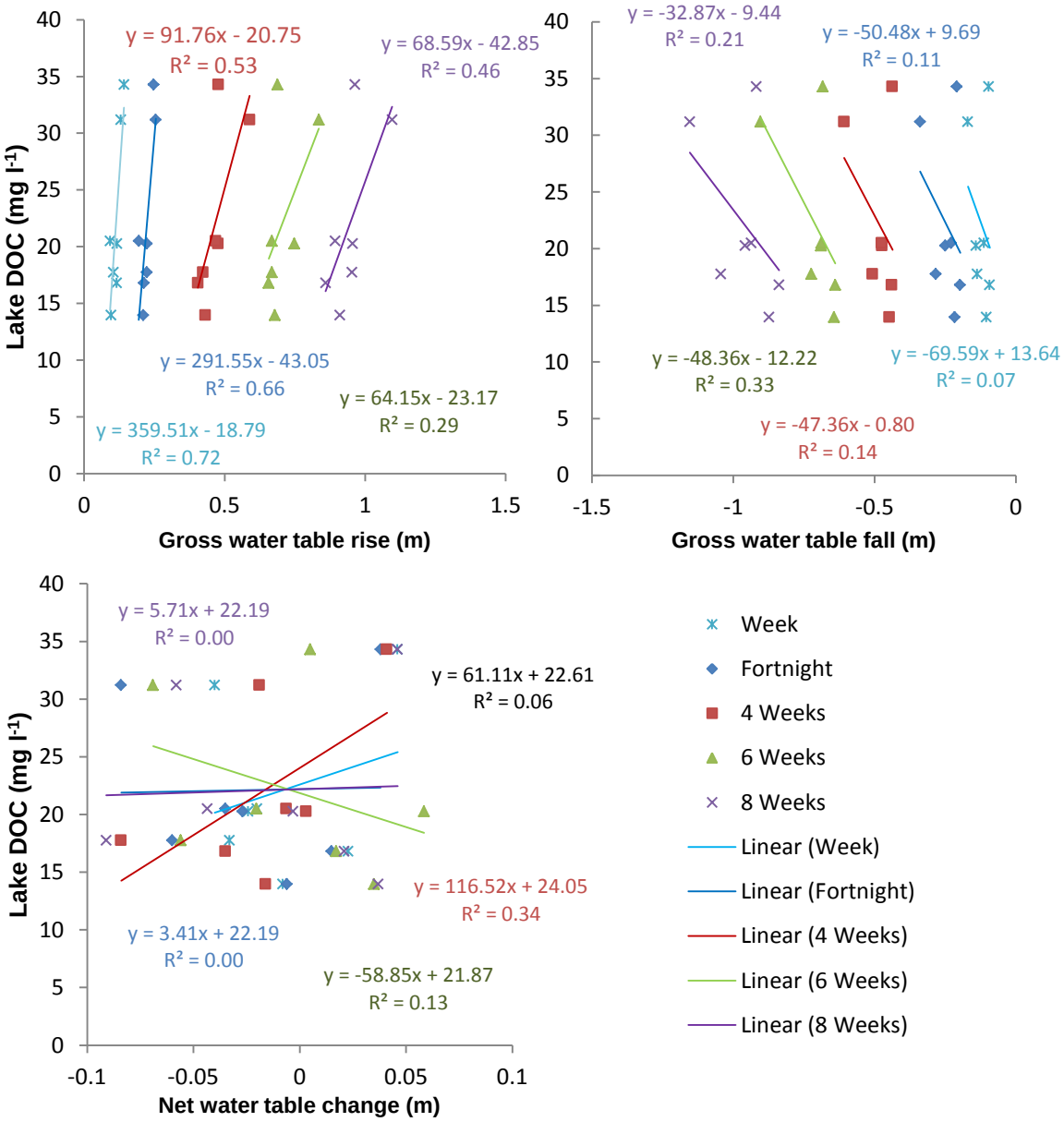

Figure 3.7:Plots of the relationship between Lake DOC concentrations and water table fluctuations, using a “memory” of one to eight weeks. Three water table-change terms were considered: gross water table rise (top left, where only increases in water table were summed), net water table change (bottom left, the sum of all 2 hourly changes over the memory period) and gross water table falls (top right, the difference between the two previous terms). Colour represents the length of time over which changes in water table were summed (5 per plot: 1, 2, 4, 6 and 8 weeks). Lines of best fit plotted by excel with the formula and R^2 value for each line given in the corresponding colour. NB: same y-axis for all plots.

		Weekly	Fortnightly	4-weekly	6-weekly	8-weekly
Lake	**Net**	ns	ns	ns	ns	ns
	Increase	y = 360x - 19 R^2 = 0.7166 P = 0.0163	y = 292x - 43 R^2= 0.6590 P = 0.0266	ns	ns	ns
	Decrease	ns	ns	ns	ns	ns
C15	**Net**	ns	ns	y = 196x + 35 R^2 = 0.8771 P = 0.0019	ns	y = 117x + 33 R^2 = 0.5842 P = 0.0454
	Increase	ns	ns	ns	ns	ns
	Decrease	ns	ns	ns	ns	ns

Table 3.1: Results of regression analysis ofDOC concentrations from two sample locations (Lake and Central 15 cm piezometer) against the water table change over previous weeks for each of the seven sampling occasions. Three scenarios were considered: one where [DOC] is related to the net change in water table (all changes were summed), one where changes are related to the gross water table increase (the sum of all positive changes) and finally where [DOC] is related to gross decreases (the difference between the previous two terms). Five timescales over which these values were summed were used, those being 1, 2, 4, 6 and 8 weeks. Only relationships with a P value < 0.05 are shown (ns indicates no significant relationship found). For all regressions, n = 7.

Despite the caveats involved with inferring seasonal mechanisms from only seven sampling periods, two relationships were found to be statistically significant:

- that between the Lake water sample DOC concentrations and gross increases in water table height,
- and the relationships between DOC concentrations from water samples taken from 15 cm at the Central site and net changes in water table height.

Lake DOC concentrations were related most strongly (P = 0.0163) to increases in water table over the previous week, although there is also a significant relationship with increases over the previous fortnight (Table 3.1). The relationship between DOC concentrations in water samples from the 15 cm Central piezometer and net changes in water table is most significant (P = 0.0019) when changes over the previous four weeks are summed, although a statistically significant relationship is also found over 8 weeks.

The positive relationship between DOC concentrations at 15 cm and net water table change is somewhat counterintuitive; Blodau et al. (2004) carried out a mesocosm experiment using intact cores from two ombrotrophic bogs and found that DOC net production was independent of water table level (at 14-15 mmol m^{-2} d^{-1}), and if DOC production is relatively constant over the timescales considered here (i.e. < 4 weeks), addition of water via rainfall (thus a net increase in water table level) might be expected to dilute near-surface waters, lowering their DOC concentration. This is evidently not the case, which may be due to production of DOC above the 15 cm depth at which porewaters are sampled (Blodau et al., 2004), which is then delivered to this depth by rainfall.

3.4 An estimation of a DOC flux term for Cors Fochno

In order to put the results from this study into a wider context, it would be useful to obtain an estimate of the flux of organic carbon lost from Cors Fochno via runoff. Although this study was not set up in such a way as to fully address this question, this is the first time measurements of seasonal DOC concentrations have been taken from the site. As such, it is thought that a conservative estimate of this flux would be a valuable addition to current knowledge of the site and, where appropriate, information from nearby locations and similar environments can be used to fill in any gaps in the calculation, albeit with clear identification of the caveats involved.

A number of methods could be used to estimate DOC losses from Cors Fochno. One possible method for measuring the flux would be to measure the concentration of DOC and flow rates in runoff channels with as high a frequency as possible. This approach was not feasible for this study, given that the bog only contributes a proportion to the Pwll Ddu (with runoff from surrounding hillsides), and that the logistics of sampling a remote site with high enough resolution were unfeasible. Instead, an estimate of the DOC flux has been made by calculating the net rainfall for the bog and multiplying this by the likely DOC concentration of this water as it leaves the site. There are several assumptions made during this calculation, which will be detailed at the end of this section. Because a *conservative* estimate is preferable

(i.e. the DOC flux will be *at least* this significant), any estimates used, where a range of values could be chosen, will minimise net rainfall and DOC concentrations.

Firstly, the net rainfall for the site was calculated. Average rainfall for the site (calculated from continuous measurements from 1981 to 2006 inclusive) is 122.1 cm yr^{-1} and, although evapotranspiration rates are not available directly from the site, pan evaporation data is available from nearby Plas Gogerddan[2] covering April to October, 1968 to 1991 (data courtesy of Mike Bailey, CCW). The average pan evaporation rate (60 cm yr^{-1}) is used for the flux estimate because, although higher evaporative losses may be expected during dry years, evapotranspiration rates will be low during the winter, and the use of average April-October rates throughout the year will compensate for this (maintaining the conservative approach). Actual evaporation rates from peatlands are known to be lower than pan evaporation rates (due to factors such as the water-holding capacity of sphagnum). A factor of 50 to 70% has been suggested (Ingram, 1983) to convert measured pan-rates to more realistic values, agreeing well with other studies of water budgets and movement in raised bogs (e.g. Waddington and Roulet, 1997). In order to arrive at a conservative flux estimate, a conversion factor of 0.7 was used, resulting in an evaporation rate of 42 cm yr^{-1} (35 mm $month^{-1}$). Assuming no net change in the water storage of the bog, this resulted in a net rainfall of 80.14 cm yr^{-1} (or 5.2×10^9 l yr^{-1} over the 650 ha site, monthly values in Table 3.2).

The DOC content of any water leaving the site will be dependent on source and flow history, but the best estimate of this is the concentration found in the Lakes near the southern edge of the bog. These will be a mixture of any water flowing towards the southern margin of the site (into the Pwll Ddu) and therefore give the most representative estimate of surface and deep water movement, weighted according to actual flow velocity. Modelling work carried out at Cors Fochno (Baird et al., 2006) has suggested that between 8 – 9.5% of net rainfall in this section of the bog is lost

[2]Situated 8 km south of Cors Fochno, this is a research station run by Institute of Grassland and Environmental Research, and assumed to similar potential evaporation to Cors Fochno (~ 30 m OD)

though water movement in the catotelm, which may bypass the lakes, but any water lost this way will have higher DOC concentrations than are used during the flux estimates, (minimum DOC concentration at depths > 50 cm at Edge of bog were 39.8 mgC l^{-1}) and so the inclusion of this flow would increase the resulting DOC flux. Above-ground runoff was not observed during any sampling period for this part of the bog, agreeing with Waddington and Roulet (1997) who found that overland flow is minimal in raised bogs due to the microtopographical features present.
Although an average Lake DOC concentration could be used for the calculation, the strong relationship between water table fluctuations and Lake DOC (see Table 3.1) allows for the DOC at any point in time to be modelled using water-table data. The DOC concentration was estimated at two-hourly intervals from weekly sums of water table gross increases using Equation 3.1, and a monthly average for these estimates found (light green and solid green lines respectively in Figure 3.5).

$$[DOC]_{(mgC\ l^{-1})} = (359.51_{(mgC\ l^{-1}\ m^{-1})} \times GWWTI_{(m)}) - 18.794_{(mgC\ l^{-1})} \quad (3.1)$$

(GWWTI = gross weekly water table increase)

These monthly averages do not deviate significantly from the average DOC concentration across all sampling periods, and offer a crude estimate of the DOC concentration, despite the simplicity of the model used. The final results of this flux estimate are given in Table 3.2. The flux is given in monthly intervals, although the rainfall figures used are the average values for 1981- 2006 (reliable rainfall data for the study period was not available).

The total flux of 17.4gC m^{-2} $yr^{-1}$is comparable with flux estimates from other studies from raised bogs (16.2 gC m^{-2} yr^{-1}, Blodau et al., 2007) and is not dissimilar from figures reported from other northern peatlands [4.2 gC m^{-2} yr^{-1} (dry year) and 11.3 gC m^{-2} yr^{-1} (wet year), Jager et al., 2009; 7-15 gC m^{-2} yr^{-1},*Scott et al., 1998*; 6-8.5 gC m^{-2} yr^{-1}, *Tegen& Dorr, 1996*; 13-26 gC m^{-2} yr^{-1}, *Tipping et al., 1998*(references in italics from Scott et al., 2001)]. The flux is around half that found (30.4 gC m^{-2} yr^{-1}total OC) by Billett et al. (2007) in drainage water from a small Scottish raised bog, although the authors did note that organic carbon content in Black Burn was high,this flux includes POC.

Month	Modelled [DOC] (mgC l^{-1})	Ave rainfall (mm)	Evaporation (mm)	Net rainfall (mm)	DOC loss (tonnes)
Jan	17.53	104.8	35	69.8	8.0
Feb	18.71	88.6	35	53.6	6.5
Mar	20.90	98.0	35	63.0	8.6
Apr	22.88	74.9	35	39.9	5.9
May	25.22	65.6	35	30.6	5.0
Jun	26.87	80.8	35	45.8	8.0
Jul	29.35	79.7	35	44.7	8.5
Aug	21.46	103.3	35	68.3	9.5
Sep	22.19	107.5	35	72.5	10.5
Oct	21.58	149.9	35	114.9	16.1
Nov	21.06	135.2	35	100.2	13.7
Dec	20.27	133.1	35	98.1	12.9
				Total (Tonnes)	**113.2**
				Total (gC $m^{-2}yr^{-1}$)	**17.42**

Table 3.2: Results from simple DOC flux estimate from Cors Fochno. The total is thought to be a conservative estimate, see text for details.

The modelled monthly flux of DOC indicates a higher delivery of OC during the autumn and a low delivery in spring. It has been reported that in an average year, DOC export at Mer Bleu (a raised bog) is highest in the summer and lowest in the winter (Blodau et al., 2007), which agrees with previous studies (e.g. Waddington & Roulet, 1997from a boreal peatland). In wet years this is not the case, and DOC fluxes decrease over the summer months. While these differences are interesting to note, the coarseness of the flux estimate detailed above does not allow confident comparison of data sets. If a simpler approach is taken and the average lake concentration is multiplied by average annual net rainfall, a value of 116.3 tonnes C or 17.9 gC m^{-2} yr^{-1} is obtained. To put this carbon flux value in context, estimated losses of carbon via DOC in runoff fall within the range of recently estimated values for methane losses from CorsFochno (2.3 – 52 gCm^{-2} yr^{-1}, Stamp, 2011 – no other estimates of components of the carbon cycle at this site have been made) and are comparable to estimated accumulation rates of ~20-25 gCm^{-2} yr^{-1} for northern peatlands (Moore et al., 1998; Turunen et al., 2002). There are a number of caveats involved in the DOC flux estimate above, which must be borne in mind:

- Although sampling was carried out over several seasons, no large storm events were sampled[3];
- No reliable rainfall data was available for the sampling period of this study, and therefore average rainfall (1981 - 2006) data is used with average concentration data from a different period (2009-2011);
- The southern transect of the bog which drains into the lakes is assumed to be representative of the entire bog;
- It is assumed that Lake DOC content represents a minimum value for all runoff.

A sensitivity analysis of the estimates used in the above estimates has been carried out and is presented in Appendix B. The estimation term with the strongest effect on the final total was annual rainfall. Using minimum or maximum estimates for all other terms combined increased the total calculated flux by +41%. See Appendix B for further details.

3.5 Conclusions

DOC concentrations vary by an order of magnitude between porewater samples, with generally low concentrations at the Central site and higher concentrations towards the edge of the bog. DOC levels were most variable with season in shallow porewaters, and were very high in intermediate depth (1-2 m) samples from the Mid-bog site.

It was found that, at depth, the average DOC concentration across all sample seasons was related to the hydraulic conductivity of the peat from which the well sampled; although the strength of the relationship was only moderate (explaining ~50% of variation between samples), it was statistically significant. DOC concentrations at15 cm below the peat surface at the Central site were significantly and positively related

[3] This may not be too significant, as studies have shown that it is less important to accurately estimate DOC losses during storm events for peatlands than for other systems (Clark et al., 2007 and references therein)

to temperature at the time of sampling. The best relationship found between DOC concentrations in the Lake sample (representative of runoff) and environmental factors was the gross increase in water table over the previous seven days, which is indicative of large amounts of rainfall. This relationship was both strong (explaining 72% of variance between samples) and statistically significant ($p < 0.02$), and was used with two-hourly data from logging pressure transducers to estimate DOC concentrations in runoff over a full seasonal cycle.

As an estimate of runoff concentrations was available, a net rainfall term (from average monthly rainfall and an estimated evapotranspiration term)was used to construct a DOC flux estimate for Cors Fochno. Despite uncertainties involved in the calculation, the estimated annual flux of 17.4 gC m^{-2} provides a useful starting point for the contextualisation of this study. The annual output of DOC from Cors Fochno into local waterways and groundwater is significant (113.2 tonnes) and, due to the proximity of the peatland to the Dyfi estuary, much of this organic matter may be delivered quickly to the marine environment.

In order to characterise the DOM pool across the peatland, several key samples will be focussed on in the next three results chapters. Firstly, to investigate what molecular changes occur with depth, samples from all depths at the Central site (the deepest) will be characterised. Those samples which have very high DOC concentrations from intermediate depth at the Mid-bog site will also be characterised, to try to ascertain the composition and source of this DOC signal. To investigate how the composition of DOC changes seasonally, a small subset of porewaters at shallow depths (15 and 30 cm at the Central site) from all sampling seasons will be characterised. Finally, characterisation of waters from the Lake site will allow an insight into what organic compounds the DOC lost to the Pwll Ddu is comprised of, and may also indicate what transformations occur when peatland-derived DOM is exposed to light, oxygen and a different microbial community on entering an open water body.

Chapter 4: molecular characterisation of porewater dissolved organic matter from Cors Fochno

4.1 Introduction to molecular characterisation in peatlands

Sphagnum species have long been known to act as ecosystem engineers, contributing through both their physical form and unique chemistry to an environment in which they out-compete other plant types and limit microbial activity to the extent that metres of dead plant material can accumulate as peat bogs (Verhoeven & Liefveld, 1997 and references therein). Phenolic compounds play a major role in these functions, creating three-dimensional polymeric networks of sphagnum acid and structurally-similar phenylpropane-based compounds which are associated with the plant cell walls (although some smaller compounds are actively excreted, Rasmussen et al., 1995). Functionally, these molecular networks lend structural protection against microbial attack (Tsuneda et al., 2001), as well as contributing to the water-holding capacity of *Sphagnum*. Simpler polymeric phenolics, particularly trihydroxy benzenes and gallic acid, have been found in water in which *Sphagnum* samples have been cultured, and it is thought that these may be the building blocks of hydrolysable tannins, which may have the same cellulose-masking role that lignin does in higher plants (Verhoeven & Liefveld, 1997). Monomeric phenols are slowly released during plant decay, as the three dimensional polymeric phenol network breaks down to its component monomers (e.g. sphagnum acid) and tannin-like structures, and when, in the dissolved phase, have been linked to enzyme binding (Verhoeven & Liefveld, 1997).

Previous studies into the biochemistry of *Sphagnum* species have found sphagnum acid ([Z]-3-(4'-hydroxyphenyl)-pent-2en-1,5-dicarboxylic acid) to be the most significant phenol produced (Verhoeven & Liefveld, 1997 and references therein),along with its peroxidative degradation product, 2,5-dihydro-5-hydroxy-4-(4'-hydroxyphenyl)-furan-2-one (hereafter referred to as hydroxybutenolide). Other significant phenols found by previous studies include *p*-hydroxyacetophenone, *p*-

hydroxybenzaldehyde, *p*-hydroxybenzoic acid, vanillic acid, ferrulic acid *p*-coumaric acid and *t*-cinnamic acid, (Rasmussen et al., 1995; Rudolph & Engmann, 1967), the structures for which are shown in figure 4.1

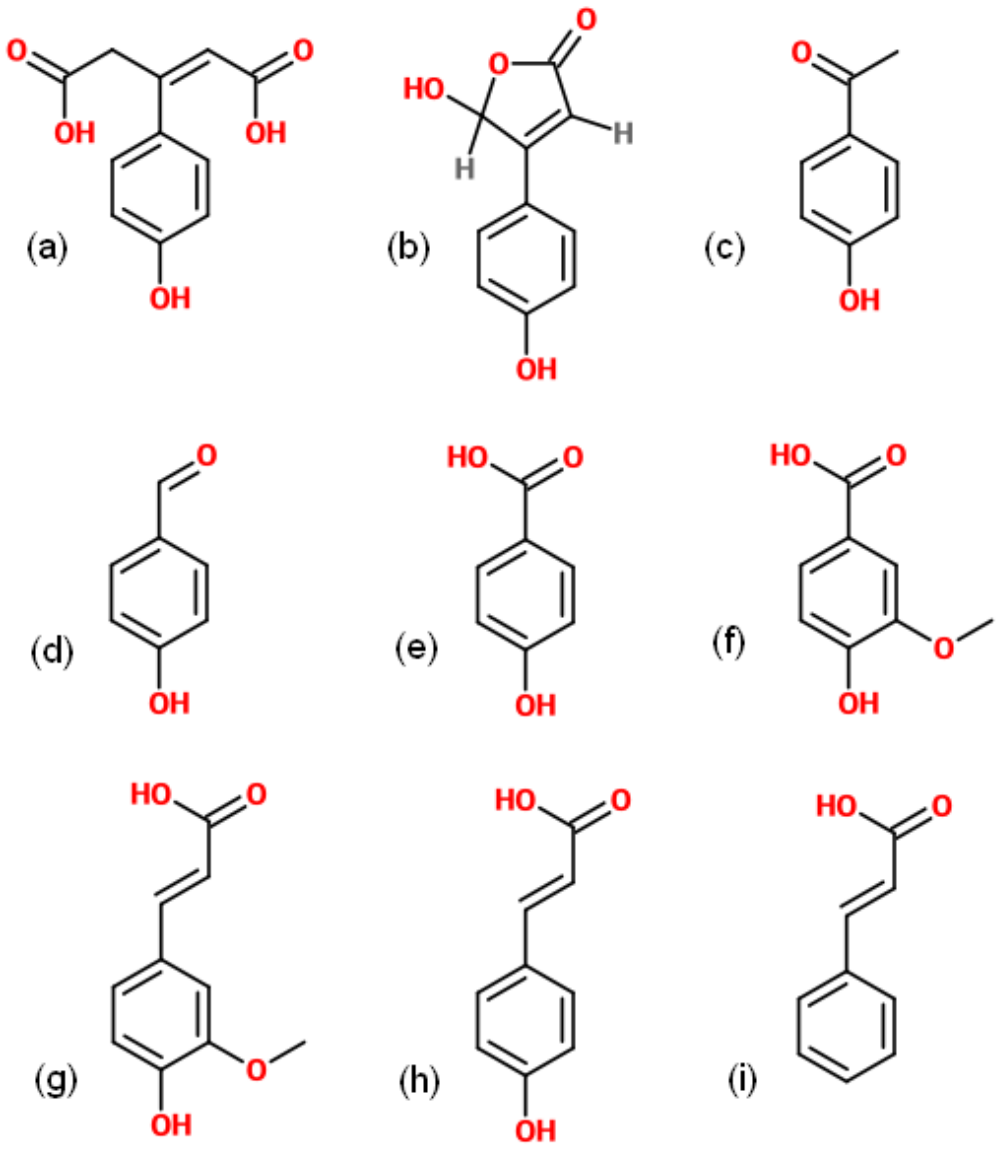

Figure4.1. Structure of key phenolic compounds found in *Sphagnum* species: (a) sphagnum acid, (b) hydroxybutenolide, (c) *p*-hydroxyacetophenone, (d) p-hydroxybenzaldehyde, (e) *p*-hydroxybenzoic acid, (f) vanillic acid, (g) ferrulic acid (h) *p*-coumaric acid (i) *t*-cinnamic acid.

Carbohydrates are known to account for a significant portion of organic matter in peat, with yields of total sugars from 233 to 395 mg g^{-1} being reported by Delarue et al. (2011), who used the molecular composition of neutral sugars in peat cores to infer plant sources and diagenetic history. To the author's knowledge, a molecular characterisation of dissolved neutral sugars has not been published for peatland

DOM. Carbohydrates have also been linked to the low degradation rates and unusual water chemistry found in *Sphagnum*-dominated bogs (e.g Hàjek et al., 2011). Galacturonic and 5-keto-D-mannuronic acid are both present in high concentrations in *Sphagnum*, mainly as long polymers associated with hemicellulose in plant cells, but also dissolved in the cells themselves (Clymo and Hayward, 1982). These contribute significantly to the high cation exchange capacity of peat bogs, and also act to acidify the water. Perhaps more importantly, they have been identified as the main tanning agent in protein and amino acid binding via an aldehyde tanning mechanism (Painter, 1991). Polymeric pectin-like structures of these, sphagnan, are released in the catotelm, and it has been suggested that they may bind with amino acids and proteins to form nitrogen rich aquatic humic acids. These recalcitrant molecules may not have central aromatic ring structures as commonly found in humic material but instead be centred around these very oxygen rich carbohydrates (Painter, 1991). This may in turn act as a sink of bioavailable nitrogen, enforcing the nutrient-poor environment in which *Sphagnum* species outcompete other plant species.

Polysaccharides in *Sphagnum*cell walls have been shown to be covered in a layer of lipids, which are believed to greatly reduce the decomposability of dead *Sphagnum* cells. These lipids, a mixture of C20-24 dicarboxylic acids, C14-26 hydroxy acids and fatty acids, are probably associated with an epicuticular wax layer on the *Sphagnum* and esterified with phenolic acids (*Van der Heijden, 1994* referenced by Verhoeven & Liefveld, 1997). Mid-length *n*-alkanes (particularly C_{23} and C_{25}) are also indicative of *Sphagnum* inputs to the peat profile and have been used as both species biomarkers and to infer changes in environmental conditions (Bingham et al., 2010; Lopez-Dias et al., 2010).

Rhizodeposition (below ground exudates and compounds released on tissue death) can provide a source of readily decomposed organic matter at depth within the peat profile, releasing simple sugars, amino acids and short chain fatty acids (Basiliko et al., 2012; Fenner et al., 2004). This injection of labile carbon can then have a priming

effect on microbial communities found within the peat, although the overall increase in heterotrophic respiration is small (Basiliko et al., 2012).

Little has been recently published on amino acid content and composition in peat bogs, but characterisation work on amino acids in solid peat has been undertaken in the past. Swain et al. (1959) obtained seven amino acids (glycine, aspartic acid, glutamic acid, threonine, alanine, valine and leucine) from peat samples taken from Dismal Swamp (Virginia, USA) and Cedar Creek Bog (Minnesota, USA) using a paper chromatography technique. Alanine was found in the highest concentrations at ~22 μmol g^{-1}. The total yield of these 7 amino acids was 0.4 – 2.9 mg g^{-1} (dry peat). Amino acid yields were higher in lower horizons of the peat, and as no free amino acids were detected it was suggested that the majority of these species were bound to or adsorbed onto humic acid micelles. Bohlin et al. (1989) conducted principal component analysis on a range of botanical and chemical properties of peat including amino acid content and found that across 41 peat samples, but found that the concentrations of the 16 amino acids they considered co-varied across samples. Yields of amino acids were 17 – 34 mg g^{-1} (OM) for *sphagnum* peats.

Advances in analytical techniques allowed Kunnas and Eronen (1994) to analyse peat samples specifically for free amino acids, quantifying 12 individual amino acids. Yields of free amino acids were highest (3.4 mg g^{-1} (dry peat)) in the upper portion of the peat profile, and the acidic amino acids (aspartic and glutamic acids) were found at high concentrations in this portion of the peat. It was suggested that plant litter decomposition sustained a higher level of free amino acids near the peatland surface than at depth. Swain et al. (1959) suggest that free amino acids are then bound within humic structures in deeper peat, but the techniques used by these studies do not allow for direct comparison of results. Lower in the peat profile, neutral free amino acids were found in highest concentrations, notably alanine (agreeing with Swain et al., 1959).

This chapter will focus on the characterisation of porewater DOM from depth profiles, seasonal profiles and also from the high-DOC intermediate-depth samples identified from the Mid-bog site (as discussed in Chapter 3). The composition of the dissolved combined amino acid and neutral sugar pools will be discussed in turn, followed by the results of TMAH thermochemolysis and gas chromatography mass spectrometry (GC-MS) on freeze dried material from porewaters. This will be followed by a synthesis of the chapter and conclusions. PCA and PC components and factor score plots are presented in Chapter 5 to assess the similarity of the above characterisation analyses of porewater samples from different depths, locations and sampling occasions.

4.1.1 Objectives and approaches taken

This chapter will address the second and third objectives summarised in Chapter 1, Section 1.4:

- To quantify both the total yield and relative contribution of individual components of the DCAA and dissolved neutral sugar pools, using a sub-set of samples from different depths, seasons and locations,
- To use TMAH thermochemolysis to provide a semi-quantitative assessment of lipids (*n*-alkanes and fatty acids) and functionally important aromatic compounds, again from a sub-set of samples as above,

In order to achieve this, the composition of each compound group (e.g. amino acids) will be described. To explore changes in composition with both depth below the peat and location, a combination of depth profiles and grouped averages (with depth) will be used to compare both yields of compound groups (amino acids and carbohydrates) and the contribution from individual components of these groups to water samples from different depths below the peat and locations on the bog. The results of TMAH thermochemolysis will then be presented, separated by compound class, considering changes with depth and season (for shallow samples) at the Central piezometers bank, and also characterising intermediate depth water samples

from the Mid-bog piezometer array. Changes in the composition of water samples will then be related to possible changes in source or to alteration of OM within the peatland (e.g. microbial degradation).

4.2 Total dissolved nitrogen (TDN) in Cors Fochno porewaters

Total dissolved nitrogen (TDN) measurements were carried out on all water samples, with values ranging from 0.55 to 8.32 mg l^{-1}. During later sampling occasions (after June 2010) it was noted that occasional very high blanks (> 5 mg l^{-1}) were measured in a small number (~5%) of vials in which samples were transported from the field and stored. For this reason, although duplicate samples were obtained and analysed, some caution must be taken when interpreting individual spikes in TDN from these sampling periods, and the depths profiles in Figure 4.2 are presented as dashed lines to represent this. The concentration of nitrogen in rainfall at Cors Fochno is ~1 mg l^{-1}(median of 32 monthly concentration measurements is 0.831 mg l^{-1} NO_3 and 0.290 mg $l^{-1}NH_4$, data courtesy of Mike Bailey, CCW[1]). Concentrations of dissolved nitrogen (which includes both the organic and inorganic forms) increase with depth, with small increases at the centre of the bog and much larger absolute increases at the edge site.

[1] For comparison, CCW monitor the nitrate and ammonia concentrations in rainfall at 11 sites across Wales, and the median of these values range from 0.677 to 1.009 mg l^{-1} for NO_3 and 0.151 to 0.536 mg l^{-1} NH_4.

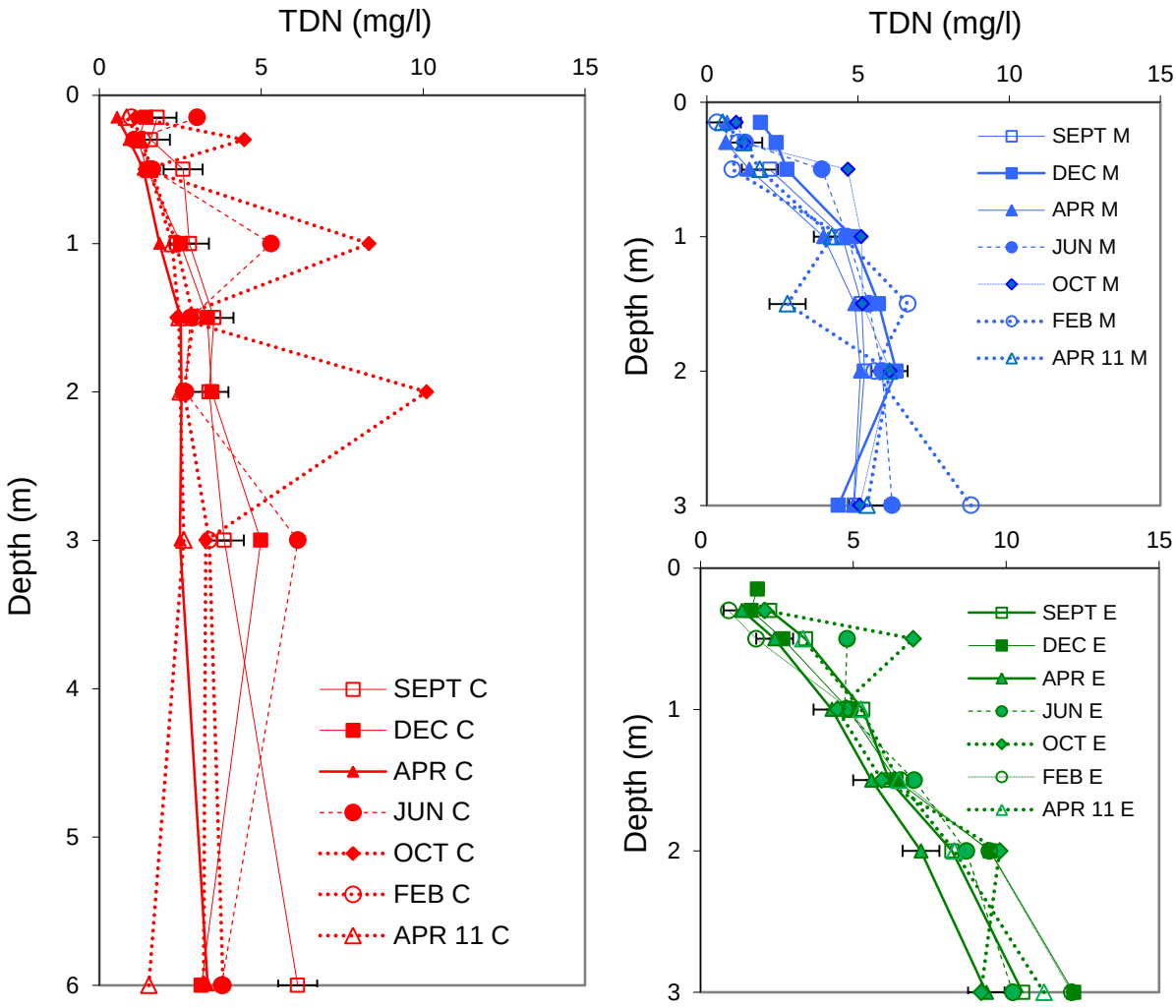

Figure 4.2: Depth profiles of TDN (mg l^{-1}) from all three sites (Red on left = Central, Blue upper right = Mid-bog, Green lower right = Edge) from all seasons. Dashed lines indicate those samples taken after Jun 2010 when sporadic high blanks were encountered in some sample vials (see text). Error bars indicate 1 σ (0.6 mg l^{-1}) of measurements (n=8) from multiple repeats of individual samples, including after 6 months sample storage – the analytical precision of the instrument(as measured by running one sample multiple times) is much higher (σ < 0.1mg l^{-1}). Error bars only shown on one sample occasion in each site for ease of reading.

The differences in the magnitude of increasing TDN concentration with depth, across locations, islikely to reflect the origin of these porewaters. Water at depth in the peat profile will move (slowly) from the centre of the bog to the bog margin (e.g. Waddington & Roulet, 1997). Nitrogen accumulates at depth (Figure 4.2, Central profile) and as a parcel of water at depth moves away from the centre of the bog, the

accumulation processes continue, leading to more extreme profile gradients and higher TDN values at depth near the edge of the bog. An increase in C:N with depth could be indicative of the contribution of microbial biomass at depth, but without knowing the organic versus inorganic contribution to TDN, this is difficult to ascertain from TDN alone. An assessment of the molecular composition of the dissolved amino acid pool may give a clearer indication of whether this is the case.

4.3 Results from amino acid analysis

The following three subsections will present and interpret the results from the analysis of amino acids in porewaters.

4.3.1 Dissolved Combined Amino Acids (DCAA) – Yields

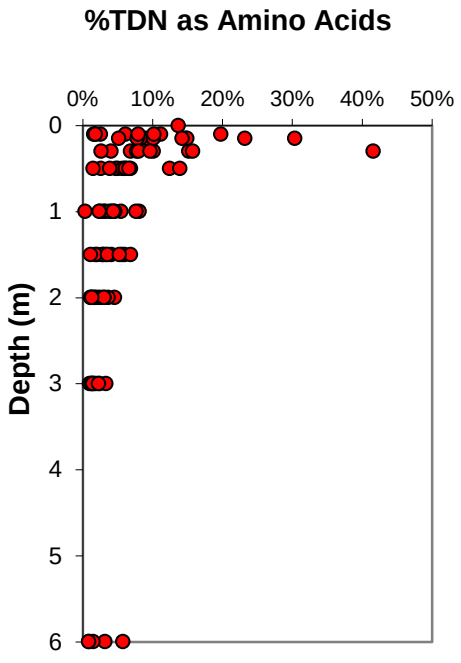

Figure 4.3: The percentage of TDN which is amino-acid bound.

Ninety six samples from locations across the bog, sampled over 7 seasons, were analysed for DCAA, with 18 individual amino acids quantified (see Section 4.3.2 for details of individual amino acids). Yields (normalised to organic carbon content of the sample) ranged from 8 to 104 mg g^{-1}OC with an average value of 29.8 mg g^{-1}OC. No clear pattern or trend in these yields was present with either depth or sampling location, although samples from 15 and 30 cm below the peat surface had higher than average amino acid yields (average of 31.0 and 37.0 mg g^{-1}OC respectively). After accounting for the molecular composition of each amino acid, this equates to a range of 0.35-4.6% of the organic carbon in samples being contained within hydrolysable amino

acids. Table 4.1 presents a summary of DCAA yields across depths and seasons at the Central piezometers array. Variability in yield is high between samples across both depth and sampling occasion.

Sampling occasion	Mean DCAA (mg g^{-1} OC)	Std Dev.	n	Depth (cm)	Mean DCAA (mg g^{-1} OC)	Std Dev.	n
Sep-09	32.7	15.6	8	**15**	35.4	10.3	6
Dec-09	53.3	46.4	8	**30**	42.6	28.1	7
Apr-10	29.1	13.3	8	**50**	33.0	8.1	6
Jun-10	37.8	15.4	7	**100**	23.2	12.1	6
Oct-10	23.5	9.3	8	**150**	24.9	17.8	6
Feb-11	24.1	12.1	8	**200**	27.2	8.6	6
Apr-11	27.6	5.0	2	**300**	22.4	7.2	6
				600	36.6	25.6	5

Table 4.1: Summary of all Central piezometers DCAA yield data. White cells to the left summarise seasonal data (all depths) with the mean, standard deviation and n for each sampling occasion. The blue summarises the depth data similarly.

Although the contribution of dissolved amino acids to DOC is relatively small, the contribution to the total nitrogen pool is (for some samples) much larger (Figure 4.3) and varies significantly with depth; the percentage contribution of amino acid-bound nitrogen to the total dissolved nitrogen pool varies by more than two orders of magnitude, accounting for between 0.34% and 42% of TDN. The highest percentage contributions are found in shallower samples (≤50 cm), due both to higher DCAA yields in some near-surface samples and increasing TDN concentrations with depth.

Yields of DCAA from intermediate depths (1 - 2 m) at the Mid-bog site range from 9.1 to 43.3 mg g^{-1}OC, with an average value of 25.0 mg g^{-1}OC (n=11). This equates to between 0.4% to 1.9% (average value 1.1%) of the OC pool being contained within hydrolysable amino acids and 1.2% to 8.1% (average value 4.6%) of the TDN pool.

4.3.2 DCAA – Molecular characterisation

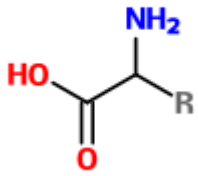

Figure 4.4, amino acid structure.

Separation of amino acids into groups according to charge classes and the functionality of side chains (represented by R in Figure 4.4) may be a useful approach for the interpretation of changes in amino acid composition with depth and location. Figure 4.5 shows a typical distribution of amino acids as a molar percentage for near-surface waters at the Central site (from the 30 cm piezometer, averaged over all seasons).

In general, the amino acids with negatively charged side-chains (glutamic acid (GLU[2]) and aspartic acid (ASP)) comprise 20-25% (molar) of the analysed amino acids, while the basic amino acids (the positively charged histidine (HIS), arginine (ARG), ornithine (ORN) and lysine (LYS)) account for only around 15% of the total. Glycine (GLY) (which has no carbon side chain, R = H) makes the largest single contribution to the total (15-20%) in the majority of samples, and the other neutral amino acids (alanine (ALA), valine (VAL), isoleucine (ISO) and leucine (LEU)) combine with glycine to account for around half the total. The polar amino acids which have hydroxyl containing side chains (serine (SER) and threonine (THR)) contribute around 10% to the total, and the remaining amino acids which contain hydrophobic side chains (tyrosine (TYR) and phenylalanine (PHEN) which both have aromatic side chains and methionine (METH), the only sulphur containing amino acid quantified) combine to make up only ~5% of the total. The non-protein (non-alpha) amino acids, β-alanine (BALA) and γ-aminobutyric acid (GABA), contribute only ~1% and 1.5% respectively to the total amino acids (note that while ornithine could be included in this group as it is not a protein amino acid, for this section it has been grouped according to its side chain and charge).

[2] Capitalised abbreviations of individual amino acids used in this chapter and Chapter 5 are given after each amino acid is first named in this section.

Few studies have previously quantified dissolved amino acids in wetland systems, but it is worth noting that the distribution of individual amino acids in our samples is remarkably similar to those found by other studies focussing on environments which are very different from that in our study, e.g. Dauwe & Middelburg (1998) who examined marine sediment cores. Dittmar et al (2001), who studied dissolved amino acids in a range of natural waters,again found relatively similar distributions, albeit with higher contributions from threonine and lower contributions from aspartic and glutamic acids in all samples they analysed (from river, estuarine, coastal and marine environments).

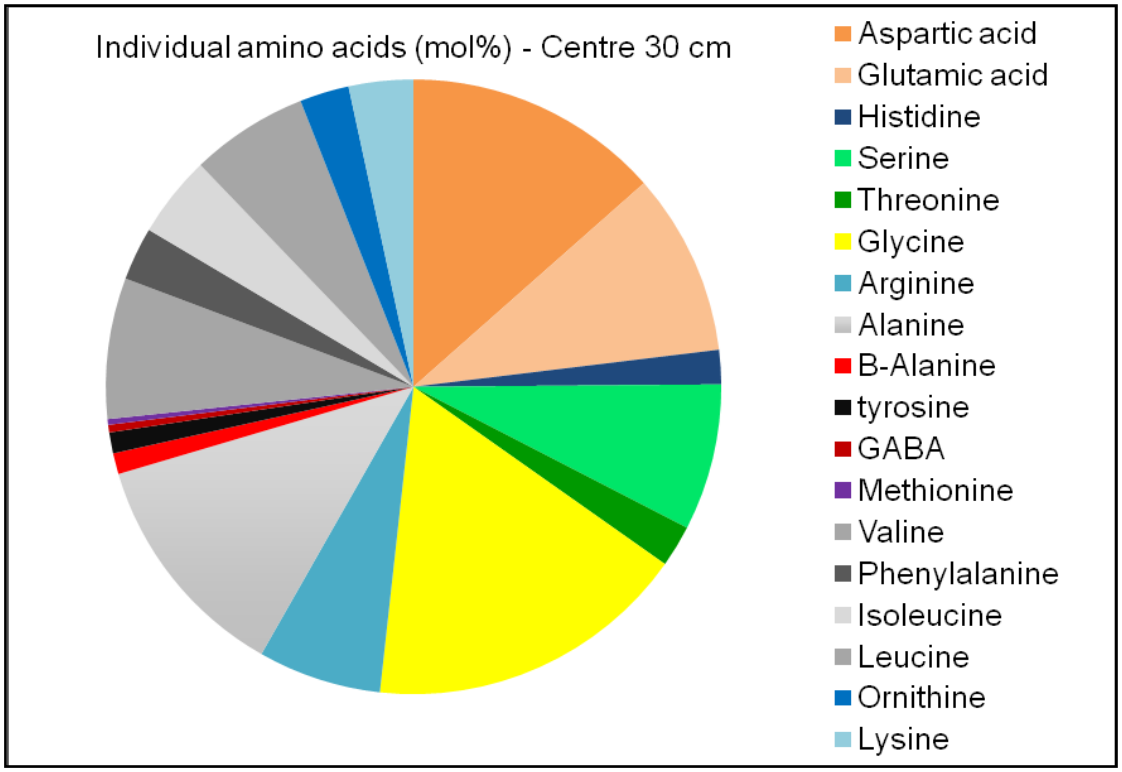

Figure 4.5: typical distribution as molar % of individual amino acids analysed. Orange sectors are the amino acids with acidic side chains, blue basic, green polar, and greys hydrophobic (with aromatic near-black). Red sectors are the non-alpha amino acids (not protein derived) and the only sulphur containing amino acid (methionine) is shown as purple. Glycine, which has no side chain, is shown in yellow.

4.3.3 DCAA – Spatial distributions and depth profiles

The depth profiles of individual amino acids display some trends, although for some individual components thereis a large degree of variation between samples. When considering depth profiles from the centre of the bog from 15 cm to 6 m below the peat surface, moving down profile, there are decreases in mol% of aspartic acid, arginine, glycine, valine and isoleucine. Ornithine, lysine, serine and threonine all increase in mol% with increasing depth.

Table 4.2 shows an example data set from Feb 2011. Not all the trends in individual amino acids distributions are evident in all depth profiles, for example, there is no clear trend in glycine content with depth in Table 4.1. To show trends in compositional changes with depth more clearly, Figure 4.6 shows the DCAA distributions averaging over broad depth horizons and all seasons. Figure 4.6 also shows that there are significant differences in the amino acid composition of the key intermediate-depth samples from the Mid-bog which have high DOC concentrations.

Molar percentage of individual dissolved amino acids from Central site, Feb 2011																		
Depth (m)	Asp (%)	Glu (%)	His (%)	Ser (%)	Thr (%)	Gly (%)	Arg (%)	Ala (%)	BALA (%)	Tyr (%)	GABA (%)	Meth (%)	Val (%)	Phen (%)	Iso (%)	Leu (%)	Orn (%)	Lys (%)
6	13	11	2.2	9	3.3	15	5.5	11	1.1	1.5	0.5	0.4	5.6	2.1	3.2	5.2	6.2	3.5
3	10	10	1.6	10	2.9	19	5.6	10	0.9	2.4	0.3	0.6	5.9	3.2	3.8	6.6	2.1	4.0
2	12	9	2.2	10	2.2	17	6.0	12	1.2	1.8	0.5	0.4	6.0	2.7	3.1	6.1	3.3	4.3
1.5	12	10	2.4	11	2.5	18	5.7	11	1.2	2.0	0.3	0.6	5.9	2.8	2.9	5.8	3.3	3.0
1	13	9	2.1	8	3.3	17	6.9	12	1.2	1.7	0.4	0.6	6.8	2.9	3.3	6.4	1.8	4.0
0.5	15	11	1.4	8	2.3	16	6.4	12	1.3	1.2	0.4	0.2	7.2	2.9	4.9	6.0	2.0	1.8
0.3	13	10	2.3	7	2.1	19	6.0	13	0.8	1.3	0.7	0.2	7.2	3.0	4.9	6.4	1.5	1.6
0.15	14	10	1.9	7	1.8	18	6.7	13	1.4	1.1	0.6	0.1	6.8	2.9	4.8	6.0	1.5	1.8

Table 4.2: Example distribution of amino acids (as molar percent of total DCAA) from Central site, sampled in February 2011.

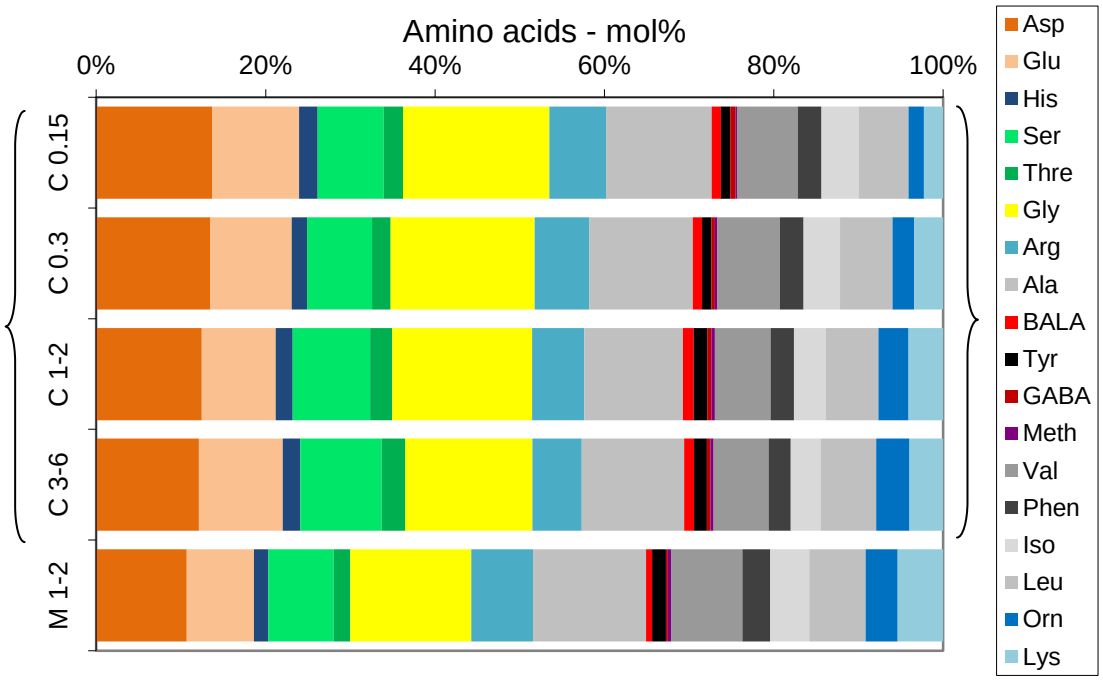

Figure 4.6: the average contribution of individual amino acids to DCAA in molar percent. Averages of 15 cm and 30 cm (top two bars) are taken from all seasons. Averages from deeper in depths profiles (from the Central site, 3rd and 4th bars, and the Mid-bog site, 5th bar) are taken from multiple depths and seasons. The sample names on the x-axis are derived from the site of sampling (C= Centre, M= Mid) and the depths (in m) over which the samples were averaged. Brackets are for ease of comparison of samples from the Central site. Colours representative of charge as Fig 4.5.

Due to the high degree of variability in yields and composition in individual samples (e.g. high %Ornithine at 6 m presented in Table 4.2), average compositional data from multiple samples will be used to discuss trends with depth. However, figure 4.3 (%TDN as DCAA) shows a clear reduction in the amount of dissolved nitrogen found as amino acids below the top 50 cm of the peat profile. Samples from 15 and 30 cm (from across the bog) had higher than average yields of amino acids, and when averaged over seasons had slightly different distributions of individual amino acids (Figure 4.6) and analysis of solid peat cores (presented in Chapter 5) shows a large peak in N content around 25 cm. For these reasons, the top two depth intervals are kept separate and not averaged with depth. The remaining five depth horizons showed little change in average composition, yield (as mg g^{-1} OC) or %TDN as amino acids, and so have been averaged, collating the intermediate depths (1-2 m) and deeper depths (3-6 m) in Figure 4.6 into depth horizons.

It is evident from Figure 4.6 that while shifts in distribution of amino acids are small and at times variable between individual samples, changes in average amino acid content with depth display clear trends. The figure also shows that the key Mid-bogintermediate depth (high DOC) samples most resemble samples from the deepest wells from the Centre of the bog, but with more extreme values for some components. For example, the aspartic acid and glycine contributions to the DCAA pool become smaller with depth at the centre of the bog, and are smaller still in Mid-bog intermediate-depth samples; likewise, the contributions from ornithine, lysine, and the hydrophobic amino acids in general (those in gray tones) increase with depth, and are greater still in the Mid-bog samples.

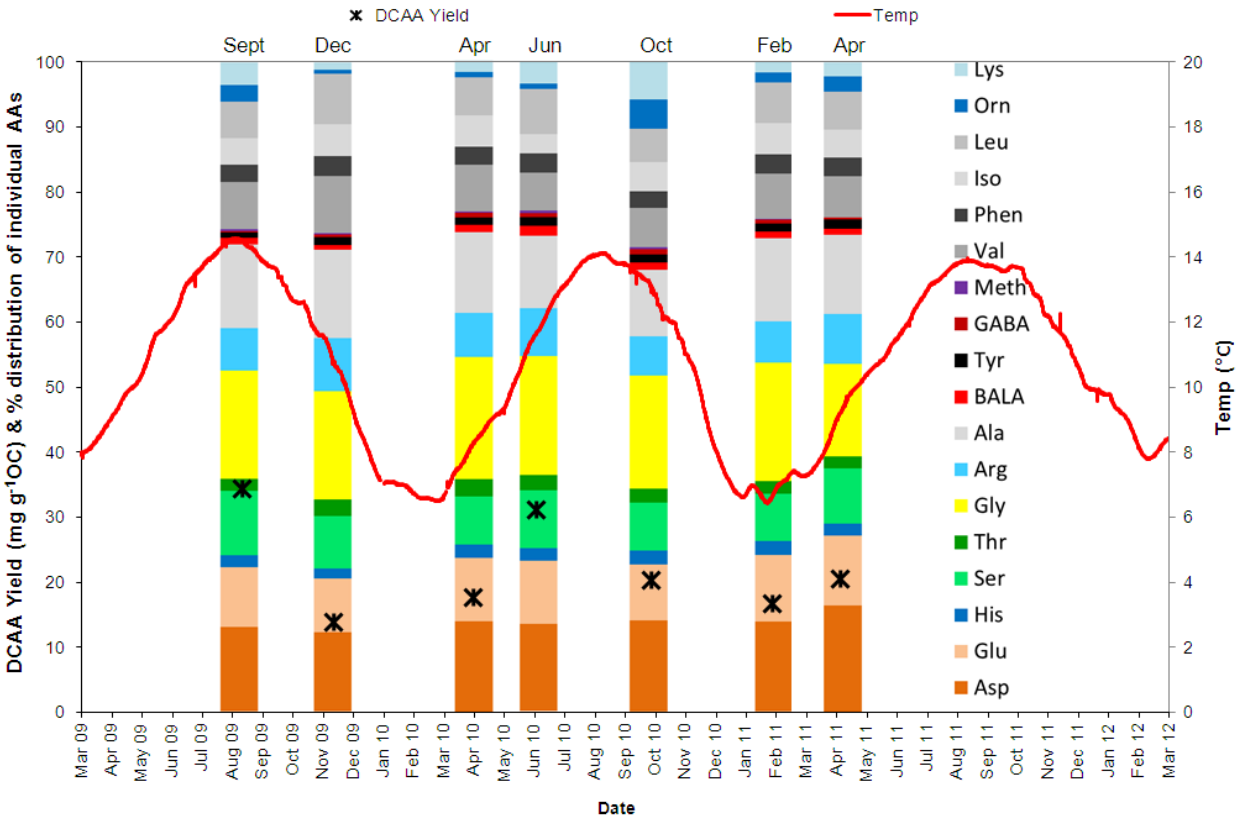

Figure 4.7:The molecular composition of DCAA (as a molar %) and yield (mg g^{-1}OC, marked by black cross) set against sub-surface water temperature measured from 15 cm piezometer by logger at R16, as used in Chapter 3. Amino acid data is taken from an average of the Central 15 and 30 cm depth samples.

Figure 4.7 shows changes in yield and molecular composition of DCAA in shallow porewaters (average of 15 & 30 cm from the Central site) over the seven sampling

periods, set against rainfall and temperature data as presented in Chapter 3. Average yields over the two depths range from 26 to 76 mg g^{-1}OC, with the highest yields in Dec 2009 due to a very high yield at 30 cm that month (104.4 mg g^{-1}OC). The average contribution of hydrolysable amino acids to the total dissolved nitrogen pool (AA-N%) range from 7.1% in Oct 2010 to 28.2% in Dec 2009 (this high value again being due to the high yield at 30 cm). The contribution to TDN is also low in Jun 2010 (8%), Sep 2009 (10%), and it is noteworthy that the three lowest AA-N% values occur in the warmest three sampling periods.

Variations in DCAA composition are in general small, although the ornithine and lycine content between months varies substantially, with the highest contribution from these compounds in Sept 2009 and Oct 2010. High ornithine content has been linked to bacterial reworking of protein-derived amino acids (Spitzy, 1988), and this may be the remnant of recycling of labile organic compounds during and at the end of the summer, when bacterial activity will be at its highest. The contribution from the other non-protein amino acids (β-alanine and γ-aminobutyric) is highest in June 2010, although variations are small and the precision of the method is not high enough to confidently draw conclusions from these changes. The three sampling periods noted above as having low AA-N% (Sep 2009, Jun 2010 and Oct 2010) are not characterised by unusual molecular composition or linked by any clear relationship.

Table 4.3 gives an overview of amino acids studied, the classification according to side-chain and charge, and the trends with depth and location discussed above. The supposition that increasing C:N with depth indicates an increase in the contribution from microbial biomass to the organic carbon pool (Section 4.2) is not supported by DCAA analysis: there is no indication that the non-protein amino acids (which are indicative of microbial biomass) increase with depth, and the AA-N% is at its lowest at 3 m (Figure 4.3).

Name	**R** "Am" refers to amino acid backbone: -CH(NH_2)COOH (structure in Figure 4.4)	**Side chain**	**Grouping** Dauwe&Middelberg (1998)	**Behaviour in depth profile**	**Comparative proportion in mid-depth (high DOC) samples**
Aspartic acid	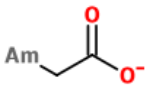	ACIDIC	NEG	Decreases with depth. Maxima at 50 cm & 6 m	LOW
Glutamic acid	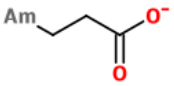	ACIDIC	NEG	Highest at surface. Variable.	LOW
Histidine	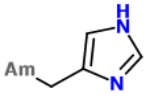	BASIC	POS		LOW
Serine		POLAR	HYDROXYL	On average, increases with depth, but variable. Lowest at surface.	LOW
Threonine	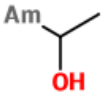	POLAR	HYDROXYL	On average, increases with depth, but variable. Lowest at surface.	LOW
Glycine			NEUTRAL	On average, decreases with depth.	LOW
Arginine	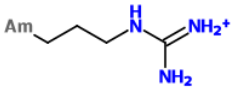	BASIC	POS	Decreases with depth.	HIGH
Alanine		H'PHOBIC	NEUTRAL	Variable.	HIGH
β-alanine	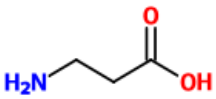	Non protein (non alpha)		Mid depth maxima around 50 cm to 1 m.	LOW
Tyrosine	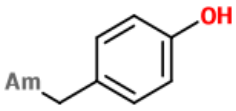	H'PHOBIC	AROMATIC		

γ-aminobutyric acid	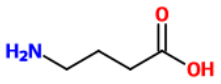	Non protein (non alpha)			LOW
Methionine	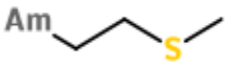	H'PHOBIC	SULPHIC	Minor component. Low variability but lowest contribution at surface (15 cm).	
Valine	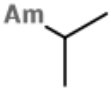	H'PHBIC	NEUTRAL	Decrease with depth.	HIGH
Phenylalanine	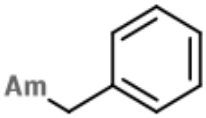	H'PHBIC	AROMATIC		HIGH
Isoleucine	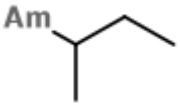	H'PHOBIC	NEUTRAL	Decreases with depth.	HIGH
Leucine	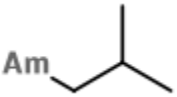	H'PHOBIC	NEUTRAL	Slight increase with depth when averaged over all seasons.	HIGH
Ornithine	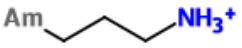	BASIC	POS	Variable. On average, increases with depth.	HIGH
Lysine		BASIC	POS	Variable. On average, decreases with depth.	HIGH

Table 4.3: Amino acids quantified, with structure, grouping by side chain and as Dauwe & Middelberg (1998), how the amino acid varies with depth through the peat profile and whether the amino acid is found in higher or lower proportional amounts in intermediate-depth Mid-bog samples. Blank boxes indicate no clear trend.

4.4 Dissolved Carbohydrates

Other studies of northern peatland-derived carbohydrates (e.g. Bohlin et al., 1989; Comont et al., 2006; Delarue et al., 2011; Estournel-Pelardy et al., 2011; Jia et al., 2008) have focussed on solid phase analysis of coresand, to the author's knowledge, no molecular characterisation of dissolved carbohydrate from peatland porewaters has been published. Therefore, although analytical problems were encountered during

the development and implementation of this technique (as evident from the low precision detailed in Chapter 2), the following results and discussion may nevertheless be useful, despite the caveats involved.

Yields of dissolved carbohydrates ranged from 24 to 275 mg g^{-1}OC, with no clear trend in total yield with either depth or location. This equates to between 1% and 10% of DOC being derived from carbohydratesand an average contribution of 3%. Carbohydrate content is highest on average at 3 m in the Mid and Central sites (208mg g^{-1}OC, or 8% of DOC), but because a smaller number of samples were analysed for dissolved carbohydrates than for other analyses, and because the precision of the method was relatively low, a cautious approach to the interpretation of changes in yield with depth must be taken.

Of the seven neutral sugars quantified for the dissolved phase, glucose is dominant in the majority of samples, although glucose also displays the largest variability between samples, with an average contribution of 28.3% to Central samples and values ranging from 8% to 52%. The remaining sugars account for similar amounts of the dissolved carbohydrate pool (Figure 4.8), with slightly lower contributions from rhamnose and fucose. Repeta et al. (2001) noted that distributions of these same 7 sugars have been found to be fairly constant in a large number of natural waters, including marine, riverine, lacustrine and sediment porewaters. From this large selection of samples, all seven sugars were found in near equal molar proportions, and there appeared to be no environmental control on this distribution.

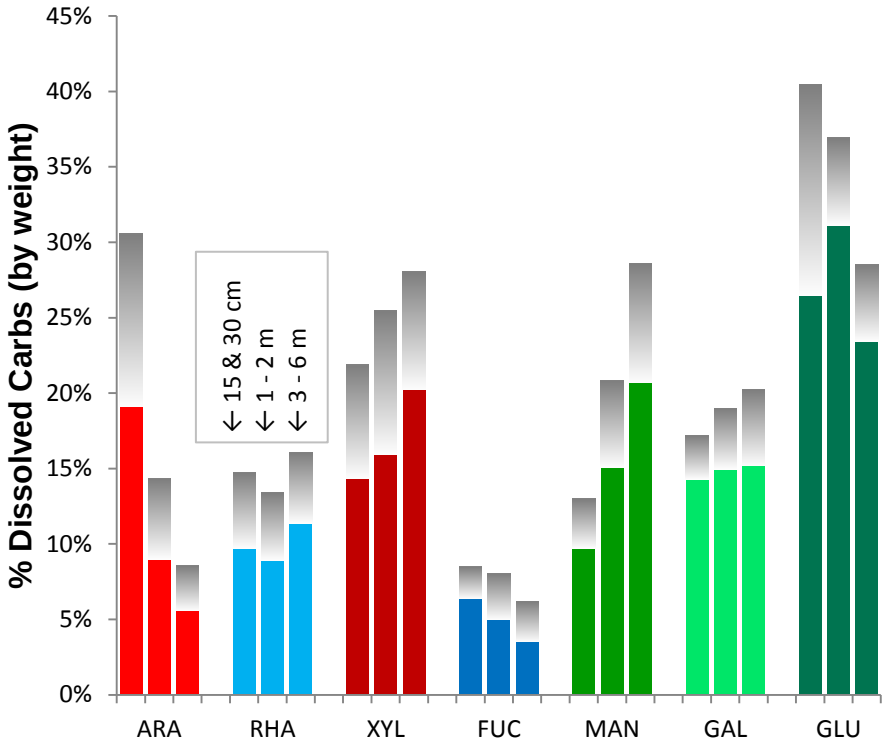

Figure 4.8: distribution of neutral sugars (as wt%) in pore water samples from the Central site, averaged with depth (15-30 cm, 1-2 m and 3-6 m, n=7, n=7 and n=4 respectively). Solid lines represent mean values, and grey shaded bars above represent 1σ. Colour indicates group; hexoses are represented in green, pentoses in red and the deoxysugars in blue.

The distribution of sugars at Cors Fochno does deviate somewhat from the equimolar distribution found in other environments; notably, rhamnose and fucose contribute less to TCHO and glucose contributes more. Fucose, and to a lesser extent rhamnose, are known to be derived largely from microbial inputs to DOC, although in peatlands are perhaps derived mainly from *Sphagnum* species (Comont et al., 2006; Jai et al., 2008). Diagenesis of neutral sugars in the solid phase has been studied in a variety of environments, and the proportion of deoxysugars has been found to increase with diagenetic alteration (e.g. Cowie & Hedges, 1984; Hedges et al., 1994; Cowie et al., 1995; Opsahl & Benner, 1995; Benner and Opsahl, 2001), but no similar downcore changes in sugar distributions are seen in peat (Jia et al., 2008). As previously mentioned, no significant changes in the distribution of dissolved carbohydrates are seen across many differing environments, so it is therefore possible that the lower contribution of fucose and rhamnose in porewaters from CorsFochno is due to the presence of DOM derived from an organic pool which does

not have a typical (diagenetically altered) sugar composition. This will be discussed further in Chapter 5.

When averages are taken over multiple seasons and depths (Figure 4.8), trends in the composition of the carbohydrate pool can be seen. There appears to be a decrease in the contribution from arabinose and fucose with increasing depth, and an increase from xylose and mannose. Changes in the distribution of galactose, rhamnose and glucose are perhaps too small to be interpreted with confidence, although glucose and rhamnose appear to act conversely to each other (glucose contributing most and rhamnose least at 1-2 m and vice versa at 3-6 m) and there is a slight increase in the relative amount of galactose with depth. Galactose shows the lowest degree of variability between all samples with a relative standard deviation of 25% compared to 77%, 53%, 52% and 46% for arabinose, xylose, fucose and mannose respectively. Analysis of the distribution of sugars by group (hexoses, pentoses and deoxysugars) shows little change with depth, as the sugars which make up each grouping appear to vary independently of one another (e.g. of the two pentoses quantified, the percentage of arabinose decreases with depth, whereas that of xylose increases). Due to the low response (and corresponding low precision) of the analysis, care must be taken when interpreting the above trends and patterns.

In studies of peat cores, several relationships between the molecular composition of the carbohydrate pool and bog function and characteristics have been proposed; for example, the ratio of arabinose and xylose to galactose, rhamnose and mannose has been proposed as an indicator of plant input material (Comont et al., 2006). Such measurements may then be used as a proxy to infer changes in the peat-forming environment of the past (Delarue et al., 2011). However, because it is not clear how these proxies or relationships would bear out in theDOM pool, the majority of discussion regarding these indicator-ratios will be deferred until Chapter 5, where a comparison between the solid and dissolved phases will be made.

4.5 TMAH Thermochemolysis and GC/MS

Analysis of DOM in porewater samples using TMAH thermochemolysis followed by GC-MS allowed for the identification of over 150 products, resulting from a variety of compounds classes including phenolics (as their methylated derivative), fatty acids (as fatty acid methyl esters, FAMES) and *n*-alkanes. The following qualitative and semi-quantitative results identify the dominant compounds that are found in the Cors Fochno samples and highlight changes in composition at different depths and environments over the peatland.

Figure 4.9 showsexample total ion count chromatograms (TICs), with peak assignments, for samples from June 2010 representing three of the key DOM environments identified in the previous chapter: **surface water** from the Central site at 15cm; the **mid depth** sample from 1.5m at the Mid-bog site(representing the intermediate-depth high DOC zone); and the **deep water**sampled at 6m depth, again at the centre of the bog. Labels are according to the numbers and symbols given in Table 4.4, which also lists the base peak and molecular ion for each compound.

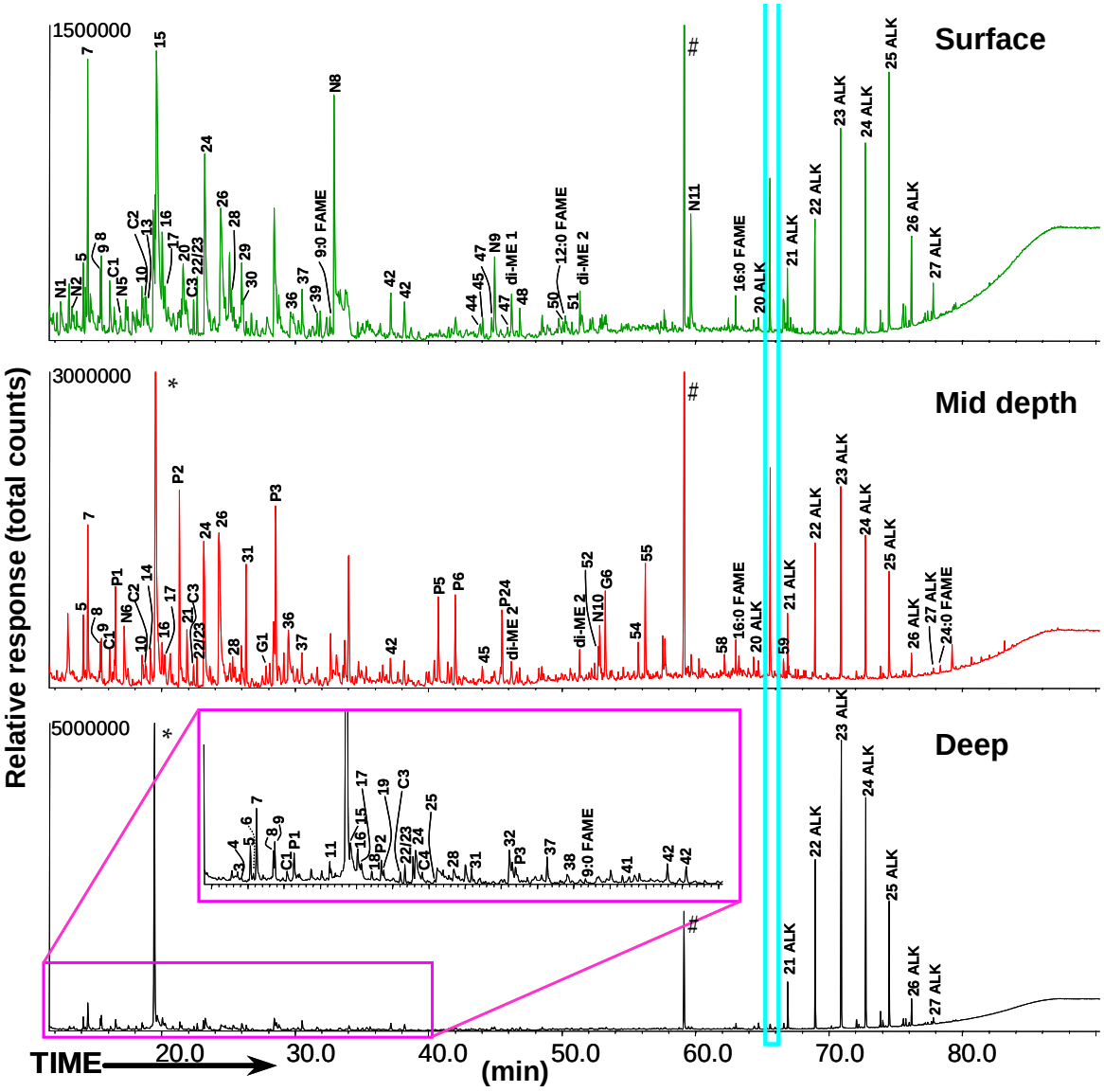

Figure 4.9: Total ion count chromatograms (TICs) for 3 porewater samples, labelled according to table 4.3; * indicates a peakreported to be an artefact of the TMAH analysis (Frazier et al., 2003) and # indicates a large peak which is present in the majority of sample from Cors Fochno but which could not been identified.Number in upper left corner of plots is response (total count), for comparison of scales only. Peak within the light blue box is 5α-androstane added as an internal standard but not used for quantification (see methods chapter section 2.4.6.2 for details).

No	Species Name	Ion	MW
1	2,3,5-trimethylfuran	110	110
2	furfural	96	96
3	2,3-dimethyl-cyclohexa-1,3-diene	93	108
4	xylene	91	106
5	ethylbenzene	91	106
6	trimethyl-1,3-cyclopentadiene	93	108
7	xylene	91	106
8	styrene	104	104
9	xylene	91	106
10	1-ethyl-3-methylbenzene	105	120
11	1-ethyl-2-methylbenzene	105	120
12	5-methyl-2-furancarboxaldehyde	110	110
13	1,3,5-trimethylbenzene	105	120
14	furancarboxylic acid ME	95	126
15	phenol	94	94
16	1,2,3-trimethylbenzene	105	120
17	benzofuran	118	118
18	1-methoxy-2-methylbenzene	122	122
19	1-ethyl-3-methylbenzene	105	120
20	2-ethyl-1-hexanol	57	130
21	butanedioic acid dimethyl ester	115	146
22	1-propynylbenzene	115	116
23	indene	115	115
24	2-methylphenol	108	108
25	4-ethyl-1,2-dimethyl-	119	134
26	4-methylphenol	107	108
27	methylthiobenzene	124	123
28	benzoic acid methyl ester	105	136
29	2,5-dimethylphenol	122	122
30	2-methylbenzofuran	131	131
31	1-ethyl-4-methoxybenzene	121	136
32	1-methyl-1H-indene	130	130
33	2-methylindene	130	130
34	(1-methyl-2-cyclopropen-1-yl)-benzene	130	130
35	1,4-dimethoxybenzene	123	138
36	4-ethylphenol	107	122
37	naphthalene	128	128
38	2,3,5-trimethylphenol	121	136
39	2,4,6-trimethylphenol	121	136
40	3-methylbenzoic acid methyl ester	119	150
41	1,3-demethyl-1H-indene	129	144
42	2-methylnaphthalene	142	142
43	1,2,4-trimethoxybenzene	168	168
44	2,7-dimethylnaphthalene	156	141
45	1,3,5-trimethoxybenzene	168	168
46	1,4-dimethylnaphthalene	156	156
47	2,3-dimethylnaphthalene	156	156
48	dimethylphthalate	163	194
49	1,2-dimethylcyclooctane	55	140
50	dibenzofuran	168	168
51	1,4,6-trimethylnaphthalene	170	170
52	3,5-dimethoxybenzoic acid ME	196	165
53	diphenylsulphide	186	186
54	2-methoxy-1,1'biphenyl	184	184
55	methyl p-methoxycinnamate, cis	161	192
56	cyclododecane	55	168
57	methyltetradecanoate	74	242
58	3-(3,4-dimethoxyphenyl)-2-propenoic acid ME	222	222
59	1,1'-(1-methylethylidene)bis[4-methoxybenzene	241	256
	Species possibly derived from carbohydrates		
C1	2-methyl-2-cyclopenten-1-one	67	96
C2	3-methyl-2-cyclopenten-1-one	96	96
C3	2,3-dimethyl-2-cyclopenten-1-one	67	110
C4	2,3,4-trimethyl-2-cyclopenten-1-one	109	124
	Species possibly derived from lignin		
P1	methoxybenzene	108	108
P2	1-methoxy-4-methylbenzene	122	122
G1	1,2-dimethoxybenzene	138	138
P3	1-ethenyl-4-methoxybenzene	134	134
P5	4'-methoxyacetophenone	135	150
P6	4-methoxybenzoic acid methyl ester	135	166
P24	4-methoxybenzeneacetic acid ME	121	180
G6	3,4-dimethoxybenzoic acid ME	165	196
	Nitrogen containing species		
N1	2-methylpyridine	93	93
N2	3-methyl-1H-pyrrole	80	81
N3	3-methylpyridine	93	93
N4	N,N-dimethyl-acetamide	87	87
N5	2,5-dimethyl-1H-pyrrole	94	95
N6	2-chloropyridine	78	113
N7	1-methyl-1H-pyrrole-2-carboxaldehyde	109	109
N8	methanamine	140	140
N9	2-methyl-1H-isoindole-1,3(2H)-dione	161	161
N10	diethyltoluamide	119	191
N11	N-butylbenzenesulphonamide	77	213
	Fatty acid methyl esters		
8:0 FAME	octanoic acid methyl ester	74	158
9:0 FAME	nonanoic acid methyl ester	74	172
di-ME 1	octanedioic acid dimethyl ester	129	202
12:0 FAME	dodecanoic acid methyl ester	74	214
di-ME 2	nonanedioic acid dimethyl ester	152	216
16:0 FAME	hexadecanoic acid methyl ester	74	270
18:0 FAME	octadecanoic acid methyl ester	74	298
24:0 FAME	tetracosanoic acid methyl ester	74	382
	Alkanes and alkenes		
12(=) ALK	1-dodecene	55	168
12 ALK	dodecane	57	170
12(=) ALK	2-dodecene (Z)	55	168
12(=) ALK	4-dodecene (Z)	55	168
20 ALK	eicosane	57	282
21 ALK	heneicosane	57	296
22 ALK	docosane	57	310
23 ALK	tricosane	57	324
24 ALK	tetracosane	57	338
25 ALK	pentacosane	57	352
26 ALK	hexacosane	57	366
27 ALK	heptacosane	57	380

Table 4.4: Table of the labelled peaks from TICs in Figure 4.9, with the molecular ion (ion) and molecular weight (MW) taken from the GC MS data library.

The earliest section of each chromatogram is dominated by lower molecular weight species, some of which are nitrogen containing. Aromatic structures dominate, with the majority of assigned peaks being identified as phenolics (or their methylated products) and alkylbenzenes. The later section of each chromatogram (after 60 mins.) is comprised almost entirely of n-alkanes, although fatty acids (present as methyl esters) are found throughout. The following results and discussion will focus on each of the major compound classes in turn, describing those compounds which are found in highest abundances and how the relative proportions of these compounds change with depth, location and season.

4.6.1 Phenolics – an overview

Many of the methoxybenzenes (the methylated products of phenolics) found in these samples have been frequently used as proxies for the study of lignin sources in natural systems (e.g. Filley et al., 2006; Shadkami & Helleur, 2010 and references therein), although lignin may not be a significant source of these compounds in our system where *Sphagnum* (a lignin-free, non-vascular plant type) is by far the dominant plant type. That being said, vascular plants are found abundantly at the site (including the cotton grasses *Eriophorumvaginatum* and *Eriophorumangustifolium* and heather *Calluna vulgaris*) and these may contribute lignin to the organic matter pool. TMAH thermochemolysis involves methylation of hydroxyl groups, thus the methylation of phenolic compounds results in methoxybenzenes. However, without the use of either another alkylating reagent or ^{13}Clabeled TMAH, it is impossible to discern between methoxy groups which were present in aromatic compounds in the original sample and those that result from the thermochemolysis reactions. This leads to difficulty during interpretation of results, for example where ferrulic acid (a lignin monomer) and caffeic acid (linked to tannin content) both appear as 3-(3,4-dimethoxyphenyl)-2-propenoic acid ME **(G18)**[3]using this method (Figure 4.10).Some lignin products have also been shown to be non-lignin specific, for example 1,2-

[3] This numeration refers to the lignin proxies which are grouped according to their base aromatic structure, either *p*-hydroxyphenyl**(P)**, guaiacyl**(G)** or syringyl**(S)**.

dimethoxybenzene **(G1)**, 1,2,3-trimethoxybenzene **(S1)** and 1,2,3-trimethoxy-5-methyl-benzene **(S5)** have been reported as derivable from carbohydrates and tannins (Frazier et al, 2003) and methoxybenzene**(P1)** and 4-methoxy benzoic acid ME **(P6)** can be derived from proteins (Ertelet al., 1984). However, despite the fact that a lignin source is not necessarily implied for these compounds, the lignin proxy numeration scheme will be used throughout, for the sake of comparability of results.

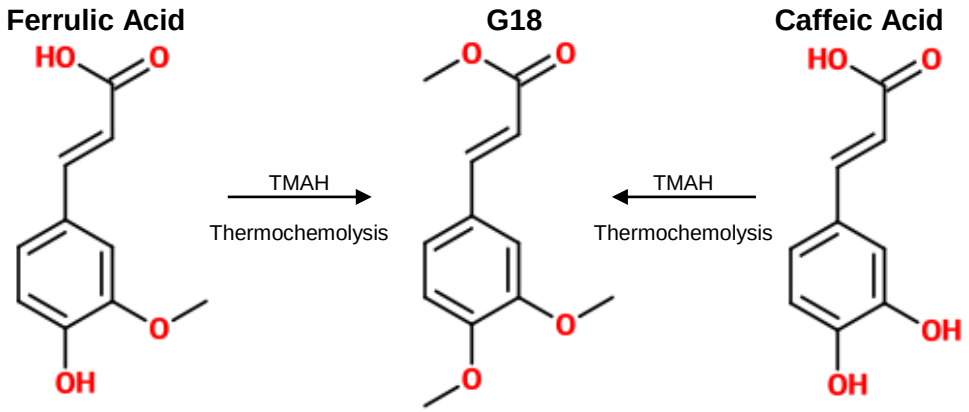

Figure 4.10: Two compounds (ferrulic acid and caffeic acid) which are indistinguishable using TMAH thermochemolysis GC-MS due to the common product **G18**, as an example of the non-specific nature of the method.

4.6.2 Phenolics – semi-quantitative characterisation

Tables 4.4 and 4.5 show the changes in peak size (relative to referencing peak) for the quantified phenolic compounds with location and depth. A full depth profile from the Central site (15 cm to 6 m) is shown, as are three samples from the Mid site (at 1.5 m) representing organic matter from the intermediate-depth, high-DOC porewaters. To investigate how the molecular composition of DOM alters with season, shallow samples (both 15cm and 30cm) from the centre of the bog were analysed overfive sampling periods, covering 14 months: Dec 2009, Apr 2010, Jun 2010, Oct 2010 and Feb 2011.The shallow central piezometersamples were chosen as the signal from the Central site may best represent the DOM released recently, rather than fresh DOM mixed with older material which is in transit from the main dome towards the lower-

lying boundaries of the site (which will be the case at the Mid and Edge sites as discussed in Chapter 3, Section 1). Figure 4.11 shows stacked TICs for each of these ten samples (5 seasons, 2 depths at each) and it can be seen that the overall character of these TICs differ significantly from each other.

It should be noted that although a good response was obtained for the 15 cm Dec 2009 sample, the TIC shown in Figure 4.11 was obtained during method testing and a different analytical set up was used for this sample. It has been included in qualitative analysis, but will not be included in the semi-quantitative analysis that follows. Surface samples are dominated by trimethoxybenzene and methoxy benzoic acid methyl esters (4-methoxy- **(P6)**, 3,4-dimethoxy- **(G6)** and 3,4,5-trimethoxy- **(S6)**). The methylated derivatives of the corresponding aldehydes (4-methoxybenzaldehyde **(P4)**, 3,4-dimethoxybenzaldehyde **(G4)** and 3,4,5-trimethoxybenzaldehyde **(S4)**) are not found in quantifiable amounts, in agreement with other studies (Templier et al., 2005). It has been shown that the acid to aldehyde ratio of lignin-derived dissolved methoxybenzenes (e.g. **G6**:**G4**) is very high in riverine waters relative to coastal and ocean settings (Del Rio et al, 1998), which may be due to a combination of the low solubility of these carboxyl-poor compounds and their preferential uptake by microbial communities (Opshal & Benner, 1995). It is worth noting that **G4** was identified in one near-surface sample (Central site at 15 cm, Feb '11, a sample with a relatively large **G6** peak, Table 4.5), but only by searching for select ions (m/z=166) and not at a high enough intensity to be reliably quantified. Methoxybenzenes with no other functional groups [e.g. methoxybenzene (**P1**) and 1,2-dimethoxybenzene (**G1**)] are also identified in the majority of samples, although the syringyl form [1,2,3-trimethoxybenzene (**S1**)] is not identified in any samples. Large peaks identified as 1-methoxy-4-methyl benzene **(P2),** 1-ethenyl-4-methoxy benzene **(P3)** and 4'methoxyacetophenone **(P5)** are also found in surface samples. At depths greater than 1m in the centre of the bog, the occurrence and abundance of methoxybenzene peaks declines, although a significant number are found at 6m depth (Table 4.6).

Figure 4.11: TICs from shallow samples (15 and 30 cm, red and blue respectively) from Central site with season. Labels on Jun 2010 15 cm as in Table 4.3 for ease of comparison.

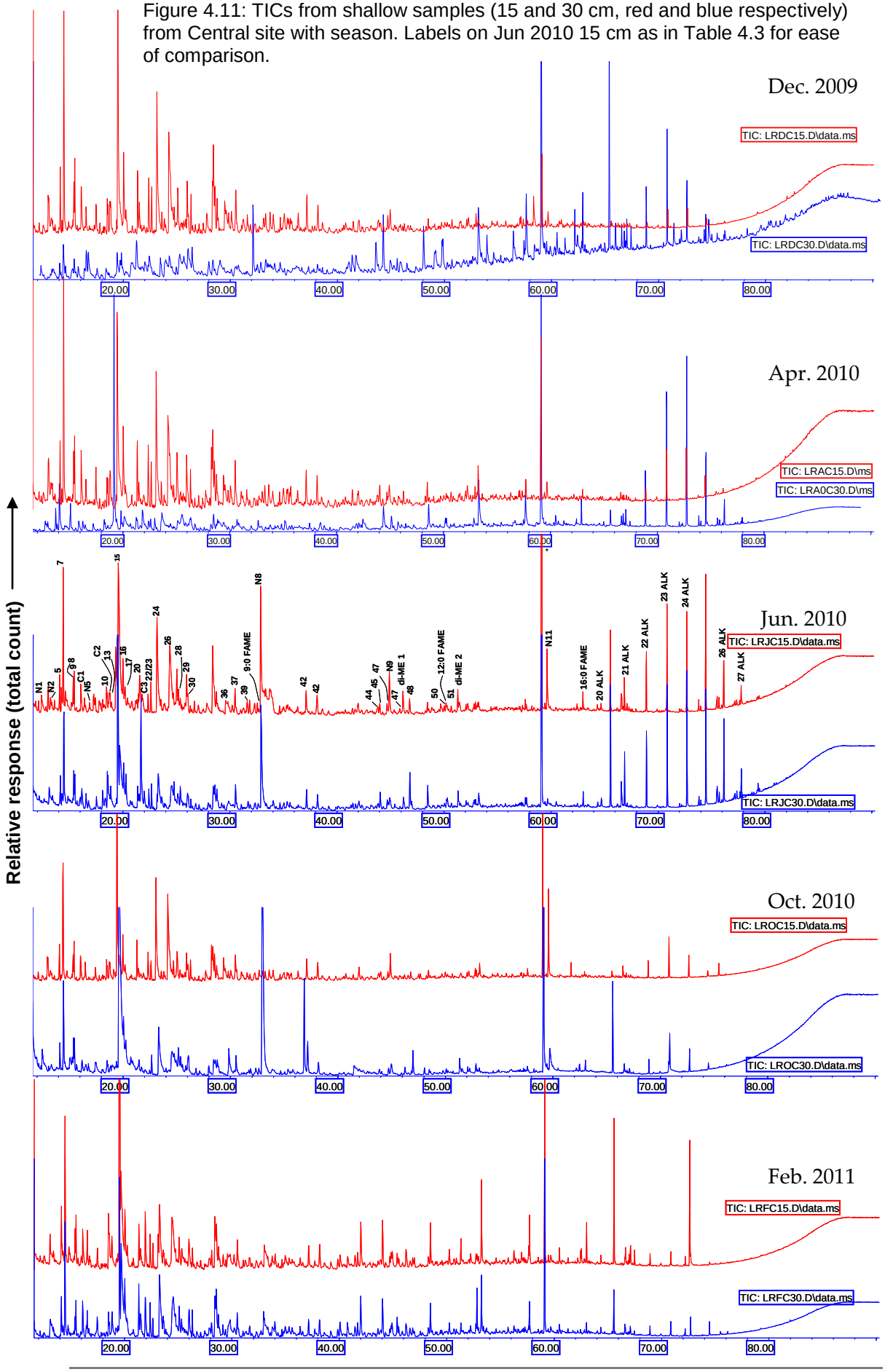

Two phenolic compounds with aliphatic side chains of greater than 2 carbon units (3-(4-methoxyphenyl)-2-propenoic acid ME **(P18)** and **(G18)**) are present in concentrations high enough to be quantified,in contrast with some other studies of natural DOM (Frazier et al., 2003; Frazier et al., 2005; Maie et al., 2006; Mannino & Harvey, 2000) and it has been suggested that biotic and photochemical reworking of degraded lignin in the aquatic environment preferentially removes these cinnamyl compounds. **P18** and **G18** have,however, been reported after analysis of lake (Peuravuori & Pihlaja, 2007) and river waters (Templier et al., 2005).

Central, 15 & 30 cm, with season		Dec 15	Apr 15	Apr 30	Jun 15	Jun 30	Oct 15	Oct 30	Feb 15	Feb 30
Benzene, methoxy-	P1	12	13	25		21	13	25	26	18
Benzene, 1-methoxy-4-methyl-	P2	33	32	24	7	26	32		31	37
Benzoic acid ME			10		23	29	13	26	24	
Benzene, 1-ethyl-4-methoxy-		19	17	34	7	9	16		15	21
Benzene, 1,2-dimethoxy-	G1	2	4	22		7	3		14	15
Benzene, 1-ethenyl-4-methoxy-	P3	27	27	11	15	27	22		32	43
Benzene, 1,4-dimethoxy-				14	3	8	2		11	9
Prop-2-ene, 2-(4-methoxyphenyl)-	$	15	12	10		14	16		15	17
But-3-enoic acid ME, 3-(4-methoxyphenyl)-	$									
Benzoic acid, 3-methoxy-4-methyl-		4	7	16	2	6	8		14	13
Acetophenone, 4-methoxy-	P5	10	6	21	5	9	8		16	22
Benzene, 1,2,4-trimethoxy-				15		8	2		13	16
Benzoic acid ME, 4-methoxy-	P6	14	15	29	16	11	18		46	48
Benzene, 1,3,5-trimethoxy-		9	15	61	13	25	11	5	42	41
Ethanone, 1-(3,4-dimethoxyphenyl)-	G5			10			8		10	10
Benzoic acid ME, 3,4-dimethoxy-	G6		17	136	4	20	11		58	50
Ethanone, 1-(3,4,5-trimethoxyphenyl)-	S5			7						
2-Propenoic acid ME, 3-(4-methoxyphenyl)-	P18	3	6				5		15	9
Benzoic acid ME, 3,4,5-trimethoxy-	S6		9	81	5	13	6		30	24
2-Propenoic acid ME, 3-(4-methoxyphenyl)-	G18								5	3

Table 4.5: relative responses of the 21methoxy-benzene species quantified, for surface samples (15 and 30 cm), over 14 month period (Dec '09; Apr, Jun & Oct '10; & Feb '11), with values relative to the response of xylene referencing peak (100). Letter and number in column header represent month and depth (cm) and the colour represents season (to aid the eye in comparison of data). $ denotes compounds known to be derived from sphagnum acid. Blank cells indicate that the compound could not be quantified.

Central, Jun 2010 Depth Profile		15	30	50	100	150	200	300	600
Benzene, methoxy-	**P1**		**21**	**19**	**23**	**13**	**11**	**8**	**47**
Benzene, 1-methoxy-4-methyl-	**P2**	**7**	**26**	**26**	**18**		**14**		**30**
Benzoic acid ME		**23**	**29**	**14**		**8**	**8**		**29**
Benzene, 1-ethyl-4-methoxy-		**7**	**9**	**12**	**11**		**8**		**19**
Benzene, 1,2-dimethoxy-	**G1**		**7**	**5**	**3**				**6**
Benzene, 1-ethenyl-4-methoxy-	**P3**	**15**	**27**	**17**	**23**	**11**	**21**		**24**
Benzene, 1,4-dimethoxy-		**3**	**8**	**3**	**3**				
Prop-2-ene, 2-(4-methoxyphenyl)-	**$**		**14**	**18**	**16**		**14**	**12**	**29**
But-3-enoic acid ME, 3-(4-methoxyphenyl)-	**$**								
Benzoic acid, 3-methoxy-4-methyl-		**2**	**6**	**15**	**11**				**7**
Acetophenone, 4-methoxy-	**P5**	**5**	**9**	**8**	**7**		**1**		**6**
Benzene, 1,2,4-trimethoxy-			**8**	**7**	**5**			**5**	**9**
Benzoic acid ME, 4-methoxy-	**P6**	**16**	**11**	**28**	**19**				
Benzene, 1,3,5-trimethoxy-		**13**	**25**	**21**	**10**			**6**	**7**
Ethanone, 1-(3,4-dimethoxyphenyl)-	**G5**			**7**					
Benzoic acid ME, 3,4-dimethoxy-	**G6**	**4**	**20**	**37**	**6**				**10**
Ethanone, 1-(3,4,5-trimethoxyphenyl)-	**S5**								
2-Propenoic acid ME, 3-(4-methoxyphenyl)-	**P18**			**6**	**4**				
Benzoic acid ME, 3,4,5-trimethoxy-	**S6**	**5**	**13**	**23**	**7**				**8**
2-Propenoic acid ME, 3-(3,4-dimethoxyphenyl)-	**G18**			**4**					

Table 4.6: relative responses of the 20methoxy-benzene species quantified for a depth profile taken from the centre of the bog in June 2010. Values are given relative to the response of referencing xylene peak (100). Number in column header represent depth (cm). $ denotes compounds known to be derived from sphagnum acid. Blank cells indicate that a compound could not be quantified.

The Mid-bog intermediate-depth samples, which have very high DOC concentrations, have abundant methoxyphenyl peaks (presented in Table 4.7), many of which are relatively large. A fuller suite of *p*-hydroxyphenyl related compounds is present, dominated by **P2**, **P3**, **P1**, **P5** and 1-ethyl-4-methoxy benzene, which shares a *p*-hydroxyphenyl structure but does not have a lignin-proxy designation. **P6**, **P18** and 4-methoxy-benzenacetic acid ME **(P24)** are also found in high abundances, and on average the *p*-hydroxyphenyl compounds make up 67% of the total peak area for all phenol-derived compounds. The proportion of compounds present with a benzoic acid structure (including **P6**, **G6** and **S6**) is lower in these intermediate depth samples, which is indicative of lower oxidative degradation of organic matter at depth (Del Rio et al., 1998; Maie et al., 2005; Maie et al., 2006). Benzoic acid compounds account for (on average) 35% of the total methoxyphenyl-peak area in the shallow (15 & 30 cm) Central porewaters, 21% in deeper Central porewaters and 16% in Mid-bog 1.5 m porewaters.

Mid site, 1.5 m, with season		Dec	Apr	Jun
Benzene, methoxy-	**P1**	76	51	63
Benzene, 1-methoxy-4-methyl-	**P2**	89	126	128
Benzoic acid ME		34	5	44
Benzene, 1-ethyl-4-methoxy-		68	117	81
Benzene, 1,2-dimethoxy-	**G1**	7		20
Benzene, 1-ethenyl-4-methoxy-	**P3**	107	83	132
Acetophenone, 4-methoxy-	**P5**	93	47	72
Prop-2-ene, 2-(4-methoxyphenyl)-	**$**	94	90	115
But-2-enoic acid ME, 3-(4-methoxyphenyl)-	**$**	5	2	5
But-3-enoic acid ME, 3-(4-methoxyphenyl)-	**$**	18	11	24
Benzoic acid ME, 4-methoxy-	**P6**	63	16	78
Benzene, 1,3,5-trimethoxy-		16		15
Benzeneacetic acid ME, 4-methoxy-	**P24**	52	22	57
Ethanone, 1-(3,4-dimethoxyphenyl)-	**G5**	8	6	10
Benzoic acid ME, 3,5-dimethoxy-		20	16	24
Benzoic acid ME, 3,4-dimethoxy-	**G6**	27	27	60
1,1'-Biphenyl, 2-methoxy-		28	13	21
Ethanone, 1-(3,4,5-trimethoxyphenyl)-	**S5**			5
2-Propenoic acid ME, 3-(4-methoxyphenyl)-	**P18**	42	39	72
2-Propenoic acid ME, 3-(4-methoxyphenyl)-	**G18**	9	4	14
Benzene, 1,1'-(1-methylethylidene)bis[4-methoxy-]		13	17	11

Table 4.7: relative responses of the 21 methoxy-benzene compounds quantified for a mid depth, high DOC samples from the Mid-bog site. Values are given relative to the response of referencing xylene peak (100). Samples from Dec '09, Apr '10 and Jun '10. $ denotes compounds known to be derived from sphagnum acid.

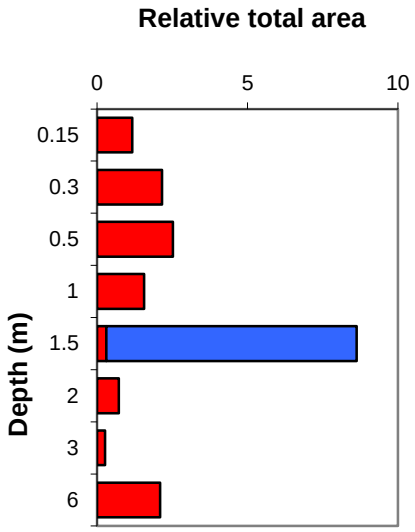

Figure 4.12 the relative abundance of methoxyphenyl compounds at the Central site (red) and Mid-bog site (blue) from Jun 2010.

In all samples, the *p*-hydroxyphenyl compounds dominate, with a lower proportion of guicyl compounds, and syringyl compounds are found in the lowest relative abundances.

In order to emphasise the relative contribution of methoxyphenyl compounds to the Mid-bog high-DOC porewaters, Figure 4.12 shows a plot of the summed relative abundance of all quantified phenol-derived peaks from the depth profile taken in Jun 2010 at the Central site (in red), and the Mid-bog 1.5 m (in blue) sample from the same day. It is clear that

high DOC concentrations at this depth are at least partially indicative of very high concentrations of phenolic compounds.

Several of the key "lignin markers" above could also be produced by the TMAH thermochemolysis of the phenolic compounds commonly found in *Sphagnum* and associated pore-waters (Figure 4.1). The methylated derivatives of these compounds are listed below (Table 4.8), and are indistinguishable from lignin components using our method, i.e. without using ^{13}C labelled TMAH. It is thereforepossible that the majority of the *p*-hydroxyphenyl lignin-marker peaks identified in our samples are derived from phenolics associated with the *Sphagnum* polymeric phenol networks and tannin-like structures, rather than from lignin as might first have been inferred. Sphagnum acid, hydroxybutenolide and *p*-coumaric acid have been found in high concentrations in effluent media in which *Sphagnum* has been grown, and active excretion mechanisms from *Sphagnum* have been suggested for these compounds (Rudolph & Rasmussen, 1992).

***Sphagnum* related phenol**	**Methylated product**	**Lignin marker**
p-hydroxyacetophenone	4'methoxyacetophenone	P5
p-hydroxybenzaldehyde	4-methoxybenzaldehyde	P4
p-hydroxybenzoic acid	4-methoxybenzoic acid ME	P6
vanillic acid	3,4-dimethoxybenzoic acid ME	G6
ferrulic acid	3-(3,4-dimethoxyphenyl)-2-propenoic acid ME	G18
p-coumaric acid	3-(4-methoxyphenyl)-2-propenoic acid ME	P18

Table 4.8, *Sphagnum* related phenols which have been identified in previous studies (see Verhoeven & Liefveld (1997) and references therein; see figure 4.1 for structures) with the methylated products following TMH and associated lignin biomarker.**P4** isin red to highlight that this compound is not present in quantifiable amounts in any THM analysis from this study.

The methylation products of sphagnum acid have been described by Abbott et al. (manuscript in review), and these compounds can be identified in samples from Cors Fochno, with strong methylated 4-isopropenylphenol[4] peaks found in the majority of

[4] Methylation results in 2-(4'methoxyphenyl)-prop-2-ene

samples, and smaller peaks assigned as methylated 3-(4'-hydroxyphenyl)-but-3-enoic acidand 3-(4'-hydroxyphenyl)-but-2-enoic acid[5] found in only some samples (Table 4.6). It has previously been assumed that sphagnum acid is primarily of functional importance only in the acrotelm of *Sphagnum*-dominated bogs, where it is actively excreted by *Sphagnum* moss (Verhoeven & Liefveld, 1997). Below this region, it is thought that sphagnum acid is quickly transformed to its peroxidative decay product, hydroxylbutenolide, and that this compound is broken down further before reaching the anoxic catotelm. At Cors Fochno, this is not found to be the case, with 2-(4'methoxyphenyl)-prop-2-ene identified in almost all samples, and at high relative abundance in the Mid-bog, high DOC samples. To the author's knowledge, this is the first time these compounds have been reported in the dissolved phase at depth.

The seasonal comparison of phenolic products (Table 4.5) shows that both the total relative abundance of methoxyphenyls and the abundance of individual compounds suggested as being actively excreted by *Sphagnum* species (e.g. **P5** and the sphagnum markers) are lowest during Jun 2010, at the height of the growing season(especially at 15 cm). These abundances are highest in Feb 2011 and Apr 2010, when primary productivity will be low (it was noted that the peatland had not started "greening up" when sampling was carried out in April). Despite this, it is not possible to draw conclusions regarding any relationship between plant activity and methoxyphenyl concentration, since sampling depths are at 15 cm and greater below the peat surface, which may not be close enough to the living *Sphagnum* communities to see an in-situ phenolic-excretion signal.

4.7 *n*-Alkanes

Medium chain-length*n*-alkanes are used as indicators of *Sphagnum* inputs into peats, as this moss displays an unusual distribution of alkanes, with high abundances of tricosane (C_{23}) and pentacosane (C_{25}) (Berdie et al., 1995; van Dongen et al.,

[5] As 3-(4'methoxyphenyl)-but-3-enoic acid ME and 3-(4'-methoxyphenyl)-but-2-enoic acid ME

2008).Tricosane(C_{23}) is dominant in low-lying, hollow and lawn *Sphagnum* species, whereas pentacosane (C_{25}) is dominant in hummock-forming species.Thus, the relative distributions of these two compounds to longer chain alkanes (usually C_{31}or C_{29}) and to each other are used as proxies for changes in peatland distribution and function (Bingham et al., 2010; Lopez-Dias et al., 2010;McClymont et al., 2011).

Medium chain, unbranched alkanes dominate the chromatograms of all samples analysed from greater than 1.5 m depth, irrespective of season or sampling location across the bog. These alkanes range from 20 to 28 carbons in length (eicosane to octacosane), and the relative abundances of each of these compounds, using the same sample set as for the previously described TMAH thermochemolysis results, are given in tables 4.9 and 4.10.

Central, June 2010 depth profile	#C	15	30	50	100	150	200	300	600
Eicosane	20	5	11	7	13	13	4	22	18
Heneicosane	21	17	35	18	65	103	23	152	113
Docosane	22	39	62	48	173	283	55	376	391
Tricosane	23	54	81	86	260	450	96	545	730
Tetracosane	24	62	90	114	182	371	130	393	571
Pentacosane	25	74	109	94	88	198	127	11	292
Hexacosane	26	35	61	32	22	53	63	43	80
Heptacosane	27	14	21	8	4	13	31	8	16
Octacosane	28		6				9		
Total *n*-alkanes		298	475	408	808	1483	539	1549	2210
Odd:Even		1.13	1.07	1.02	1.07	1.06	1.06	0.86	1.09

Table 4.9: relative responses of the nine n-alkanes quantified for a depth profile taken from the centre of the bog in June 2010. Values are given relative to the response of the xylene referencing peak (100). Number in column header represent depth (cm). The ratio of odd- to even-numberedn-alkanes is also noted.

For the majority of samples, tricosane (C_{23}) is the dominant alkane present, as might be expected from a peatland where the majority of the peat surface is covered by lower-lying microtopography, e.g. lawns and hollows. Pentacosane (C_{25}) is the dominant *n*-alkane in only one sample, from porewaters 30cm below the centre of the dome in June. This may be due to heterogeneity in the peat profile, with layers of peat formed from different *Sphagnum* species, or because the hydrology of the underlying peat layers brings water to this sampling well from a hummock-

dominated location. Unusually, the depth interval below this (50cm, June) is dominated by tetracosane (C_{24}), and this, coupled with the general lack of strong odd-over-even dominance, suggests some alteration of the chain lengths compared with the parent material. *n*-alkanes with an odd number of carbons dominate most plant sources (e.g. from plant waxes) including *Sphagnum*(e.g. Bingham et al., 2010; Lopez-Dias et al., 2010). It is likely that the alkanes identified in porewater samples by TMAH thermochemolysis are moieties of larger complex molecules or assemblages derived from plant waxes, as pure alkanes are insoluble in water.Whatever the mechanism for these compounds being suspended or dissolved into water samples from Cors Fochno, their odd-even distribution appears to be altered during this process.

The abundance of *n*-alkanes also increases significantly with depth, and at depths greater than 1m, they contribute between 40-70% to the total area of all quantified peaks. Alkanes have been used as biomarkers for plant inputs by many studies (e.g. Bingham et al., 2010; Lopez-Dias et al., 2010) due in part to their longevity in nature. This recalcitrance may explain the increased proportion that alkanes make to the DOM pool at depth, where utilisation of other organic compounds leads to an accumulation of the most recalcitrant OM. Another possibility is that the mechanisms which disperse alkanes into porewater, whether biotic, physical or chemical, occur at depth.

The distribution of n-alkanes in shallow porewaters shows a distinct seasonal signal, with much higher abundances and fuller suites of chain-lengths in April and June than in other months (Table 4.11). This is also the case for the June Mid-bog sample at 1.5m below the peat surface (the data from Mid-bog 1.5 m samples is given in Table 4.10), and indeed all samples taken during that month, regardless of location or depth (qualitative analysis only). There are several possible explanations for this finding, including: a) the mechanismsthat disperse nominally-non-soluble *n*-alkanes into the soluble phase occur only in the summer, and these compounds are only preserved in porewaters year-round at depth; or b) that compounds or waters are

moving from depth towards the surface during the summer due to enhanced evapotranspiration and reduced recharge rates. The latter possibility is seen to be implausible when data relating to the variability of the water table at the site (discussed in Chapter 3) is considered. Although reversal of the direction of hydraulic head and subsequent upward flow of water has been reported in peatlands during summer months (Beer & Blodau, 2007; Waddington & Roulet, 1997), the magnitude of this flow is small, and at Cors Fochno the water table moves at most ~20 cm over the course of a year. There has also been no suggestion in previous modelling studies of the site that upward movement of water occurs, even during the summer (A. Baird, pers comm.).

Central, 15 & 30 cm with season	#C	D15	A15	A30	J15	J30	O15	O30	F15	F30
Eicosane	20			*5*	5	*11*				*2*
Heneicosane	21	2		*15*	17	*35*	2			*2*
Docosane	22	2	5	*61*	39	*62*	11	*10*	6	*5*
Tricosane	23	5	14	*173*	54	*81*	19	*30*	7	*10*
Tetracosane	24	5	14	*168*	62	*90*	11	*15*	9	*10*
Pentacosane	25	3	8	*97*	74	*109*	4	*6*	2	*7*
Hexacosane	26			*31*	35	*61*				
Heptacosane	27			*7*	14	*21*				
Octacosane	28					*6*				
Total *n*-alkanes		17	41	*554*	298	*475*	48	*61*	25	*36*
Odd:Even		1.35	1.12	*1.10*	1.13	*1.07*	1.21	*1.40*	0.59	*1.10*

Table 4.10: relative responses of the nine n-alkanes quantified for surface samples (15 and 30 cm, italic denoting 30cm samples), over 14 month period (Dec '09; Apr, Jun & Oct '10; & Feb '11), with values relative to the response of the xylene referencing peak (100). Letter and number in column headers represent month and depth (cm). Colours represent different season, to aid the eye. The ratio of odd-numbered (with respect to number of carbons) to even-numberedn-alkanes is also noted.

The possibility that the high *n*-alkane contribution could be an artefact of sampling was also considered, as particularly unusual distributions (i.e. high abundance across all depths) were observed in all samplesfrom only June 2010, but this is deemed very unlikely as deep waters (most notably from 6m depth at centre of bog) display high contributions from *n*-alkanes which are relatively stable across all seasons.

Mid-bog1.5 m, with season	#C	Dec	Apr	Jun
Eicosane	20			11
Heneicosane	21	11	4	28
Docosane	22	16	5	4
Tricosane	23	7	6	94
Tetracosane	24		6	80
Pentacosane	25		7	53
Hexacosane	26		4	11
Heptacosane	27		2	2
Octacosane	28			
Total *n*-alkanes		35	35	284
Odd:Even		1.16	1.25	1.67

Table 4.11: relative responses of the nine n-alkanes quantified for 1.5 m samples (representing the high-DOC porewaters) taken from the Mid-bog site in Dec 2009, Apr 2010 and Jun 2010. Values are given relative to the response of xylene referencing peak (100). The ratio of odd- to even-numberedn-alkanes is also noted. Blank cells indicate that the compound could not be quantified.

4.8 Fatty acid methyl esters (FAMEs)

FAMEs were present in the majority of samples, and in some were a major constituent of the GC-MS TIC. Table 4.12 gives an example of the relative abundances of FAMEs (15 and 30 cm samples at the Central site over 5 sampling periods). Coelution of FAME peaks with unknown compounds resulted in few or no FAMEs being identified in some TICs, and therefore a further identification step for the saturated long-chain FAMEs was undertaken by focusing on the m/z 74 (indicative of FAMEs) spectra.

Qualitatively, although FAMEs are present in most samples, no single TIC contains all FAMEs which have been identified. Of the saturated FAMEs, hexadecanoic acid ME is the most prevalent, followed by octanoic- and nonanoic-acid MEs. Butanedioic acid dimethyl ester is a dominant peak in most of the surface samples, has higher responses in the lower part of the acrotelm (30cm compared to 15cm below the peat surface), and is not present at all in the centre samples which come from deeper than 50cm (i.e. in the depth profile). This compound is present in the Mid-bog, intermediate-depth, high DOC concentration samples however, and is the dominant FAME present here. Octane- and nonane-dioic acid dimethyl esters are also present

in the majority of samples, occurring with similar intensities, although octanedioic acid dimethyl ester is usually the dominant of the two peaks.

Central, 15 & 30 cm, seasonal	D15	A15	A30	J15	J30	O15	O30	F15	F30
Hexanoic acid ME				12		9	15		
Butanedioic acid di-ME		9	59	5	26			45	36
Octanoic acid ME				12		9	11	4	
Nonanoic acid ME			20	9	8		9		
Decanoic acid ME			15	10			5		
Octanedioic acid di-ME				24	23			23	13
Dodecanoic acid ME				8				17	15
Nonanedioic acid di-ME				16	20		18	16	4
9-Hexadecanoic acid ME			14					6	
Hexadecanoic acid ME		3	30	11	11	3	10	20	7
9-Octadecenoic acid ME			4					7	
8-Octadecenoic acid ME			20			2		14	
Octadecanoic acid ME			5					7	
Tetracosanoic acid ME									

Table 4.12: An example of the relative abundance of FAMEs found at shallow depths (15 & 30 cm) at the Central site over 5 sampling periods (Dec '09, Apr '10, Jun '10, Oct '10 and Feb '11). Number and letter in column header indicate month and depth (in cm). Colours denote month for ease of comparison.

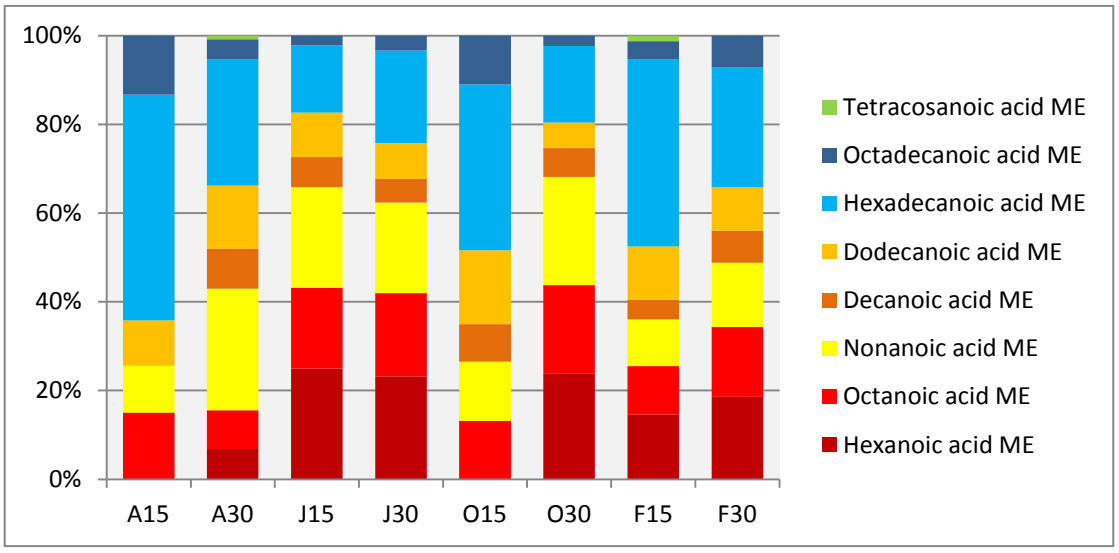

Figure 4.13: The distribution of FAMEs (as identified using single ion mode with a m/z of 74) for shallow depth samples (15 and 30 cm depth) from the Central site across 4 sampling seasons (Apr '10, Jun '10, Oct '10 and Feb '11). The red-yellow palette show the 6:0 (hexanoic-) to 12:0 (dodecanoic-) FAMEs and the blue palette identify 16:0 and 18:0 FAMEs. 24:0 (tetracosanoic acid ME), the only FAME with a main chain of more than twenty carbon atoms is shown in green. Sample names on x-axis identify month and depth (cm).

Note that in Table 4.12, numerous FAMEs are missing from the semi-quantitative analysis. Although it is not possible to directly compare the results of the single ion

mode spectra from m/z 74 and the TIC, Figure 4.13 shows the FAMEs identified using the m/z 74 spectra and the relative proportion of these peaks. The two months which had the lowest identifiable contributions from FAMEs in TIC mode also had characteristic distributions of FAMEs identified in single ion mode, with a larger proportion of the total coming from hexadecanoic acid ME and with no hexanoic acid ME identified.

The shortest chain FAMEs are most easily degraded by microbial communities (Frazier et al., 2005), and the two months with the lowest apparent FAME concentrations show the lowest contributions from these compounds, suggesting that in Apr and Oct 2010, the FAME pool at 15 cm has been depleted by microbial degradation. No *iso-* or *aneiso*-C_{15} or C_{17} FAMEs, which would be indicative of high bacterial inputs (Deport et al., 2006), were identified in any samples. The largest contribution from the ubiquitous 18:0 and 16:0 are found at 15 cm in Apr 2010, Oct 2010 and Feb 2011. In June 2010 however, the contribution from FAMEs < 16:0 is much higher, which may be indicative of high bacterial contributions (Deport et al., 2006).

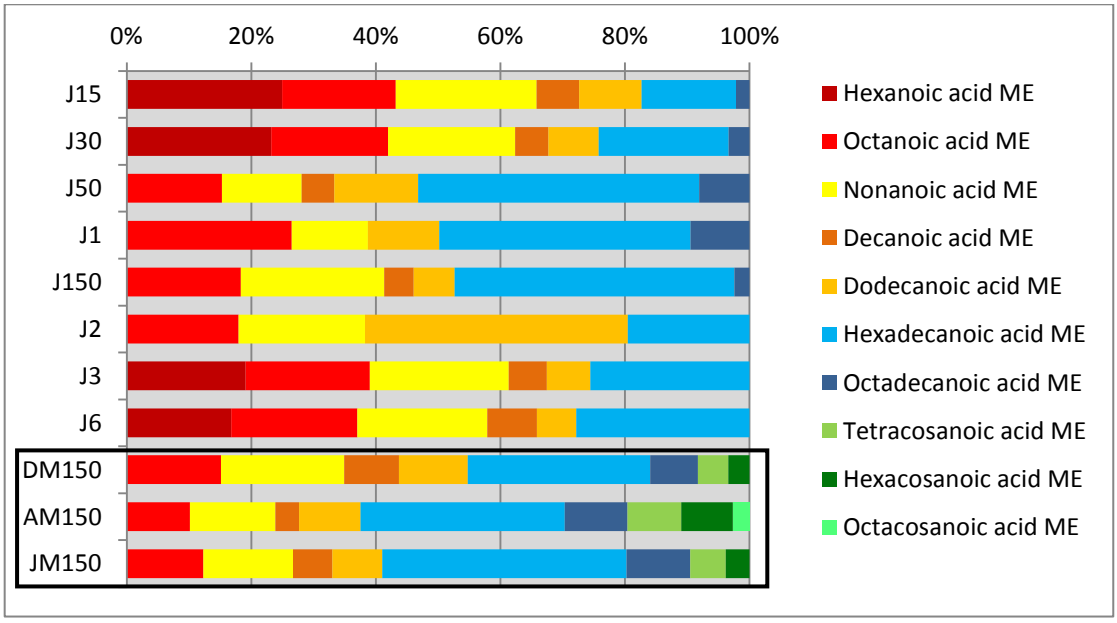

Figure 4.14: The distribution of FAMEs (as identified using single ion mode with a m/z of 74) for a depth profile Central site taken in June 2010, and also three seasonal samples from the Mid-bog site at 1.5 m depth (Dec '09, Apr '10 and Jun '10, highlighted by black box). The red-yellow palette show the 6:0 (hexanoic-) to 12:0 (dodecanoic-) FAMEs and the blue palette identify 16:0 and 18:0 FAMEs. The green palette identified long-chain FAMEs (>C_{20}) which are only found in Mid 1.5 m samples. Sample names on y-axis identify month and depth (cm).

Figure 4.14 shows the proportions of saturated FAMEs in a depth profile, as well as from the Mid-bog site at 1.5 m. Notably, three FAMEs with a chain-length of >20 carbon atoms were identified in the Mid-bog 1.5 m samples. Although FAMEs can be produced from a number of sources, microbial sources do not produce FAMEs > 18:0 (Frazier et al., 2003), and so these FAMEs must be derived from plant sources. It is striking how similar the distributions of FAMEs are in the two shallowest and two deepest samples from the June 2010 Central depth profile. All samples from intermediate depths (50 cm to 1.5 m) showed a different distribution pattern, with lower contributions from FAMEs < 16:0 and no identified hexanoic acid ME (6:0).

4.9 Nitrogen-containing compounds

There is a distinct shift in the main nitrogen-bearing species found with increasing depth. Figure 4.9 includes a selection of nitrogen bearing species, and these are mainly found in the surface samples. These heterocyclic species are pyridine- and pyrrole-related and appear in the early portion of the TICs. In deeper samples, nitrogen isalso found in nitrile species, notably in benzylnitrile[6] (2-phenylacetonitrile), octadecanitrile, hexadecanitrile and ethylbenzonitrile. At a depth of 3m in the centre of the bog, the variety of nitrogen bearing species has increased significantly, and this is supported by evidence from hydrolysable dissolved combined amino acid analysis which shows that a decreasing proportion of the measured total dissolved nitrogen in the water is attributable to specific amino acids.

It has been proposed that the unusual oxopolysaccharides in peat bogs (sphagnan) bind with amino acids and proteins at depth to produce aquatic humic substances, binding nitrogen into highly recalcitrant structures (Hàjek et al, 2011). The breakdown of proteins releases amino acids which can then undergo Maillard reactions in the presence of carbohydrates, to form stable humic substances (Kalbitz&

[6]Reported as a decarboxylation product of phenylalanine standard upon TMAH thermochemolysis by Gallois et al. (2007).

Geyer, 2002). This acts to increase the humic pool and protect organic nitrogen from mineralisation, preserving N within the peat profile and decreasing N availability in the peatland (Verhoeven & Liefveld, 1997). However, because specific nitrogen containing compounds were frequently found only in one sample or found to coelute with unknown compounds, it was not possible to include N-containing compounds in the current semi-quantitative analysis.

In order to assess the nitrogen content and chemically characterise the humic and fulvic fractions of DOM, further techniques are required, and this will be discussed in Chapter 6 which focuses on the high accuracy and precision mass spectrometry of four samples of DOM from Cors Fochno via electrospray ionisation Fourier transform ion cyclotron mass spectrometry (ESI FT-ICR-MS).

4.10 Carbohydrate-derived compounds

Four carbohydrate-derived compounds were identified in the majority of samples analysed (all 2-cyclopenten-1-one based compounds with alkyl side chains of 2-methyl-, 3-methyl-, 2,3-dimethy- and 2,3,4-trimethyl-) as have also been identified in other studies of natural DOM (Frazier at al., 2003; Frazier et al., 2005; Templier et al., 2005).

The relative response of the carbohydrate derived compounds is lower in deeper Central samples (depth < 1 m) and slightly lower in the Mid-site (1.5 m) samples than the 15 & 30 cm Central samples from the same periods (Table 4.13). Other than this change with depth, differences between samples are relatively minor and will not be focussed on individually.

	Dec 15	Apr 15	Apr 30	Jun 15	Jun 30	Oct 15	Oct 30	Feb 15	Feb 30	Jun 50	Jun 100	Jun 150	Jun 200	Jun 300	Jun 600	Dec Mid	Apr Mid	Jun Mid
C1	31	28	34	29	32	26	25	32	33	17	26	16	16	16	19	29	22	26
C2	16	21		10	29	18	10	27	28	14	21	8	12			14		17
C3	28	29	21	17	22	21	5	24	27	16	15	9	11	8	16	15	*	17
C4	10	11	13	14	21	9		16	8	14	17	9	6		20			

Table 4.13: The relative intensity of the four quantified carbohydrate-derived compounds for all samples: C1 = 2-methyl-2-cyclopenten-1-one, C2 = 3-methyl-2-cyclopenten-1-one, C3 = 2,3-dimethy-2-cyclopenten-1-one and C4 = 2,3,4-trimethyl-2-cyclopenten-1-one. Samples are as previously discussed, with month and depth (cm) indicated in the column header. The final three samples (indicated in red) are from the Mid-bog site at 1.5 m. Colours of table data are by season to aid the eye. Grey columns indicate depth profile.*Peak was present but coeluted with a very strong phenol peak and was not quantifiable.

TMAH thermochemolysis GC-MS does not have good sensitivity to carbohydrates (e.g. Cheftez et al., 2000; Shadkami & Helleur, 2010) and the addition of a methylation reagent (in this case TMAH) to conventional pyrolysis-GC-MS, while increasing the degree of information obtained on polar compounds, has been found to decrease the amount of information obtained on carbohydrates and related compounds (Templier et al., 2005). However, this data will be discussed further in Chapter 5, where principal component analysis (PCA) of all measured variables will be used to characterise samples.

4.11 Chapter synthesis and conclusions

Analysis of dissolved amino acids, carbohydrates, phenolic compounds, *n*-alkanes and fatty acid methyl esters revealed a high degree of heterogeneity between porewaters. Yields of DCAA and carbohydrates each span more than an order of magnitude, each contributing only a small amount (~3%) to the total dissolved organic carbon pool.Molecular characterisation was challenging as yields were low for the majority of samples. Despite the low analytical precision for some individual components of these pools, average distributions show clear trends.Semi-quantitative analysis of the products formed after TMAH thermochemolysis by GC-MS added further information on the composition of porewater DOM, and allowed a

more detailed characterisation of peatland DOM than has been published by any previous study.

The deepest porewaters were characterised by compounds which are of generally low solubility. *n*-alkanes dominate the TICs obtained by THM, although the products of phenolic compounds are also abundant at 6 m depth. Nitrogen concentrations are high, but the contribution from amino acids to the TDN pool are low, and there is a higher abundance of the more hydrophobic amino acids. THM also reveals a larger suite of nitrogen containing compounds at depth, including numerous nitrile-bearing compounds. FAMEs are also found in high relative abundance in the deepest porewaters, and are dominated by shorter-chain FAMEs (< 16:0) which may be indicative of a bacterial source, but are also the most labile of the FAMEs identified.

Intermediate depth porewaters (1-2 m) vary hugely between sample sites, although this may be a product of the hydraulic conductivity of the peat in which piezometers are embedded rather than location. Intermediate depth samples from the Central site resemble deeper waters, but with higher neutral sugar yields. Average distributions of individual neutral sugars reveals clear trends, with increased arabinose and fucose in shallow porewaters and a higher contribution from mannose and xylose at depth. Intermediate depth porewaters from the Mid-bog site (from piezometers sampling low hydraulic conductivity peat) have very high contributions from phenol derived compounds, which have mainly *p*-hydroxybenzyl and cinnamic structures. These compounds have been linked with the phenolics produced by *Sphagnum* species, and sphagnum acid derivatives are found abundantly in these DOM samples[7]. FAMEs are present in low apparent concentrations at intermediate depth, and have a low contribution from FAMEs < 16:0. Mid-bog samples at these depths contain longer chain (>20:0) FAMEs indicating a source from plant waxes or similar.

[7] No published studies have shown sphagnum acids derivatives from peatland porewaters, and they have not previously been thought to be significant at depth.

Porewaters from shallow depths are characterised by higher contributions of amino acids than at other depths, and these amino acids are made up of the less hydrophobic amino acid compounds (with, for example, low contributions from the aromatic amino acid tyrosine). Amino acids which are indicative of microbial activity and (the non-protein amino acids) are at their highest in Jun 2010, and ornithine (which is indicative of bacterial turnover of the protein pool)contributions are highest in Sep 2009 and Oct 2010. Phenolic compounds are dominated by benzoic acid structures, which are indicative of oxidative degradation. The phenolic compounds which have been linked to active excretion mechanisms by *Sphagnum* species (e.g. **P5** and the cinnamic compounds **P18** and **G18**) were found in highest relative abundance in Feb 2011 and Apr 2010, possibly indicating a slow build-up of these compounds over the winter, when microbial and bacterial activity will be low and therefore degradation rates will be at their slowest.

The significant changes in the composition of the DOM pool, over both spatial and temporal scales, is somewhat surprising considering the similar plant source materials and the apparent stability of this carbon reservoir as implied by its ^{14}C age (which has been shown to be 500-1000 years younger than the surrounding peat, Clymo & Bryant, 2008).However, internal cycling of DOC has been shown to be fast, with internal production and consumption rates many times higher than DOC export (Blodau et al., 2007). It must be borne in mind that firstly, the characterised portions of the DOM pool only contribute a small amount to total DOC, and secondly they are the most closely related to the plant and microbial source material and are more likely to be in the actively cycling carbon pool. Thus, although significant changes in composition are found between samples, it is possible that only a small fraction of the total DOM pool falls within the analytical windows of the techniques used so far, and a larger uncharacterised carbon pool is falling outwith these analyses. An insight into this uncharacterisable DOM will be obtained using ESI-FT-ICR-MS, which will be discussed in Chapter 6.

Chapter 5: The sources and fate of peatland derived DOM – a comparison of porewaters to the solid phase and runoff

5.1 Introduction

Chapter 4 reported the molecular characterisation of DOM in water samples taken from piezometers installed at different depths across Cors Fochno. The following chapter will compare the results presented in Chapter 4 with the analysis of solid peat material taken from two cores using complementary techniques and the water samples taken from a site which is thought to represent water leaving the peatland.

5.1.1 The source of peatland DOM – A comparison of solid and dissolved phases

Two cores from contrasting microtopographical features of the bog were analysed for C and N content, stable isotopes, amino acids, neutral sugars and phenolic compounds. A hummock and hollow were sampled to represent two end members of the peat which makes up Cors Fochno. Although these two cores won't encapsulate the chemical makeup of all peat on the site, they represent the wettest and driest environments found on the main dome of Cors Fochno and provide a useful reference against which the porewater characterisation presented in Chapter 4 can be compared. Peatland structures such as hollows, lawns and hummocks are formed and maintained by the differential between growth and decay rates between *Sphagnum* species in the different microhabitats (Rydin et al., 2006). Hollow species generally have a higher capacity for photosynthesis than hummock species, but are more prone to desiccation due to the hydrological controls exerted by tightly packed *Sphagnum* shoots in hummock features. Hummock species also exhibit higher resistance to decay, which allows hummock species to build topographical highs, and may help maintain capillary networks to greater depth than in hollows (Rydin et al., 2006 and references therein).

It has been noted that, at the centre of the bog, peat which underlies hummock-like features (with higher cover of non-*Sphagnum* species such as *Calluna vulgaris* and sedges e.g. *Eriophorum* spp.) is more decomposed than that found beneath lawns and hollows, which contain high cover of *Sphagnum* (Baird et al., 2006). Baird & Milner (manuscript in preparation) conducted a detailed study of the degree of decomposition and structure (measured on the Von Post scale) of 2 m cores from the centre of the bog. They found that, below raised features, a horizon of more decomposed peat frequently occurs at depths of 30-45 cm below the peat surface. A similar feature was found under some hollows (again at 30-45 cm below the peat surface), but generally the degree of decomposition was much less than under hummocks or ridges.

5.1.2 Transformations of organic matter – molecular characterisation of "lake" water and comparison to porewaters

When considering the transect along which the banks of piezometers have been placed, there is a flow of water from the central dome, through the mid section of the bog where drain blocking has raised the water table, to the edge of the site to then be drained by the Pwll Ddu. Figure 5.1 shows a schematic diagram of the drainage channels surrounding the bog, identifying several key fluxes of DOC between carbon reservoirs over the site. Modelling work on the southern side of the bog (Baird et al., 2006) has suggested that only 8-9.5% of net rainfall bypasses the lakes, flowing through the catotelm to the Pwll Ddu, and therefore characterisation of the water within the lakes provides an excellent opportunity to assess the molecular composition and quality of organic matter leaving Cors Fochno as DOM.

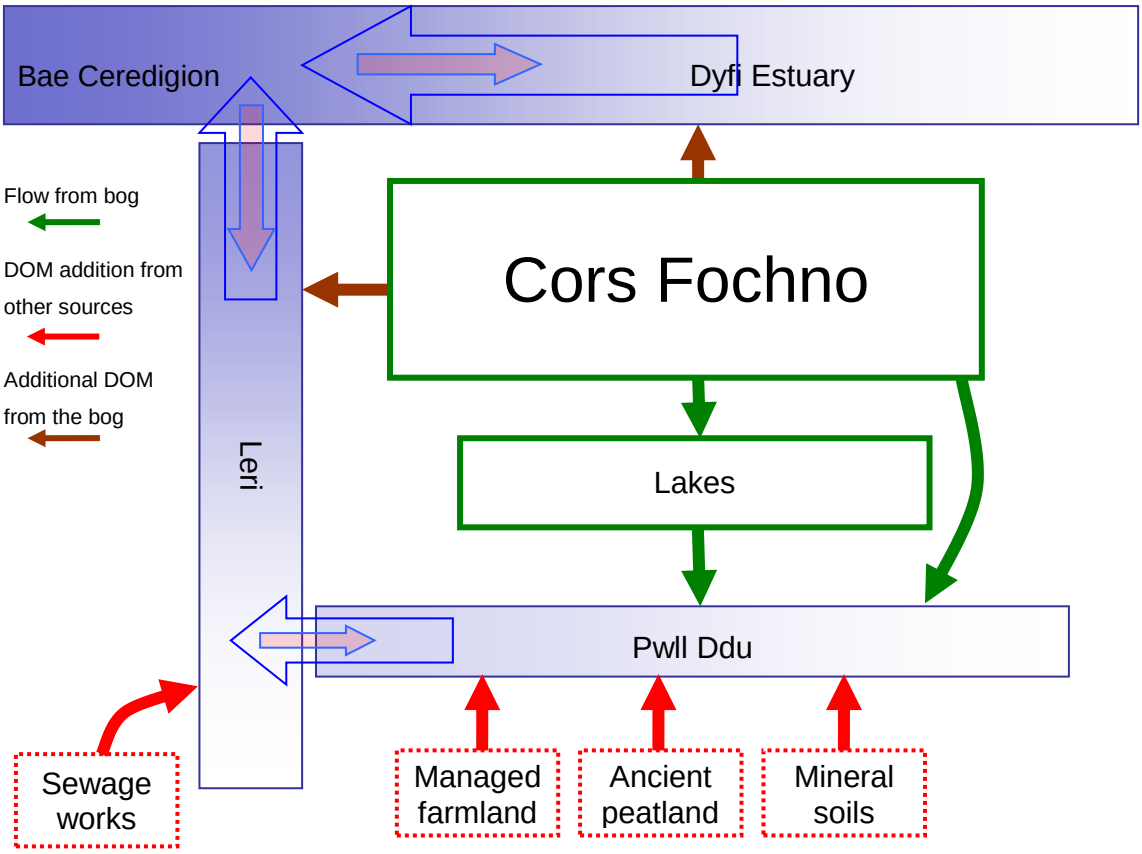

Figure 5.1.Schematic of water flow from Cors Fochno to the Bae Ceredigion via the Pwll Ddu and Leri. Green boxes represent sources of peat-derived DOM, red dotted boxes represent other possible sources of DOM, and long blue boxes represent waterways. Blue colouring in boxes denotes tidal influence (and presence of saline waters at high tide, with more intense blue indicating greater influence). Blue lined arrows denote water flow along waterways at high and low spring tide.

5.1.3 Objectives and approaches

The following chapter will focus on two objectives summarised in Chapter 1:

- To compare the DOM pool against solid phase peat cores using complimentary techniques
- Using the information gained from molecular characterisation, to assess the sources of peatland DOM and the molecular transformations or alterations this OM undergoes in different environments in the peatland

Comparison with the solid phase may help determine the sources of the DOM which has been characterised in previous chapters, and the degree of similarity between the solid and

dissolved phase may shed light on the mechanisms for release or production of DOM.Significant transformations may occur when porewater DOM leaves the peatland and becomes exposed to light, oxygen, changing water chemistry and new biotic communities. For this reason, the molecular composition of peatland porewater will also be compared to that of samples from the Lake, where many sources of OM will be similar, but environmental conditions differ considerably.

The approach taken will be similar to that taken in Chapter 4. Results from each analysis will be presented and interpreted in turn, using depth profiles and simple graphical representation to aid comparison. The carbohydrate and amino acid compositions of the solid phase will be compared to porewater compositions, and these will then be compared to compositions in runoff. Analysis of phenolic compounds in the solid phase by CuO oxidation will then be compared to the results from TMAH thermochemolysis in the same way. Two proxies (which have been adapted by the author for this study) will be used to assess degradation of phenolic compounds within water samples (see Section 5.5.3).

Finally, the results from multiple techniques will be analysed using principal component analysis (PCA) performed on a correlation matrix to assess compositional patterns and transformations which DOM undergoes in differing environments. Preliminary analysis of the data from each technique (separately) will be conducted in order to collate those variables from an analysis which co-vary (in order to reduce skewing of the PCA by, for example, the 18 quantified amino acids – See Section 5.6 for further details). The PCA will then be conducted using a final set of variables and the principal components used to explore differences between samples considering all analyses.

5.2 Carbon and nitrogen in peat cores

Figure 5.2 shows the results of CN content and stable isotope analysis from both cores. Analysis for total organic carbon (TOC) and total nitrogen (TN) of both cores showed an organic carbon content of 43 to 51% and a nitrogen content of 0.5 to 2.8%, values which agree well with other measurements from ombrotrophic peat cores (Comont et al., 2006). TOC

content was higher in the hummock setting, and increased with depth in both cores, corresponding to the decomposition of more labile material which generally has a larger number of functional groups and is richer in oxygen and heteroatoms. This may also account for the higher C content in the hummock, where decomposition rates may be higher due to a lower water table and more oxygen availability (e.g. Belyea & Clymo, 2001). As decay of fresh plant material proceeds, the organic pool becomes enriched in recalcitrant, carbon rich, unsaturated and aromatic material (Stevenson, 1994). Nitrogen content increases slightly with depth in both cores, with a deviation towards higher N content at between 24 and 28 cm seen in both cores (although this is more pronounced in the hollow).

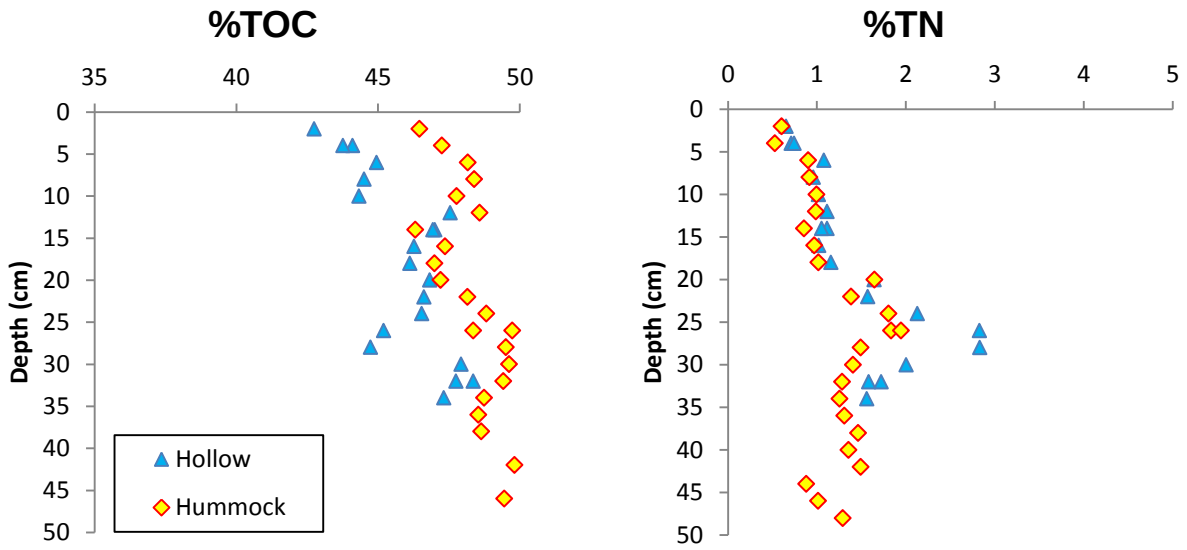

Figure 5.2: Percent total organic carbon and total nitrogen of solid core material.

5.3 Characterisation of carbohydrates in the solid phase and runoff waters

The following sections will focus firstly on the carbohydrate composition from two peat cores, then a comparison of the solid phase to the dissolved phase as characterised in Chapter 4. Finally, samples from the Lake site will be discussed, representing the flux of carbohydrates to surrounding water bodies.

5.3.1 Characterisation of neutral sugars in the solid phase

The yield of total sugars in core slices ranged from 344 to 1198 mgTCHO g^{-1}OC. Both cores from the hummock and hollow show the maximum percentage of TCHO carbon (48% in the hummock and 37% in the hollow) in the topmost 5 cm of the core, decreasing to ~20-30% in lower portions of both cores. A minimum (14-15%) in the %TCHO C is present in the hummock between 19 and 25 cm. Other than a maximum value near-surface, there is no clear trend in total sugar yields, but this finding is similar to those from other studies of peat profiles (Bohlin et al., 1989; Delarue et al., 2011). Yields are on average higher in the hollow (791 mg TCHO g^{-1} OC) than in the hummock core (641 mg TCHO g^{-1} OC), although this mainly reflects higher yields near-surface, and averages from below 20 cm are more similar (589 and 616 mg TCHO g^{-1} OCfor hummock and hollow respectively).

In order to address not only changes in total sugar yield, but also changes in the composition of this carbon pool, the weight percentage of each individual sugar quantified was calculated. Total sugars are dominated by glucose, which makes up 49-76% (by weight) of TCHO. Galactose and mannose also contribute significantly to TCHO, making up 4-20% of the sugars, whereas ribose and fucose only make up 0.03-1.3% of TCHO (see table 5.1).

	Ara	Rha	Rib	Xyl	Fuc	Man	Gal	Glu
MAX	7.52%	5.79%	0.27%	21.6%	1.26%	14.4%	20.5%	75.9%
MIN	1.24%	2.59%	0.03%	4.08%	0.42%	4.34%	5.41%	48.7%
MEAN	4.00%	4.33%	0.13%	10.4%	0.80%	8.05%	12.1%	60.2%

Table 5.1: the composition (as weight percent) of neutral sugars from both cores, showing maximum, minimum and mean values for each sugar.

Figure 5.3 shows contributions from individual sugars in down-core profiles. In the hummock core, galactose, rhamnose and mannose all have decreases in contribution with increasing depth (Figure 5.3). It is noteworthy that these sugars have been identified as being diagnostic of moss inputs, notably including *Sphagnum spp.* (Delarue et al., 2011; Comont et al., 2006). A decreasing proportion of these compounds with depth may therefore imply that either, in the past, mosses made up a smaller proportion of the fresh material from which the peat is derived, or that these moss-derived carbohydrates are being preferentially mineralised or

undergoing chemical transformations which remove them from the hydrolysable pool. Delarue et al. (2011) recently also found that these same moss indicators decreased with depth, and attributed this to changes in environmental conditions, having considered but rejected the possibility of preferential *Sphagnum* degradation. Although increased sedge inputs in the past (as Delarue et al. (2011) invoke) may be the driver in other systems, there is no supportive evidence that this is the cause of decreasing moss indicators at Cors Fochno. It is instead proposed that vascular plant root systems, which extend below the most microbially-active portion of the acrotelm (the top ~5 cm, Blodau et al., 2004), introduce a vascular plant signal at depth, which is then retained due to slow decomposition rates in the catotelm. Mapping of root biomass in cores taken from peatland hollows has shown that some root systems[1]can extend significantly below the water table, with substantial root densities (4 g dm^{-3}) found between 10 to 30 cm below the peatland surface (Moore et al., 2002) and it has also been shown that rates of decomposition can be several orders of magnitude slower in the catotelm than in the acrotelm (Beer & Blodau, 2007).

The glucose component of the cores increases with depth (Figure 5.3) which is further evidence against decreasing *Sphagnum* input in the past. Glucose is a structural component found in high concentrations in the cellulose of *Sphagnum* species (Jia et al., 2008), and an increase in the contribution of glucose suggests preferential removal of mannose, galactose and rhamnose from the hydrolysable monosaccharide pool, rather than a decrease in moss-input.

[1] Moore et al. (2002) mapped shrub roots, which may extend to different depths from sedge roots, but very little data is available in the literature regarding the depth of active root systems in peatlands.

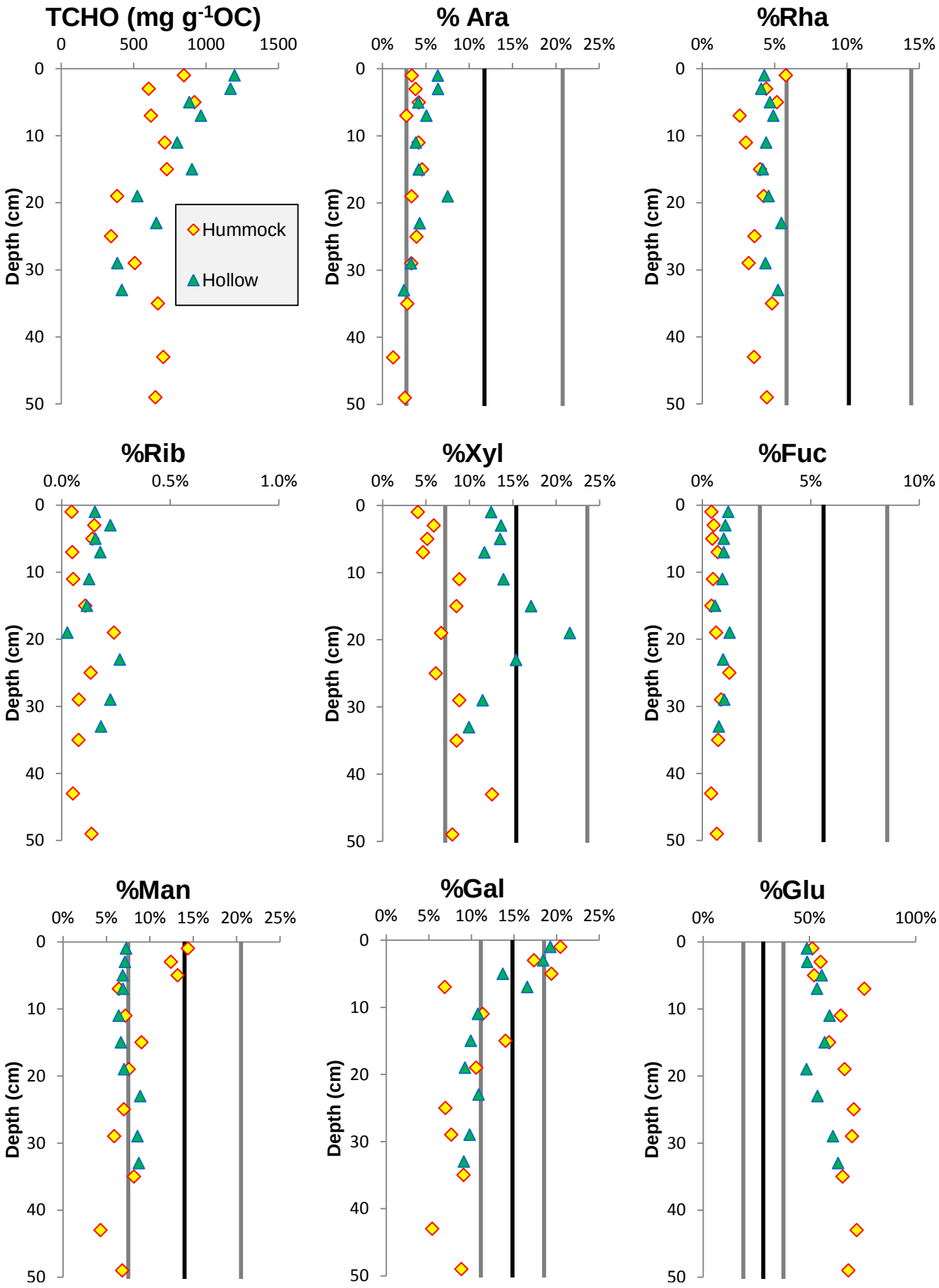

Figure 5.3: Total yield and weight percent of individual sugars found in core segments (yellow diamonds for hummock, green triangles for hollow). Also shown for reference is the average weight percent from the central piezometer array (black line) and degree of variation (+/- 1 standard deviation, grey lines) over all central piezometer depths. (Note: ribose was not included in dissolved carbohydrate quantification).

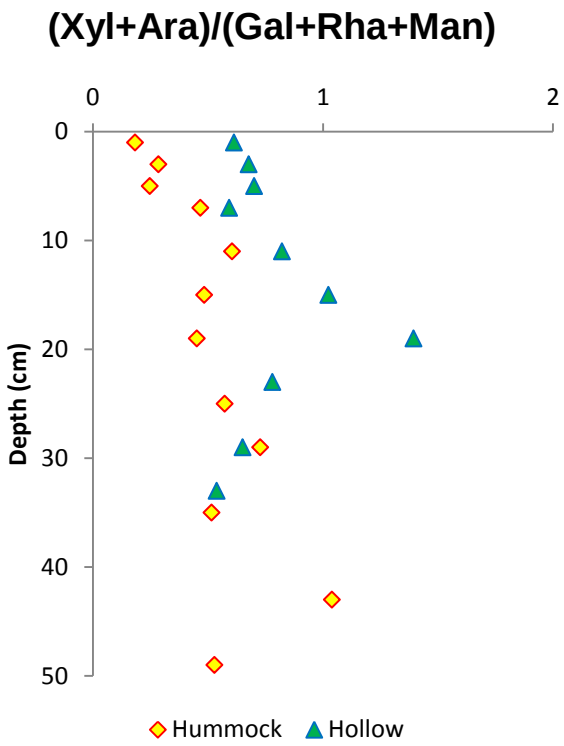

Figure 5.4: *Sphagnum* vs. sedge input indicator as suggested by Comont et al. (2006).

Comont at al., (2006) suggested that the proportion of xylose and arabanose to galactose, rhamnose and mannose [(Xyl + Ara) / (Gal + Rha + Man)] may be used as an indicator of peat source-material. Xylose and arabinose are diagnostic of *Cyperaceae*, and therefore an increase in this proportion suggests an increase in the contribution of sedges to the peat. Figure 5.4 shows this proportion for both the hummock and hollow cores, which display two clear features. Firstly, above 10 cm the hummock core displays the lowest values, indicating high *Sphagnum* input. Although cotton grass was present in both settings, it is possible that heterogeneity within the hummock features resulted in no fresh cotton grass being sampled in the hummock core. Secondly, there is a clear peak in the ratio at a depth of 19 cm in the hollow, perhaps indicating a layer of peat at this depth which has a high sedge input. A similar feature may be present at a greater depth in the hummock (only seen at 43 cm), but because the elevations of the two sampling locations were not measured (relative to a set datum), it is impossible to directly compare depths at which trends are seen between cores.

Carbohydrate analysis of solid cores provides an insight into the source material from which the DOM pool is mainly composed. The next section will focus on how the solid and dissolved OM pools differ with respect to neutral sugar content and composition.

5.3.2 Comparison of neutral sugars in the solid versus dissolved phase

The yield of neutral sugars is much higher in the solid phase than the dissolved phase (344 – 1198 mg g^{-1} OC for core samples compared to 35 – 275 mg g^{-1} OC for central porewaters). Figure 5.3 also shows how the composition of the dissolved phase differs from the solid phase. The solid black line in each plot in Fig. 5.3 of % contribution for an individual sugar (apart from ribose, which was not quantifiable in the dissolved phase) shows the mean % contribution in the porewater samples from the centre of the bog (all depths). This average is used because the precision of the method was low at low yields. It should be borne in mind that the weight percentage for the dissolved phase does not include ribose and, although ribose is only a minor constituent of peat cores, the percentage of all other sugars in the dissolved phase will be slightly higher because of this (~1%). The only sugar which is present in the solid phase at higher weight percent than in porewaters is glucose, which makes up around 50% of the solid peat material. Fucose, and to a lesser extent rhamnose, are particularly enriched compared to the total carbohydrate pool. Arabinose, xylose, galactose and mannose are also somewhat enriched in the aqueous phase, with average compositions above that of the peat. Notably, enrichment of arabinose in the dissolved phase has been suggested as an indicator of microbial activity (Spitzy, 1988) although care must be taken when interpreting the contribution of individual sugars due to the low precision of the analysis. Deviations in the dissolved pool away from the carbohydrate-composition of the solid phase (from which the majority of dissolved sugars will be derived) again suggest a preferential removal of some compounds from the peat as it is undergoes decay. As such, caution must be used when interpreting carbohydrate compositions in peat and inferring changes in vegetation input, with associated paleoclimatic implications (e.g. Comont et al., 2006; Jai et al., 2008).

Jia et al. (2008) determined the carbohydrate composition of 24 common peatland plant species, and found that not only are fucose and rhamnose present in high abundances in *Sphagnum*, but that they contribute most to the carbohydrate pool in hollow and lawn species, which the authors suggest may be due to the presence of bacteria in hyaline cell walls of submerged *Sphagnum*. Fucose has also been used as a biomarker for microbially-sourced organic matter (Comont et al., 2006) and it is likely that both fucose and rhamnose are present

due to mixed microbial and moss sources in peat cores. It is worth noting that galactose contribution varies substantially with depth through both cores, but shows less variation in porewaters (as indicated by the size of the standard deviation for all central porewaters, see Fig 5.3). Galactose content was suggested as an indicator of peat-decomposition by Bohlin et al. (1989), who found that arabinose, galactose and xylose content decreased with increasing degree of decomposition in peat, as measured on the von Post scale (*H*-value), although this did vary with peat type. Other authors have noted that arabinose and galactose are components of polysaccharides which are more degradable than other carbohydrates found in peatland environments (Jia et al., 2008).

5.3.3 The peatland as a dissolved carbohydrate source

Yields of neutral sugars are on average higher in the Lake samples than for porewater samples, with an average TCHO yield of 128 mg g^{-1}OC (min in Oct 2010 of 85.7 mg g^{-1}OC and max in Feb 2011 of 248 mg g^{-1}OC). This corresponds to between 3% and 10% of DOC as being derived from neutral sugars. The waters in the lake are sourced from runoff (both shallow and deep) and rainfall, and the high yields of carbohydrates may reflect inputs from very shallow depth horizons (i.e. < 15 cm which is the shallowest piezometer depth). Blodau et al. (2004) have shown that the majority of DOC is produced at or just below the vegetation zone (~ 5 cm) and these authors also found highest porewater DOC concentrations at this depth. Vertical movement of water is thought to be less significant than horizontal movement in peatlands (e.g. Waddington et al., 1998) therefore, if DOC is produced very close to the surface of the peatland, this fresh DOM may be better represented in lake samples than in piezometers.

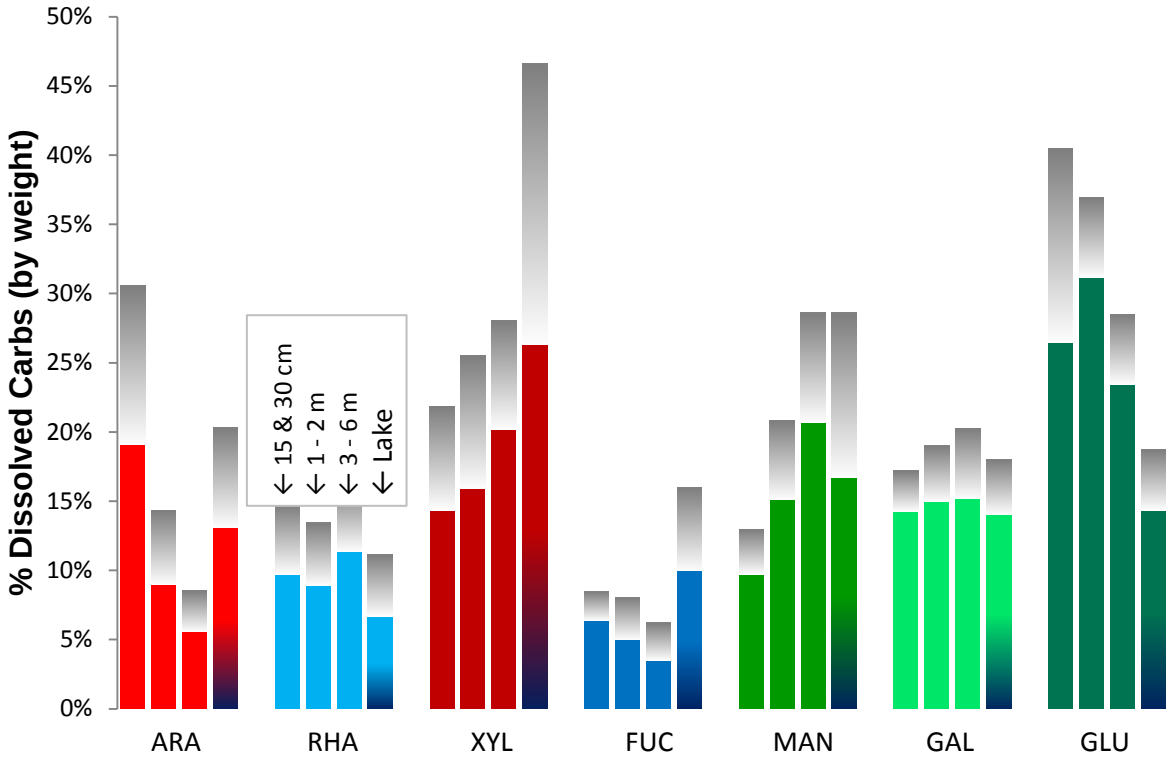

Figure 5.5: distribution of dissolved neutral sugars (as wt%) in porewater samples from the Central site and lake, with the Central samples averaged with depth (15-30 cm, 1-2 m and 3-6 m, n=7, n=7 and n=4 respectively) and the lake averaged over all analysed samples(n=5). Solid lines represent mean values, and grey shaded bars above represent 1σ. Colour indicates group; hexoses are represented in green, pentoses in red and the deoxysugars in blue. 4th sample in each set (the lake sample) highlighted with mixed shading to distinguish between sample locations.

Figure 5.5 shows the average distribution of neutral sugars quantified (note that ribose is not included due to low yields and poor peak resolution). Xylose and fucose are found in high relative abundance, particularly in Feb 2011, when xylose contributed 61% to the TCHO pool.If this anomalously high peak is removed from the calculation, an average Lake value of 17%[2] is found, which is intermediate between the deepest (3-6 m) and mid-depth (1-2 m) porewaters (Figure 5.5). Glucose and rhamnose appear to contribute proportionally less to the TCHO pool in the Lake than in other porewaters, but this is somewhat due to the very high xylose content of these samples. Again, due to the low precision of individual sugar analyses, caution must be used when interpreting individual numbers.

5.4 Characterisation of amino acids in the solid phase and runoff waters

[2]Which shifts all other values by ≤ 2%.

As in the previous sections, the following results and interpretation of amino acid analyses will focus firstly on the analysis of two peat cores, then a comparison of the solid phase to the dissolved phase and finally samples from the Lake site will be discussed.

5.4.1 Characterisation of amino acids in the solid phase

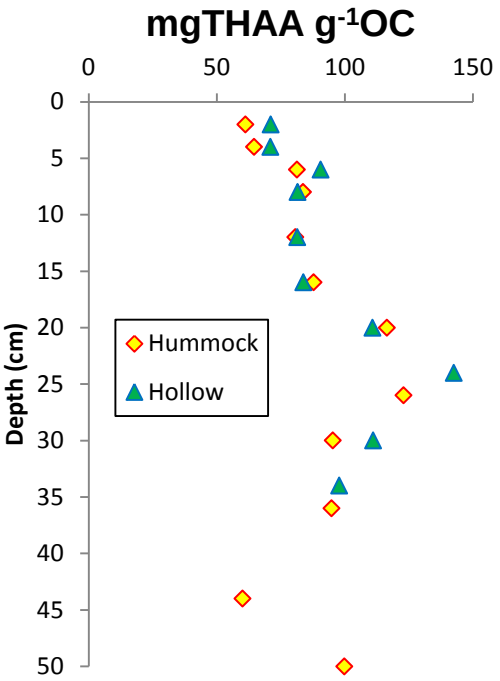

Figure 5.6: Total hydrolysable amino acids with depth for hummock and hollow cores.

The yield of total hydrolysable amino acids (THAA) varies between 60 and 143 mgTHAA g^{-1}OC (Figure 5.6) with a maximum value in both cores at ~25 cm depth below the peat surface. Yields are remarkably similar between the two cores, both showing a distinct increase with depth in the upper 25 cm of the core and a decrease below this depth. Amino acid-bound N makes up between 41-85% of the total nitrogen pool, contributing more substantially to TN near the top of cores; amino acids are evidently an important component of the nitrogen pool in the peat, and this is supported by the fact that the maxima in amino acids yield fit very closely with the maxima in TN content discussed above.

Solid cores show only small amounts of variability in the molar percentages of individual amino acids. If the variability between the molar percentage contribution of each individual amino acid is considered, a higher degree of variation can be seen in the hummock core (Table 5.2) which may be due to more variation in environmental factors (e.g. redox conditions) through the core profile which result from the core spanning the acrotelm/catotelm boundary. The dominant amino acids found in both cores are alanine (~14% molar contribution), glycine (~13%), aspartic acid (~10%) and glutamic acid (~10%).

The amino acids with the strongest downcore trends (that is with systematic changes, although not necessarily of large magnitude) are the acidic pair, aspartic- and glutamic-acid,

and threonine which all decrease in relative concentration with increasing depth, and alanine, tyrosine, and valinine which all contribute more to the overall yield downcore (Figure 5.7). Ornithine also contributes more with depth, although there is a slight decrease in the molar percentage at depths greater than 30 cm in the hummock core. Phenlyalanine and leucine do not show any large trends, although there may be a slight decrease with depth in the upper 25 cm to then increase with depth below this point; the clear trend is that these amino acids, in addition to lysine, all decrease with increasing depth in the upper 20 cm of both cores. The contribution from arganine increases over the first 8 cm in the hummock core, then remains stable at ~9%, which is similar to the contribution to the hollow core throughout. Contributions from serine, histadine, methionine and glycine all vary slightly with depth, although there is no clear trend in these changes, and isoleucine varies little with depth.

	Hummock Std Dev	Hollow St Dev	Hummock Mean	Hollow Mean	Hummock Rel. Std Dev	Hollow Rel. Std Dev	Trend with depth
Asp	0.8%	0.5%	10.2%	10.4%	8.0%	5.2%	↓
Glu	1.1%	0.9%	9.8%	9.4%	11.1%	9.7%	↓
Ser	0.4%	0.5%	7.8%	7.7%	5.2%	6.6%	
His	0.3%	0.2%	2.2%	2.2%	12.3%	10.4%	
Gly	0.6%	0.6%	12.7%	12.5%	4.6%	5.0%	
Thr	0.5%	0.4%	0.9%	0.9%	59.0%	42.0%	↓
Arg	0.8%	0.4%	9.0%	8.5%	9.1%	4.1%	↑*
Ala	0.6%	0.8%	13.6%	14.1%	4.5%	5.7%	↑
B Ala			0.1%	0.0%			
Tyr	0.2%	0.2%	2.4%	2.7%	6.7%	7.3%	↑
GABA	0.1%	0.1%	0.2%	0.2%	45.0%	69.1%	↓
Meth	0.1%	0.1%	0.9%	0.8%	12.1%	14.8%	
Val	0.6%	0.4%	8.4%	8.4%	7.0%	4.4%	↑
Phe	0.2%	0.1%	4.1%	4.1%	5.9%	2.2%	
Iso	0.2%	0.1%	5.1%	5.2%	4.6%	2.7%	
Leu	0.4%	0.4%	8.4%	8.2%	5.3%	5.2%	↓
Orn	0.1%	0.1%	0.2%	0.3%	39.0%	20.4%	↑
Lys	0.3%	0.2%	4.0%	4.4%	6.9%	5.2%	

Table 5.2: Statistics from analysis of amino acids in two cores, showing the standard deviation, mean and relative standard deviations of each amino acid quantified. Also shown is any trend found with increasing depth (down arrows in pink indicate a decreasing contribution with increasing depth; up arrows in blue indicate an increasing contribution). Note that no values are given for the standard deviation of β-alanine as it was only found in levels above the detection limit of the method in one core slice. *The downcore increase in the contribution from arganine is only seen in the upper section of the hummock.

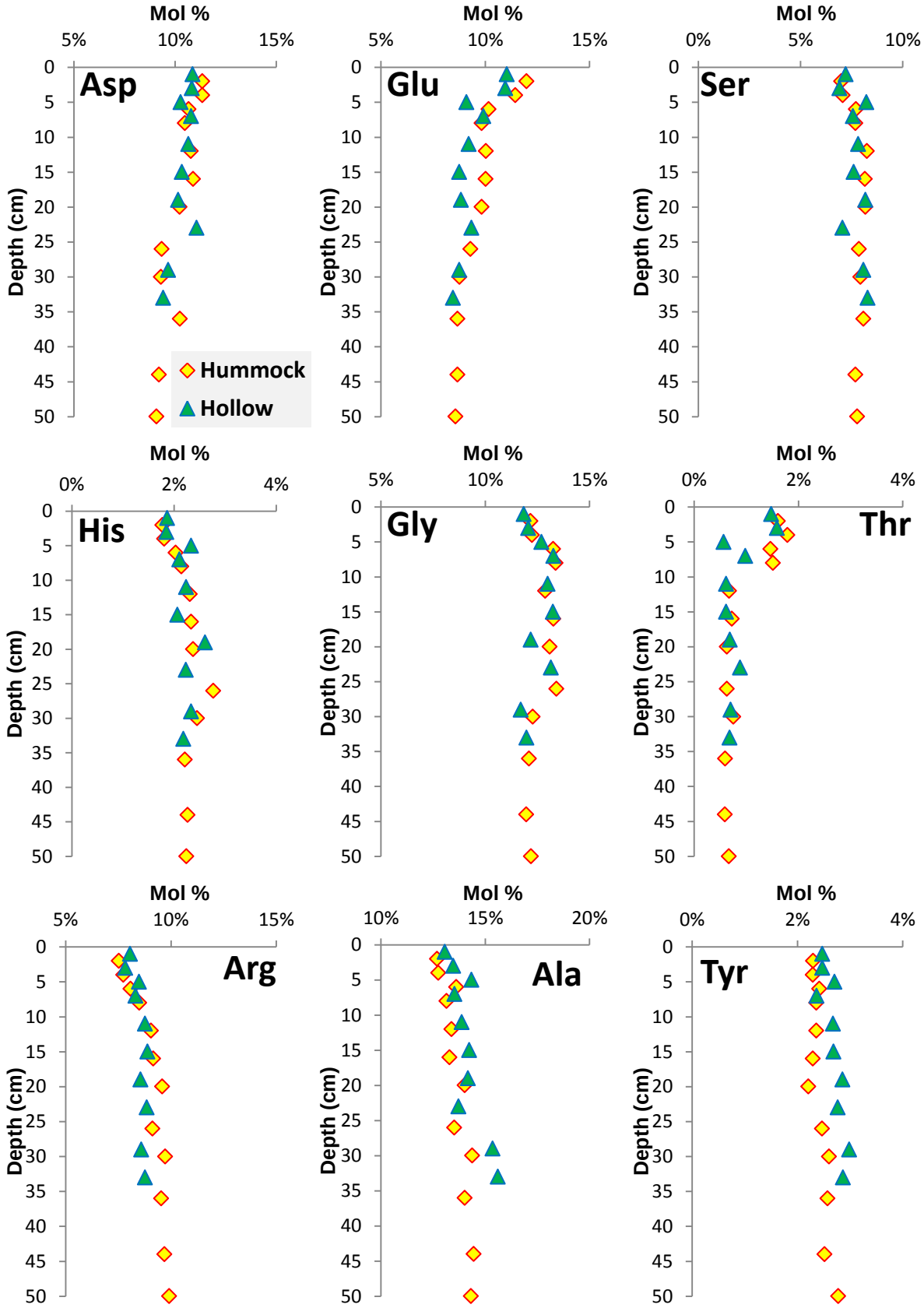
Asp
Glu
Ser
His
Gly
Thr
Arg
Ala
Tyr
Mol %
Depth (cm)
Hummock
Hollow

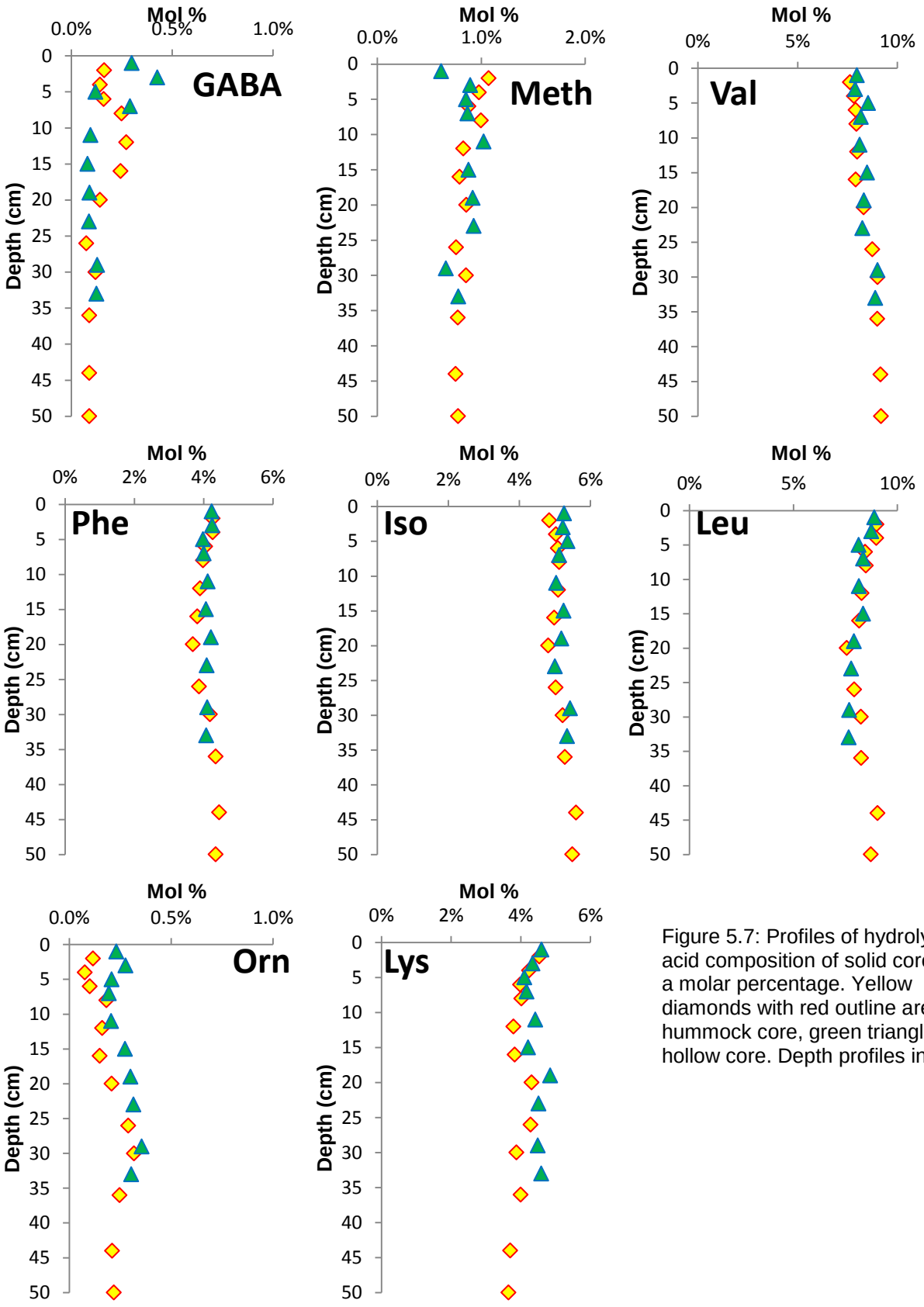

Figure 5.7: Profiles of hydrolysable acid composition of solid cores as a molar percentage. Yellow diamonds with red outline are hummock core, green triangles are hollow core. Depth profiles in cm.

The non-protein amino acids (the non-alpha β-alanine and γ-amino butyric acid and ornithine) all contribute very small amounts to the hydrolysable amino acid pool, in total making up less than 1% of the total yield (by molar ratio). β-alanine is only found in one core slice (the hummock at 26 cm), and so is effectively absent from the core analysis. The depth at which β-alanine is found has a particularly high amino acid yield, and may also have small peaks in the non-protein ornithine as well as glycine and alanine which have been shown to be the degradation products of other amino acids (Riboulleau et al., 2002). There is no peak in γ-amino butyric acid contribution at this depth.

5.4.2 Comparison of amino acids in the solid versus dissolved phase

Hydrolysable amino acids make up a larger proportion of the organic carbon pool in the peat cores than in porewaters (60 to 143 mgTHAA g^{-1}OC in the solid phase compared to 8 to 104 mg g^{-1}OC from porewaters). The solid phase amino acid composition in the hummock and hollow cores are remarkably similar, as can be seen from the mean values in Table 5.2. Only small amounts of variation occur (systematically) with depth (Fig 5.6) and therefore this variation (with depth) between core samples can be captured by averaging the top and bottom sections of both cores. Figure 5.8 shows a comparison of the average amino acid composition with depth in the dissolved phase (Central site as presented in Chapter 4) with the average composition found in the top and bottom of the core segments. The "top" slice is averaged over the upper 6 cm of both cores (i.e. the first three 2 cm slices, n=6) and include fresh plant material. The "bottom" slice is an average of the analysed slices from the deepest 30% of each core (the deepest two slices from hollow and three from the hummock). These two average segments have been created to act as two "end members" (shallow and deep) to aid comparison with porewaters.

The proportion of amino acids with hydrophobic side chains is higher in the solid phase than the dissolved, and there are some stark contrasts between the solid and dissolved phases; non-protein amino acids are almost entirely absent from the solid phase, with much higher contributions from the non-alpha amino acids β-alanine and γ-amino butyric acid (β-alanine is only found in one core slice) and the alpha, but non-protein amino acid ornithine. The relatively high contribution of non-alpha amino acids is indicative of a microbial influence,

and enrichment of ornithine in the dissolved phase has been shown to indicate bacterial reworking of protein-derived amino acids (Spitzy, 1988). Glycine, threonine and aspartic acid contribute more to the dissolved pool of amino acids, whereas the less soluble and aromatic tyrosine and phenylalanine are relatively more abundant in the core material. Methionine, the only quantified sulphur-containing amino acid, is also present in higher relative abundance in the solid cores than in the dissolved phase, although it remains only a minor constituent.

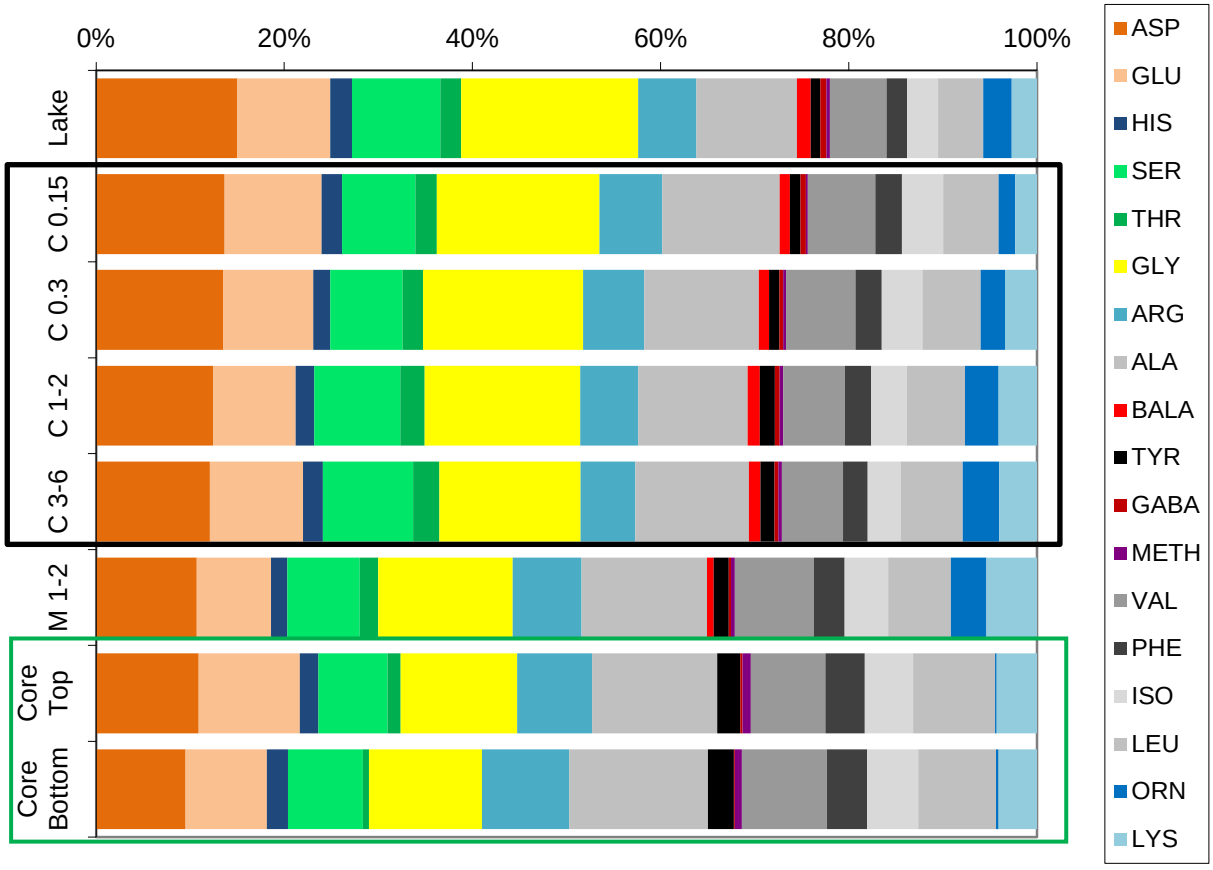

Figure 5.8: the average contribution of individual amino acids to THAA in molar percent. The top six bars are all from water samples and represent contribution to DCAA. The bottom two bars are a comparison to the solid phase. The sample names on the y-axis are derived from the site of sampling (C= centre, M= mid) and the depths in m over which the samples were averaged. The box in black is to aid the eye in comparison of a depth profile from the same site (centre, depths 15 cm to 6 m). The samples in the green box at the bottom of the plot (solid phase analysis of cores) represent the average contribution of the top 6 cm and the bottom 30% of the two cores studied to give an indication of downcore changes.

5.4.3 Cors Fochno as a dissolved amino acid source

Amino acid analysis was carried out on all samples from the Lake site. Yields of total DCAA are on average slightly lower than the majority of porewater samples, averaging 25.8 mg g^{-1}OC

(with a minimum of 16.5 mg g^{-1}OC in Feb 2011 and a maximum of 47.4 mg g^{-1}OC in Apr 2010, Table 5.3). To some extent this may be because yield is here being expressedin mg g^{-1}OC and are thus influenced by DOC concentrations: higher DOC concentrations were observed in the lake when samples were taken in October, whereas low concentrations were found in April 2010. Changes in the overall size DOM pool may not be coupled with changes in the size of the amino acid pool. The average yield of DCAA equates to an average of 8% of TDN and 1.1% of DOC being bound in dissolved amino acids, which is again lower than the corresponding values for shallow porewaters (≤ 30 cm depth) at the central site.

Sampling Month	[DOC] (mg C l^{-1})	[TDN] (mg N l^{-1})	$C:N_{(a)}$	Total DCAA (mg g^{-1}OC)	%AA-N	%AA-C
Sep 09	34.3	1.43	28.0	18.9	6.1%	0.8%
Dec 09	14.0	0.53	30.7	32.1	11.2%	1.4%
Apr 10	17.8	0.61	33.8	47.4	19.8%	2.0%
Jun 10	31.2	1.35	27.0	25.0	8.0%	1.1%
Oct 10	20.3	3.91*	6.0	30.3	2.2%	1.3%
Feb 11	16.8	0.37	53.4	16.5	10.2%	0.7%
Apr 11	20.5	0.81	29.4	32.1	11.2%	1.4%

Table 5.3: Amino acid data from the Lake site across all sampling periods (month in first column). Total yield of DCAA and associated percentages of TDN and DOC which are amino acid derived (%AA-N and %AA-C). DOC, TDN and the atomic C to N ratio are also presented for comparison. *Possible contamination.

The lowest TDN concentration (at the Lake site) was found in Feb 2011 which corresponds with the lowest DCAA yield. A high TDN was measured for Oct 2010 and the C:N ratio falls to 6.0 (> 5 times lower than the average), but as previously discussed in Chapter 4, the precision of TDN measurements in the later sampling seasons may be low due to a small number of sample vials having large nitrogen blanks. Although it is possible that DOC and TDN become decoupled at certain times, no duplicate Lake sample was available from Oct 2010 to confirm the high TDN concentration and therefore this feature will not be discussed further.

Figure 5.8 shows the average molecular distribution of amino acids from all Lake samples, with comparisons to porewaters and cores. The non-α amino acids (β-alanine and γ-amino butyric acid) have high relative abundances, indicative of a significant contribution from microbial biomass. Ornithine (the other non-protein amino acid) does not make a significantly higher contribution to the DCAA pool, varying from 1.8% to 3.9% which is well within the

range of values from porewaters taken from within the peat profile. Aspartic acid and glycine have larger molar percentage abundances in the Lake samples than in all other sample types, contributing more than a third in total to the DCAA pool, with much higher contributions than to solid cores.

All the amino acids with hydrophobic side chains (arganine, alanine, tryrosine, valine, phenylalanine, isoleucine and leucine, displayed in grey to black tones in Figure 5.8) are found in lower relative abundances in the Lake sample than in the piezometer water samples, and are found in much lower abundances than in the core samples.

5.5 Characterisation of phenolic compounds in the solid phase and runoff waters

As in the previous sections, the following results and interpretation of phenolic compound analyses will focus firstly on the analysis of two peat cores (with data from CuO oxidation), followed by comparisons to semi-quantitative data from TMAH thermochemolysis GC MS from both porewaters and Lake samples.

5.5.1 Characterisation of phenolic compounds in solid peat

Analysis of phenolic compounds fromthe two cores used in this study was carried out as part of two undergraduate projects (D. Elias and J. Dallas-Ross, both at the University of Edinburgh), and will be presented here for purposes of comparison to the dissolved phase. CuO oxidation allows quantification of eleven phenols which are separated into groups by methylation state and functionality, those groups being the unmethylated *para*-hydroxybenzenes (P), methylated vanillyl compounds (V), di-methylated syringyl compounds (S) and cinnamic compounds (C) which contain a trans propenoic acid side-chain. The P, V, and S groups each contain three phenols, an aldehyde, ketone, and carboxylic acid, and the C group contains two acids which differ by methylation state (see Table 5.4). Core slices were chosen according to visual assessment of the core (aiming as best as possible to sample at or

between any changes in colour or texture) at low resolution; only six slices per core were analysed due to the time constraints of the associated projects.

Compound		IUPAC nomenclature	THM analogue
p-hydroxybenzaldehyde	P	4-hydroxybenzaldehyde	P4
p-hydroxyacetophenone	P	4'-hydroxyacetophenone	P5
p-hydroxybenzoic acid	P	4-hydroxybenzoic acid	P6
vanillin	V	4-hydroxy-3-methoxybenzaldehyde	G4
acetovanillone	V	1-(4-hydroxy-3-methoxyphenyl)ethanone	G5
vanillic acid	V	4-hydroxy-3-methoxybenzoic acid	G6
syringaldehyde	S	4-hydroxy-3,5-dimethoxybenzaldehyde	S4
acetosyringone	S	1-(4-hydroxy-3,5-dimethoxyphenyl)ethanone	S5
syringic acid	S	4-hydroxy-3,5-dimethoxybenzoic acid	S6
p-coumaric acid	C	3-(4-hydroxyphenyl)prop-2-enoic acid	P18
ferulic acid	C	3-(4-hydroxy-3-methoxyphenyl)prop-2-enoic acid	G18

Table 5.4: Phenolic compounds quantified using CuO method, their grouping, IUPAC name (as these are used throughout discussion of TMAH thermochemolysis etc.) and the analogous methylated compound from thermally assisted hydrolysis and methylation.

Table 5.5 lists the composition of the lignin phenol pool in both cores as weight percentages. Note that the THM analogue name is used in the table for ease – the results from CuO oxidation are usually expressed as the compound names in the first column of Table 5.4.

Total phenol yields from the CuO oxidation of cores range from 10.9 to 57.3 mg g^{-1}OC, which is comparable to yields of amino acids from cores (Table 5.5). This equates to between 0.6% and 3%of carbon in the organic pool. There is an increase in the yield of phenols with increasing depth in the hummock core, especially over the top 10 cm of the core, after which concentrations are comparable to the hollow core, where the yield varies with depth but with no clear pattern. Given the low resolution, it is not possible to assign a mechanism for these changes, although it may be that, due to the availability of oxygen below the hummock, lignin or phenolic compounds are partially degraded, removing material from the compound pool that is quantifiable by CuO oxidation GC-MS. Enzymatic degradation of large aromatic structures usually occurs via phenol oxidase, and the oxygen requirements for this mechanism are high (Freeman et al., 2001).

	Depth (cm)	P4 (P)	P5 (P)	P6 (P)	G4 (V)	G5 (V)	G6 (V)	S4 (S)	S5 (S)	S6 (S)	P18 (C)	G18 (C)	Yield (mg g^{-1} OC)	% Phenol C
Hummock	1-2	3%	1%	5%	21%	5%	6%	28%	7%	6%	10%	9%	10.9	0.6%
	7-8	3%	2%	5%	24%	6%	7%	21%	5%	6%	9%	12%	19.7	1.0%
	19-20	3%	2%	12%	21%	7%	11%	14%	4%	6%	6%	14%	22.1	1.1%
	25-26	3%	1%	13%	19%	8%	14%	12%	4%	5%	7%	14%	24.1	1.2%
	35-36	4%	4%	8%	18%	6%	8%	17%	5%	6%	12%	11%	30.6	1.6%
	49-50	5%	5%	11%	16%	5%	7%	14%	4%	5%	12%	17%	28.7	1.6%
Hollow	1-2	8%	11%	8%	10%	3%	3%	16%	6%	4%	22%	10%	43.0	2.5%
	11-12	7%	10%	10%	17%	4%	5%	18%	5%	4%	12%	8%	33.6	1.8%
	15-16	6%	8%	6%	20%	4%	5%	24%	5%	4%	11%	6%	48.1	2.6%
	19-20	5%	5%	4%	23%	5%	7%	21%	5%	5%	13%	7%	57.3	3.0%
	29-30	6%	7%	7%	19%	6%	8%	18%	6%	6%	10%	8%	36.6	1.9%
	33-34	7%	8%	8%	18%	5%	8%	18%	5%	6%	9%	8%	31.8	1.7%

Table 5.5: The composition, total yield and percentage of organic carbon as phenols for all samples analysed. Cores are identified in column one, and depths of the core slices analysed in column two. Compositional data are given as weight percentages, named (for ease) using THM homologues (see Table 5.4). The % phenol C is the percentage of TOC which can be attributed to phenolic compounds. Columns with data in green highlight those compounds which have been reported as being produced by *Sphagnum* (i.e. not as part of the lignin pool).

The major constituents of the phenol pool are the vanillyl and syringyl aldehydes (equivalent to G4 and S4).There is a relatively small contribution from *p*-hydroxyphenyls, and these compounds decrease in relative abundance over the top 20 cm of the hollow core. *p*-hydroxybenzoic acid and the cinnamic compounds are particularly variable in abundance, although with no clear patterns with depth.

CuO analysis of fresh plant material from Ryggmossen bog in central Sweden (analysed using same equipment and protocol; unpublished data courtesy of G. Cowie) has indicated that cottongrass (*Eriophorum vaginatum*) has a very high phenol component from *p*-hydroxyacetophenone (P5 homologue) which accounts for 55% of the total lignin-phenol yield. If, as suggested by the composition of neutral sugars, sedge inputs were high at ~19 cm in the hollow core (see Section 5.3), the phenol distribution might be expected to reflect this. This is not the case, which may indicate that the lignin component of cottongrass is derived more from the above-ground plant material, and the monosaccharides which are indicative of sedge input at 19 cm result from root material. This lends further support to the view that the [(Xyl +

Ara) / (Gal + Rha + Man)] ratio changes discussed in Section 5.3 do not reflect an increased input from sedges in the past.

5.5.2 Comparison of phenolic compounds in the solid versus dissolved phase

Because different methods are used to analyse solid phase and dissolved phase samples for phenolic compounds, the results are not directly comparable. CuO oxidation GC-MS (as used for the analysis of the solid phase samples) results in a simple suite of lignin proxies: TMAH thermochemolysis (used on the dissolved phase samples) results in a larger suite of phenol-derived compounds which are then used to infer the parent material, but conventional (non ^{13}C labelled) TMAH treatment results inphenol indicators which are less indicative of plant source (i.e. resulting from hydrolysable tannins, lignin and polyphenolics). During this study, a semi-quantitative approach has been taken when analysing data from TMAH thermochemolysis GC-MS, whereas CuO oxidation GC-MS is quantitative. Comparative studies have shown that even when used quantitatively, yields from the two methods differ significantly (e.g. Wysocki et al., 2008).

Comparisons can be made between the relative distribution of those 8 compounds that are measured in both analyses (i.e. the ketone and acidic functionalities of P, V and S groups and the cinnamic compounds). In the analysis of cores, the acidic and ketone containing P, V and S compounds are found in similar average abundances, with the acidic group (equivalent to P6, G6 and S6) found at similar or slightly higher abundances than their ketone homologues (P5, G5 and S5). The average contributions (as weight %) from all six of these compounds only vary from 5% to 8%, together contributing just more than a third to the total phenol pool, and split by group, their abundance order is P > G > S. Both the cinnamic compounds (equivalent to P18 and G18) individually contribute > 10 % on average to the core phenols.

The equivalent 8 methoxybenzene products resulting from TMAH thermochemolysis GC-MS are dominated by the acidic functionalities (P6, G6 and S6), but with no clear compound as the dominant of the three. For example, on average, porewater samples from the Central wells at 15 cm (all seasons) have highest contributions from P6 (average abundance relative to

referencing peak of 21.8), then G6 (17.7) and S6 (10.1) followed by G5, P5, P18 and G18 (all < 10). At 30 cm, G6 becomes dominant (51.5) followed by S6 then P6 (29.3 and 22.0 respectively), and P5 is also found in greater abundance (12.9). The cinnamic equivalents (P18 and G18) are found in only low abundances (average < 10), but as discussed in Chapter 4, several other studies of natural DOM have found no phenolic compounds with alkyl side chains of greater than two carbons in length (Frazier et al., 2003; Frazier et al., 2005; Maie et al., 2006; Mannino & Harvey, 2000) and it has been suggested that biotic reworking of phenolic compounds preferentially removes these cinnamic derivatives.

Porewaters from intermediate-depth at the Mid-bog site have very high methoxybenzene abundances, and are worth considering separately in comparison to the cores. Of the 8 compounds which result from both analysis techniques, the Mid porewater samples are dominated by the *p*-hydroxy ketone and acid (equivalent to P5 and P6), followed by *p*-coumaric acid, vanillic acid and ferulic acid (P18, G6 and G18). These compounds are notably the most variable components from the solid phase analysis; Table 5.6 shows the standard deviation and relative standard deviation in the solid phase and the average relative abundance of all phenolic compounds identified after CuO oxidation GC-MS.

	P4 (P)	P5 (P)	P6 (P)	G4 (V)	G5 (V)	G6 (V)	S4 (S)	S5 (S)	S6 (S)	P18 (C)	G18 (C)
Ave wt %	5	**5**	**8**	19	**5**	**7**	19	**5**	**5**	**11**	**10**
St Dev	2	**3**	**3**	4	**1**	**3**	5	**1**	**1**	**4**	**3**
Rel St Dev (A)	36%	**65%**	**37%**	20%	**27%**	**41%**	25%	**16%**	**13%**	**36%**	**33%**
M1.5 Ave abundance THM (B)	-	71	52	-	8	38	-	5	0	51	9

Table 5.6: A comparison of the variability of phenolic compounds in the solid phase with the concentration in porewaters from the high-DOC regions at mid-depth in the Mid bog site. The first three rows show the average molecular composition of all core slices (as a weight percentage) and the standard deviation (both absolute and relative) of each compound (n=12). The 4th row (highlighted in orange) shows the average abundance (relative to the referencing peak) of the equivalent methoxybenzene compounds (see table 5.4) derived from TMAH thermochemolysis for all Mid-bog 1.5 m samples analysed (n=3).

The TICs resulting from TMAH thermochemolysis of Mid intermediate-depth (high DOC) porewaters show much higher abundances of methoxybenzene compounds than all other porewater samples (as discussed in Chapter 4). Although the 8 compounds derived from the CuO oxidation method are not the dominant methoxybenzene compounds in the M1.5

samples, there does appear to be a strong relationship between the relative abundance of these compounds in the dissolved phase and their variability in the solid phase. Figure 5.9 shows a basic linear regression of the relative methoxybenzyl abundances (Mid 1.5 m depth porewater)against the standard deviation of homologues from the solid phase analysis with a line of best fit as calculated by Excel. The high R^2 value (0.7687) corresponds to a p-value of < 0.01, suggesting that the relationship has a high level of statistical significance.

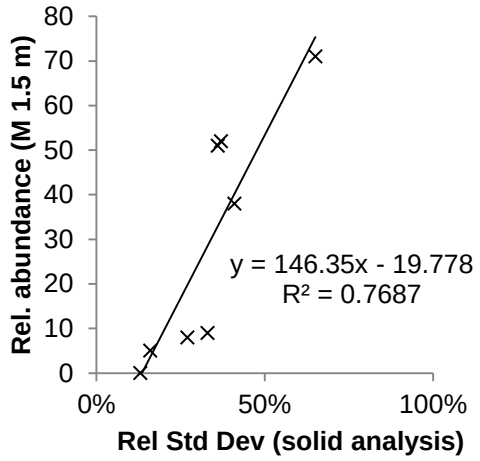

Figure 5.9: The strong relationship between the relative standard deviation of individual phenolic compounds as found in solid cores by CuO oxidation, and the relative abundance of those phenols in the Mid intermediate-depth porewater samples.

Generally, there is a large difference between the distribution of phenolic compounds found by the two different methods, but this is likely due to the inclusion of compounds resulting from the methylation of tannin and polyphenolic compounds in the thermochemolysis results (Filley et al., 2006). Because this technique is only being used semi-quantitatively and without ^{13}C labelled TMAH in this study, it is impossible to ascertain the contribution from these different phenol pools.

5.5.3 Cors Fochno as a dissolved phenolic compound source

Three samples collected from the Lake site in April, June and October 2010 were analysed using TMAH thermochemolysis GC-MS. Figure 5.10 shows the TICs for these three samples, with samples labelled for reference in the Jun 2010 sample according to Table 4.4 in Chapter 4.Methoxybenzyl compounds are found in total relative abundances from 88.2 (Oct) to 158.5 (Apr 2010, Table 5.7).This is lower than in shallow Central porewaters by ~ 50% (average for 15 & 30 cm at Central is 261, and is comparable to the level found in deeper porewaters (for 50 cm to 6m, the average is 143).

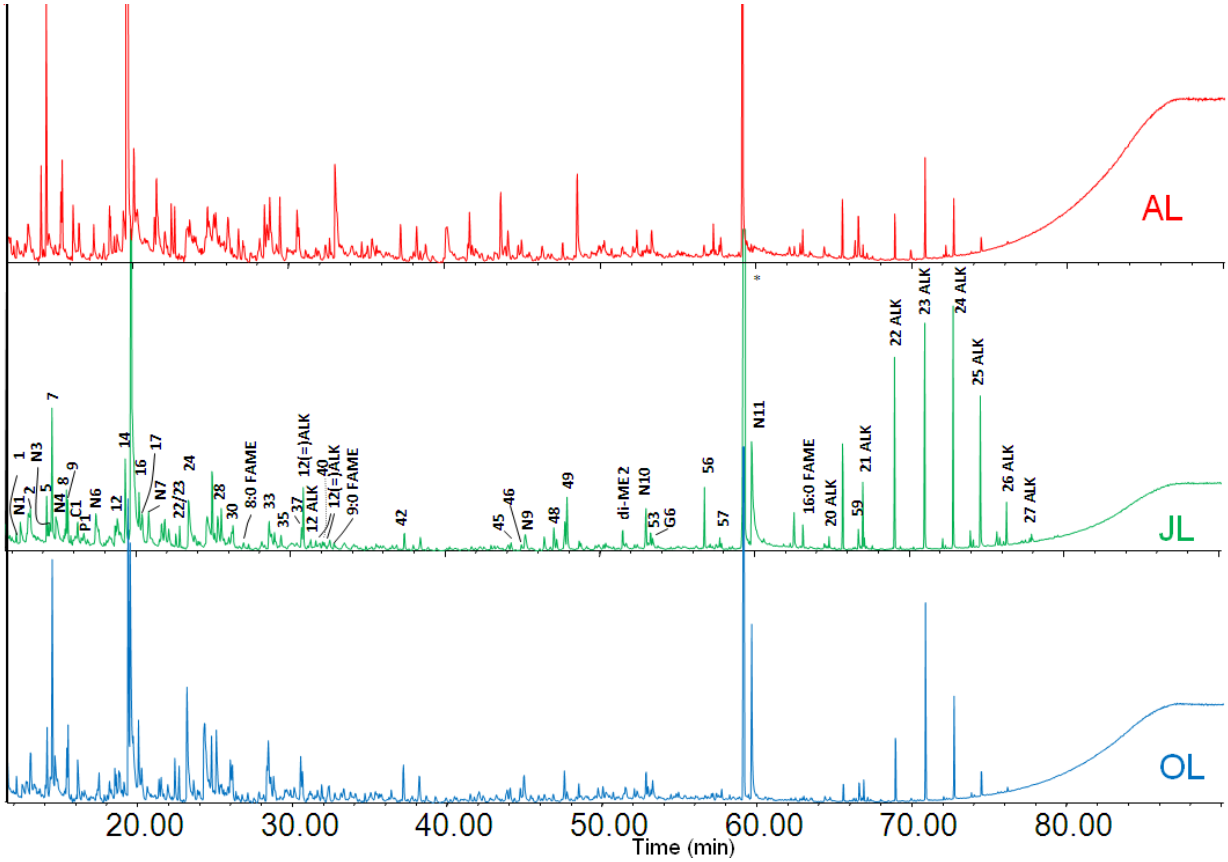

Figure 5.10: TICs for Lake samples from April (red), June (green) and October (blue) with peak assignments labelled according to Table 4.4 to allow comparison to previous figures.

The distribution and composition of methoxybenzyl compounds (Table 5.7)show some similarities to surface samples (15 and 30 cm) from the Central site: there is a high trimethoxybenzene abundance, and the dominant peaks are the acidic methoxybenzenes (**P6**, **G6** and **S6**), and those with no other functional groups (**P1** and **G1**, but with no detectable **S1**). *p*-hydroxybenzyl structures dominate over guicyl and, of the syringyl structures, only S6 is present. In contrast to porewaters, the Lake samples contain no quantifiable cinnamic compound homologues (**P18** and **G18**). Therefore the only methoxybenzene structures with side chains of more than 2 carbons which are detectable in the Lake are those compounds which are known to be derived from sphagnum acid [2-(4-methoxyphenyl)-prop-2-ene, and 3-(4-methoxyphenyl)-but-3-enoic acid ME, Abbott et al., 2010]. As previously discussed in Section 4.6.2, several studies of natural DOM have found no longer chain (> 2) methoxy benzenes, and it has been suggested that these are removed by photochemical and biotic reworking of DOM (Frazier et al., 2003; Frazier et al., 2005; Maie et al., 2006; Mannino & Harvey, 2000).

Lake, with season (2010)		Apr	Jun	Oct
Benzene, methoxy-	**P1**	14	13	9
Benzene, 1-methoxy-4-methyl-	**P2**	18	6	10
Benzoic acid ME		26	46	6
Benzene, 1-ethyl-4-methoxy-		4		6
Benzene, 1,2-dimethoxy-	**G1**	22	4	4
Benzene, 1-ethenyl-4-methoxy-	**P3**	16		
Acetophenone, 4-methoxy-	**P5**		2	
Prop-2-ene, 2-(4-methoxyphenyl)-	**$**	15		8
Benzoic acid, 3-methoxy-4-methyl-			2	4
But-3-enoic acid ME, 3-(4-methoxyphenyl)-	**$**		6	
Benzoic acid ME, 4-methoxy-	**P6**		3	12
Benzene, 1,3,5-trimethoxy-		19	10	10
Benzeneacetic acid ME, 4-methoxy-	**P24**			
Ethanone, 1-(3,4-dimethoxyphenyl)-	**G5**			
Benzoic acid ME, 3,5-dimethoxy-				
Benzoic acid ME, 3,4-dimethoxy-	**G6**	15	11	14
Benzoic acid ME, 3,4,5-trimethoxy-	**S6**	10	4	5
Ethanone, 1-(3,4,5-trimethoxyphenyl)-	**S5**			
2-Propenoic acid ME, 3-(4-methoxyphenyl)-	**P18**			
2-Propenoic acid ME, 3-(4-methoxyphenyl)-	**G18**			
TOTAL		**159**	**107**	**88**

Table 5.7: The relative response (relative to referencing peak) of methoxybenzenes after TMAH thermochemolysis GC-MS analysis of Lake samples from April, June and October 2010. $ denotes compounds known to be derived from sphagnum acid.

Maie et al. (2006) used the ratio of the smallest vanillyl and syringyl compounds (termed DV and DS respectively) to the largercompounds of the same groups (termed V and S) to assess photodegradation of lignin moieties. DV and DS are considered to be the products of photodegradation of V and S respectively. The terms were defined as follows:

DV = **G1** + **G2** + 1-methoxy-2-hydroxybenzene

DS = **S1** + 1,2-dimethoxy-3-hydroxybenzene

V = **G3** (3,4-dimethoxy-1-ethenylbenzene) + **G4** + **G5** + **G6** + **P24** + **G18** + **G12** [3-(3,4-dimethoxyphenyl)-propanoic acid ME]

S = **S5** + **S6** + **S18**

Adapting this interpretation method to use the TMAH thermochemolysis homologues given in Table 5.4 and including compounds not found using CuO oxidation (as used by Maie et al., 2006), a ratio of [P1 + P2 + G1] / [∑P(n>2) + ∑G(n>2) + ∑S(n>2)] was calculated, where ∑P(n>2) indicates the sum of all *p*-hydroxyl compounds minus P1 and P2. This ratio [hereafter referred

to as (R1 + R2) : (R>2)] assumes that photodegradation of methoxybenzyl structures with larger and more numerous side chains results in the production of methoxybenzenes and methoxytoluenes with no other functional groups (as Maie et al., 2006). The (R1 + R2) : (R>2) ratios from shallow porewaters (Central site, 15 & 30 cm) vary between 0.16 to 0.88, with an average value of 0.46 (Table 5.8). The (R1 + R2) : (R>2) becomes higher with increased depth, reaching 1.75 at 6 m. The intermediate depth Mid-bog porewaters have (R1 + R2) : (R>2) values which range from 0.42 to 0.72. Lake water (R1 + R2) : (R>2) values range from 0.75 in Oct 2010 to 1.33 in Apr 2010, averaging 1.08. Maie et al. (2006) report a low ratio of [(DV + DS) : (D + S)] for plant leachates (0.2 – 0.5), low values for DOM from freshwater and mangrove sites (0.5 and 0.4 respectively) and high values (8.4) for DOM from the Florida Bay where extensive light exposure is expected.The results are not directly comparable, as a different suite of compounds is used, but the (R1 + R2) : (R>2) does not show as high a degree of variation in Cors Fochno samples.

While it is possible that the (R1 + R2) : (R>2) ratio is indicative of a certain degree of photochemical degradation of OM in the Lakes, the increases with depth in peatland porewater are unlikely to be explained by this mechanism. It is more probable that slow *in-situ* OM degradation at depth results in a similar suite of phenolic compounds as the initial photodegradation experienced in the Lake samples, with microbial communities attacking the same side-chain functionalities that are more susceptible to photochemical alteration. Another proxy for the degradative state of lignin-derived DOM used by Maie et al. (2006) is the percentage contribution of all benzoic acid methyl esters (e.g. P6, benzoic acid ME) to the total methoxybenzyl pool. This degradation state proxy is indicative of oxidative degradation of lignin.The following equation was devised using the compounds quantified in the current study:

%benzoic acids = [P6 + G6 + S6 + benzoic acid ME + 3,5-dimethoxy benzoic acid ME + 3-methoxy-4-methylbenzoic acid] / ∑all methoxybenzenes (5.1)

The %benzoic acids in shallow porewaters range from 11% at 15 cm in Dec 2009 to 51% at 30 cm in April 2010, with an average value of 35% (Table 5.8). Values were lower at greater depth

(10% at 2 m and 0% at 3 m) but were higher (22%) at 6 m. The %benzoic acids in intermediate-depth Mid samples were low, ranging in value from 9% in Apr 2010 to 18% in Jun 2010. Values in Lake samples varied from 26% in Apr 2010 to 53% in Jun 2010. This proxy appears to differentiate between the chemistry of deep porewaters and those closer to the surface. Although oxidative degradation of phenols may be occurring extensively in Lake samples, the benzoic acid products are also photo-labile, and may therefore be lost via photodegradation (Maie et al., 2006). In order to further assess these proxies, and integrate them into the data set from all analyses of water samples, principal component analysis was applied to all samples for which the TMAH thermochemolysis results had been quantified.

Degradation indices from TMAH thermochemolysis		
Sample month, location and depth	**%benzoic acids**	**(R1 + R2) : (R>2)**
Dec 2009, Central, 15 cm	**11.3%**	**0.88**
Apr 2010, Central, 15 cm	**27.7%**	**0.61**
Apr 2010, Central, 30 cm	**50.8%**	**0.24**
Jun 2010, Central, 15 cm	**43.8%**	**0.16**
Jun 2010, Central, 30 cm	**32.5%**	**0.67**
Jun 2010, Central, 50 cm	**42.0%**	**0.38**
Jun 2010, Central, 100 cm	**24.1%**	**0.65**
Jun 2010, Central, 150 cm	**26.0%**	**1.16**
Jun 2010, Central, 200 cm	**9.7%**	**1.07**
Jun 2010, Central, 300 cm	**0.0%**	**1.00**
Jun 2010, Central, 600 cm	**22.0%**	**1.75**
Oct 2010, Central, 15 cm	**26.8%**	**0.62**
Oct 2010, Central, 30 cm	**46.1%**	**1.00**
Feb 2011, Central, 15 cm	**39.8%**	**0.33**
Feb 2011, Central, 30 cm	**33.1%**	**0.33**
Dec 2009, Mid, 150 cm	**15.4%**	**0.43**
Apr 2010, Mid, 150 cm	**6.8%**	**0.72**
Jun 2010, Mid, 150 cm	**16.5%**	**0.42**
Apr 2010, Lake	**29.3%**	**1.33**
Jun 2010, Lake	**53.4%**	**1.15**
Oct 2010, Lake	**41.8%**	**0.75**

Table 5.8: Samples on which semi-quantitative analysis of TMAH TICs was carried out, with values for degradation indices %benzoic acids and (R1 + R2) : (R>2). Colours of text to highlight different sample types (black: shallow samples; blue: June 2010 Central depth profile; red: high DOC intermediate depth samples from Mid-site; green: Lake sample).

5.6 Transformations of DOM from Cors Fochno – characterisation across all environments by principal component analysis (PCA)

In addition to the semi-quantitative analysis of phenol derivatives, FAMES and *n*-alkanes, the integrated areas of more than 30 alkylbenzene, phenol and naphthalene derived peaks were quantified from the TICs of TMAH thermochemolysis porewater analysis. Although the origin of these compounds in the DOM is unknown, they may be indicative of certain OM reservoirs or transformations between reservoirs. TMAH thermochemolysis GC-MS, combined with the analysis of the DCAA and neutral sugars and bulk measurements of DOC, TDN and $C:N_{(a)}$, results in a large and diverse data set, with many components varying on different scales. PCA provides a useful interpretation tool, amalgamating many varying terms into a small number of principal components which can explain variance between samples.

The number of variables resulting from each analysis technique differs significantly, for example 18 amino acids were quantified in DCAA analysis, 7 *n*-alkanes were identified by TMAH thermochemolysis whereas only one number (a concentration) is obtained by DOC analysis. For some sets of variables (e.g. *n*-alkanes), all individual relative abundances co-vary, which leads to a skewing of the PCA. In order to compensate for this, PCA using a correlation matrix was carried out on the results from each analysis technique, and a subset of variables was selected which best represented variance between samples. The example in Figure 5.11is from the PCA of all amino acids distributions as a molar percentage. The first principal component (PC1) explains 38% of variance across all samples, and the second (PC2) explains only 12%. PC1 is dominated by the hydrophobic amino acids on the negative, and the remaining amino acids on the positive. PC2 does not represent a large degree of variance, and so the distribution of individual amino acids can be summarised by only one variable: the percentage of hydrophobic amino acids. The total yield of amino acids and the %AA-N are also included.

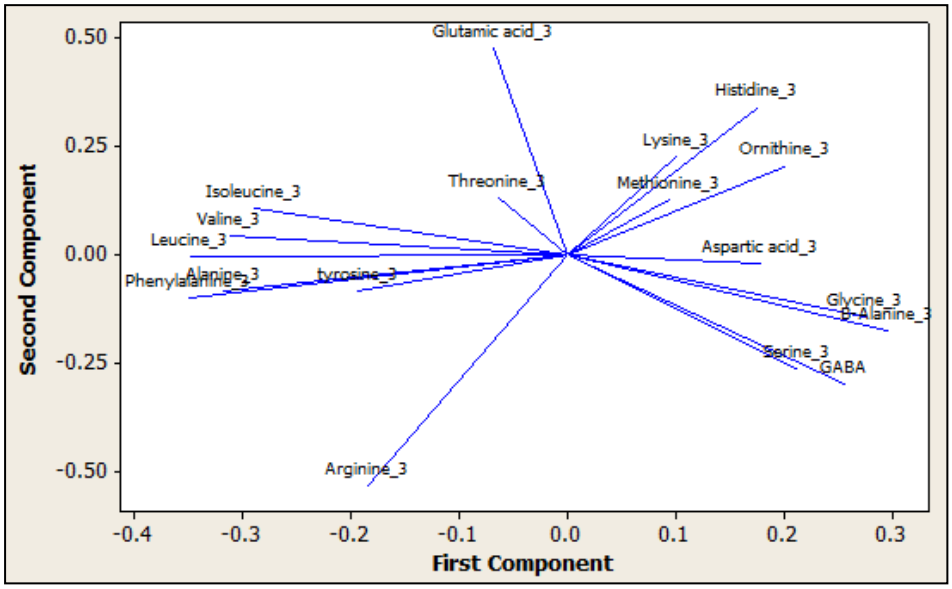

Figure 5.11: PCA loading plot (using Mintab 15) of the molar percent amino acids for all DOM samples.

For the final PCA (again using a correlation matrix), DOC and TDN concentrations are used, as is the atomic C:N ratio. Based on the preliminary analysis discussed above, DCAA yields, the % hydrophobic amino acids and %AA-N are used to summarise results from the amino acid analysis. No results from the dissolved carbohydrate analysis were used due to both uncertainties in absolute numbers and lack of data for a number of samples. From the TMAH themochemolysis results, the total relative abundance FAMES was used, as was the total methoxybenzene abundance. The percentage 16:0 and 18:0 FAMES (to the total FAME pool) was found to represent large degree of variation between samples, in addition to the relative abundances. Of the methoxybenzenes, the percentages of trimethoxybenzenes, sphagnum acid derivatives, benzoic acids, cinnamic and *p*-hydroxyphenyl compounds were carried forward to the final PCA, as was the (R1 + R2) : (R>2) ratio. The total *n*-alkane abundance, the odd to even ratio of *n*-alkanes and the C_{25} to C_{23} ratio were also used in the final PCA. Of the four 2-cyclopenten-1-one based carbohydrate-derived compounds, the relative abundance of 2-methyl-2-cyclopenten-1-one and 3-methyl-2-cyclopenten-1-one were considered. Finally, the phenols and naphthalenes which were quantified but not assigned a clear source were summarised by the combined abundance of naphthalene and 2-methylnaphthalene and the combined abundance of 2-methylphenol and 2,5-methylphenol (see Table 5.9 for summary and abbreviations used).

Summary of PCA variables with abbreviations used in plots		
Variable	**Abbreviation**	**Comment**
DOC conc.	DOC	Elemental information
TDN conc.	TDN	
Atomic C:N ratio	C:N(a)	
Total FAMEs	FAMES	Ubiquitous class of compounds – distribution may be indicative or plant or microbial source
% (16:0 + 18:0)	%16&18	
2-methyl-2-cyclopenten-1-one	C1	Derived from carbohydrates – may indicate plant sources of DOM
3-methyl-2-cyclopenten-1-one	C2	
Total methoxybenzenes	MOBs	Indicative of lignin or sphagnum source and known to be functionally significant (see Chapter 4, Section 4.1) – these terms may also be indicative of oxidative or photochemical decay and reworking of organic matter.
%cinnamic	%Cin	
(R1+R2) : (R>2)	R1R2:R	
%*p*-hydroxybenzyl	%p	
%benzoic acids	%AMOB	
%trimethoxybenzenes	%TMB	
% sphagnum acid derivatives	%SPH	
DCAA yield	AA yield	Amino acids and their distributions may be indicative of microbial activity
%AA-N	%N	
% hydrophobic DCAA	%hydrophobic	
Phenols	PH1+PH2	Unknown source
Total *n*-alkanes	nAlk	Indicative of plant wax source – lack of odd to even dominance may indicate chemical alteration
Odd:Even ratio of *n*-alkanes	O:E	
Naphthelenes	N1+N2	Unknown source

Table 5.9: Summary of PCA variables used for final analysis, with abbreviations used in plots. Variables have been grouped and coloured accordingly (e.g. all terms in purple are related to DCAA analysis). See text for further information.

19 samples were included in the final analysis, these being the samples which had values for the full suite variables included in the PCA. In order to carry out PCA, every variable included in the analysis needs to be measured for every sample, and for example, no DCAA data was available for Central 15 cm sample from Jun 2010 due to sample loss during analysis. The samples used in the analysis include a depth profile (from the centre of the bog sampled in June) from 30 cm to 6 m depth as well as water samples from different seasons and locations across the bog. Table 5.10 lists all samples included.

Samples included in PCA with abbreviations used in plots		
Samplemonth, location and depth	**Abbreviation**	**Comment**
Dec 2009, Central, 15 cm	Dec C15	Seasonal variations
Apr 2010, Central, 15 cm	Apr C15	
Apr 2010, Central, 30 cm	Apr C30	
Jun 2010, Central, 30 cm	Jun C30	Depth profile from Central piezometer array (and seasonal variations)
Jun 2010, Central, 50 cm	Jun C50	
Jun 2010, Central, 100 cm	Jun C100	
Jun 2010, Central, 150 cm	Jun C150	
Jun 2010, Central, 200 cm	Jun C200	
Jun 2010, Central, 300 cm	Jun C300	
Jun 2010, Central, 600 cm	Jun C600	
Oct 2010, Central, 15 cm	Oct C15	Seasonal variations
Oct 2010, Central, 30 cm	Oct C30	
Feb 2011, Central, 15 cm	Feb C15	
Feb 2011, Central, 30 cm	Feb C30	
Dec 2009, Mid, 150 cm	Dec Mid	Other key locations – high DOC mid-depth samples from Mid piezometer array and Lake samples
Jun 2010, Mid, 150 cm	Jun Mid	
Apr 2010, Lake	Apr L	
Jun 2010, Lake	Jun L	
Oct 2010, Lake	Oct L	

Table 5.10: Summary of samples included in final PCA, with abbreviations used in plots.

The eigenvalues for the final PCA are fairly low, indicating that a large portion of variability between samples is not represented in the first two principal components: PC1 explains 25% of variation between samples, and PC2 explains 24.4%. PC1 is strongly positively influenced by the percentage of TDN measured as amino acids, the presence of carbohydrate indicators and FAMEs in TMAH thermochemolysis TICS, the atomic C:N ratio of the DOM sample and the contribution benzoic acids make to the methoxybenzene pool. The negative element is dominated by the TDN concentration of the DOM sample, the percentage of sphagnum acid derivatives in the methoxybenzene pool, the (R1 + R2) : (R > 2) ratio of methoxybenzenes and the *n*-alkane contribution to TMAH thermochemolysis TICs.

The positive element of PC2 is dominated by the contribution of phenols to TMAH thermochemolysis TICs, the percentage of hydrophobic amino acids in the DCAA pool, the DOC concentration of the water sample, the contribution from methoxybenzenes to TICs and percentage of these with cinnamic structures. The negative element of PC2 is mainly

influenced by components of the methoxybenzene pool: the percentage found with a trimethoxybenzene structure, the contribution of benzoic acids to this pool, and the (R1 + R2) : (R > 2) ratio.

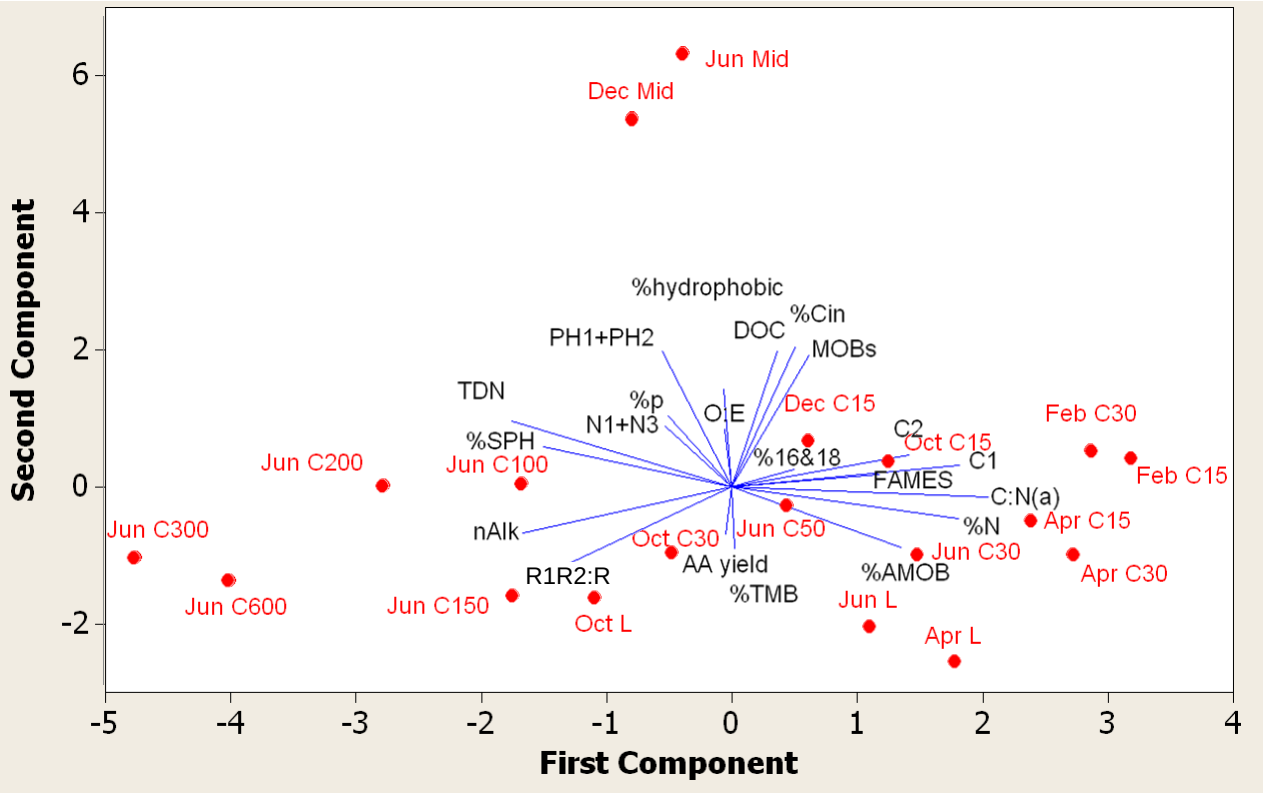

Figure 5.12a:Biplot of the first two principal components from PCA of samples with both a loading plot (blue lines with black labels) to show how variable combined to form components, and a score plot showing samples (red dots) plotted with respect to the first two principal components. See Tables 5.9 and 5.10 for a list of samples, variables and the relevant abbreviations.

Although the analysis is missing some key samples, the sample set covers enough seasons, depths and locations that some key patterns emerge. Figure 5.12b shows the biplot from Figure 5.12a, annotated with sample groupings to aid interpretation. Firstly, PC1 appears to differentiate between sample depths. Deeper samples from the June Central depth profile (> 50 cm) plot negatively on PC1, with the two deepest samples (from 3 m and 6 m) having the most negative PC1 scores. Water samples from near the peat surface (15 and 30 cm) plot positively on PC1 (with the exception of a sample from 30 cm taken in October 2010).The variables which contribute most to positive PC1 values (more "shallow-like "character) involve the proportion of sample which is non-humic, i.e. most closely resembles plant and microbial OM (Sleighter &

Hatcher, 2007), with higher %AA-N values and larger contributions from FAMEs and carbohydrate derived compounds after TMAH thermochemolysis.

PC2 separates samples by location: water samples from the Lake site plot negatively on PC2 and those from the Mid piezometer array (at 150 cm) plot positively on PC2. All samples from the Central piezometer array (from all depths and all seasons) plot between -2 and +1 on PC2 (Figure 5.12b). Samples from the Lake site come from a relatively oxic environment, where UV light may influence sample degradation.The variables which contribute to negative PC2 scores include the two proxies for degradation of phenolic compounds, (R1 + R2) : (R > 2) and the %benzoic acids (see Section 5.5.3). Intermediate depth, high DOC samples from the Mid bog site have been shown earlier in this chapter to most closely resemble the solid phase peat from which much of the porewater DOM will be derived. PC2 therefore may represent the oxidative- or photo- degradation state of DOM from Cors Fochno.

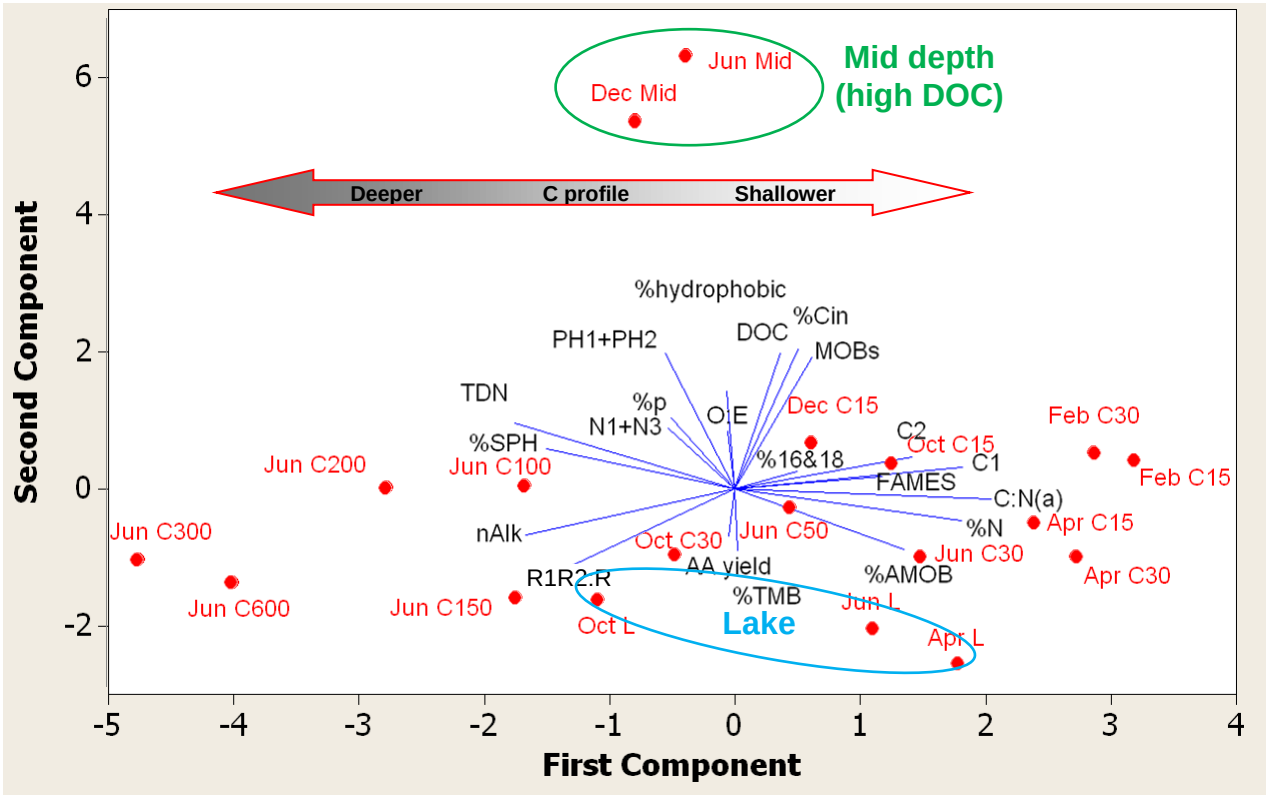

Figure 5.12b: As Figure 5.12a annotated with sample groupings to highlight interpretation. Biplot of the first two principle components from PCA of samples with both a loading plot (blue lines with black labels) to show how variables combined to form components, and a score plot showing where samples (red dots) plotted with respect to the first two principle components.See Tables 5.9 and 5.10 for a list of samples, variables and the relevant abbreviations.

There may also be a seasonal component to PC1.Shallow Central samples (15 & 30 cm) plot more positively on PC1 in February and April and more negatively in October, with the June and December samples plotting between these extremes. The same is true for the samples taken from the Lake, although only three months of Lakes samples are included in the analysis (April, June and October). In this sense, porewaters from 15 & 30 cm have a more extreme "shallow" character during the late winter and spring. The Lake samples from April and June have a more peatland-surface-like character than in October, which may be indicative of inputs of fresh plant material or more labile OM. PCA provides a powerful tool for the integration of multiple data sets. Although only a small number of samples were quantified for every variable which contributed to the analysis, PCA resulted in clustering of samples into several groups, providing more confidence that the analysis of four samples using an ultrahigh resolution mass spectrometry technique (in Chapter 6) will provide information that will be relevant to a larger number of samples.

5.7Chapter synthesis and conclusions

Characterisation of solid phase material from two contrasting cores revealed that there was much lower levels of variability in the chemical composition of the cores (both downcore and with different microtopography) than were found in porewaters. A much higher percentage of the solid organic carbon was characterisable as amino acids and carbohydrates. Carbohydrate yields were highest in the top 5 cm of both cores. Changes in composition were generally low, with glucose being the major component of the TCHO pool at all depths, although xylose did show a large peak in relative yield at ~20 cm below the hollow. Similar changes in xylose contribution have been observed in other studies (Comont et al., 2006) and attributed to changes in vegetation with time, with increased sedge inputs in the past being related to changing environmental conditions. It was deemed unlikely that this was the cause in the current study, as other possible cottongrass biomarkers (*p*-hydroxyacetophenone) did not show similar trends. The peak in sedge-derived carbohydrates may instead have been due to an input of belowground carbon via root systems, or simply due to heterogeneity of the peat profile.

At approximately 25 to 30 cm depth, a maximum in the percentage total nitrogen was observed, which coincided with a maximum in THAA yields and a minimum in carbohydrate yields. Contributions of individual compounds to the total amino acid pool do not change substantially with depth, with the majority of variation seen in the top 5 cm of each core. Contributions from the non-protein amino acids (β-alanine, α-amino butyric acid and ornithine) are very low in the solid phase, suggesting a high contribution from microbial sources in the dissolved phase. Amino acids in peat cores had a higher contribution from compounds with hydrophobic side chains than porewaters (particularly those amino acids with aromatic side chains), and lower contributions from glycine, which is a product of degradation of other amino acids and proteins. Microbial activity is also indicated by an enrichment of the neutral sugar arabinose in the dissolved phase relative to the core material.

Lake samples were characterised by an amino acid pool that had only a small contribution from compounds with hydrophobic side chain and high non-protein amino acid yields (relative to all other samples). Carbohydrate yields were on average high, with a relatively high contribution from xylose.

Only a small portion of the organic carbon in cores was attributable to phenolic compounds, the majority of which were aldehydes and cinnamic structures. Lignin yields were particularly low above the water table, which may be indicative of phenol oxidase activity in the oxygen-rich peat below the hummock. Both solid phase and dissolved phase phenolic compounds are dominated by *p*-hydroxyphenyl structures. Porewater samples, particularly those near the surface of the peatland, had much higher contributions from acidic phenolic compounds than the solid phase, which may be indicative of oxidative degradation of larger polymeric structures (e.g. hydrolysable tannins). Lake samples in particular had a high proportion of P1, P2 and G1 compounds relative to the total methoxybenzene pool (as quantified from TMAH thermochemolysis data) and no cinnamic compounds. This may be indicative of photodegradation, although analysis of deep peat porewater samples (6 m) also resulted in a highdegradation state using this proxy, indicating that, used alone, it is not selective for photochemical alteration.

Of all the water samples, those from intermediate depth at the Mid-bog site (characterised by high DOC water from wells with low hydraulic conductivity) were most similar to the solid phase with respect to both amino acids and phenolic compounds. Amino acids were dominated by compounds with hydrophobic side chains, and large suites of methoxybenzenes were found which were shown to relate strongly to the phenolic compounds in the solid phase that were most variable with depth and location. This may lend support to the idea that high DOC measurements from wells with low hydraulic conductivities is due to sampling from micropores or closed pore-spaces which are normally closed off from water flow, increasing the residence time of the porewaters they hold. In comparison, the water samples which have the least contact time with the solid phase peat (represented by the Lake sample)have the most hydrophilic character and are compositionally least like the core material.

PCA was carried out, combining data from multiple analyses. PC2 separates samples from differing sites and appears to be representative of the influence of oxic-degradation, and possibly photodegradation. PC1 separates samples by depth, and the variables which contribute most to PC1 are linked to the degree of humification or the presence of components which closely resemble fresh plant-source materials (e.g. the percentage of nitrogen that is attributable to amino acids). PCA of Lake samples revealed that in April and June (2010), the lake had a more peatland surface-like character than in October (2010), possibly indicating a greater input from fresh plant material or more labile OM.

Although a number of complementary methods have been utilised in order to characterise DOM from Cors Fochno, a large fraction remains uncharacterisable by most methods. Electrospray ionisation Fourier transform ion cyclotron resonance mass spectrometry is a powerful tool, allowing the molecular characterisation thousands of chemical species within a mixture such as humic and fulvic acids. The next chapter (6) will describe the analysis of four DOM samples from Cors Fochno using this technique.

Chapter 6: Characterisation of humic substances and identification of transformational relationships by electrospray ionisation Fourier transform ion cyclotron resonance mass spectrometry (ESI-FT-ICR-MS)

6.1 Introduction

Humic substances (HS) are a major component of natural organic matter (NOM), accounting for 70-90% of dissolved organic carbon (DOC) (Thurman, 1985). HS are a complex and heterogeneous mix of organic material, formed by the decay and transformation of plant and microbial remains, which exhibit a wide range of hydrophobicities, reactivities and molecular sizes (Grinhut et al., 2011; Sleighter & Hatcher, 2008). Most studies which attempt to characterise HS do so by referring to the average chemical properties within an extracted portion of a sample, which may include a large array of compounds with differing structures (Grinhut et al., 2011). These studies in general agree that the chemical properties of HS are remarkably similar across many environments (Stevenson, 1994). While TMAH thermochemolysis gas chromatography mass spectrometry (GC-MS) provides an insight into components of this pool (fragmenting the organic matter (OM) into compounds which are amenable to GC-MS by hydrolysis and methylation as in Chapters 4 and 5), FT-ICR-MS is the only technique which is capable of molecular characterisation of the thousands of individual compounds within these mixtures (e.g. Bae et al., 2011; D'Andrilla et al., 2010; Koch et al., 2005; Schmidt et al., 2011; Sleighter & Hatcher, 2007; Sleighter & Hatcher, 2008).

FT-ICR-MS is increasing our understanding of the complexity of HS. These macromolecular structures, which are comprised of many smaller molecular units, tend to aggregate and act as a polymeric unit (Sleighter & Hatcher 2007). While

studies of (NOM) have shown that the majority of molecular weights and molecular compositions which are chemically feasible are found (Hertkorn et al., 2008), fractionation of fulvic acid (FA) has demonstrated that this fraction is structurally less diverse (Witt et al., 2009), with many aromatic structures dominated by carboxyl functionalities.

FT-ICR-MS is an incredibly powerful tool for examining the nature of NOM, and the biogeochemical community is still exploring new ways of utilising it. Kejawinski et al. (2009) used multivariate statistical methods to analyse FT-ICR-MS spectra from marine DOM, to identify m/z (mass to charge) markers for terrestrial and surface ocean sources. D'Andrilla et al. (2010) used FT-ICR-MS to investigate porewater from northern peatlands in Minnesota, using an Aromaticity Index to identify the large array of condensed and phenol type compounds from this environment and Stenson et al. (2003) used FT-ICR-MS to identify the degradation of lignin as a source of FAs in Suwannee River Fulvic Acid (SRFA).

Thousands of compounds may be compared between similar samples using FT-ICR-MS, and as such, it is a useful tool to track molecular transformations of OM. It has also been used to track changes in the quality of organic matter along a river-ocean transect in Chesapeake Bay (Sleighter & Hatcher, 2008) showing that DOM becomes more aliphatic with fewer oxygen rich molecules as organic matter moves from near-shore to off-shore, although considerable similarities were found across all salinities, highlighting the refractory nature of a large portion of DOM. FT-ICR-MS has been used (Stubbins et al., 2010) to identify changes in Congo river DOM after irradiation (i.e. after photo-oxidation) finding that aromatic compounds were most susceptible to degradation via this mechanism, and that the diversity of formulae identified after treatment with UV was significantly reduced. The technique has also been used to track changes in in plant biomass during humification and the formation of soil organic matter (Ohno et al., 2010), finding steadily reducing H:C ratios as the plant precursors transform into refractory HAs.

Although no structural information is obtained directly from FT-ICR-MS, it has been combined with others techniques to suggest structures in humic substances. Witt et al. (2009) combined FT-ICR-MS with collision induced dissociation (CID), showing the on CID of single peaks from SRFA, CO_2 and H_2O units were released, suggesting the presence of carboxyl and hydroxyl structures in these FAs.

A small amount of work has also been undertaken to utilise FT-ICR-MS in studies of dissolved organic nitrogen (DON). McKee and Hatcher (2010) used the technique to identify a possible new abiotic mechanism for N sequestration in marine sediments, suggesting the presence of a homologous series of CHON containing compounds, identified using GC-MS as alkyl amides, may be due to the amidation of esters by sedimentary ammonia. Schmidt et al. (2011) also investigated DON release from marine sediments, tracing the degradation of protein structures in anoxic sediments in the Black Sea. The above examples are given to highlight the wide scope of FT-ICR-MS studies, and there is great potential to bring this relatively young technique to new avenues of research.

ESI-FT-ICR-MS instrumentation is limited to a relatively small number of laboratories across Europe, and instrument time is both difficult and expensive to acquire. Thanks to an Academic Research Collaboration (ARC) project, jointly funded by the British Council and the German Academic Exchange Service (DAAD), four DOM samples from this study were analysed using ESI-FT-ICR-MS at Helmholtz Zentrum (Munich).

6.1.1 Objectives and approaches

This chapter aims to address the final two objectives as summarised in Chapter 1, Section 1.4:

- To use a ultrahigh resolution mass spectrometry technique to investigate humic substances within peatland porewater,

- Using the information gained, to assess the sources of peatland DOM and the molecular transformations or alterations this OM undergoes in different environments in the peatland.

FT-ICR-MS provides a very powerful tool for assessing molecular transformations and alterations between samples. The water samples which will be discussed in this chapter cover four of the key DOM environments as discussed in Chapter 3:

- A sample from the upper 15-30 cm of the bog (referred to as Integrated Acrotelm, IA) – this is a composite of samples from four pairs (15 and 30 cm) of shallow piezometers installed within 10 m of each other at the Central site in order to obtain large volumes of sample;
- A sample from 6 m depth at the Central site (C6), representing the deepest water sampled;
- A sample from the intermediate-depth horizon (1.5 m) of high DOC concentration water at the Mid-bog site (M1.5);
- And a sample from the Lake (L), which is considered to be representative of runoff from the site.

All samples were collected in April 2010.

Due to the enormous complexity of DOM, data sets acquired by FT-ICR-MS are very large and difficult to interpret (e.g. Bae et al., 2011). Visualisation techniques are paramount to assessing FT-ICR-MS data (e.g. Sleigter & Hatcher, 2007). Van Krevelen diagrams are frequently used (after Kim et al., 2003) to visually assess the character of samples analysed using FT-ICR-MS, as different regions on a Van Krevelen plot, representing differing H:C and O:C ratios, may be indicative of different classes of organic compound. The distribution of peaks over H:C and O:C space has been shown to be similar for many natural DOM samples (e.g. Kim et al., 2003; Ohno et al., 2010; Sleighter & Hatcher, 2008; see Figure 6.1).

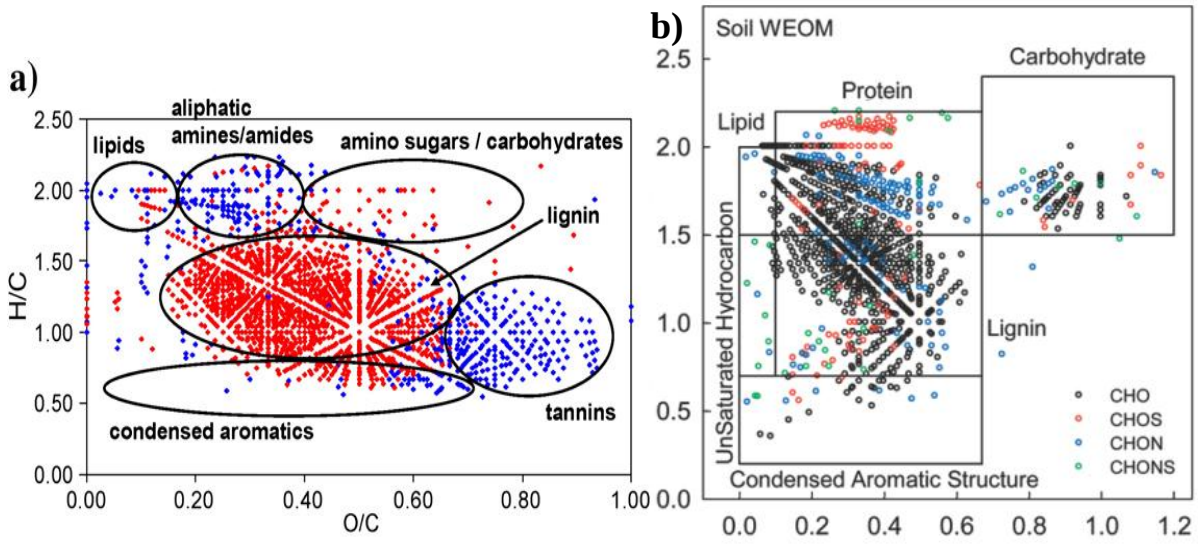

Figure 6.1: Van Krevelen diagrams taken (with minor adaptations) from previously published studies, showing the prevalence of peaks with H/C values between 0.5 and 1.5 and O/C values of 0.2 to 0.6; a) Dismal Swamp DOM showing the effect of C_{18} extraction (red in both extracted and whole water, blue in only whole water sample, from Sleighter and Hatcher 2008), b) water extractable organic matter from Caribou soil from USA (Ohno et al., 2010) showing heteroatom content by colour. Note that diagrams have been taken from publications, therefore scales differ slightly.

Van Krevelan diagrams will be used to interpret the FT-ICR-MS data presented in the following chapter, and then a number of entirely novel approaches will be explored to assess similarities and transformations between samples.

6.2 Description of FT-ICR-MS spectra

Figure 6.2 shows the full mass spectrum of the shallow porewater sample which is a mixture of several 15 cm and 30 cm porewaters from the centre of the bog (IA) from m/z 200-650. Due to the high resolving power of FT-ICR-MS, a large number of peaks could be resolved at each nominal mass, and up to 29 peaks were assigned molecular formulae per molecular mass integer. Several important aspects of the mass spectra are discernable from Figure 6.2, notably that there is a clear repeating pattern of 14 Da, which comes about due to the presence of many similar molecular formulae which differ from each other only by the addition or subtraction of a CH_2 unit (e.g. via the lengthening and shortening of side chains). There is also a clear 2 Da pattern, with higher intensity and a greater number of peaks at odd m/z values than even.

The even m/z peaks result only from either compounds which contain N_1 or N_3, or the ^{13}C-containing isotopic analogue of an odd m/z peak. Due to the spacing of these ^{13}C peaks, it can be shown that the negative mode electrospray ionisation has only produced singly deprotonated ions; these peaks are found at intervals of 1.0034 Da (the mass difference between ^{13}C and ^{12}C) whereas if the ionisation resulted in doubly charged ions, ^{13}C peaks would be observed at an interval of 0.5015 Da (Sleighter & Hatcher, 2007).

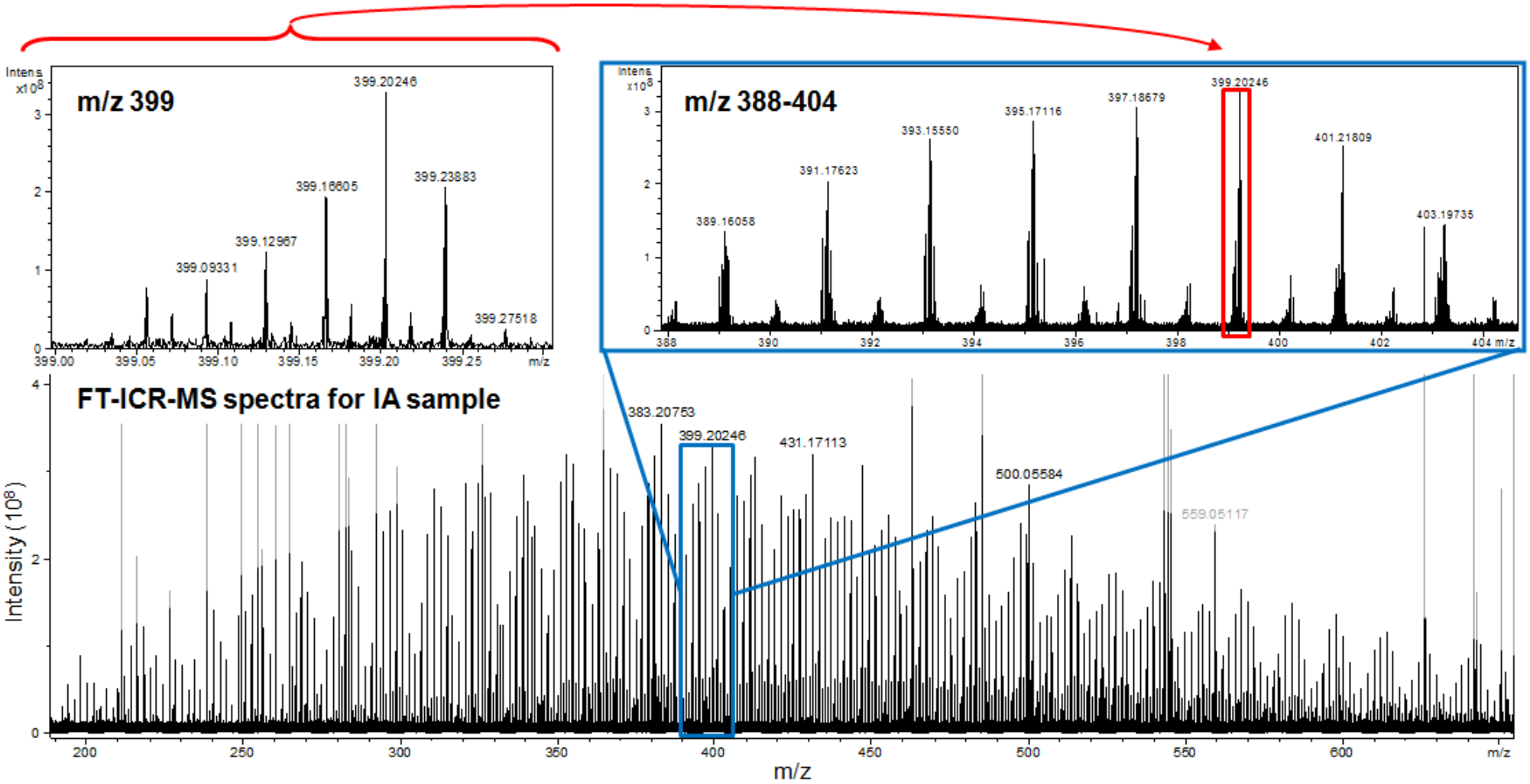

Figure 6.2: Lower plot is full FT-ICR-MS spectrum for integrated acrotelm sample (IA). Higher intensity peaks which were not considered when assigning intensity reference peak (as relative intensity of 100 at m/z = 383.20753) are greyed out, but include fatty acids (<300 m/z), instrumental contamination peaks (as identified by blank MeOH runs) and chlorine adducts (at m/z ~ 545). A zoomed in view of m/z 388 to 404 is shown in upper right (highlighted on lower plot in blue) and a further zoomed in image of all peaks found at m/z 399 is shown in top left.

Peaks present in FT-ICR-MS spectra are measured in intensity, in the range of 10^8, but the strength of the signal is affected by a number of factors such as instrumental set up and competition for charge during ESI within the sample. All NOM samples exhibit an arc of increasing then decreasing intensity peaks with m/z (Figure 6.2), overlain by a number of anomalously high intensity peaks. In order to allow comparison of peak sizes between samples, it is standard practice for the largest peak within the arc to be identified and given a nominal relative intensity of 100. Note that this peak may not be the highest intensity peak from the middle section of the spectrum, but will be the peak with the highest intensity from the background signal found in all NOM samples. In the spectrum from IA, this reference peak was found at 383.20753 (Figure 6.2).

The signal to noise (S/N) ratio is calculated using the data analysis software (Bruker Daltronics DataAnalysis) and it is this value which is used to separate those peaks which are considered for formula assignment. A S/N ≥ 5 was used as a discriminator for the majority of analyses; where a higher cut-off was used it will be clearly indicated.

An average of 3826 peaks were assigned molecular formulae in each of the four key extracted samples, the makeup of which are represented in figure 6.3. The majority of peaks (64%) were assigned formulae containing only carbon, oxygen and hydrogen (CHO compounds), with the remaining assignments being dominated by nitrogen-containing formulae. That being said, the abundance of heteroatom-containing formulae is high compared with other studies of terrestrial NOM (e.g. 90% of Dismal Swamp DOM found to be CHO, Bae et al., 2011). While the largest number of assigned peaks are found in the Mid-bog (M1.5) sample, it is notable that the number of CHO peaks in each sample is very similar. However, looking at the total number of peaks in this manner is somewhat misleading, as many of the peaks assigned CHO formulae are not present in all samples (at S/N ≥ 5). Only 2435 of the 6074 assigned molecular formula are common to all four samples, of which 1920 are CHO assignments (from a total of 3095 CHO formulae assigned over all samples). This

shows that while the number of CHO peaks varies little between samples (as can be seen from the similar sizes of the CHO bars in Figure 6.3), the make-up of those peaks is much more variable.

Although the characterisation of thousands of compounds by molecular formula does provide a huge amount of information, there are some limitations associated with the technique. Firstly, as with the majority of characterisation methods, the utilisation of a solid phase extraction followed by ESI will result in only a sub-section of the total organic pool being ionised (Flerus et al., 2011; Tfaily et al., 2011), especially compounds with oxygen rich and acidic functionalities. For example, fatty acids are readily ionised in negative ESI mode (Sleighter & Hatcher, 2007), and the peaks at these masses are found at high intensity (Figure 6.2), which does not necessarily indicate that fatty acids are present in high abundance within the original sample. This highlights another limitation of the technique, which is that due to lack of calibration methods and variable response from different compound classes, the technique is not quantitative, and care must be taken when comparing samples which have been run on different equipment and with different analytical set-ups.

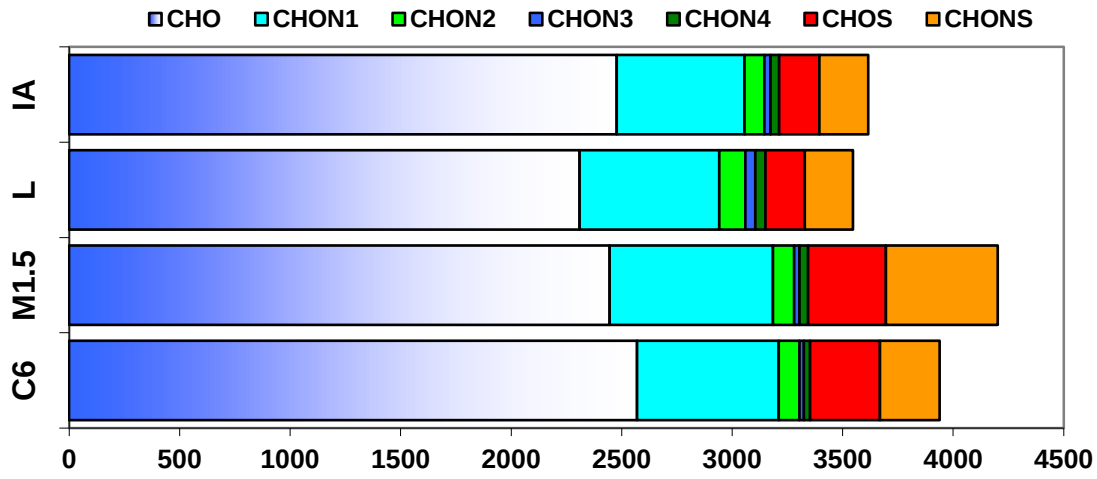

Figure 6.3: The number of peaks assigned molecular formulae for each extracted sample, with colour denoting the heteroatom content (e.g. CHON2 is all peaks with no sulphur and two nitrogen atoms in their assigned formula). CHOS includes both R-S_1 and R-S_2 assignments and CHONS is all peaks with molecular formula containing both nitrogen and sulphur atoms, irrespective of number.

A final limitation is that although a molecular formula is obtained for thousands of peaks, no structural information is directly measured; it must instead be inferred from atomic ratios. A single peak may represent a variety of structural isomers, which may well differ substantially in both chemistry and response to the analysis.

Calculation of the weight-averaged molecular composition of samples provides further information on the bulk chemistry. Average values for the mass, double bond equivalent (DBE, a measure of hydrocarbon saturation) and C, O, N and S content of samples, as well as molar O:C and H:C ratios, were calculated, where the contribution from each formula was weighted according to the intensity of the associated peak. DBE represents the number of double bonds or rings required to build a molecular structure from the assigned elemental formula, with a DBE of zero indicating a fully saturated molecule. Some examples of the equations for these calculations are given below for formula *x*, with molecular composition $C_cH_hO_oN_nS_s$ and intensity Int_x:

$$DBE = c - (½\ h) + (½\ n) + 1 \quad (6.1)$$

$$DBE_{wa} = \frac{\sum(DBE_x)\ X\ Int_x}{\sum Int} \quad (6.2)$$

The weight averaged DBE value and H:C ratio both indicate a higher degree of saturation in the surface samples (L and IA) than in deeper samples (C6 and M1.5) with the average formula containing fewer double bonds and having a higher H:C ratio (Table 6.1). The mid-bog sample (M1.5) has an average composition which is substantially less saturated. The oxygen content (both as weight averaged number of oxygen atoms per formula $O_{wa,}$ and the weight averaged molar oxygen to carbon ratio $O:C_{wa}$) shows little variation between samples. Although the average number of oxygen atoms per assigned formula in M1.5 (8.7) is slightly higher than in other samples (mean = 8.4), this is partly due to a greater significance of formulae with high mass (and associated higher number of carbon atoms), and is reflected in the similar $O:C_{wa}$ across all samples. There is a substantial increase in the presence of

organo-sulphur compounds in M1.5, and this is reflected in the number of CHOS and CHONS species present (i.e. the high weight averaged sulphur content, $S_{wa,}$ is not due only to an increased intensity of sulphur-bearing peaks).

Sample code	Peaks	m/z_{wa}	DBE_{wa}	C_{wa}	O_{wa}	N_{wa}	S_{wa}	$O:C_{wa}$	$H:C_{wa}$
L	3547	434.85	7.35	21.91	8.35	0.26	0.096	0.40	1.44
IA	3616	432.42	7.81	21.83	8.47	0.21	0.083	0.39	1.39
M1.5	4402	441.40	9.30	22.31	8.70	0.24	0.117	0.39	1.27
C6	3939	425.91	8.13	21.51	8.38	0.19	0.089	0.39	1.35

Table 6.1: The number of assigned peaks and weight averaged molecular composition of all four samples. Molecular composition information is as weight averaged mass (m/z_{wa}), double bond equivalent (DBE_{wa}), the weight averaged number of C, O, N and S atoms in all formulae (C_{wa}, O_{wa}, N_{wa} and S_{wa}), and weight averaged molar O:C and H:C ratio ($O:C_{wa}$ and $H:C_{wa}$) Example equations for the calculations are given above.

6.3 Characterisation using Van Krevelen diagrams

Figure 6.4 shows where all the larger CHO formulae (S/N ≥ 10) plot on a Van Krevelen diagram by colour. Also marked are the areas in which typical molecules belonging to a number of compound classes would plot. It should be noted that where a series of formulae may fall within one of the regions typical to a compound class, this does not necessarily imply that those formulae represent compounds from that class in any these samples. All samples considered have many peaks in and surrounding the area associated with lignin derived material and "above" this region of the plot (i.e. with higher H:C ratio) in agreement with many previous studies of natural DOM. Figure 6.1 shows a selection of examples from the analysis of freshwater DOM by ESI FT-ICR-MS (many similar results have been published) which illustrates the ubiquitous nature of peaks which plot in the lignin portion of a Van Krevelen diagram. A large number of peaks also plot in the tannin region of the Figure 6.4 and tannic structures are known to be of significance in peatland environments (as discussed in previous chapters). Although there are a number of peaks present in all samples with assigned formulae which would plot in the carbohydrate region of the diagram, the majority of these are of low intensity, and

many contain heteroatoms, therefore they did not meet the selection criteria for Figure 6.4.

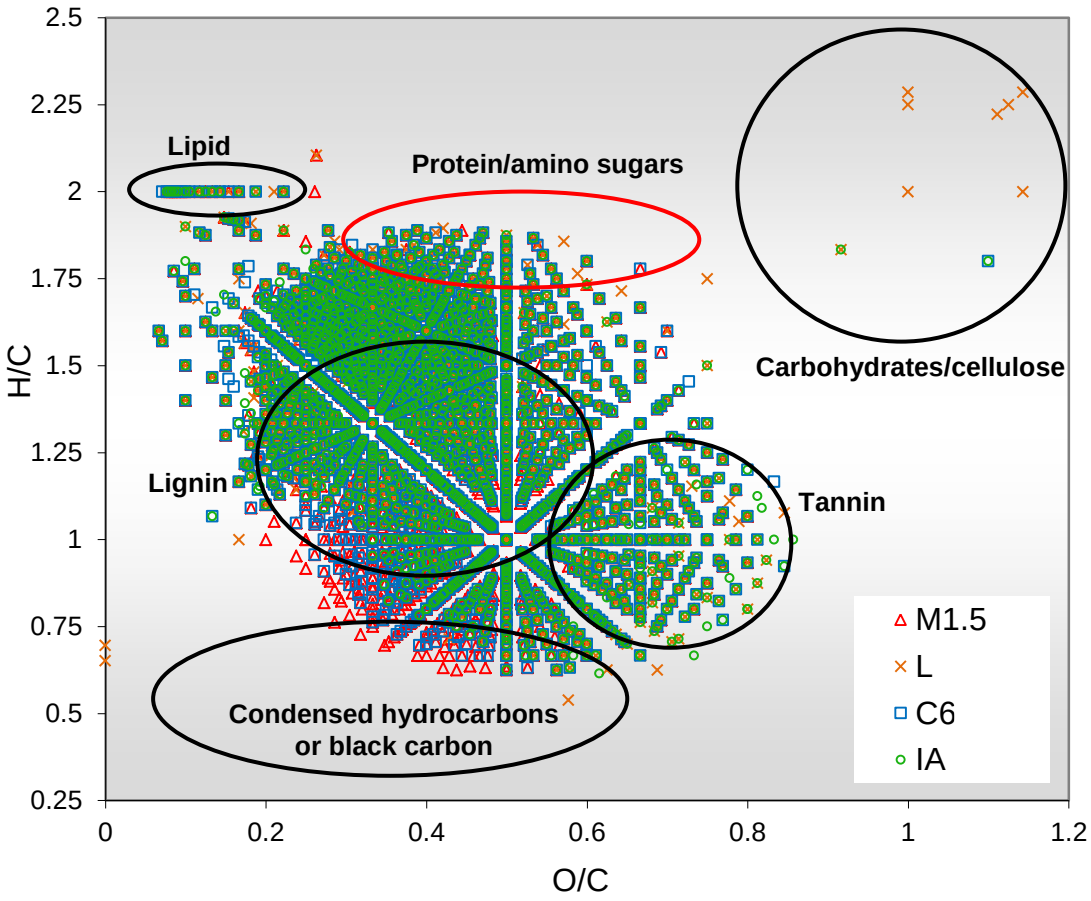

Figure 6.4: Van Krevelen plot of CHO peaks with S/N ≥ 10 for all four samples. The regions of the Van Krevelen in which several compound classes would plot have been marked. Amino sugars and proteins are highlighted in red as they are nitrogen-containing and therefore not relevant for the data plotted. Diagram produced after Sleighter & Hatcher, 2008.

Figure 6.5 shows the distribution of nitrogen containing formulae over a Van Krevelen diagram, also indicating the low relative intensity of the majority of CHON peaks. Nitrogen is contained in chemical species which span almost the entire H/C and O/C compositional space of peaks from Cors Fochno.

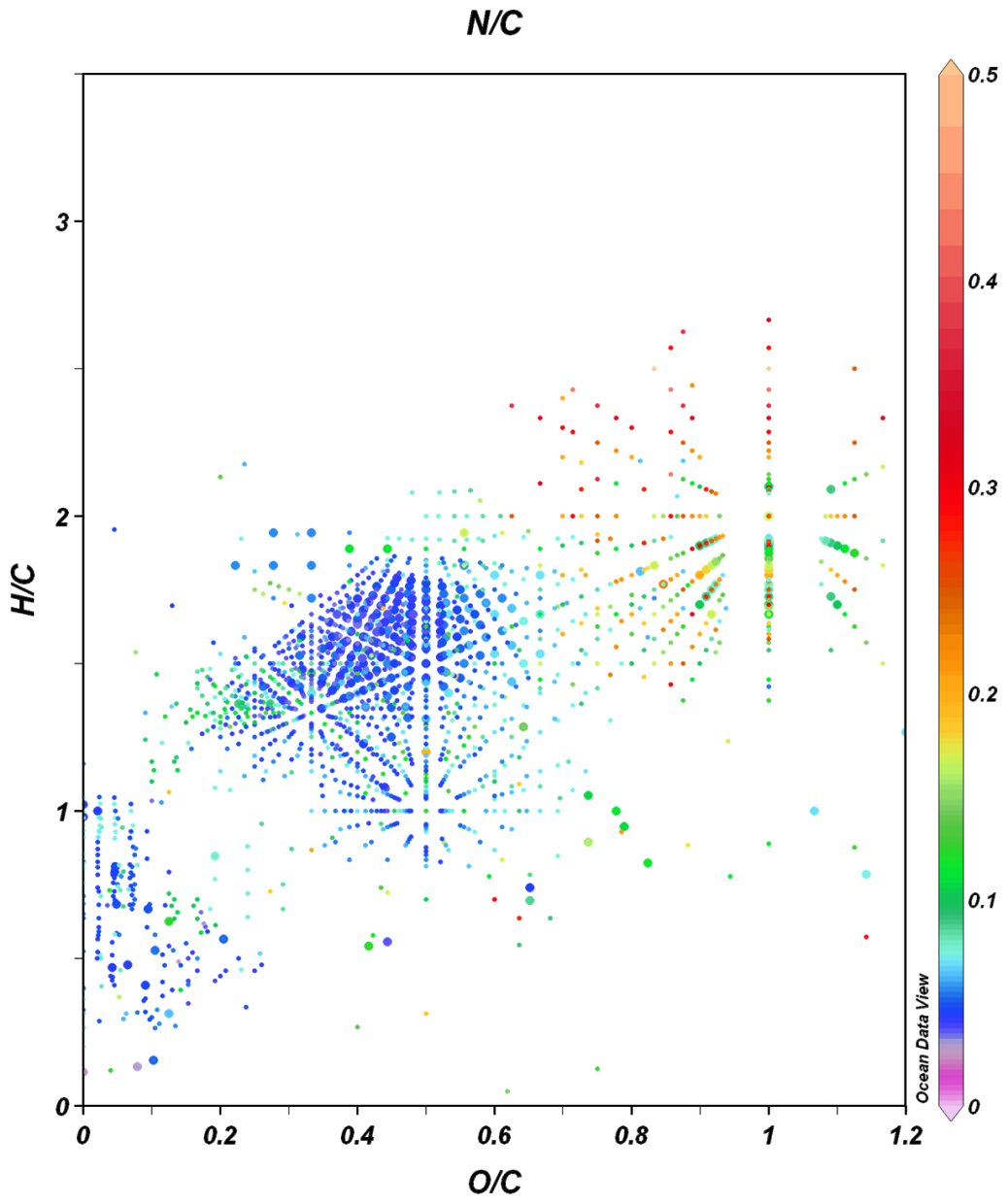

Figure 6.5: All CHON containing formulae (from all four samples) on a modified 3D Van Krevelen diagram with the N/C ratio on the z-axis by colour. Dots are two different sizes: larger dots represent peaks with a relative intensity greater than 10.

The N/C ratio of the majority of peaks in the lignin and tannin regions of the Van Krevelen diagram are low (~ 0.05). CHON Formulae with O/C > 0.8 and H/C > 1.5 are abundant, but confirmation that these unusual formulae are correctly assigned is not available.

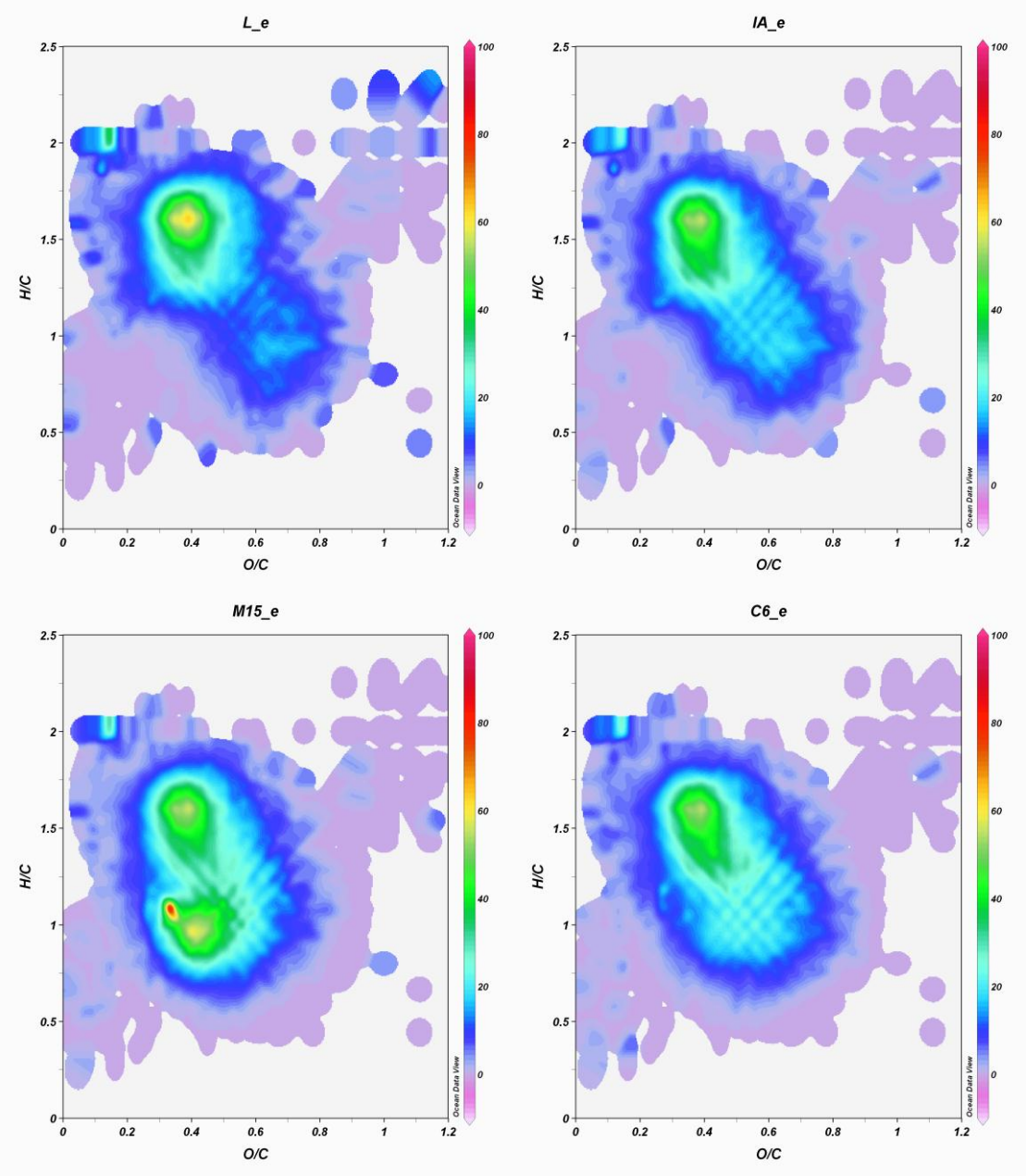

Figure 6.6: 3-D Van Krevelen plots of all samples, with relative intensity on the z-axis represented by colour. Plots made with Ocean Data View (ODV) using VG gridding to smooth z-axis. (The "e" in the sample name is to differentiate between data from extracted and non-extracted samples in ODV only, and can be ignored: non-extracted data is not presented for this study). See Appendix C for enlarged versions of the panels.

Figure 6.6 shows how the intensity of peaks plots on a Van Krevelen diagram (with intensities averaged to create a colour-contour plot). Generally the H:C 0.8-1.7, O:C 0.3-0.6 area of the Van Krevelen diagram contains the highest peak intensities in each sample. Sample M has a second region of high intensity peaks at lower H:C and O:C ratios. The area of very high intensity peaks indicated by the red "smudge" on the M1.5 plot (at H:C ~0.35 and O:C ~1.1) relates to a number of peaks which are

present in very high intensities (>100); these very high intensity peaks will be discussed in detail in Section 6.5. High intensity peaks are also found at low O:C ratios and H:C ratios of 2, the region indicative of lipids and fatty acids. As mentioned previously, these compound classes are known to be readily ionised by ESI (Sleighter & Hatcher, 2007) and therefore the high intensity of peaks in this region of the Van Krevelen does not necessarily represent high concentrations of these compounds.

6.4 Comparison of samples using Van Krevelen diagrams:

The above diagrams (Figure 6.6) contain a great deal of information (the intensity and atomic ratios of thousands of compounds) but are difficult to compare; many of the details are lost due to the use of gridding and because subtle changes in intensity are not easily read. Because the intensity of a peak does not necessarily reflect the actual collective concentration of molecules with the associated molecular formula (due to selective ionisation for example), it is useful to compare the relative intensity of individual peaks between comparable samples run at the same time under the same conditions (which eliminates changes in response due to instrumental set-up).

Comparative Van Krevelen plots of all four samples, showing the log-ratio of the relative intensities across different samples are shown below (Figure 6.7). Taking a pair of samples, for every peak which has been identified and assigned a molecular formula in both samples, the ratio of the intensities of that peak in each sample is found and plotted on the z-axis as colour (x- and y-axes are as regular Van Krevelen). A logarithmic scale is not commonly used for diagrams of this type, but has been used here as it is felt that it reduces bias caused by decimal versus non-decimal scale.

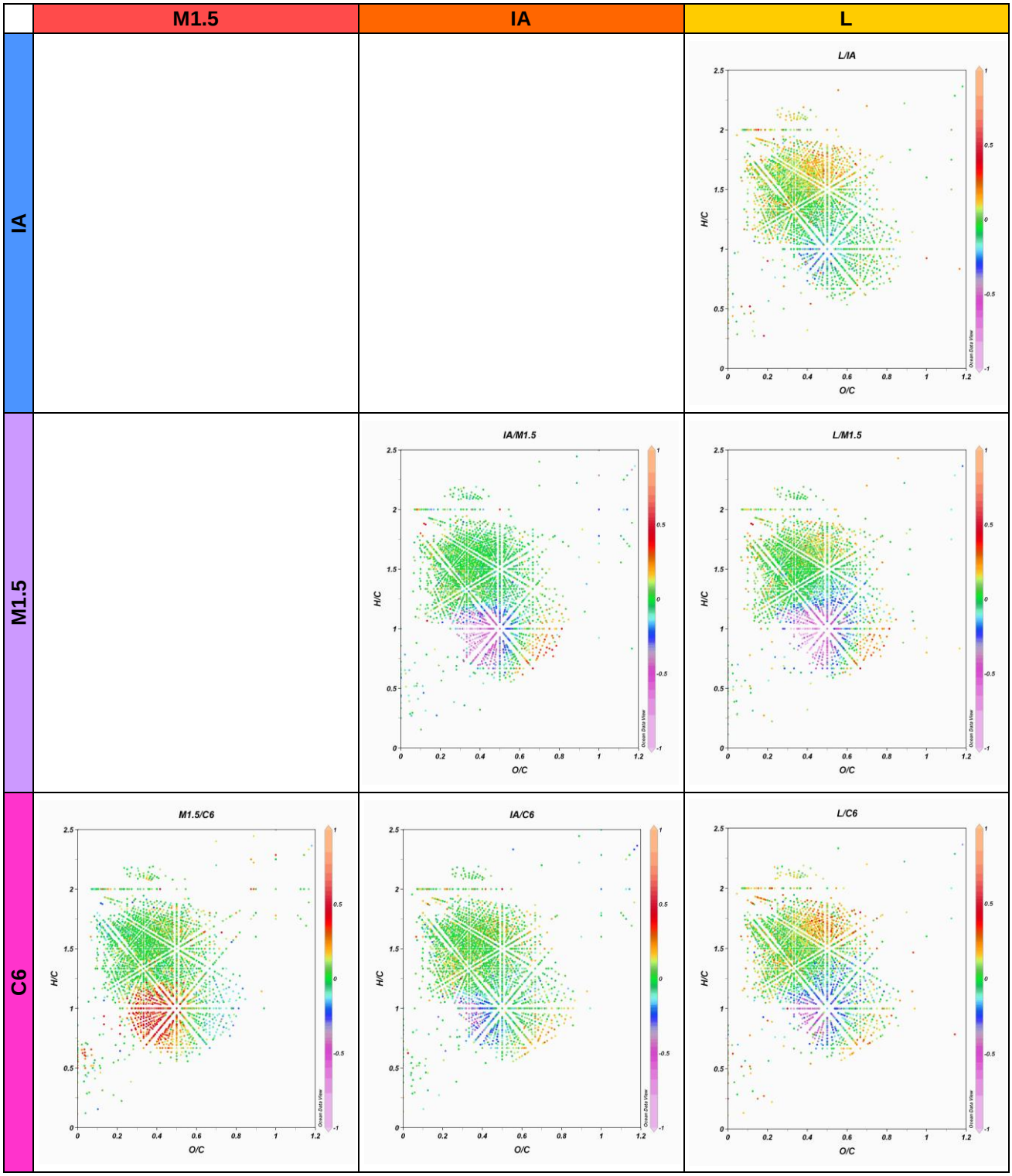

Figure 6.7: Comparison of the intensity of shared peaks plotted on Van Krevelen diagrams. On the z axis (by colour) is the $\log_{10}$ ratio of each shared peak with the numerator of the ratio labelled in the top row and the denominator of the ratio in the first column; green is a value of ~0 (ratio is close to 1, therefore little change in intensities between samples). For ease of comparison, the column and row labels are coloured in the colour palette which indicated higher intensities of the relevant sample; for example, the bottom right Van Krevelen diagram compared the intensity of all peaks found in both L and C6. L is the numerator (in the hot coloured palette) therefore z values > 0 (again in the hot palette) indicates a peak with higher intensity in the Lake sample. See Appendix C for enlarged versions of the panels.

The region of the Van Krevelen diagrams associated with lignin derived compounds shows a great deal of variation between samples, despite the fact that peaks falling within this region dominate all four spectra. The mid-peat sample (M1.5) from the low hydraulic conductivity region of the peat profile has much higher intensity peaks in the lower H:C and O:C region of this area, while the sample representing run-off from the bog (L) has many higher intensity peaks in the higher H:C ratio region, toward the protein-related region shown in Figure 6.3. The lake sample also shows higher intensity peaks where H/C > 2, specifically from O/C 0.2 to 0.4; many S containing formulae are found in this region in agreement with previous studies (e.g. Ohno et al., 2010, as shown in Figure 6.4). Although the L sample does not contain as many CHOS formulae as M1.5, those that do occur have are of moderate to high intensity and mainly appear in a confined region of H/C : O/C space, suggesting chemical similarity.

Both surface samples (L and IA) have higher intensity peaks in the more oxygen rich area of the lignin-associated region, with particularly high intensity peaks in the Lake sample. The region of H:C 1.2-1.7, O:C 0.2-0.6 shows remarkably similarity between all samples from bog porewaters (C6, M1.5 and IA); only the lake sample has noteworthy differences in peak intensities in this region, with many high intensity peaks, some with a relative intensity > 100.

6.5 Peaks unique to certain samples

Although the comparison of samples via 3D Van Krevelen diagrams provides a powerful visualisation method, only those peaks which are found in both samples being compared are considered. If a sample contains compounds with formulae which are unique to that sample, these will not be adequately represented using any of the visualisation techniques employed so far. Figure 6.8 shows another Van Krevelen diagram which compares the Lake and Mid samples, this time plotting those peaks which are unique to one of the samples being compared. Although 268 peaks are identified in the Lake sample but not in the Mid (blue), only 26 of these

have a S/N ≥ 10. The remainder are low intensity peaks, and their presence is likely dependant somewhat on the signal to noise ratio chosen as the cut-off for peak identification. There are a large number of unique peaks in the Mid-bog sample, and many of these are present at a S/N ≥ 10, largely found within the low H:C and O:C ratio region of the diagram.

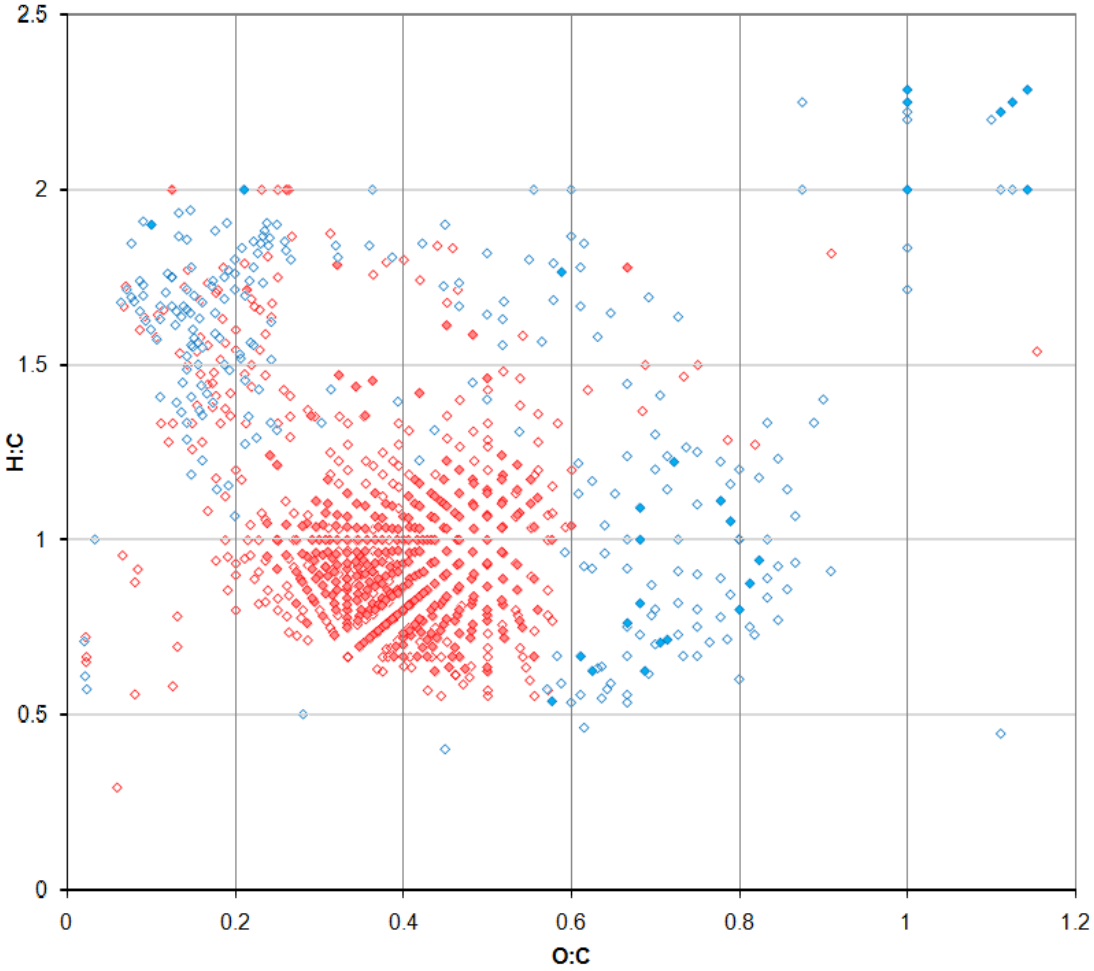

Figure 6.8: Van Krevelen diagram of CHO peaks which, when Lake and Mid samples are compared, are found in only one of the spectra. Colour denotes sample, with red marks indicate peaks only found in M1.5 and blue in L; open diamonds have 5 ≤ S/N < 10, filled S/N ≥ 10.

In order to investigate the peaks which are not common to all samples, the number of CHO peaks per nominal mass was calculated and plotted in Figure 6.9. To the author's knowledge, this approach has not been taken in any published studies. While most peaks per nominal mass integer are found at similar masses for all samples, more peaks per mass occur at high masses (>550 Da) in M1.5, and this high-mass region also has the fewest peaks in L. The 14 Da repeating pattern that was

present in the spectra presented in Figure 6.1 is even clearer in Figure 6.9. Another notable feature of this plot is that although the nominal masses which have the most peaks per mass have a similar number across all samples, the troughs in the "wave" created by the 14 Da repeating pattern are much lower in L and IA. The implications of this relate to the degree of similarity between all chemical species identified in a sample, with respect to CH_2 addition and subtraction, and will be discussed below.

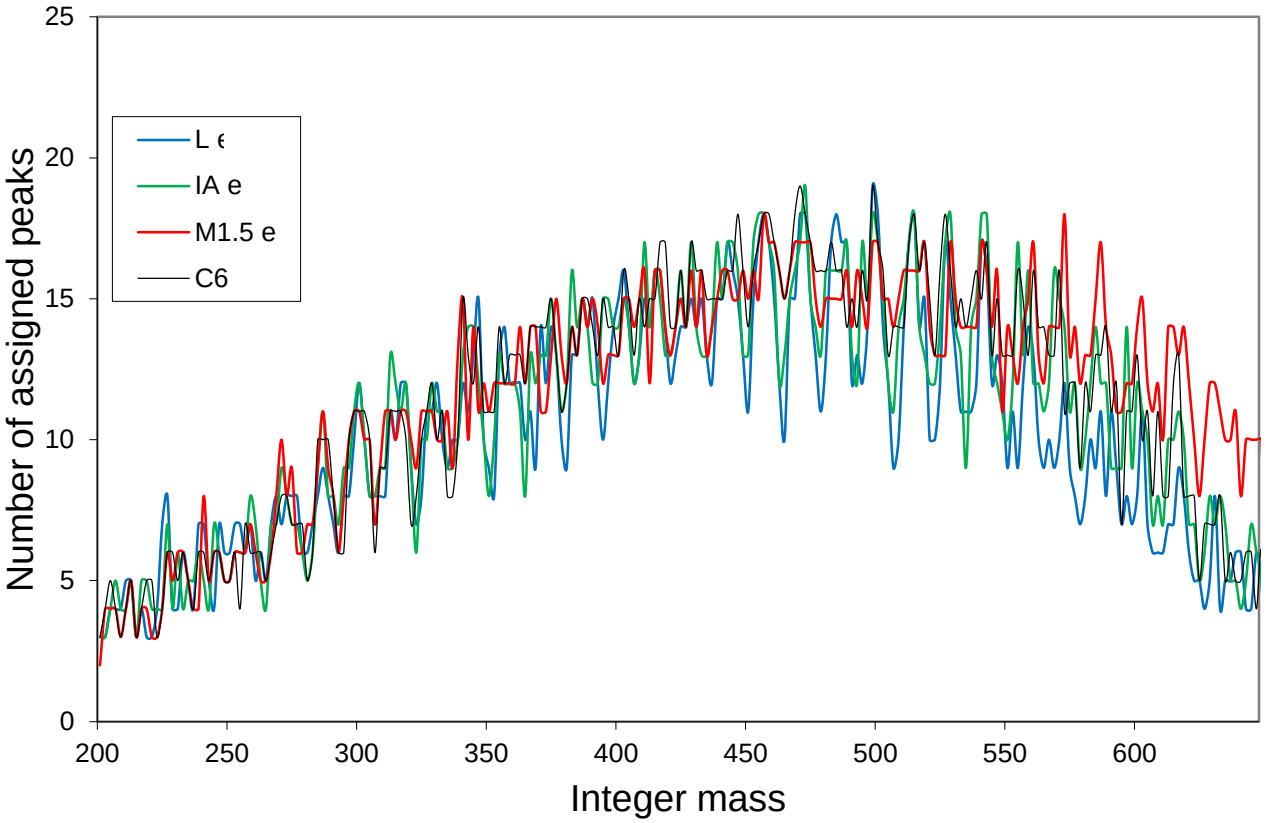

Figure 6.9: The number of CHO peaks per integer mass identified in each sample. As only CHO assignments are included, even integer masses (which are limited to ^{13}C-COH, $CHON_1$ and $CHON_3$) are not considered.

The 14 Da recurring pattern in Figure 6.9 comes about because many formulae within each sample are related to each other by CH_2 additions, forming semi-homologous series (e.g. Stenson et al., 2003). If the sample is dominated by several long chains of semi-homologous series, it is likely that there will be a strong 14 Da pattern in the spectra. Conversely, if the sample is made up of many short chains, with large numbers of unrelated compounds, it is likely that there will only be a weak 14 Da pattern.

To quantify the strength of the recurring patterns in Figure 6.9, software (AnalySeries v. 2.0.4.2, freely available online at http://ngdc.noaa.gov/paleo/softlib/softlib.html) was used to perform wave analysis on all four plots. The resulting frequency data (plotted in Figure 6.10) shows a large peak at 14 Da.

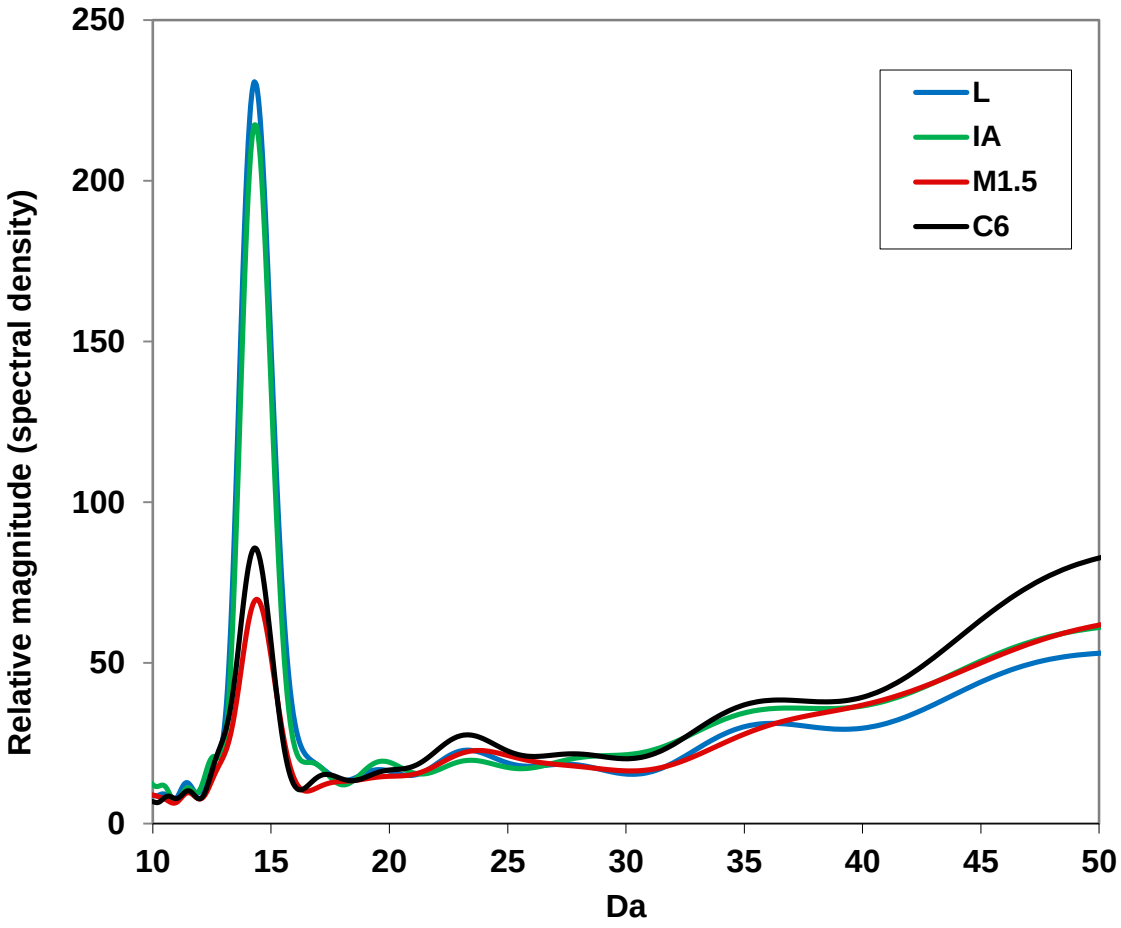

Figure 6.10: spectral analysis of data from Figure 6.9. (BTukey spectrum using Bartlett window with a bandwidth of 0.0110294; obtained using AnalySeries 2.0.4.2)

6.6 The use of Kendrick Mass Defect to identify transformational relationships in complex NOM mixtures

As illustrated by Figures 6.9 and 6.10 (and discussed above) there is a strong 14 Da pattern in the mass spectra obtained by ESI-FT-ICR-MS because many formula are very similar to each other, and differ only by the addition or subtraction of a CH_2

unit (e.g. the lengthening of an alkyl side-chain). By collecting all the formulae related to each other in this way (or by other molecular transformations, as will be discussed later), it is possible to see the degree of inter-relatedness in the large and complex mixtures of compounds found in NOM. The groups of these inter-related formulae are referred to in this work as semi-homologous series or chains.

All the peaks within a sample can be sorted into semi-homologous series by calculation of the Kendrick mass defect (KMD) (Hughey et al., 2001). Initially, the series being considered link all those species which are related to each other by the addition or subtraction of a CH_2 unit. The mass difference between all members of a series will therefore be a multiple of 14.01565 Da, the exact mass of CH_2 (Hughey et al., 2001). In order to identify these mass differences, it is useful to convert all CHO masses from IUPAC mass (based on a ^{12}C atom having a mass of 12.000) to a "Kendrick" mass, where the mass of a CH_4 unit is nominally assigned the value of 14.000 (Kendrick, 1963) by using the following equation:

$$\text{Kendrick mass} = \text{IUPAC mass} \times (14 / 14.01565) \quad (6.3)$$

In this new mass scale, all compounds which differ only by the addition or subtraction of CH_2 units have masses which differ by multiples of exactly 14, so will have the same numbers after the decimal place. This is termed the Kendrick mass defect, where:

$$\text{KMD} = \text{nominal Kendrick mass (integer)} - \text{exact Kendrick mass} \quad (6.4)$$

Now all members of a semi-homologous series have the same KMD, and if they are a CHO compound, the semi-homologous series can be defined by its DBE and O content. Figure 6.11A shows a plot of KMD with nominal mass for the samples M1.5 and L. In order to differentiate more easily between semi-homologous series, they have been coloured according to their z* value. Although it has little physical

meaning, this term separates all nominal masses according to where they lie on a 14 Da cycle[1] and is calculated using Equation 6.5 below:

$$z^* = (\text{modulus [nominal mass / 14]}) - 14 \quad (6.5)$$

Once data has been plotted as a KMD/mass diagram, samples can be compared using similar visualisations as for Van Krevelen diagrams. Figure 6.11B shows examples of these, for the same samples, where the intensity (averaged in H:C and O:C space to create a colour contour) is plotted as the z-axis and then the intensities of all shared peaks are compared using a log-ratio (Figure 6.11C).

From plotting the intensities on a KMD/mass diagram, it is again clear that the region of very high-intensity peaks seen previously in the M1.5 Van Krevelen plots spans a wide range of intermediate masses (~350 – 550 Da), and that the peaks which are present in M1.5 but not in L are mainly of high mass (> 550 Da) and high KMD (which relates to low H:C ratio). Figures 6.11-A and -B offer a complimentary visualisation technique, but the KMD/mass diagram is of most value when used to plot the relationships between individual peaks.

[1] all nominal masses that divide exactly by 14 are given a value of -14, all masses 2 mass units above these have a z* value of -12 etc.

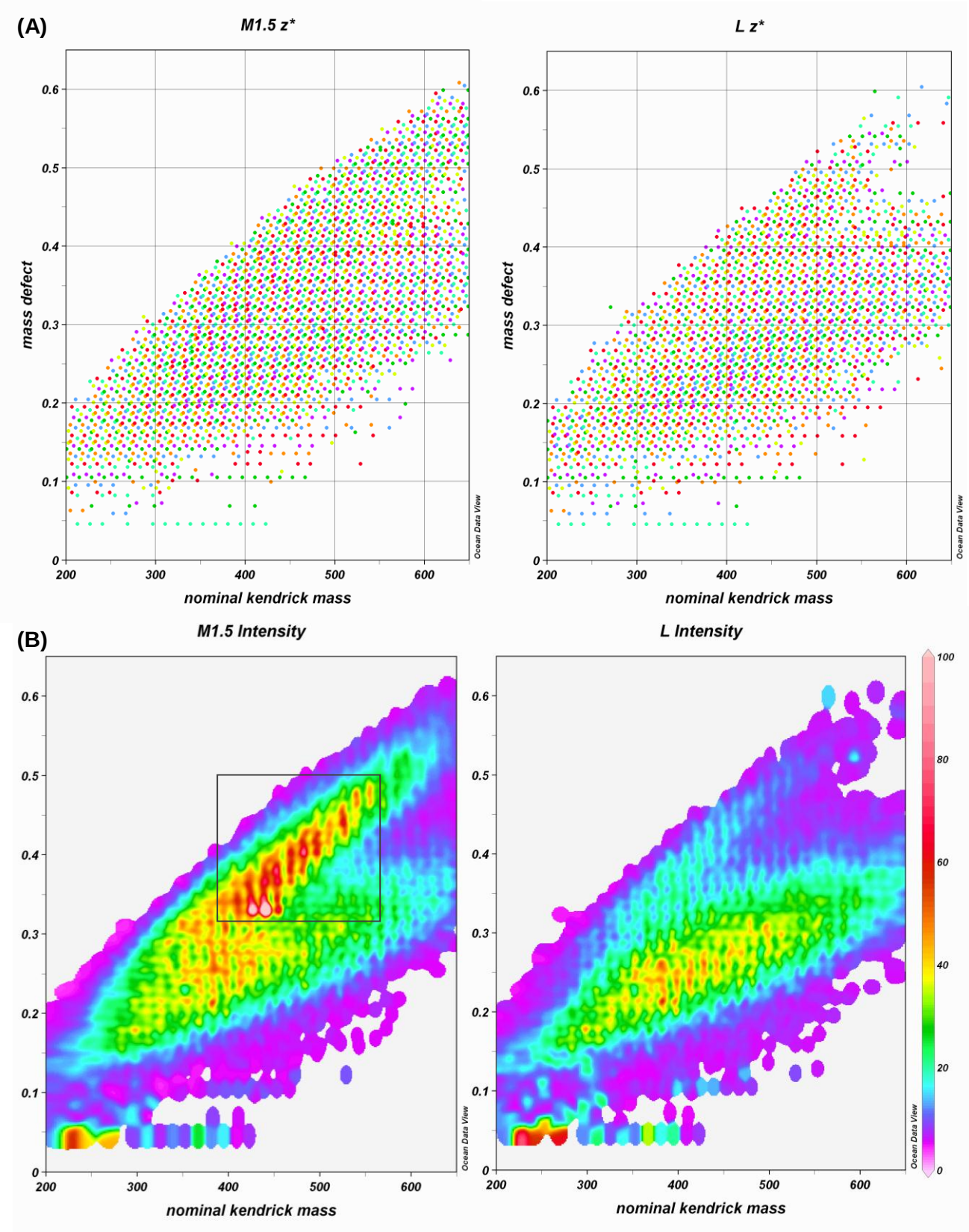
(A)
M1.5 z*
L z*
mass defect
nominal kendrick mass
Ocean Data View
(B)
M1.5 Intensity
L Intensity
nominal kendrick mass
Ocean Data View

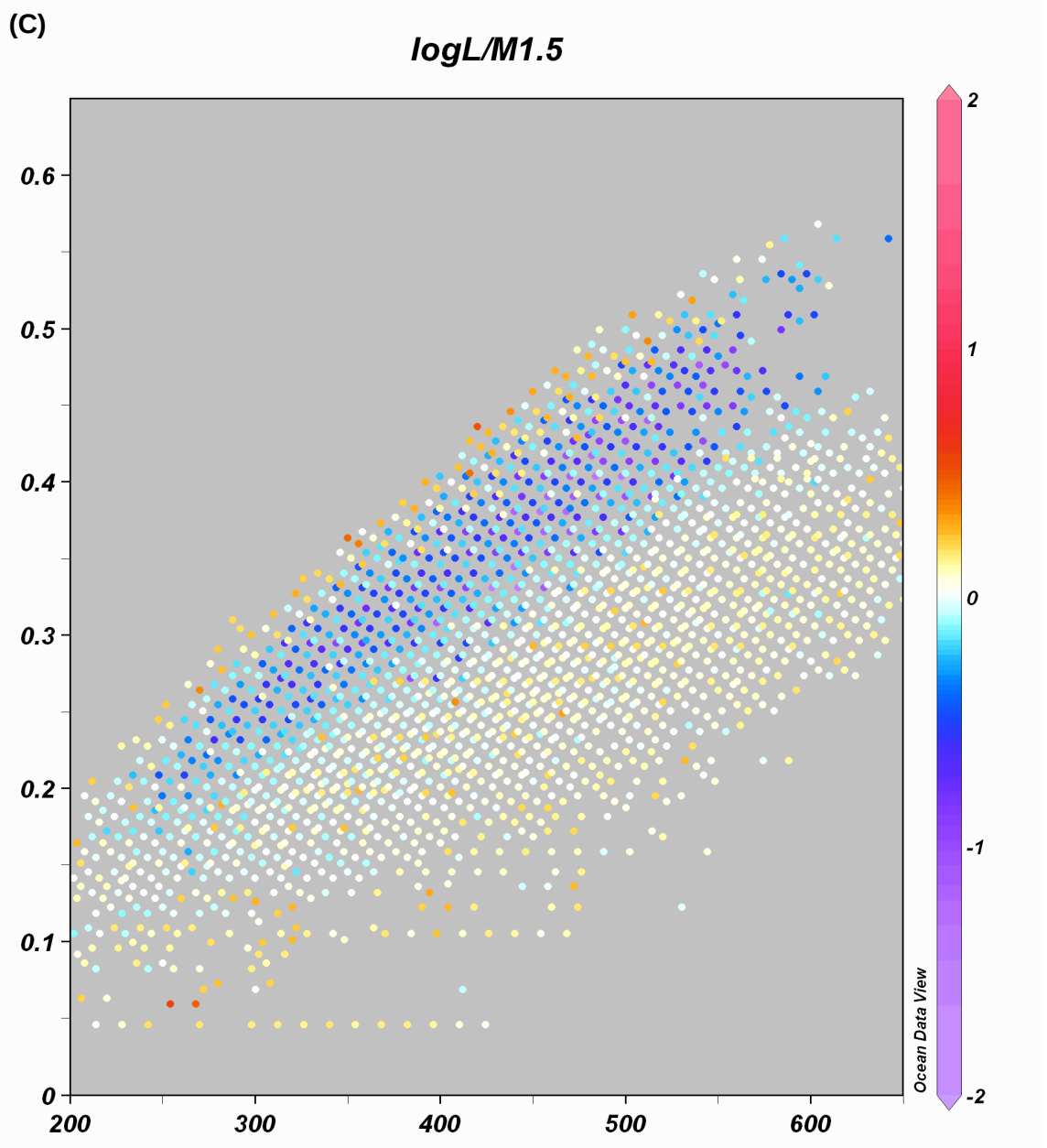

Figure 6.11A (upper two plots on previous page): Kendrick mass defect of CHO species plotted against nominal mass for L and M1.5 with all formulae sorting by z* value (shown by colour). Figure 6.11B (two lower plots on previous page) show the same plots but with relative intensity on the z-axis, using Ocean Data View VG gridding to smooth z-axis into colour contour plot. The grey box identifies the region of the diagram which is investigated further below (see Figures 6.13 and 6.14). Figure 6.11C (this page) is a comparative plot: the $\log_{10}$ ratio of intensities (L/M1.5) is plotted on the z-axis, with warm colours denoting peaks present in both spectra but at a higher relative intensity in L, whereas those in cool colours have higher intensities in M1.5 and peaks of similar intensity are pale or white.

Although separating NOM according to DBE, z* values and oxygen content is a valuable step to molecular characterisation, the number of terms and variables is still large. Koch et al., (manuscript in preparation) have proposed that, although complex,

all NOM can be characterised by one equation, which combines the previously utilised terms into an ORganic Compound Class (ORCC, Equation 6.6):

$$ORCC = DBE - O + (z^* / 2) \quad (6.6)$$

For all CHO compounds, ORCC can theoretically only have 18 chemically feasible solutions, although the vast majority of molecules found in NOM belong to three ORCCs: -13, -6 and 1 (Koch et al., in prep.) and 92% of peaks identified in samples from Cors Fochno have a ORCC or -6 or 1. Figure 6.12 shows histograms of the number of peaks at each nominal mass separated by ORCC, and it is clear that compounds with an ORCC of -6 are found throughout the mass range, whereas ORCC 1 compounds are more abundant at high masses in the Mid sample. Koch et al. (in prep) note that around half of all detectable molecular formulae are present in all marine samples, and these compounds, which represented the refractory background in DOM, almost all have ORCC values of -6.

Van Krevelen diagrams have highlighted a region of high intensity peaks in the Mid samples (centred around H/C ~ 1 and O/C ~ 0.4) which is accompanied by many peaks which are unique to this sample. KMD/mass diagrams have provided further information on the mass range and high KMD values for these peaks. By filtering the CHO peak selection (minus fatty acids) to only include those peaks with high relative intensity (>60), 238 peaks are selected. These peaks all have ORCC values of either -6 or 1, the distribution of which are shown on a Van Krevelen diagram in Figure 6.13.

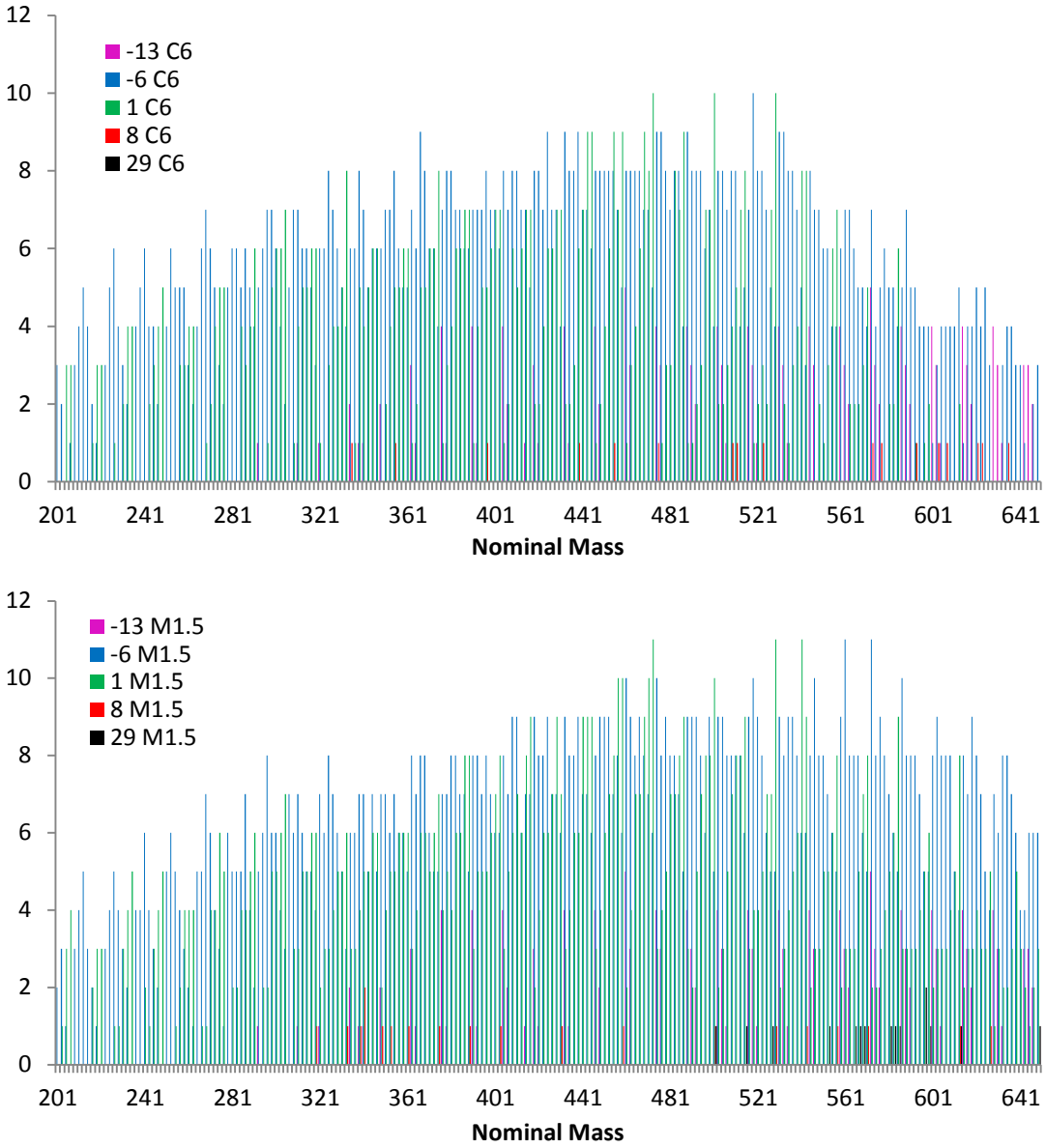

Figure 6.12: Histograms of the number of CHO compounds identified per nominal mass separated by ORCC (above for C6 and below for M1.5).

Those peaks from the region of the Van Krevelen diagram which has been identified as particularly significant in M1.5 (high intensity, with unique peaks) all share an ORCC of 1, whereas all those peaks which are present in high concentrations in all samples belong to ORCC -6. The organic carbon class separation has provided the final tool by which these compounds can be systematically filtered. By simple comparison of the number of peaks in each semi-homologous series for ORCC of 1 versus an ORCC of -6, the ubiquitous character of ORCC -6 can be confirmed. While the average "chain length" for ORCC -6 semi-homologous series is 15.2 peaks and

the standard deviation of the lengths is 1.046 (7%), the average length for ORCC 1 is 10.0 peaks, with a standard deviation of 2.201 (22%).

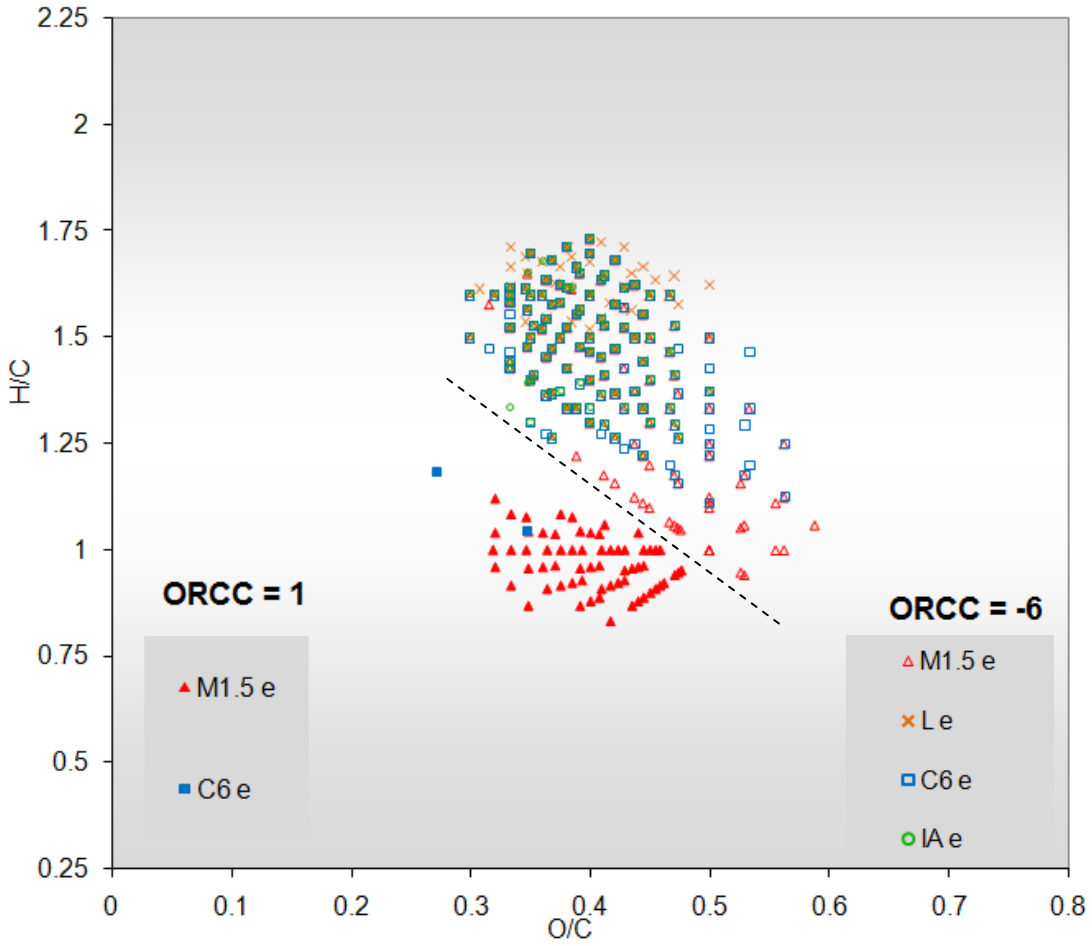

Figure 6.13: Van Krevelen diagram of all CHO peaks with intensity > 60 (excluding fatty acids) identified in all samples. Filled markers indicate ORCC = 1 (below the dashed line, which is presented only to aid the eye) and open markers indicate ORCC = -6.

By considering only high intensity (> 60) peaks which do not belong to ORCC -6, those peaks which are found ubiquitously in all samples may be discounted and the remaining formulae can be plotted on a KMD/mass diagram to show possible transformational relationships between these species (Figure 6.14). It is worth noting the different distribution of higher intensity CHO ORCC -6 peaks and particularly those regions of the Van Krevelen diagram which are occupied by peaks from only one sample: the Lake sample has numerous peaks at high H/C, both C6 and M1.5 have peaks at high O/C and the area around H/C = 1 and O/C = 0.5 is dominated by

peaks from M1.5, supporting the previous comparisons of bulk chemistry and Van Krevelen diagrams.

The points on a KMD/mass diagram are arranged such that transpositions along the horizontal equate to addition or subtraction of CH_2 units (Figure 6.14). All points along one line will have the same number of rings and double bonds (DBE) and oxygen content, and changes in horizontal position may indicate lengthening or shortening of alkyl side chains. In the same way, near-vertical relationships equate to a change in the saturation state of organic structures (resulting in the same C and O numbers but altered DBE). These networks of homo-oxic formulae (composed of several semi-homologous series) then overlap, with further transformations (indicated by curved arrows on Figure 6.14) representing changes in oxygen content. This final visualisation method shows how, with only a few simple chemical transformations, all the large peaks responsible for the unusual character of M1.5 can be linked.

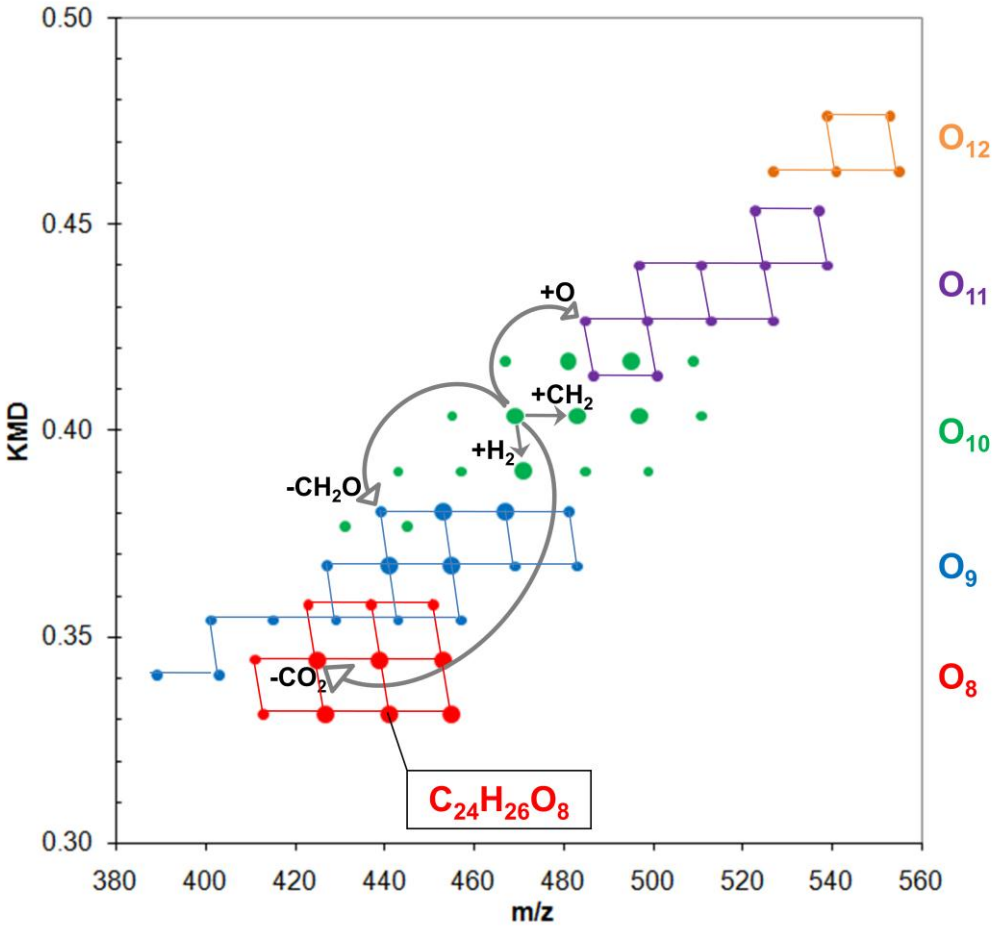

Figure 6.14: KMD vs mass plot for all assigned CHO peaks from the Mid sample with a relative intensity >60 and belonging to ORCC = 1.

It is important to note however that structural information is still only inferred from molar ratios; two peaks may lie close to each other on the above diagram but represent multiple compounds with structures which cannot be related by simple transformations (for example the structures shown in figure 6.15, which belong to the same semi-homologous series but are structurally very different). When considering a very long semi-homologous series (such as the DBE = 7, O = 7 series which has 28 members in C6; the maximum mathematical chain length for a mass range of 200-650 is 32), it seems unlikely that all structures are linked simply by stepwise changes in alkyl chain length. When considered as part of a large interlinked network however, the multiple transformational pathways available allow for substantial changes to structure through many small steps.

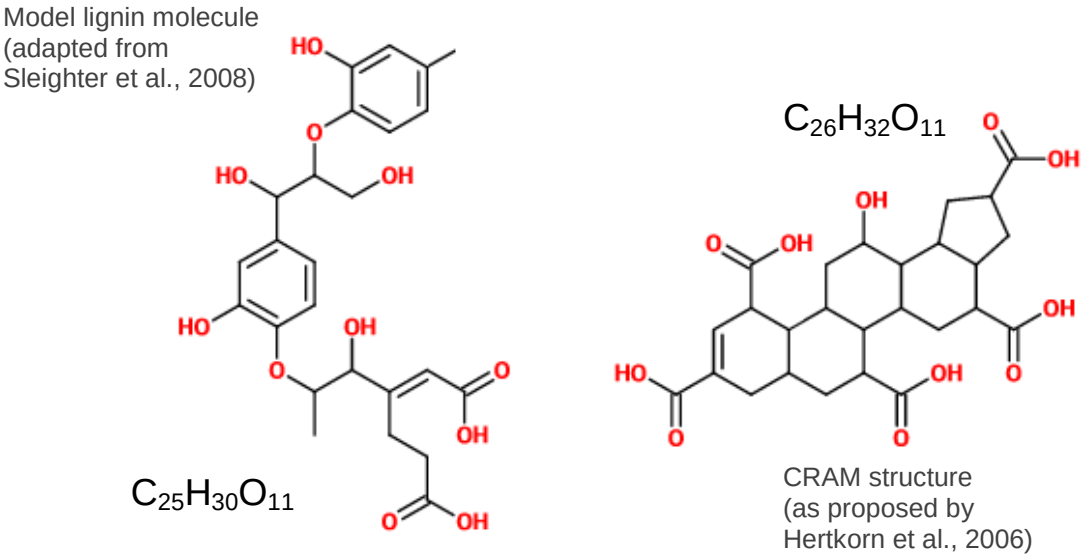

Figure 6.15: Two possible structures for members of the same CHO semi-homologous series (DBE = 11, O = 11). The structure on the left is an adapted lignin model structure from Sleighter et al. (2008) and that on the right is one proposed for Carboxyl-Rich Alicyclic Molecules (CRAM) by Hertkorn et al. (2006).

Even though transformations, as represented graphically in Figure 6.14, may not be chemically relevant for all formulae which appear to be linked, the visualisation of these interlinking networks provides a powerful interpretation tool. Using these networks, the mechanisms affecting the composition of DOC in an organic carbon pool may be deduced. If all the peaks within a ESI-FT-ICR-MS spectrum were plotted on a diagram such as Figure 6.14, it would be impossible to track all these transformations, but there would still be many peaks aligning along trajectories representing the same chemical transformations (i.e. linking formulae that are related to each other by the addition or subtraction of a simple molecular unit). In order to interpret the entire data set, semi-homologous series are required for a number of transformations. This is a novel approach to the interpretation of ESI-FT-ICR-MS data, which has been developed by the author for this study.

Where the standard KMD series provides information on how linked the array of molecular structures is by CH_2 addition or subtraction, similar mass defect series can be constructed for any transformation of interest by the use of Equations 6.7 and 6.8 where U is the molecular unit being either added or removed during the

transformation. Seven further transformations were considered (listed in Table 6.2) and all CHO compounds were arranged into "transformational series".

$$\text{Kendrick mass (U)} = \text{IUPAC mass} \times [(\text{nominal mass of U}) / (\text{exact mass of U})] \quad (6.7)$$

$$\text{KMD (U)} = \text{nominal Kendrick mass (integer)} - \text{exact Kendrick Mass (U)} \quad (6.8)$$

Transformation	Unit	Mass	Transformation	Unit	Mass
Methylation/ chain lengthening	CH_2	14	Saturation	H_2	2
Hydration	H_2O_2	34	Decarboxylation	COO	44
Hydrolysis	H_2O	18	Carboxyl to hyrdroxyl transformation	CO	28
Oxygen addition (e.g. ring cleavage)	O	16	Oxidation	$+O$ $-H_2$	14

Table 6.2: The molecular transformations considered when creating "transformational series" based on the Kendrick mass defect of molecular unit U (with nominal masses).

Once KMD(U) values have been calculated for all CHO formulae, they can be assigned to a "transformational chain" and these chains can then be investigated. The four samples investigated all contain DOM which has been produced from the same pools of living matter: peatland plants (both vascular and moss) and bacterial/microbial and fungal communities. Differences between the samples may be due to a large number of factors, such as oxygen availability, age or decomposition history, and the presence of light (driving photo-oxidation processes). Remnant signals of the molecular transformations which this DOM has undergone may be left in the size and distribution of the transformational series identified by FT-ICR-MS. For example, if a large proportion of formulae in one sample are related by oxidation and therefore belong to a series of long $+O-H_2$ transformational chains, this may indicate that oxidation is one of the key mechanisms which has led to the large array of OM present.

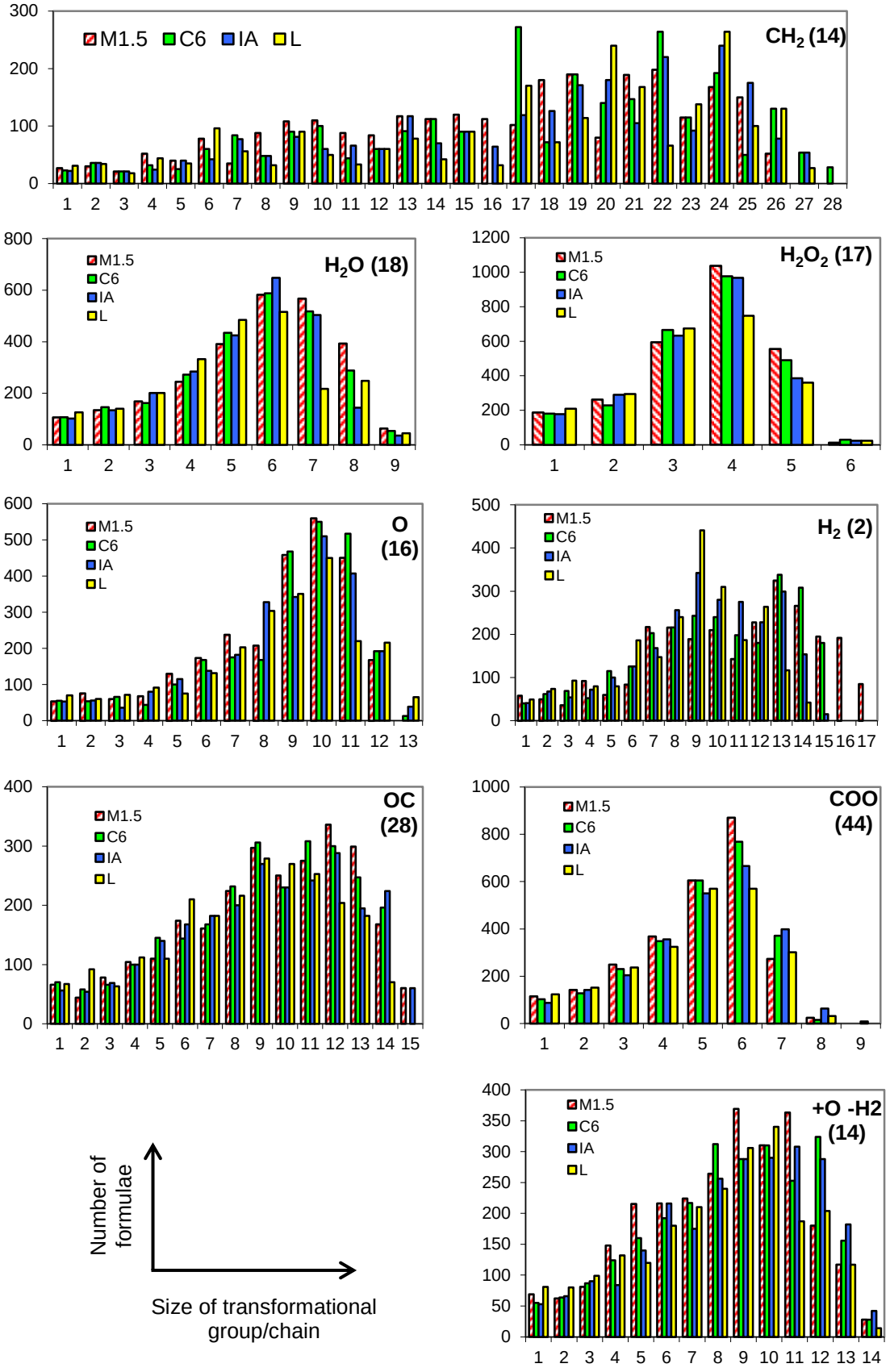

Figure 6.16: The number of formulae found within transformational series of different sizes. For each transformation (indicated by both molecular unit and nominal mass to which Kendrick mass was normalised), the x-axis shows sizes of groups (or chain-length) and the bars represent the number of formulae found in groups of that size. Different samples represented by colour.

Figure 6.16 shows plots of the number of peaks belonging to all calculated transformational series separated by series-size; that is, if we consider all members of a series to be part of a transformational chain, chains are sorted by "length" and the number of formulae contained within a chain of each specific length are summed. As an example, in the top chart of Figure 6.16, there is a large bar at chain length 17 in light green, the C6 sample. The bar is 272 tall on the y-axis (the number of formulae). This means that 272 formulae are found within chains connecting 17 formulae in a semi-homologous series, i.e. that (dividing 272 by 17) there are 16 such "chains" in the C6 sample.

Kujawinski et al. (2002) arranged mass peaks from two HS samples (Suwannee River FA and Mt. Rainier humic acid) into CH_2 semi-homologous series, and found that the majority of these series contained fewer than ten members. This may indicate that HS from Cors Fochno is more structurally related (with respect to CH_2 addition) than other terrestrial HS as the majority of CH_2 series shown in Fig 6.16 are larger than this. The other information contained in Figure 6.16 (from those plots not relating to CH_2 addition) is difficult to compare to previous work as, to the author's knowledge, nothing similar has been published. Grinhut et al., (2011) used a similar series of transformations to assess the transformations of HS on degradation by white rot fungi but the approach and interpretation differs. For this reason, discussion of absolute "chain lengths" will be kept to a minimum. The multitude of compounds which make up NOM will of course have many apparent relationships between them, especially if the pool is limited to only those molecules which contain no heteroatoms (CHO compounds). But, whatever the typical interlinking of compounds in NOM, shifts away from this, and thus differences between the four Cors Fochno samples, may provide a novel way of exploring transformational relationships.

Firstly considering the length of CH_2 transformational series presented in Figure 6.16, all CHO formulae belong to CH_2 semi-homologous series which range in size from 1 (a sample not linked to any others) to 28. These series cover the full range of chemical

compositions found, from saturated and oxygen rich to aromatic carbon rich compounds, and can therefore characterised by DBE and oxygen content (the two parameters which categorise CH_2 semi-homologous series). The larger series (containing ≥5 formulae) were split into five categories:

- those series which varied in size significantly between samples (standard deviation of size >1.5) were separated into four groups (A-D), according to which sample contained the largest example of that series;
- all large series (containing ≥ 15 formulae in at least one sample) which vary little in size between all samples (standard deviation < 1)[2] were designated category E.

These five categories were then characterised by average DBE and oxygen content, the results of which are shown in Table 6.3. Only 5 CH_2 transformational series were largest in the Lake sample, and those 5 semi-homologous series were characterised by very low double bonding and aromaticity and relatively low oxygen content. Many of the series which are variable in length (categories A-E) are largest in the Mid-bog sample (48% of the relevant series), and this group is characterised by very high DBE. On average, the most oxygen rich series are longest in the integrated acrotelm (IA) sample, whereas the least oxygen rich are largest in the deepest porewaters (C6). The largest and most stable series of compounds have on average a relatively low DBE value and high oxygen content. These ubiquitous chains of semi-homologous formulae likely represent the background HS present in all DOM samples.

[2] Although somewhat arbitrary, these values were chosen so that the number of series over which averages were taken were comparable between categories.

Category	CH_2 transformational series category (described in text)	Number of series in category	Average DBE	Average O content
A	Variable size, largest in L	5	5.2	8.00
B	Variable size, largest in IA	14	11.7	11.1
C	Variable size, largest in M1.5	45	15.0	9.98
D	Variable size, largest in C6	30	10.5	7.83
E	Very large and ubiquitous	54	8.24	10.2

Table 6.3: The properties (average DBE and molecular oxygen content) of CH_2 semi-homologous series, as sorted by prevalence in different samples. See text above for description of categories.

Considering the other transformational series presented in Figure 6.16, the largest series include saturation, oxidation, O addition and that of the hydroxyl to carboxyl (or similar) transformation, represented by the addition of a CO unit. Fewer formulae are linked by either hydrolysis or hydration transformations. The length of decarboxylation series is also noteworthy considering the mass change of the transformation (44 Da) and the mass range over which compounds were measured (450 Da). The differences in the size of transformational series between samples may be indicative of the mechanisms by which the mixture of organics within the DOM is produced. DOM in the Mid 1.5 m sample has many formulae which may be related by multiple hydration steps; it also has fewer formulae linked by oxidation or O addition. Fewer formulae in the Lake sample are related by OC addition or subtraction than in other samples, and there are also fewer formulae possibly linked by multiple saturation steps. Instead, more formulae are linked by O addition, which could be indicative of ring cleavage (Grinhut et al., 2011). Finally, the shallow porewater sample (IA) is characterised by many formulae which are linked by decarboxylation and by oxidation, and also has large series suggestive of hydroxyl to carboxyl transformations.

6.7 Chapter synthesis and conclusions:

The comparison of transformational series provides a powerful tool for assessing possible mechanisms involved in the formation of the DOM pool, particularly with

respect to the formation and transformation of HS. There is now a clear distinction between samples: those series of compounds which are least saturated, with many double bonds are most prevalent in the Mid 1.5 m sample. The Mid 1.5 m sample is also most linked by apparent saturation transformations, and contains many formulae which are linked by what may be changes in the aromatic backbone of structures, but have few links relating to the addition or subtraction of oxygen rich functional groups. The Mid 1.5 m sample has many very high intensity peaks which have been assigned formulae which lie within the Van Krevelen compositional space traditionally attributed to lignin, but which is also occupied by phenolic compounds, e.g. sphagnum acid. These peaks are all related by a simple series of transformations, as can be seen when plotted on a KMD diagram.

The most oxygen rich series contain a greater number of formulae in the shallow porewater sample (IA), and on entering the Lake environment the molecular formulae become less related by CH_2 addition or subtraction, with an increase in much more saturated compounds. More formulae in IA are linked by the addition or subtraction of a carboxyl group, or by transformation of carboxyl groups to hydroxyl groups (or vice versa), whereas more formulae in the Lake are possibly linked by O addition, indicative of ring cleavage. Comparison of the relative intensity of shared peaks between pairs of samples agrees with this. IA and L samples both have numerous peaks with higher intensity than L and C6 samples at higher O/C ratios, and L in particular has many larger peaks at high H/C ratios. All of this agrees well with data from TMAH thermochemolysis GC-MS presented in Chapter 5. The use of % benzoic acid and (R1 + R2) : (R>2) proxies suggested that oxidative degradation produced a suite of acidic functionalities at shallow depths, and that in the Lake environment these were susceptible to photodegredation.

The Lake sample had many fewer peaks with assigned formulae in the higher mass range (>500 Da) than in other samples, and the greatest number of high mass formulae were found in the Mid 1.5 m sample. The loss of high mass aromatic compounds in the Lake sample may be another indicator of photoxidative

degradation (Stubbins et al., 2010). The largest number of identified peaks was found in the Mid 1.5 m sample; not only is the DOC concentration higher in this sample than in others, but it is also composed of a more diverse mix of HS.

Finally, the well established use of comparative Van Krevelen diagrams shows that peaks plotting in the lignin/polymeric phenol region are highest in the Mid 1.5 m sample. This is further strengthened when comparing 3-D Van Krevelen diagrams with relative peak intensity on the z-axis. In these diagrams, the C6, IA and L samples contain a single dominant (high intensity) area which is similar to a degraded HS (degraded lignin) source, whist the M1.5 sample has two dominant regions, the other being centred around the compositional space of phenols such as sphagnum acid. Nitrogen containing formulae plot over a large range of H/C and O/C ratios, but are rarely present at high intensity. There are also few high intensity N-containing formulae which plot within the amino-sugar and protein regions of the Van Krevelen diagram. This may suggest that nitrogen is incorporated into a large array of chemically diverse macromolecular structures, and that the organic compounds containing nitrogen bear little resemblance to the plant or microbial source materials from which they were originally derived.

The use of novel visualisation techniques and interpretation of these provides a new tool for assessing the simplicity and inter-relatedness of compounds within a sample. Histograms of the numbers of identified CHO formulae per integer mass turns the 14 Da pattern in FT-ICR-MS spectra into a wave pattern that can be analysed using common spectral analysis tools to quantify this pattern. The strength of this pattern may be indicative of a) the many differing fundamental building blocks of macromolecular HS, and b) how linked all formulae are by CH_2 addition or subtraction, which may depend on the diagenetic or decompositional history of the sample. Further work (outwith the scope of this study), requiring the reinterpretation of FT-ICR-MS data from differing NOM environments, would assess whether this technique is of use as an interpretive tool.

Chapter 7: Synthesis and conclusions

The following chapter will summarise and compile the findings from the previous chapters by first identifying key samples or sample types, then addressing each of these key samples in turn, tying in information from all chapters. The objectives, novelty and limitations of the study will then be considered.

7.1 Carbon dynamics and key samples

The measurement of dissolved organic carbon (DOC) concentrations across a number of sites, at a range of depths and over 18 months, has provided a new insight into the heterogeneity of DOM within a northern peatland. DOC concentrations varied over the site by more than an order of magnitude, and seasonal changes in DOC concentration were dramatic, to depths of 50 cm below the peatland surface. Four key sample types were identified which would represent the chemical environments for the majority of samples collected:

- Shallow depth samples (15 and 30 cm) from the Central site exhibited seasonal changes in DOC concentration;
- Porewater samples from deep within the peat profile (3-6 m) may represent a more stable DOC pool;
- Intermediate depth samples (1 – 2 m) from the Mid-bog site had very high DOC concentrations, observed as a broad peak in the DOC depth-profiles from this site;
- Samples from a pool at the southern edge of the bog (Lake) were thought to be representative of runoff from the site into nearby water-bodies.

Although variations in DOC concentration were large across spatial and temporal scales, relationships between environmental and physical factors (i.e. water table, temperature and the hydraulic conductivity of the peat) and DOC concentrations were observed. At shallow depths (Central site at 15 cm), the DOC concentration was related to the temperature at the time of sampling, suggesting that at this depth the

production of DOC by microbial communities and plants (e.g. by root exudation) is the main control on DOC concentrations. The same is not true in the Lake sample, where DOC concentrations appear instead to be controlled by delivery of water to the Lake site. The gross increase in water table height (measured at two hourly intervals at a piezometer between the Mid and Edge sites) over the seven days prior to sampling was shown to have a statistically significant positive relationship to Lake DOC concentrations. Finally, the average DOC concentration of porewaters from deeper wells (≥ 50 cm) had two controlling factors: concentrations increased with lateral distance from the centre of the site (concentrations were highest near the edges of the bog) and a statistically significant negative relationship between the hydraulic conductivity measured in the sampling well and average DOC concentrations was observed.

The relationship between Lake DOC concentrations and water table increases was used to estimate DOC concentrations in the Lake for the 3 year period over which water table measurements were taken. These values were then combined with monthly average rainfall data to calculate a DOC flux for the entire site of 113.2 tonnes yr^{-1} or 17.4 gC m^{-1} yr^{-1} which is similar to studies of other peatland sites and is comparable to estimated accumulation rates, demonstrating the significance of DOC fluxes for the overall carbon balance of the peatland. Although the estimate comes with a number of caveats, it is the first for the site, and provides a useful starting position from which other studies could build.

Samples forming depth profiles, seasonal profiles and from different locations across the site were characterised using a novel combination of techniques. These included dissolved combined amino acid (DCAA) analysis, dissolved carbohydrate analysis (characterising neutral sugars) and TMAH thermochemolysis gas chromatography with mass spectrometry (GC-MS) which gave a semi-quantitative analysis of phenolic compounds (as their methylated derivatives), *n*-alkanes and fatty acids (as fatty acid methyl esters, FAMEs). Generally only a small proportion of the DOC of a water sample could be attributed to either carbohydrates or amino acids (a much

lower proportion than in the solid phase), leaving a large portion as phenolic compounds, lipids and uncharacterisable humic substances (HS). In the following three sections, the characterisation of the key sample types identified above will be reviewed and discussed.

7.2 Characterisation of Central porewaters including depth profiles

Amino acids from porewaters taken at the Central site were characterised, relative to the solid phase, by lower contributions from amino acids with hydrophobic side chains and higher contributions from the non-protein amino acids β-alanine (BALA) γ-amino butyric acid (GABA) and ornithine. The elevated contribution from non-protein amino acids is indicative of microbial activity, which is supported by an enrichment of arabinose in the dissolved phase (compared to carbohydrates in solid cores). Total dissolved nitrogen (TDN) concentrations and nitrogen to carbon ratios increased with depth in porewater depth profiles. DCAA were shown to have higher total yields near the surface of the peatland than at depth, and make up a substantial portion of the TDN pool (up to 42%) in shallow-depth porewaters (< 50 cm), contributing less to the TDN pool in deeper porewaters. The decrease in DCAA yields, and a decrease in the proportion of charged amino acids may indicate the incorporation of nitrogen (from enzymes and amino acids) into larger macromolecular structures, which is supported by evidence from both TMAH thermochemolysis GC-MS and FT-ICR-MS:

- Total ion count (TICs) chromatograms resulting from TMAH thermochemolysis show an increased diversity of nitrogen-containing compounds in deeper water samples, including many with nitrogen which is strongly bound (via nitrile bonds) into the organic matrix;
- FT-ICR-MS suggests that nitrogen is bound into many HS (there are a large number of nitrogen-containing assigned molecular formulae), with the largest number of nitrogen containing formulae at depth in the porewater profile.

TICs from the deepest porewaters were dominated by *n*-alkanes. These compounds were only shown to be present in near-surface waters during summer months, which may be indicative of the mechanism by which these nominally non-soluble compounds enter the dissolved phase. FAMEs, especially the shorter chain FAMES (shorter than hexadecanoic acid methyl ester) were also prevalent in deep waters, and had a seasonal signal in shallower waters, again showing highest relative abundance in summer (June 2010). Lipids are known to coat the surface of *Sphagnum* leaves, creating a protective waxy layer, and the high abundance of both *n*-alkanes and short-chain FAMEs may indicate that a component of plant waxes is being transferred to the dissolved phase. This may be either through a physical or microbially mediated mechanism (e.g. a utilisation of recalcitrant organic matter by microbial communities after priming in the spring), but elucidating what this mechanism is has not been possible.

Phenolic compounds identified in Central porewaters were dominated by *p*-hydroxyphenyl structures. The methylated products of sphagnum acid have also been identified in the majority of peatland porewaters for the first time. Benzoic acid structures were particularly abundant in near-surface waters, which is indicative of oxidative degradation at these depths. Much lower contributions from benzoic acids were seen at depth. This was supported by analysis of FT-ICR-MS data using a novel visualisation method. Those series of chemically related HS which are most prevalent in shallow waters were particularly rich in oxygen, and many species were related by transformations indicative of carboxylation and oxidation reactions. Conversely, those series which were most prevalent in the deepest porewaters (6 m at the Central site) had on average the lowest oxygen content. An adapted photodegradation index [(R1 + R2) : (R>2)] has shown an increase in the degree of degradation with depth, and a loss of longer side chains and oxygen rich functionalities; although this proxy was intended to assess photodegradation, it appears to also be indicative of general degradation state.

7.3 Characterisation of intermediate-depth, high-DOC Mid-bog porewaters

Samples from intermediate depth at the Mid-bog site (representative of those waters from within the broad peak in DOC concentrations) had very high relative abundances of methoxybenzyl peaks in TICs, dominated by *p*-hydroxybenzyl compounds. Cinnamic compounds were also abundant at these intermediate depths. Several aspects of the phenolic component of intermediate-depth Mid-bog porewaters are noteworthy:

- Benzoic acid structures contributed only a small amount to the total methoxybenzene pool indicating little oxidative degradation, and the (R1 + R2) : (R>2) ratio was low, possibly indicative of a low degree of degradation generally;
- The methoxybenzenes identified using TMAH thermochemolysis are closely linked to the phenols liberated after CuO oxidation of solid phase samples; the thermochemolysis homologues of the phenolic compounds which vary most in abundance in down-core profiles (solids) have high abundances in these high-DOC waters;
- FT-ICR-MS analysis of other samples showed highest intensity peaks with one intermediate H/C and O/C region of their Van Krevelen diagrams, indicative of degraded HS. The intermediate-depth samples contained a second very high intensity region, which plots in the compositional space of sphagnum acid and other polymeric phenols known to be important in *Sphagnum* dominated peatlands.

Comparison of transformational series derived from FT-ICR-MS data has shown that many more formulae in the Mid-bog sample are related by saturation transformations than in other samples, and there are fewer transformations involving oxygen addition or subtraction (either alone or in combination with hydrogen or carbon). Those series of chemically related HS which were largest in the Mid-bog sample have high average double bond equivalence (BDE) values. Long-chain FAMEs (tetracosanoic acid ME and longer) were unusually present in these

samples, which is indicative of a plant source. Amino acids in the dissolved phase were particularly high in compounds with hydrophobic side chains, and the dissolved phase generally resembled the solid phase more closely in these high-DOC samples than in other porewaters.

7.4 Characterisation of runoff via Lake samples

DCAA yields from Lake waters were on average lower than from porewaters. The amino acids present had the lowest contributions from compounds with hydrophobic side chains and high non-protein amino acid content suggested high microbial biomass inputs. Fewer methoxybenzene peaks were identified in TICs from Lake samples, and these were found at lower relative abundance. The phenol-derived compounds which were present had a high contribution from benzoic acid structures (indicative of oxidative degradation) and a high (R1 + R2) : (R>2) ratio, possibly indicative of photodegradation. This was supported by interpretation of FT-ICR-MS data as follows:

- More formulae were related by oxygen addition transformations in the Lake sample than in other samples, which is indicative of ring cleavage;
- The series of related chemical species which were most prevalent in the Lake had very low average DBE values, indicating few aromatic ring structures;
- There was a loss of high molecular weight formulae in the Lake sample relative to other samples, which is the more photo-labile portion of the DOM pool.

Principal component analysis (PCA), performed on a correlation matrix, was carried out combining data from multiple analyses of a sub-set of samples which covered the key sample types identified in Section 7.1. On a score plot, the first principal component (PC1) separated samples from differing sites, with the samples from the Lake site having negative PC1 scores, the Central samples plotting intermediately, and the intermediate depth, Mid-bog samples having positive PC1 scores. PC1 appears to be representative of the influence of oxic-degradation, and negative PC1

scores may indicate photodegradation of the DOM sample. PC2 separated samples by depth, with Lake and 15 cm deep samples having negative PC2 scores and the 3 m and 6 m having positive scores. The variables which contribute most to PC2 are linked to the degree of humification of a sample, and the presence of components which can be attributed to plant source materials (e.g. the percentage of nitrogen that is attributable to amino acids). There may also be a seasonal component to the PCA, which will be reviewed in the following section.

7.5 Seasonal changes in molecular character of dissolved organic matter (DOM)

Substantial changes in the composition of near-surface and Lake waters were shown to occur over a seasonal cycle. Due to the low precision of some individual analyses, care must be taken when attempting to interpret individual results, but several points are noteworthy:

- PCA of Lake samples revealed that in April and June (2010), the lake had a more surface-like character than in October (2010) i.e. more negative values for PC1 and PC2. This may indicate a greater input from fresh plant material or more labile OM;
- In February 2011, when the rainfall proxy (increases in water table height) indicates high rainfall, xylose concentrations were found to be exceptionally high in the Lake sample. This could be due to a flushing of sedge derived organic matter from nearby regions of the bog after die back introduced plant litter to the bog surface and increased carbohydrate storage in belowground reserves;
- The phenolic compounds shown to be actively excreted by *Sphagnum* species (e.g. cinnamic compounds and *p*-hydroxyacetophenone) were found in highest relative abundances not at the height of the growing season (as may be expected for root exudates for example) but in the late winter and early spring. Excretion may occur throughout the year, with these compounds

only building up during the winter when microbial activity is low and degradation rates are slow.

7.6 Evaluation of this project's success relative to its objectives

Chapter 1, Section 1.4 outlined a series of aim and objectives of the work, which will be addressed in the following section individually, highlighting the successes and limitations of the project with regards these specific aims.

- To quantify DOC concentrations across different locations and depths over more than a full annual cycle in order to ascertain how DOC concentrations change over both time and space, the heterogeneity of DOC concentrations with depth and location, and to gain an insight into controls upon the magnitude of this important carbon pool

Samples were collected from three arrays of piezometers, over a range of depths from 15 cm to 6 m across Cors Fochno. Changes in DOC concentration were evident across season, location and depth, but the most surprising result was the very large DOC concentrations found at mid depth from the Mid-bog piezometers array (see Chapter 3 Figure 3.1).

Three different environmental factors were suggested to influence of control DOC concentrations from different types of water sample across the bog. Using regression analysis, it was shown that DOC concentrations at shallow depths in the peat profile (specifically from the Central site at 15 cm) were related to the temperature at the time of sampling. Regression analysis of samples from deeper in the peat profile (all piezometers ≥ 50 cm depth) showed that there was a significant negative relationship between the DOC concentration and the hydraulic conductivity of the sampling piezometers, and DOC concentrations were also found to increase with lateral distance from the centre of the bog. The concentration of DOC in Lake samples (linked to runoff water) was found to have a strong relationship with gross increases in water table height over the previous seven days (see Chapter 3, Section 3.3). This is

significant as numerous studies have sought to explain the drivers of DOC release from peatlands (e.g. Freeman et al., 2001; Worrall et al., 2003; Worral et al., 2004; Evans et al., 2007; Strack et al., 2008) but no to the authors knowledge, no study has linked this combination of drivers with different environments across a peatland.

In addition to the above, simple modelling, using the relationships found by regression analysis, allowed for an estimate of the DOC flux from Cors Fochno (See chapter 3, section 3.4). Although ambitious (the estimate comes with a number of caveats due to the assumptions and limited environmental data available), this estimate of DOC export is the first for the site, and may inform the site owners (NRW) when considering management options in the future.

- To quantify both the total yield and relative contribution of individual components of the DCAA and dissolved neutral sugar pools, using a sub-set of samples from different depths, seasons and locations

87 water samples were analysed for DCAA (with 18 individual amino acids quantified) and 43 samples were successfully analysed for dissolved carbohydrates (quantifying 8 individual neutral sugars). Although several depth profiles were analysed for both amino acids and carbohydrates, poor recovery of hydrolysis products and instrumental problems led to significant gaps in the sample set (see Chapter 2 Figure 2.6). The analysis of dissolved carbohydrates in particular was hampered by low yields and poor analytical precision, and the discussion of neutral sugars in water samples was subsequently limited.

- To use TMAH thermochemolysis to provide a semi-quantitative assessment of lipids (*n*-alkanes and fatty acids) and functionally important aromatic compounds, again from a sub-set of samples as above

Initially, it was hoped that TMAH thermochemolysis would provide some degree of quantitative data (without standards for all compounds studied, it is difficult to ascertain exact response factors) as discussed in Chapter 2, Section 2.4.6.2. However, recovery of the internal standard used was variable, and as such, a new method for

gaining semi-quantitative data from TICs was developed by the author. Instrumental set-up was not optimised for analysis of freeze dried DOM, and this, combined with limited instrument availability and lack of resilience when samples were lost meant that some key samples from the analysis (e.g. sample from Lake, Feb 2011, see Chapter 2, Figure 2.6). Despite this, samples from all locations across multiple depth profiles from different sampling occasions were analysed. Using the novel semi-quantitative method of peak area comparison, the relative response of a large number of lipids and phenolic compounds was measured. A novel technique for quantification of co-eluting peaks within a thermochemolysis TIC was also developed by the author for this study (see Chapter 2, Section 2.4.6.2).

- To compare the DOM pool against solid phase peat cores using complimentary techniques

Due to the limitations (particularly of the dissolved carbohydrate analysis) aspects of the comparison between DOM and the solid phase are subject to strong caveats, as highlighted in Chapter 5. However, the comparison between phases aided interpretation of the results from the dissolved phase analysis, for example showing that water samples from intermediate depth at the Mid-bog site (characterised by high DOC) were most similar to the solid phase with respect to both amino acids and phenolic compounds.

- To use a ultrahigh resolution mass spectrometry technique to investigate humic substances within peatland porewater

A series of novel techniques and visualisation approaches was developed during this study and used to analyse the huge amount of data generated by this technique. Subtle differences in the humic substances in the four water samples analysed were highlighted (e.g. that humic substances were less saturated with more double bonding in the M1.5 sample and the most oxygen rich groups of HS were found in shallow porewaters (IA)). The main strengths of this analysis (and the novel data analysis techniques) lie in its ability to identify similarities and possible relationships between the thousands of molecular formulae identified from each sample.

- Using the information gained from the above molecular characterisation, to assess the sources of peatland DOM and the molecular transformations or alterations this OM undergoes in different environments in the peatland.

The source of DOM at Cors Fochno was only poorly constrained, although some significant phenolic compounds were detected in porewaters by TMAH thermochemolysis (e.g. sphagnum markers). Several indicators of microbial inputs (e.g. non protein amino acids and enrichment in arabinose) suggested

The investigation of molecular transformations within the peatland was better addressed. The novel adaptation of two proxies which evaluate the oxidative and photochemical degradation state of phenolic compounds (via their methoxybenzene TMAH thermochemolysis techniques) was used assess possible molecular transformations and alterations which DOM undergoes in different environments. Decreases in DCAA yield, and a decrease in the proportion of charged amino acids in the dissolved phase suggested the incorporation of organic nitrogen into larger macromolecular structures, which was supported by evidence from both TMAH thermochemolysis GC-MS and FT-ICR-MS. PCA, performed on a correlation matrix, was carried out combining data from multiple analyses of a sub-set of samples, resulting in principal components that separated samples by depth, location and included some seasonal component. Novel approaches to interpretation of ESI-FT-ICR-MS data provided the most exciting evidence for transformational relationships between humic substances (which make up the majority of DOM) but these haven't been tested in any other environments or studies, and are hard to integrate with current literature.

The fate of DOM exported from Cors Fochno was only partially addressed, and a small study to investigate the DOM as it left the site and made the transition from Lake to drainage channel (Pwll Ddu) to the nearby estuary failed because the characterisation techniques used in this study were not capable of yielding quantifiable results from the brackish to saline water samples. The oxidative and

photochemical transformations that OM undergoes when entering the Lake may be indicative of the fate of DOM exported from Cors Fochno, but residence times for the water in the Lake would be needed to infer changes through time.

7.7 Highlighting novel aspects and limitations of this work

The estimation of the DOC export flux from Cors Fochno presented in Chapter 3 is the first for this site. Because the ideal or conventional data (e.g. Billett et al. 2004) necessary to make this estimate (environmental, hydrological and chemical) was patchy or entirely unavailable, a novel combination of modelled DOC concentrations in runoff (from water table height) and a water export term (estimated from average annual rainfall and evapotranspiration rates) was employed.

Contributions to peatland DOM from individual dissolved neutral sugars have not been previously reported, and so the numbers presented as part of this study are the first of their kind. A large limitation of the study however was the low yields and associated low precision of the dissolved carbohydrate analysis resulted in unreliable interpretation of individual sugars. Instrumental and analytical problems also led to significant gaps within the data set, with patchy data available for water samples across depths, locations and seasons (see Chapter 2, Figure 2.6).

Other instrumental and set-up problems limited the interpretation of TMAH thermochemolysis results, which were only semi-quantitative due to failure of an internal standard. However, the problems created by the failed internal standard led to two innovative techniques to be developed by the author in order to address these difficulties. A novel method of gaining relative abundances of peaks by comparison to a xylene peak was used, as was a new method for accurately splitting coeluting peaks.

A step-wise interrogation of ESI-FT-ICR-MS data, as presented in Chapter 6, led to the creation of several novel visualisation techniques by the author. Histograms of the number of peaks per nominal mass could be analysed for the strength of their 14 Da signal using spectral analysis. This may be indicative of how linked all formulae are by CH_2 addition or subtraction, which may depend on the diagenetic or decompositional history of the sample. From here, KMD theory was used to find the level of relatedness between complex mixtures of molecules in HS, with relation to a series of additions or subtractions of simple molecular units. The distribution and "length" of these semi-homologous series or chains was then interrogated further to provide a measure of subtle changes in the character of HS between samples.

7.8 Relevance to other studies and avenues for further work to complement this study

The results relating to carbon dynamics at Cors Fochno (both the apparent differing controls on DOC and the estimate of DOC fluxes and export from the site) will provide the site managers (NRW) with valuable information, and may help inform policy and management decisions in the future. Policy makers and researchers are aware that there is a lack of data relating to carbon dynamics in lowland peats in the UK (Pers Comm. Chris Evans) and to this end a large DEFRA project us currently investigating carbon dynamics in a range of UK peatlands (SP1210, Lowland peatland systems in England and Wales – evaluating greenhouse gas fluxes and carbon balances) and although Cors Fochno was not included in the final lists of field sites, it is possible that the data collected during this project could be included in the reports from the SP1210.

The novel visualisation techniques for interpreting ESI-FT-ICR-MS data which were developed during this study may provide a meaningful assessment of the degree of relatedness and simplicity of an organic mixture. Both the spectral analysis of the number of peaks per nominal mass, and the interpretation of semi-homologous series relating to the addition/subtraction of different simple molecular units may

provide promising avenues for further work. These need to be tested on existing data sets from differing environments and instruments, and it is hoped that this may provide further possibilities to build on research with colleagues in Germany. Although currently very time consuming to generate, the coding required to mine complex spectra for the necessary information in order to carry out multiple-KMD analysis would be simple to generate, and could provide another useful tool for other researchers to use when first interrogating their data.

The TMAH thermochemolysis method used in this study requires further development for use on freeze dried material from peatlands. Specifically, the internal standard addition step requires testing, and the reasons for its failure needs to be found, whether this is related to the sample matrix of freeze-dried peatland-DOM or the incomplete reaction of TMAH due to high concentrations of phenolic compounds. The addition of ^{13}C labelled TMAH would allow further distinction of methoxybenzenes, and this would require testing when applied to freeze-dried material.

If the TMAH thermochemolysis could be optimised for the analysis of freeze dried DOM, the phenolic degradation indices adapted for this study ((R1 + R2) : (R>2) and %benzoic acid) could be calibrated to other phenolic sources or be used to provide an indicator of fresh or photochemically/oxidatively degraded peatland-derived DOM. Other chemical indicators (such as the percentage of xylose in the dissolved carbohydrate pool being indicative of sedge inputs) would require the development of much more robust characterisation techniques.

A number of studies (e.g. Hagedorn et al., 2007, Stutter et al., 2007 and Dawson et al., 2008) have shown how the quality, hydrophobicity and lability of soil organic matter and DOM change seasonally in other environments (as discussed in Chapter 1, section 1.3). The release of labile DOM in the spring then primes the soil system to release older and more recalcitrant DOM later in the summer and autumn. The results of PCA from this study may provide indicators for this labile pulse of DOM,

tracking priming in raised peats, but full analysis of water samples from other sites would be needed to test this.

Finally, if the quality and quantity of water obtained from wells at intermediate depth is affected by the hydraulic conductivity measured in those wells, a study which molecularly characterises different fractions of water from a peat core (e.g. free flowing water compared to water extracted by squeezing) may elucidate why this is the case. This project could be manageable as an undergraduate project for example, and the results may be publication worthy, but it was unfortunately beyond the time, money and instrumental constraints of this study.

References

Abbott G. D., Swain E. Y., Muhammad A. B., Allton K., Belyea L. R., Laing C. G., Cowie G. L. (2013) Effect of water-table fluctuations on the degradation of Sphagnum phenols in surficial peats. Geochimica et Cosmochimica Acta 106 (177-191).

Bae E., Yeo I. J., Jeong B., Shin Y., Shin K.-H., and Kim S. (2011) Study of double bond equivalents and the numbers of carbon and oxygen atom distribution of dissolved organic flatter with negative-Mode FT-ICR MS. Analytical Chemistry 83(11), 4193-4199.

Baird A. J., Eades P. A., and Surridge B. W. J. (2008) The hydraulic structure of a raised bog and its implications for ecohydrological modelling of bog development. Ecohydrology 1(4), 289-298.

Basiliko N., Stewart H., Roulet N. T., and Moore T. R. (2012) Do Root Exudates Enhance Peat Decomposition? Geomicrobiology Journal 29(4), 374-378.

Beer J. and Blodau C. (2007) Transport and thermodynamics constrain belowground carbon turnover in a northern peatland. Geochimica et Cosmochimica Acta 71(12), 2989-3002.

Belyea L. R. and Clymo R. S. (2001) Feedback control of the rate of peat formation. Proceedings of the Royal Society of London Series B-Biological Sciences 268(1473), 1315-1321.

Benner R. and Opsahl S. (2001) Molecular indicators of the sources and transformations of dissolved organic matter in the Mississippi river plume. Organic Geochemistry 32(4), 597-611.

Berdie L., Grimalt J. O., and Gjessing E. T. (1995) Hydrocarbons, alcohols and sterols in the dissolved plus colloidal and particulate phases of the waters from a dystrophic lake, Skjervatjern Lake (Norway). Water Research 29(9), 2017-2030.

Billett M. F., Garnett M. H., and Harvey F. (2007) UK peatland streams release old carbon dioxide to the atmosphere and young dissolved organic carbon to rivers. Geophysical Research Letters 34(23).

Billett M. F., Palmer S. M., Hope D., Deacon C., Storeton-West R., Hargreaves K. J., Flechard C., and Fowler D. (2004) Linking land-atmosphere-stream carbon fluxes in a lowland peatland system. Global Biogeochemical Cycles 18(1).

Billett M. F., Deacon C. M., Palmer S. M., Dawson J. J. C., and Hope D. (2006) Connecting organic carbon in stream water and soils in a peatland catchment. Journal of Geophysical Research-Biogeosciences 111(G2).

Bingham E. M., McClymont E. L., Valiranta M., Mauquoy D., Roberts Z., Chambers F. M., Pancost R. D., and Evershed R. P. (2010) Conservative composition of n-alkane

biomarkers in Sphagnum species: implications for palaeoclimate reconstruction in ombrotrophic peat bogs. Organic Geochemistry 41(2), 214-220.

Blodau C., Basiliko N., and Moore T. R. (2004) Carbon turnover in peatland mesocosms exposed to different water table levels. Biogeochemistry 67(3), 331-351.

Blodau C., Roulet N. T., Heitmann T., Stewart H., Beer J., Lafleur P., and Moore T. R. (2007) Belowground carbon turnover in a temperate ombrotrophic bog. Global Biogeochemical Cycles 21(1).

Bohlin E., Hamalainen M., and Sunden T. (1989) Botanical and chemical characterization of peat using multivariate methods. Soil Science 147(4), 252-263.

Chefetz B., Chen Y., Clapp C. E., and Hatcher P. G. (2000) Characterization of organic matter in soils by thermochemolysis using tetramethylammonium hydroxide (TMAH). Soil Science Society of America Journal 64(2), 583-589.

Clark J. M., Lane S. N., Chapman P. J., and Adamson J. K. (2007) Export of dissolved organic carbon from an upland peatland during storm events: Implications for flux estimates. Journal of Hydrology 347, 438-447.

Clymo R. S., and Bryant C. L. (2008) Diffusion and mass flow of dissolved carbon dioxide, methane, and dissolved organic carbon in a 7-m deep raised peat bog. Geochimica et Cosmochimica Acta 72 (2048-2066).

Comont L., Laggoun-Defarge F., and Disnar J.-R. (2006) Evolution of organic matter indicators in response to major environmental changes: The case of a formerly cut-over peat bog (Le Russey, Jura Mountains, France). Organic Geochemistry 37(12), 1736-1751.

Cowie G. L. and Hedges J. I. (1984) Determination of neutral sugars in plankton, sediments and wood by capillary gas-chromatography of equilibrated isomeric mixtures. Analytical Chemistry 56(3), 497-504.

Cowie G. L. and Hedges J. I. (1992) Sources and reactivities of amino acids in coastal marine environments.Limnology and Oceanography 37(4), 703-724.

Cowie G. L., Hedges J. I., Prahl F. G., and Delange G. J. (1995) Elemental and major biochemical changes across an oxidation front in a relict turbidite – and oxygen effect. Geochimica et Cosmochimica Acta 59(1), 33-46.

D'Andrilli J., Chanton J. P., Glaser P. H., and Cooper W. T. (2010) Characterization of dissolved organic matter in northern peatland soil porewaters by ultra high resolution mass spectrometry. Organic Geochemistry 41(8), 791-799.

Dauwe B. and Middelburg J. J. (1998) Amino acids and hexosamines as indicators of organic matter degradation state in North Sea sediments. Limnology and Oceanography 43(5), 782-798.

Davidson E. A. and Janssens I. A. (2006) Temperature sensitivity of soil carbon decomposition and feedbacks to climate change. Nature 440(7081), 165-173.

Dawson J. J. C. and Smith P. (2007) Carbon losses from soil and its consequences for land-use management. Science of the Total Environment 382(2-3), 165-190.

Dawson J. J. C., Billett M. F., Hope D., Palmer S. M., and Deacon C. M. (2004) Sources and sinks of aquatic carbon in a peatland stream continuum. Biogeochemistry 70(1), 71-92.

Dawson J. J. C., Soulsby C., Tetzlaff D., Hrachowitz M., Dunn S. M., and Malcolm I. A. (2008) Influence of hydrology and seasonality on DOC exports from three contrasting upland catchments. Biogeochemistry 90(1), 93-113.

Delarue F., Laggoun-Defarge F., Disnar J. R., Lottier N., and Gogo S. (2011) Organic matter sources and decay assessment in a Sphagnum-dominated peatland (Le Forbonnet, Jura Mountains, France): impact of moisture conditions. Biogeochemistry 106(1), 39-52.

Dittmar T., Fitznar H. P., and Kattner G. (2001) Origin and biogeochemical cycling of organic nitrogen in the eastern Arctic Ocean as evident from D- and L-amino acids. Geochimica et Cosmochimica Acta 65(22), 4103-4114.

Eimers M. C., Watmough S. A., and Buttle J. M. (2008) Long-term trends in dissolved organic carbon concentration: a cautionary note. Biogeochemistry 87(1), 71-81.

Erlandsson M., Buffam I., Folster J., Laudon H., Temnerud J., Weyhenmeyer G. A., and Bishop K. (2008) Thirty-five years of synchrony in the organic matter concentrations of Swedish rivers explained by variation in flow and sulphate. Global Change Biology 14(5), 1191-1198.

Ertel J. R., Hedges J. I., and Perdue E. M. (1984) Lignin signature of aquatic humic substances. Science 223(4635), 485-487.

Estournel-Pelardy C., Delarue F., Grasset L., Laggoun-Defarge F., and Ambles A. (2011) Tetramethylammonium hydroxide thermochemolysis for the analysis of cellulose and free carbohydrates in a peat bog. Journal of Analytical and Applied Pyrolysis 92(2), 401-406.

Evans C. D., Chapman P. J., Clark J. M., Monteith D. T., and Cresser M. S. (2006) Alternative explanations for rising dissolved organic carbon export from organic soils. Global Change Biology 12(11), 2044-2053.

Evans C. D., Freeman C., Cork L. G., Thomas D. N., Reynolds B., Billett M. F., Garnett M. H., and Norris D. (2007) Evidence against recent climate-induced destabilisation of soil carbon from C-14 analysis of riverine dissolved organic matter. Geophysical Research Letters 34.

Fenner N., Ostle N., Freeman C., Sleep D., and Reynolds B. (2004) Peatland carbon afflux partitioning reveals that Sphagnum photosynthate contributes to the DOC pool. Plant and Soil 259(1-2), 345-354.

Filley T. R., Nierop K. G. J., and Wang Y. (2006) The contribution of polyhydroxyl aromatic compounds to tetramethylammonium hydroxide lignin-based proxies. Organic Geochemistry 37(6), 711-727.

Flerus R., Koch B. P., Schmitt-Kopplin P., Witt M., and Kattner G. (2011) Molecular level investigation of reactions between dissolved organic matter and extraction solvents using FT-ICR MS. Marine Chemistry 124(1-4), 100-107.

Flerus R., Lechtenfeld O. J., Koch B. P., McCallister S. L., Schmitt-Kopplin P., Benner R., Kaiser K., and Kattner G. (2012) A molecular perspective on the ageing of marine dissolved organic matter. Biogeosciences 9(6), 1935-1955.

Frazier S. W., Kaplan L. A., and Hatcher P. G. (2005) Molecular characterization of biodegradable dissolved organic matter using bioreactors and [C-12/C-13] tetramethylammonium hydroxide thermochemolysis GC-MS. Environmental Science & Technology 39(6), 1479-1491.

Frazier S. W., Nowack K. O., Goins K. M., Cannon F. S., Kaplan L. A., and Hatcher P. G. (2003) Characterization of organic matter from natural waters using tetramethylammonium hydroxide thermochemolysis GC-MS. Journal of Analytical and Applied Pyrolysis 70(1), 99-128.

Freeman C., Evans C. D., Monteith D. T., Reynolds B., and Fenner N. (2001) Export of organic carbon from peat soils. Nature 412(6849), 785-785.

Freeman C., Fenner N., Ostle N. J., Kang H., Dowrick D. J., Reynolds B., Lock M. A., Sleep D., Hughes S., and Hudson J. (2004) Export of dissolved organic carbon from peatlands under elevated carbon dioxide levels. Nature 430(6996), 195-198.

Gallois N., Tempher J., and Derenne S. (2007) Pyrolysis-gas chromatography-mass spectrometry of the 20 protein amino acids in the presence of TMAH. Journal of Analytical and Applied Pyrolysis 80(1), 216-230.

Goni M. A. and Hedges J. I. (1992) Lignin dimers – structures, distribution, and potential geochemical applications. Geochimica et Cosmochimica Acta 56(11), 4025-4043.

Gorham E. (1991) Northern Peatlands - role in the carbon-cycle and probable responses to climatic warming. Ecological Applications 1(2), 182-195.

Grinhut T., Hertkorn N., Schmitt-Kopplin P., Hadar Y., and Chen Y. (2011) Mechanisms of Humic Acids Degradation by White Rot Fungi Explored Using H-1 NMR Spectroscopy and FTICR Mass Spectrometry. Environmental Science & Technology 45(7), 2748-2754.

Hagedorn F., Saurer M., and Blaser P. (2004) A C-13 tracer study to identify the origin of dissolved organic carbon in forested mineral soils. European Journal of Soil Science 55(1), 91-100.

Hajek T., Ballance S., Limpens J., Zijlstra M., and Verhoeven J. T. A. (2011) Cell-wall polysaccharides play an important role in decay resistance of Sphagnum and actively depressed decomposition in vitro. Biogeochemistry 103(1-3), 45-57.

Hayward P. M. and Clymo R. S. (1982) Profiles of water content and pore size in sphagnum and peat, and their relation to peat bog ecology. Proceedings of the Royal Society of London Series B-Biological Sciences 215(1200), 299-325.

Hedges J. I. and Ertel J. R. (1982) Characterisation of lignin by gas capillary chromatography of cupric oxide oxidation products.

Hedges J. I., Cowie G. L., Richey J. E., Quay P. D., Benner R., Strom M., and Forsberg B. R. (1994) Origins and processing of organic matter in the Amazon river as indicated by carbohydrates and amino acids. Limnology and Oceanography 39(4), 743-761.

Hertkorn N., Frommberger M., Witt M., Koch B. P., Schmitt-Kopplin P., and Perdue E. M. (2008) Natural Organic Matter and the Event Horizon of Mass Spectrometry. Analytical Chemistry 80(23), 8908-8919.

Hughey C. A., Hendrickson C. L., Rodgers R. P., Marshall A. G., and Qian K. N. (2001) Kendrick mass defect spectrum: A compact visual analysis for ultrahigh-resolution broadband mass spectra. Analytical Chemistry 73(19), 4676-4681.

Jager D. F., Wilmking M., and Kukkonen J. V. K. (2009) The influence of summer seasonal extremes on dissolved organic carbon export from a boreal peatland catchment: Evidence from one dry and one wet growing season. Science of the Total Environment 407(4), 1373-1382.

Jia G., Dungait J. A. J., Bingham E. M., Valiranta M., Korhola A., and Evershed R. P. (2008) Neutral monosaccharides as biomarker proxies for bog-forming plants for application to palaeovegetation reconstruction in ombrotrophic peat deposits. Organic Geochemistry 39(12), 1790-1799.

Kalbitz K. and Geyer S. (2002) Different effects of peat degradation on dissolved organic carbon and nitrogen. Organic Geochemistry 33(3), 319-326.

Kendrick E. (1963) A mass scale based on CH2=14.0000 for high resolution mass spectrometry of organic compounds. Analytical Chemistry 35(13), 2146-&.

Kim S., Kramer R. W., and Hatcher P. G. (2003) Graphical method for analysis of ultrahigh-resolution broadband mass spectra of natural organic matter, the van Krevelen diagram. Analytical Chemistry 75(20), 5336-5344.

Koch B. P., Witt M. R., Engbrodt R., Dittmar T., and Kattner G. (2005) Molecular formulae of marine and terrigenous dissolved organic matter detected by electrospray ionization Fourier transform ion cyclotron resonance mass spectrometry. Geochimica et Cosmochimica Acta 69(13), 3299-3308.

Kujawinski E. B., Longnecker K., Blough N. V., Del Vecchio R., Finlay L., Kitner J. B., and Giovannoni S. J. (2009) Identification of possible source markers in marine dissolved organic matter using ultrahigh resolution mass spectrometry. Geochimica et Cosmochimica Acta 73(15), 4384-4399.

Kinnas A. V., and Eronen M. (1994) Identification of free amino acids in peat by gas chromatography and mass spectrometry. European Journal of Soil Science 45, 378-392.

Limpens J., Berendse F., Blodau C., Canadell J. G., Freeman C., Holden J., Roulet N., Rydin H., and Schaepman-Strub G. (2008) Peatlands and the carbon cycle: from local processes to global implications a synthesis (vol 5, pg 1475, 2008).Biogeosciences 5(6), 1739-1739.

Lopez-Dias V., Borrego A. G., Blanco C. G., Arboleya M., Lopez-Saez J. A., and Lopez-Merino L. (2010) Biomarkers in a peat deposit in Northern Spain (Huelga de Bayas, Asturias) as proxy for climate variation. Journal of Chromatography A 1217(21), 3538-3546.

Maie N., Yang C. Y., Miyoshi T., Parish K., and Jaffe R. F. (2005) Chemical characteristics of dissolved organic matter in an oligotrophic subtropical wetland/estuarine ecosystem. Limnology and Oceanography 50(1), 23-35.

Maie N., Jaffe R., Miyoshi T., and Childers D. L. (2006) Quantitative and qualitative aspects of dissolved organic carbon leached from senescent plants in an oligotrophic wetland. Biogeochemistry 78(3), 285-314.

Mannino A. and Harvey H. R. (2000) Terrigenous dissolved organic matter along an estuarine gradient and its flux to the coastal ocean. Organic Geochemistry 31(12), 1611-1625.

Mason S. L., Filley T. R., and Abbott G. D. (2009) The effect of afforestation on the soil organic carbon (SOC) of a peaty gley soil using on-line thermally assisted hydrolysis and methylation (THM) in the presence of 13C-labelled tetramethylammonium hydroxide (TMAH). Journal of Analytical and Applied Pyrolysis 85(1-2), 417-425.

McClymont E. L., Bingham E. M., Nott C. J., Chambers F. M., Pancost R. D., and Evershed R. P. (2011) Pyrolysis GC-MS as a rapid screening tool for determination of peat-forming plant composition in cores from ombrotrophic peat. Organic Geochemistry 42(11), 1420-1435.

McKee G. A. and Hatcher P. G. (2010) Alkyl amides in two organic-rich anoxic sediments: A possible new abiotic route for N sequestration. Geochimica et Cosmochimica Acta 74, (6436-6450).

Moore T. R., Bubier J. L., Frolking S. E., Lafleur P. M., and Roulet N. T. (2002) Plant biomass and production and CO2 exchange in an ombrotrophic bog. Journal of Ecology 90(1), 25-36.

Moore T. R., Pare D., and Boutin R. (2008) Production of dissolved organic carbon in Canadian forest soils. Ecosystems 11(5), 740-751.

Moore T. R., Roulet N. T., and Waddington J. M. (1998) Uncertainty in predicting the effect of climatic change on the carbon cycling of Canadian peatlands. Climatic Change 40(2), 229-245.

Myklestad S. M., SkÃ¥nÃ¸y E., and Hestmann S. (1997) A sensitive and rapid method for analysis of dissolved mono- and polysaccharides in seawater. Marine Chemistry 56(3â€“4), 279-286.

Ohno T., He Z. Q., Sleighter R. L., Honeycutt C. W., and Hatcher P. G. (2010) Ultrahigh Resolution Mass Spectrometry and Indicator Species Analysis to Identify Marker Components of Soil- and Plant Biomass-Derived Organic Matter Fractions. Environmental Science & Technology 44(22), 8594-8600.

Opsahl S. and Benner R. (1995) Early digenesis of vascular plant tissue lignin and cutin decomposition and biogeochemical implications. Geochimica et Cosmochimica Acta 59(23), 4889-4904.

Opsahl S. and Benner R. (1997) Distribution and cycling of terrigenous dissolved organic matter in the ocean. Nature 386(6624), 480-482.

Painter T. J. (1991) Lindlow Man, Tollund Man and other peat bog bodies – the preservative and antimicrobial action of sphagnam, a reactive glycuronoglycan with tanning and sequestering properties. Carbohydrate Polymers 15(2), 123-142.

Peuravuori J. and Pihlaja K. (2007) Advanced TMAH and TMAAc thermochemolysis-pyrolysis techniques for molecular characterization of size-separated fractions from aquatic dissolved organic matter. Analytical and Bioanalytical Chemistry 389(2), 475-491.

Repeta D. J., Quan T. M., Aluwihare L. I., and Accardi A. M. (2002) Chemical characterization of high molecular weight dissolved organic matter in fresh and marine waters. Geochimica et Cosmochimica Acta 66(6), 955-962.

Riboulleau A., Mongenot T., Baudin F., Derenne S., and Largeau C. (2002) Factors controlling the survival of proteinaceous material in Late Tithoniankerogens (Kashpir Oil Shales, Russia). Organic Geochemistry 33(9), 1127-1130.

Robertson K. J., Williams P. M., and Bada J. L. (1987) Acid-Hydrolysis of Dissolved Combined Amino-Acids in Seawater - a Precautionary Note. Limnology and Oceanography 32(4), 996-997.

Roulet N. T., Laffeur P. M., Richard P. J. H., Moore T. R., Humphreys E. R., and Bubier K. (2007) Contemporary carbon balance and late Holocene carbon accumulation in a northern peatland. Global Change Biology 13(2), 397-411.

Rudolph H. and Engmann B. (1967) Neue Ergebnissezur Konsitution des Sphagnols. Berichte Der Deutschen Botanischen Gesellschaft 80(2), 114-&.

Rudolph H. and Rasmussen S. (1992) Studies on secondary metabolism of Sphagnum cultivated in bioreactors. Cryptogamic Botany 3(1), 67-73.

Rydin H., Gunnarsson U., and Sundberg S. (2006) The role of Sphagnum in peatland development and persistence. In Ecological Studies, Vol. 188 (ed. R. K. Wieder and D. H. Vitt), pp. 47-65.

Schmidt F., Elvert M., Koch B. P., Witt M., and Hinrichs K. U. (2009) Molecular characterization of dissolved organic matter in pore water of continental shelf sediments. Geochimica et Cosmochimica Acta 73(11), 3337-3358.

Schmidt F., Koch B. P., Elvert M., Schmidt G., Witt M., and Hinrichs K.-U.(2011) Diagenetic Transformation of Dissolved Organic Nitrogen Compounds under Contrasting Sedimentary Redox Conditions in the Black Sea. Environmental Science & Technology 45(12), 5223-5229.

Scott M. J., Jones M. N., Woof C., Simon B., and Tipping E. (2001) The molecular properties of humic substances isolated from a UK upland peat system - A temporal investigation. Environment International 27(6), 449-462.

Shadkami F. and Helleur R. (2010) Recent applications in analytical thermochemolysis. Journal of Analytical and Applied Pyrolysis 89(1), 2-16.

Sleighter R. L. and Hatcher P. G. (2007) The application of electrospray ionization coupled to ultrahigh resolution mass spectrometry for the molecular characterization of natural organic matter. Journal of Mass Spectrometry 42(5), 559-574.

Sleighter R. L. and Hatcher P. G. (2008) Molecular characterization of dissolved organic matter (DOM) along a river to ocean transect of the lower Chesapeake Bay by ultrahigh resolution electrospray ionization Fourier transform ion cyclotron resonance mass spectrometry. Marine Chemistry 110(3-4), 140-152.

Spencer R. G. M., Ahad J. M. E., Baker A., Cowie G. L., Ganeshram R., Upstill-Goddard R. C., and Uher G. (2007) The estuarine mixing behaviour of peatland derived dissolved organic carbon and its relationship to chromophoric dissolved organic matter in two North Sea estuaries (UK). Estuarine Coastal and Shelf Science 74(1-2), 131-144.

Stenson A. C., Marshall A. G., and Cooper W. T. (2003) Exact masses and chemical formulas of individual Suwannee River fulvic acids from ultrahigh resolution electrospray ionization Fourier transform ion cyclotron resonance mass spectra. Analytical Chemistry 75(6), 1275-1284.

Stoddard JL K. J., Deviney FA, DeWalle DR, Driscoll CT, Herlihy AT, Kellogg JH, Murdoch PS, Webb JR, Webster KE. (2003) Response of Surface Water Chemistry to the Clean Air Act Amendments of 1990. EPA Report EPA 620/R-03/001.

Strack M., Toth K., Bourbonniere R., and Waddington J. M. (2011) Dissolved organic carbon production and runoff quality following peatland extraction and restoration. Ecological Engineering 37(12), 1998-2008.

Strack M., Waddington J. A., Bourbonniere R. A., Buckton E. L., Shaw K., Whittington P., and Price J. S. (2008) Effect of water table drawdown on peatland dissolved organic carbon export and dynamics. Hydrological Processes 22(17), 3373-3385.

Stubbins A., Spencer R. G. M., Chen H. M., Hatcher P. G., Mopper K., Hernes P. J., Mwamba V. L., Mangangu A. M., Wabakanghanzi J. N., and Six J. (2010) Illuminated darkness: Molecular signatures of Congo River dissolved organic matter and its photochemical alteration as revealed by ultrahigh precision mass spectrometry. Limnology and Oceanography 55(4), 1467-1477.

Stutter M. I., Lumsdon D. G., and Cooper R. J. (2007) Temperature and soil moisture effects on dissolved organic matter release from a moorland Podzol O horizon under field and controlled laboratory conditions. European Journal of Soil Science 58(5), 1007-1016.

Swain E. Y., Perks M. P., Vanguelova E. I., and Abbott G. D. (2010) Carbon stocks and phenolic distributions in peaty gley soils afforested with Sitka spruce (Piceasitchensis). Organic Geochemistry 41(9), 1022-1025.

Swain F. M., Blumentals A., and Millers R. (1959) Stratigraphic distribution of amino acids in peats from Cedar Creek Bog, Minnesota, and Dismal Swamp, Virginia. Limnology and Oceanography, 4(2), 119-127.

Templier J., Derenne S., Croue J. P., and Largeau C. (2005) Comparative study of two fractions of riverine dissolved organic matter using various analytical pyrolytic methods and a C-13 CP/MAS NMR approach. Organic Geochemistry 36(10), 1418-1442.

Tfaily M. M., Podgorski D. C., Corbett J. E., Chanton J. P., and Cooper W. T. (2011) Influence of acidification on the optical properties and molecular composition of dissolved organic matter. Analytica Chimica Acta 706(2), 261-267.

Thurman E. M. (1985) Developments in biogeochemistry – Organic geochemistry of natural waters. New York, Springer.

Tsugita A., Uchida T., Mewes H. W., and Ataka T. (1987) A rapid vapour phase acid (hydrochloric and trifluoroacetic acid) hydrolysis of peptide and protein. Journal of Biochemistry 102(6), 1593-1597.

Turunen J., Tomppo E., Tolonen K., and Reinikainen A. (2002) Estimating carbon accumulation rates of undrained mires in Finland - application to boreal and subarctic regions. Holocene 12(1), 69-80.

vanDongen B. E., Zencak Z., and Gustafsson O. (2008) Differential transport and degradation of bulk organic carbon and specific terrestrial biomarkers in the surface waters of a sub-arctic brackish bay mixing zone. Marine Chemistry 112(3-4), 203-214.

Verhoeven J. T. A. and Liefveld W. M. (1997) The ecological significance of organochemical compounds in Sphagnum. Acta Botanica Neerlandica 46(2), 117-130.

vonLutzow M. and Kogel-Knabner I. (2009) Temperature sensitivity of soil organic matter decomposition-what do we know? Biology and Fertility of Soils 46(1), 1-15.

Waddington J. M. and Roulet N. T. (1997) Groundwater flow and dissolved carbon movement in a boreal peatland. Journal of Hydrology 191(1-4), 122-138.

Wallage Z. E., Holden J., and McDonald A. T. (2006) Drain blocking: An effective treatment for reducing dissolved organic carbon loss and water discolouration in a drained peatland. Science of the Total Environment 367(2-3), 811-821.

Wieder R. K. (2001) Past, present, and future peatland carbon balance: An empirical model based on Pb-210-dated cores. Ecological Applications 11(2), 327-342.

Witt M., Fuchser J., and Koch B. P. (2009) Fragmentation Studies of Fulvic Acids Using Collision Induced Dissociation Fourier Transform Ion Cyclotron Resonance Mass Spectrometry. Analytical Chemistry 81(7), 2688-2694.

Worrall F., Burt T., and Adamson J. (2004) Can climate change explain increases in DOC flux from upland peat catchments? Science of the Total Environment 326(1-3), 95-112.

Worrall F., Burt T., and Shedden R. (2003) Long term records of riverine dissolved organic matter. Biogeochemistry 64(2), 165-178.

Worrall F., Burt T. P., and Adamson J. (2006) Do nitrogen inputs stimulate dissolved organic carbon production in upland peat bogs? Global Biogeochemical Cycles 20(3).

Worrall F., Burt T. P., and Adamson J. (2006) The rate of and controls upon DOC loss in a peat catchment. Journal of Hydrology 321(1-4), 311-325.

Appendix A: Sample storage tests

7 replicate samples were collected from three depths from the September 2009 sampling run. One was analysed for DOC concentration as part of the regular measurements, then three months later, three repeat vials were opened and analysed (with the Dec 2009 run) and the final three repeats analysed after 6 months (with the April 2010 run). The results are presented below.

	Repeat DOC concentration measurements (mg $l^{-1)}$		
	Edge 1 m	**Mid 3 m**	**Central 30 cm**
Month 1	55.55	69.19	36.71
Month 3	54.67	68.41	37.41
	53.79	69.14	35.47
	52.94	73.71	36.11
AVE	53.80	70.42	36.33
Month 6	50.14	67.14	33.74
	56.14	65.81	36.97
	*	66.79	36.50
AVE	53.14	66.58	35.74
Change over 6 months	-4.3%	-3.8%	-2.7%

Table A1: Results of DOC storage experiment. * Sample lost.

Appendix B: Sensitivity analysis of assumptions involved in DOC flux calculations

Several assumptions and estimates were made in the calculation of DOC flux from the site (Chapter 3, Section 3.4). In order to assess how large an impact different possible values of these estimates may have made to the final flux term, a sensitivity analysis was carried out. The main estimates or assumptions (as detailed in Chapter 3, Section 3.4) were as follows:

- Mean annual rainfall (1981 to 2006 inclusive) was used
- A factor of 0.7 was applied to pan evaporation rates to obtain an estimated evaoptranspiration rate
- Evapotranspiration was assumed to be constant throughout the year (although the pan evaporation rate was for March to October)
- It was assumed that no DOC was lost via flow through the catotelm.

The following scenarios (and combinations) were tested:

- Minimum and maximum annual rainfall (1981 to 2006 inclusive) were used instead of a mean value (these being 961.6 cm from 1995 and 1586.9 cm from 2000).
- A factor of 0.5 was applied to pan evaporation rates to estimate evapotranspiration (Ingram (1983) suggest a factor from 0.5 to 0.7)
- Evapotranspiration was assumed to shut down during the winter (November to February)
- 9% of water lost from the site was assumed to flow through the catotelm (as modelled by Baird et al., 2006) with a DOC concentration of 48.81 mg l^{-1}, the average of all samples taken from piezometers of depths ≥ 50 cm at the Edge site over all seasons ($n = 42$, $\sigma = 8.97$).

The results of the sensitivity analysis are shown in Table B.1 below.

Scenario	DOC flux from site (Tonnes)
1) As original estimate but using min. '81-'06 rainfall	78.6
2) Using min. '81-'06 rainfall and 9% catotelm flow	87.0
3) Using min. '81-'06 rainfall and 0.5 pan evaporation factor	96.0
4) Using min. '81-'06 rainfall and 0.5 pan evaporation factor and 9% catotelm flow	106.3
5) Initial estimate (as in Chapter 3, Section 3.4)	113.2
6) Average rainfall and 9% catotelm flow	128.7
7) Average rainfall with only seasonal evapotranspiration	130.9
8) Average rainfall with 0.5 pan evaporation factor	133.8
9) Average rainfall with seasonal evapotranspiration and 0.5 pan evaporation factor	143.3
10) Average rainfall with seasonal evapotranspiration and 9% catotelm flow	146.0
11) Average rainfall with 0.5 pan evaporation factor and 9% catotelm flow	148.0
12) Average rainfall, seasonal evapotranspiration, a 0.5 pan evaporation factor and 9% catotelm flow	159.5
13) Using max. '81-'06 rainfall	169.4
14) Using max. '81-'06 rainfall and 9% catotelm flow	186.8
15) Using max. '81-'06 rainfall and 0.5 pan evaporation factor	187.5
16) Using max. '81-'06 rainfall and 0.5 pan evaporation factor and 9% catotelm flow	206.8

Table B.1: Results from sensitivity analysis of assumptions made during DOC flux estimate.

Using the minimum and maximum annual rainfall numbers had the largest effect on the flux estimate, resulting in the highest and lowest estimates (Figure B.1).

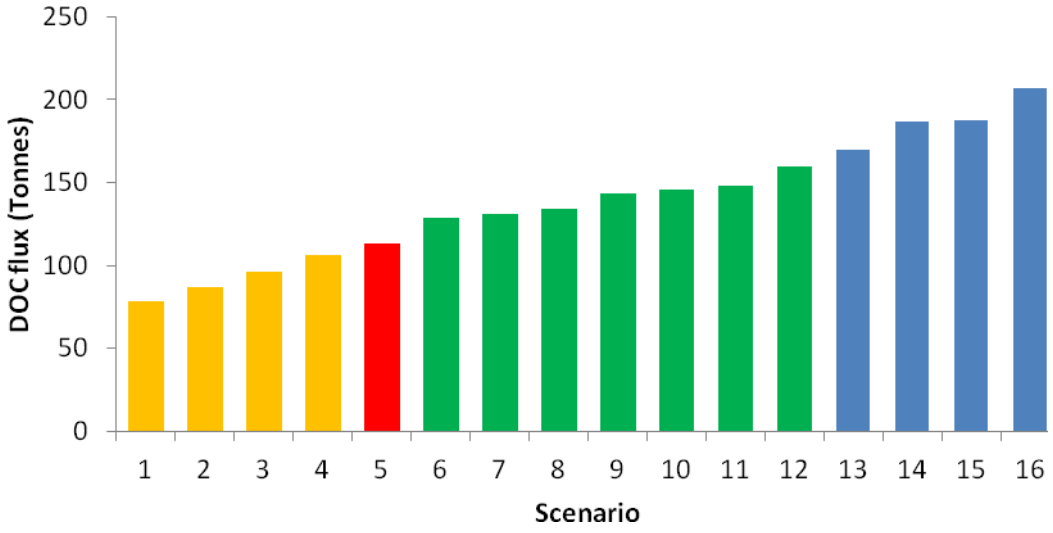

Figure B.1: DOC flux estimates from the site in tonnes with each scenario as listed in Table B.1. Yellow bars indicate the estimates using the lowest rainfall data, blue the highest. The green bars show the estimates using average annual rainfall and the red bar is the original estimate as described in Chapter 3, Section 3.4.

Appendix C: Large Van Krevelen plots (Chapter 6)

The following four images are enlarged versions of the panels in Figure 6.6. Sample ID at the top of the image.

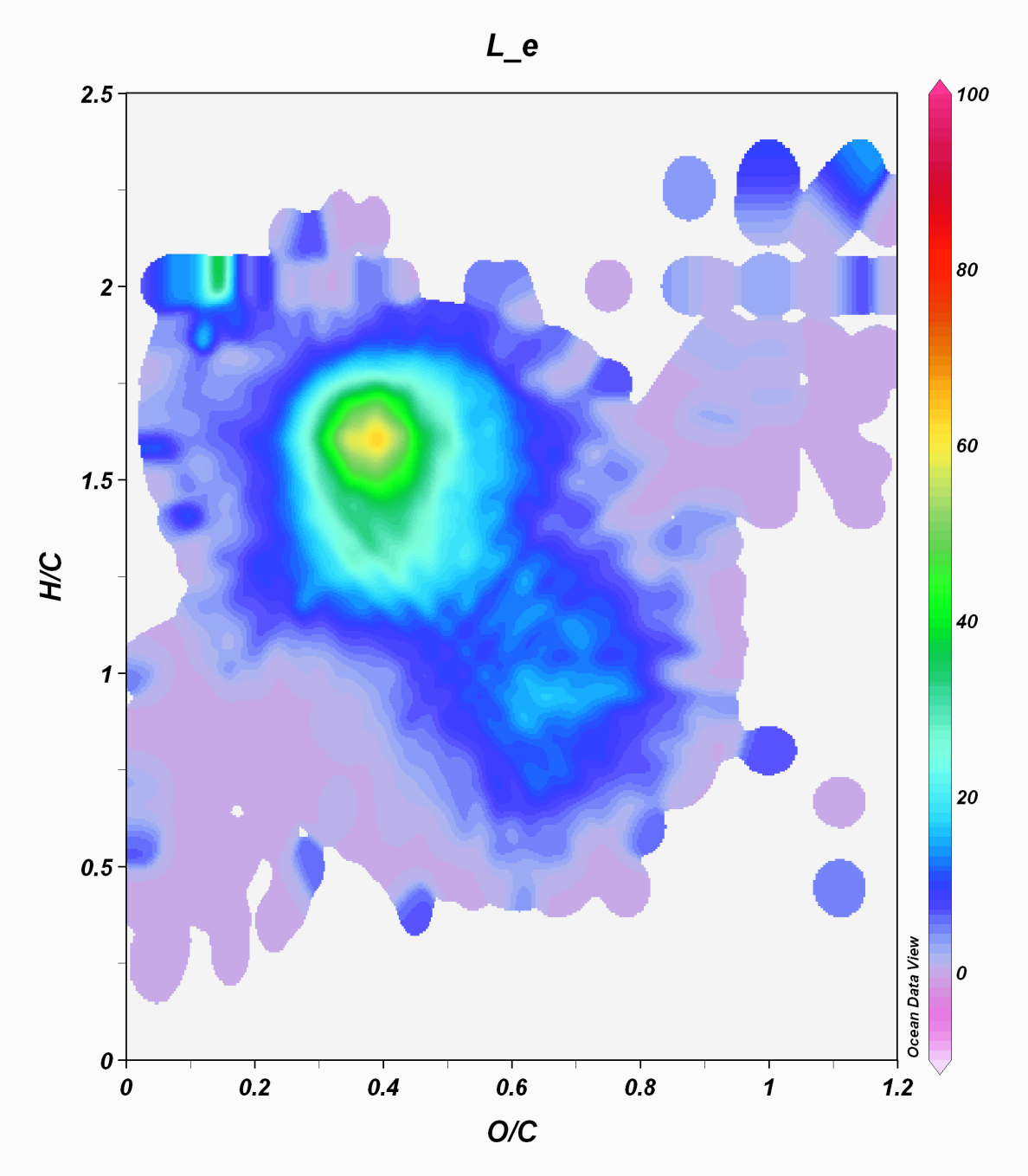

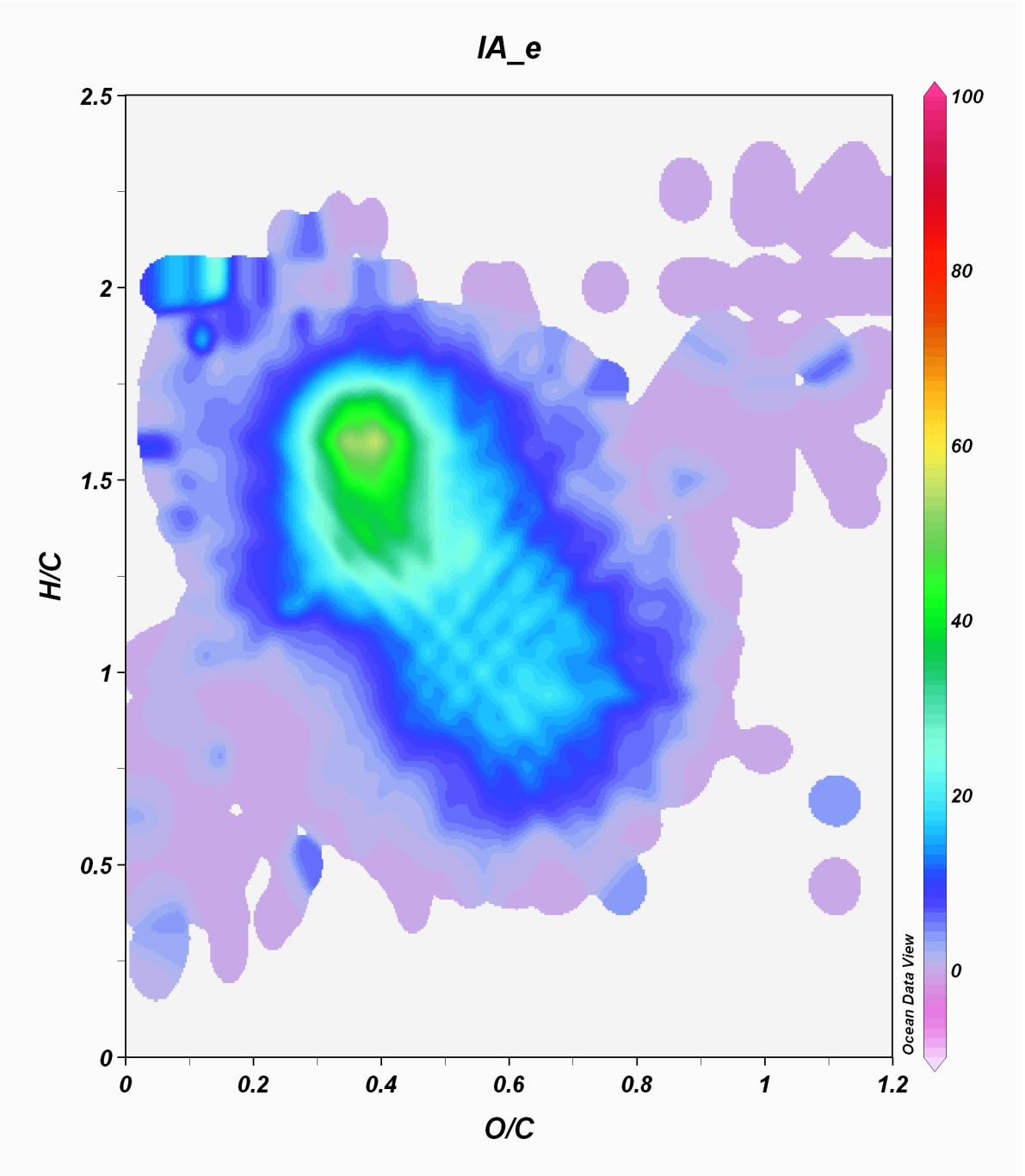
IA_e
2.5
2
1.5
1
0.5
0
H/C
0
0.2
0.4
0.6
0.8
1
1.2
O/C
100
80
60
40
20
0
Ocean Data View

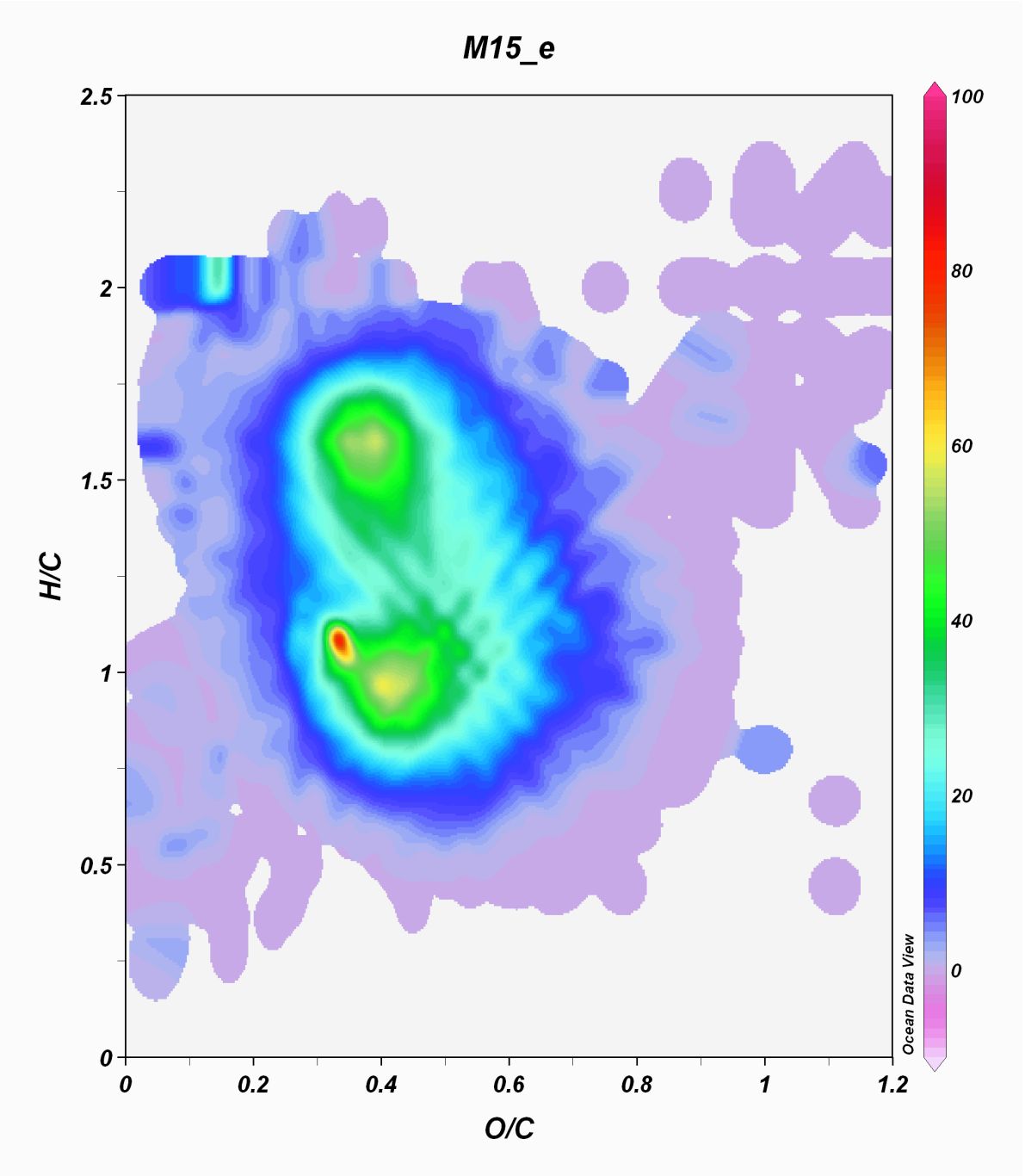
M15_e
2.5
2
1.5
1
0.5
0
H/C
0
0.2
0.4
0.6
0.8
1
1.2
O/C
100
80
60
40
20
0
Ocean Data View

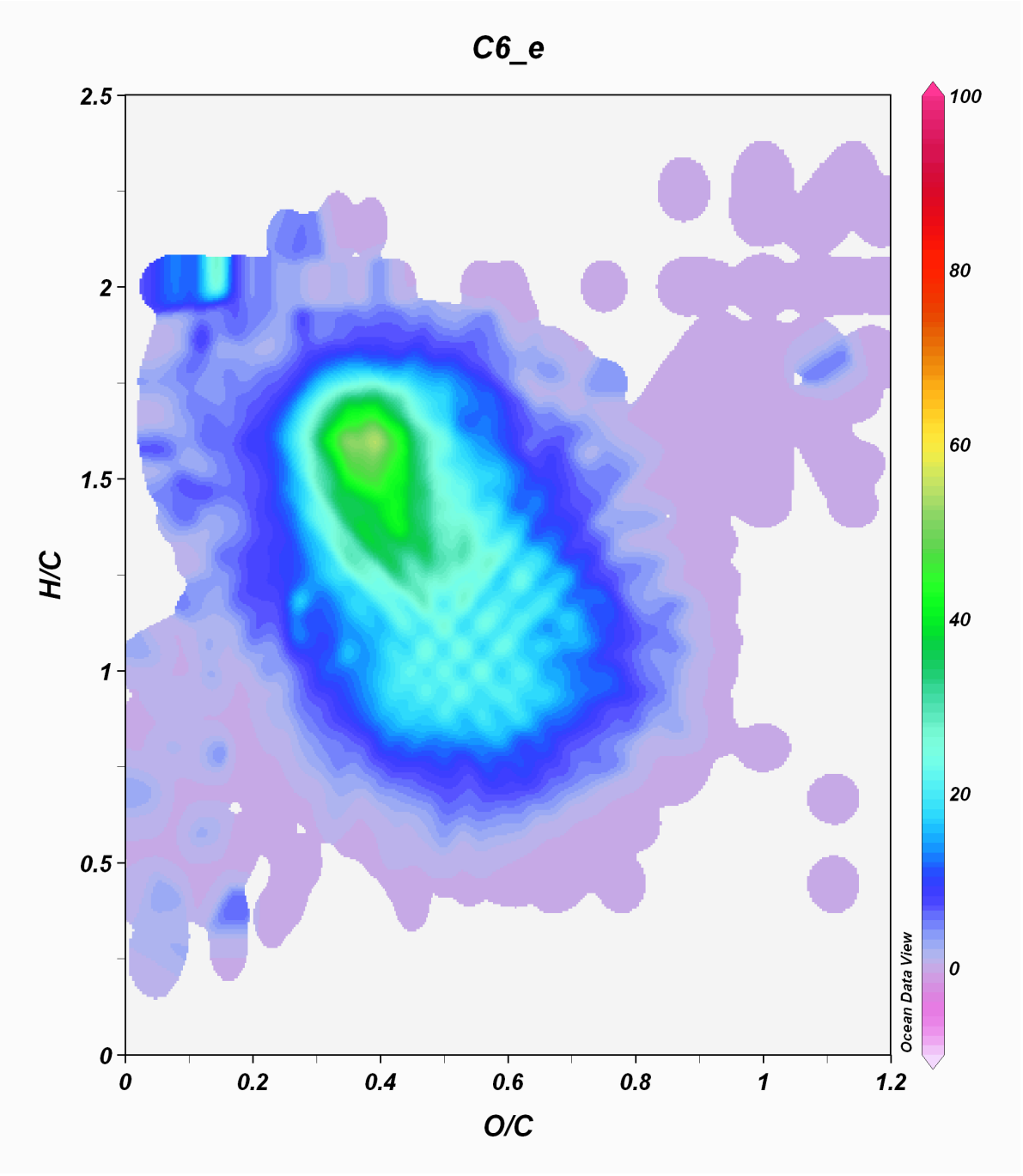
C6_e
2.5
2
1.5
1
0.5
0
H/C
0
0.2
0.4
0.6
0.8
1
1.2
O/C
100
80
60
40
20
0
Ocean Data View

The following six images are enlarged versions of the panels in Figure 7.6. Sample IDs at the top of the image indicate the comparison made (see Figues 7.6 for details).

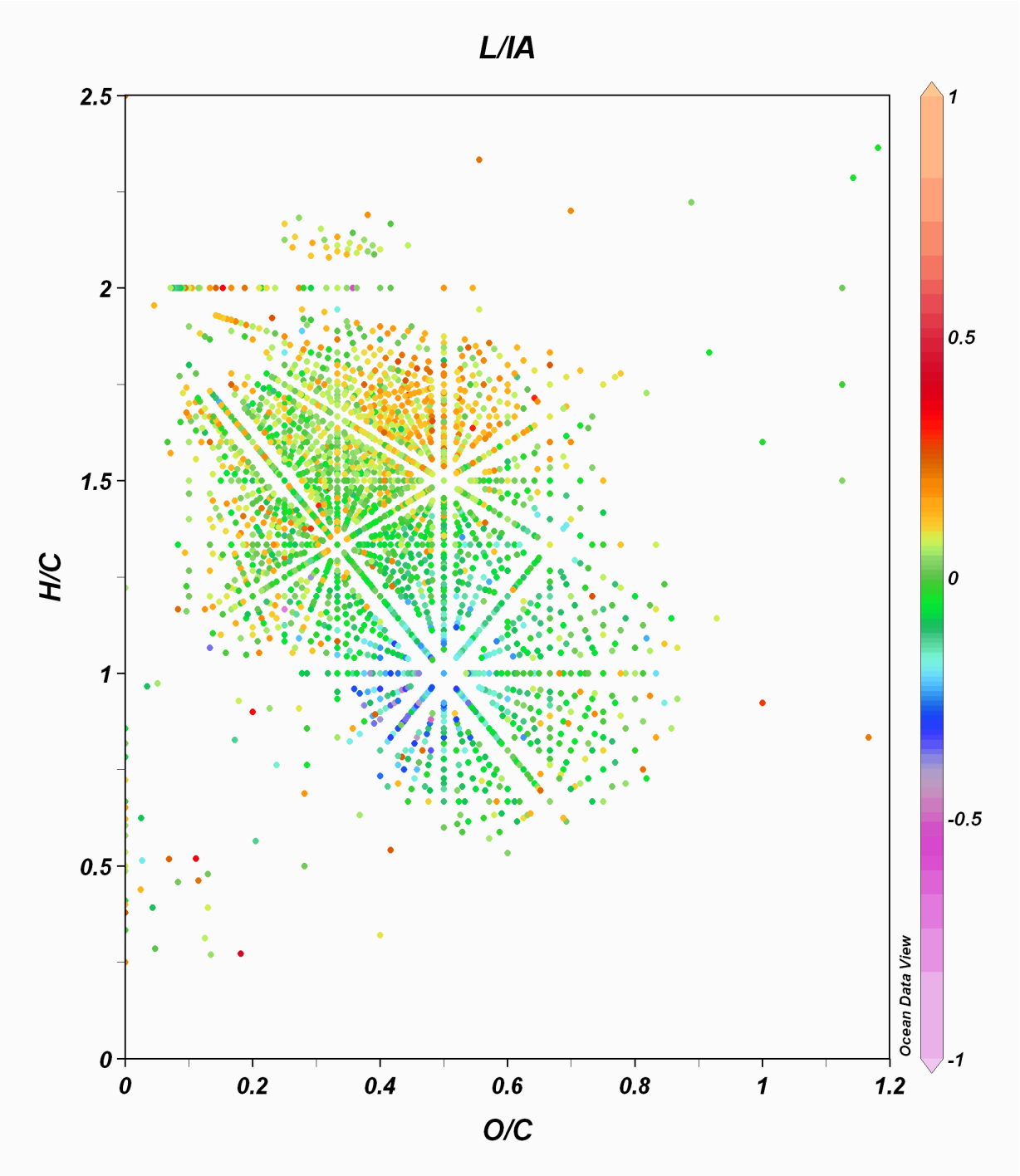

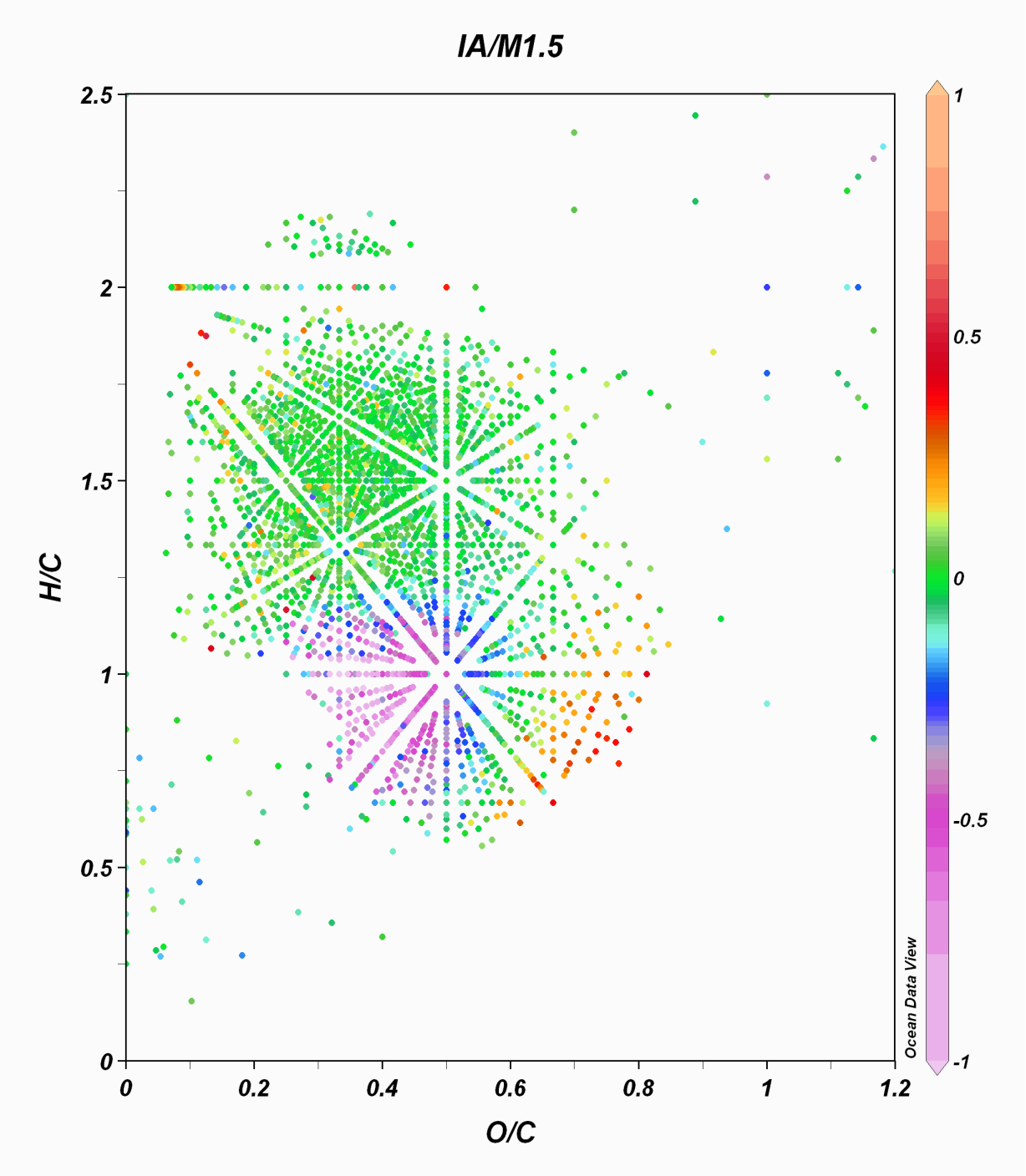
IA/M1.5
H/C
O/C
2.5
2
1.5
1
0.5
0
0
0.2
0.4
0.6
0.8
1
1.2
1
0.5
0
-0.5
-1
Ocean Data View

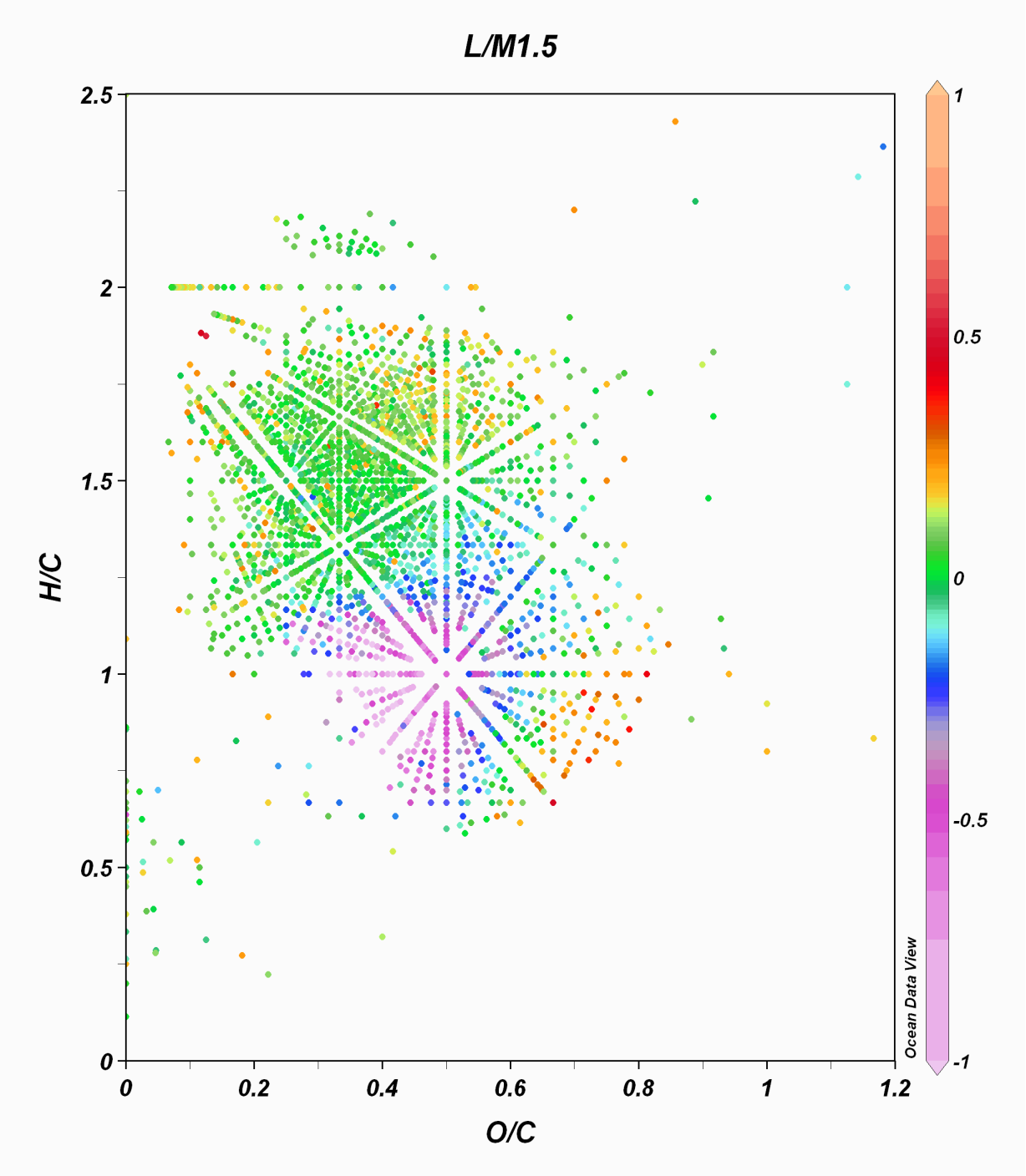
L/M1.5
H/C
O/C
2.5
2
1.5
1
0.5
0
0
0.2
0.4
0.6
0.8
1
1.2
1
0.5
0
-0.5
-1
Ocean Data View

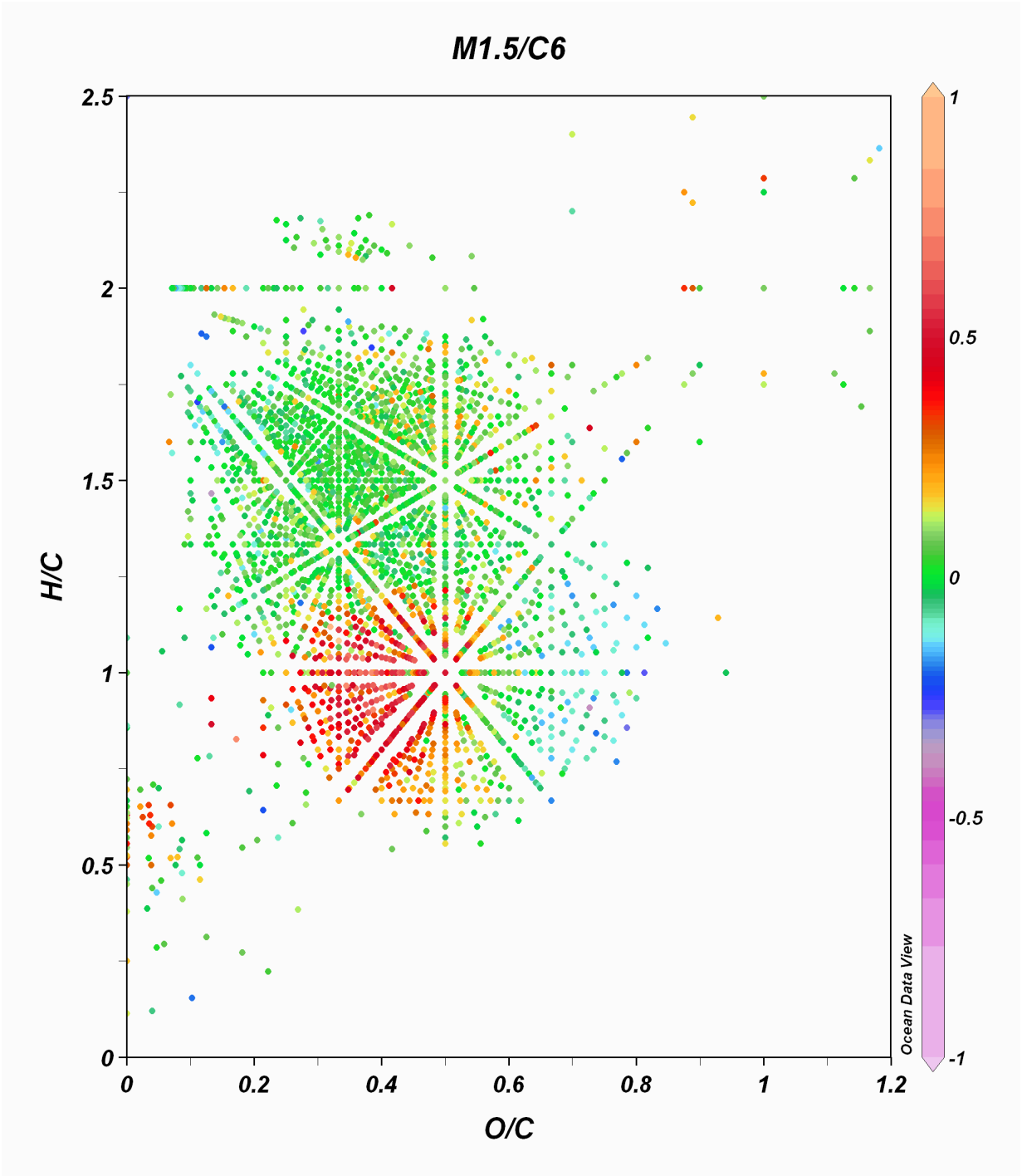
M1.5/C6
2.5
2
1.5
1
0.5
0
H/C
0
0.2
0.4
0.6
0.8
1
1.2
O/C
1
0.5
0
-0.5
-1
Ocean Data View

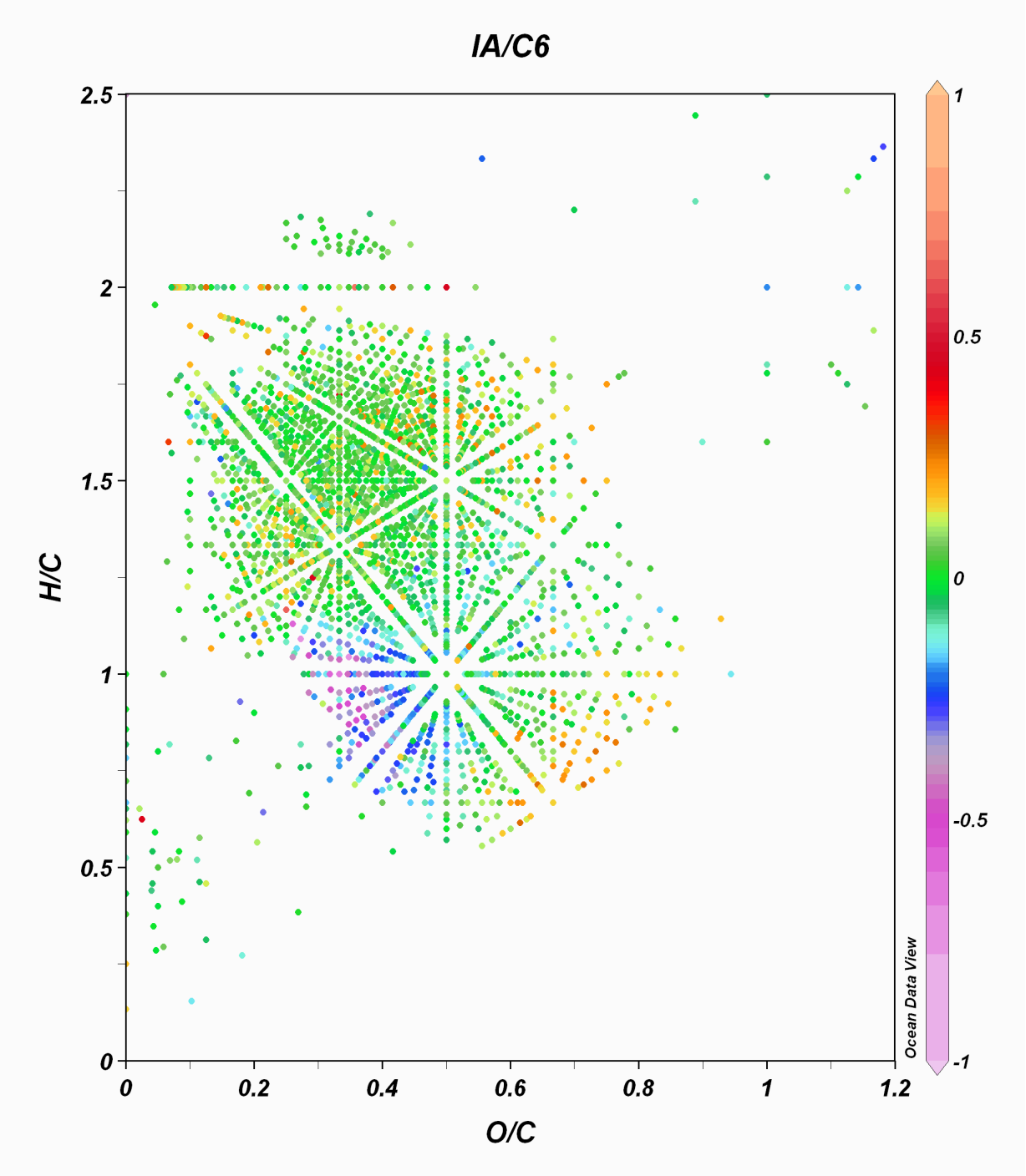
IA/C6
H/C
O/C
2.5
2
1.5
1
0.5
0
0
0.2
0.4
0.6
0.8
1
1.2
1
0.5
0
-0.5
-1
Ocean Data View

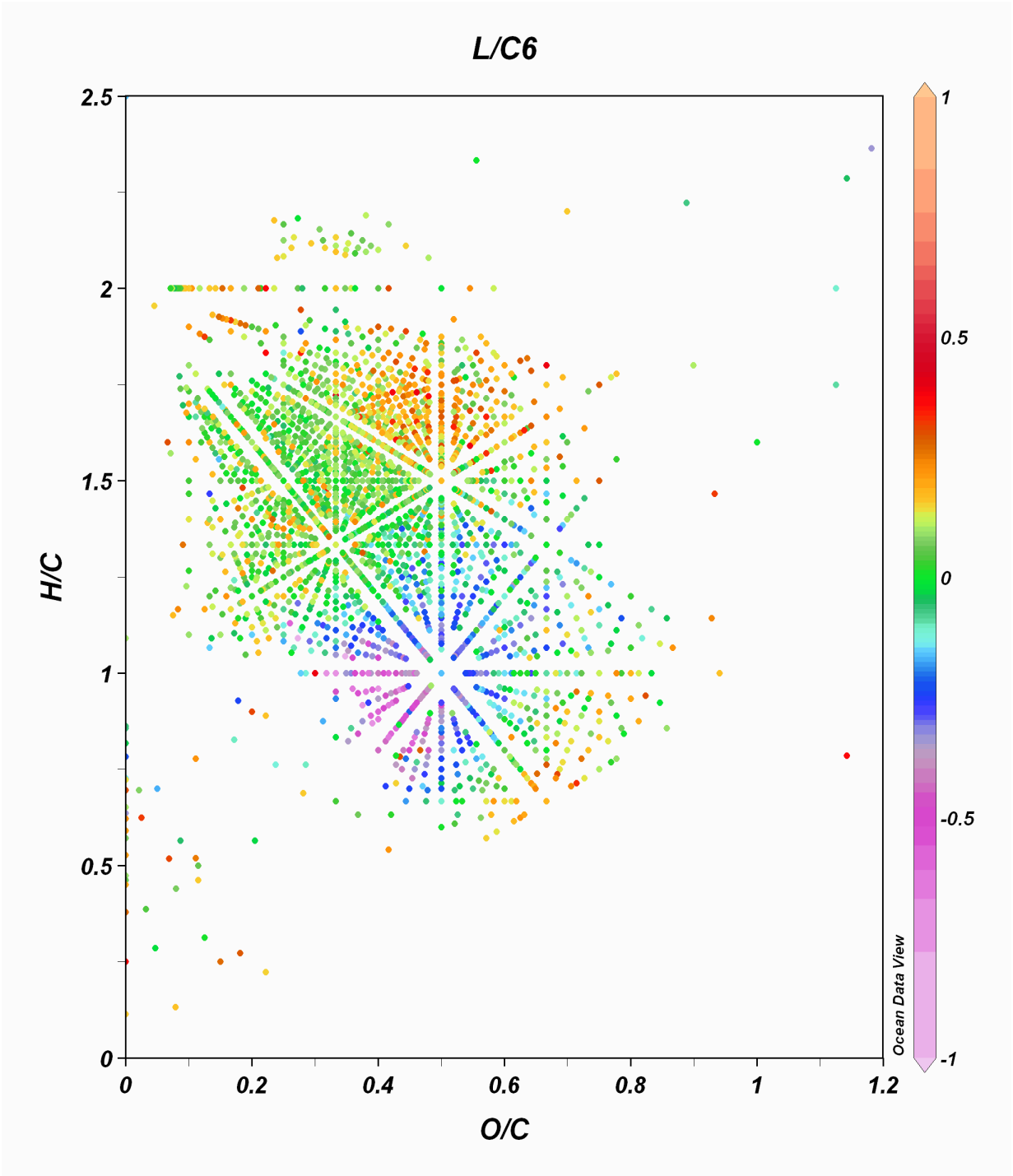
L/C6
2.5
2
1.5
1
0.5
0
H/C
0
0.2
0.4
0.6
0.8
1
1.2
O/C
1
0.5
0
-0.5
-1
Ocean Data View